DISSERTATION

INVESTIGATING BIOSYNTHETIC PATHWAYS OF THE *ASPERGILLUS* GENUS THROUGH BIOMIMETIC TOTAL SYNTHESIS OF SECONDARY METABOLITES

Submitted by

Brooke Benson

Department of Chemistry

In partial fulfillment of the requirements

For the Degree of Doctor of Philosophy

Colorado State University

Fort Collins, Colorado

Spring 2022

Doctoral Committee:

Advisors: Robert M. Williams (deceased)
Alan Kennan

Robert Paton
Debbie Crans
Dean Crick

ABSTRACT

INVESTIGATING BIOSYNTHETIC PATHWAYS OF THE *ASPERGILLUS* GENUS THROUGH BIOMIMETIC TOTAL SYNTHESIS OF SECONDARY METABOLITES

The prenylated indole alkaloids are a class of secondary metabolites containing a unique bicyclo[2.2.2]diazaoctane core and a wide range of biological activity. This complex structure has prompted extensive investigation into the biochemical synthesis of these compounds. Currently, three disparate biochemical strategies are known to be used by producing fungi to construct the bicyclic core: (1) NADPH-dependent bifunctional reductase/Diels-Alderase-mediation in formation of the monooxopiperazines; (2) brevianamide assembly through cofactor-independent pinacolase resulting in spontaneous intramolecular Diels-Alder (IMDA) generation of the bicyclo[2.2.2]diazaoctane core; (3) Diels-Alderase mediated enantiodivergent generation of the dioxopiperazines via cytochrome P450 oxidation to achiral azadienes and successive enzyme-mediated stereoselective IMDA reaction. This work aimed to employ biomimetic total synthesis to aid in elucidation of the biosynthetic pathways in the *Aspergillus* genus, which utilizes the third strategy. This author reports the first total syntheses of 6-*epi*-Notoamides T10-12 and Notoamide T2, as well as an improved total synthesis of 6-*epi*-Notoamide T. Also reported are synthetic efforts towards 6-*epi*-Notoamide T9, Notoamide TI, and Citrinalin C.

ACKNOWLEDGEMENTS

I would first like to thank Professor Robert Williams for guiding me on so much of this journey. Bob gave me the space to become an independent scientist, while always having a suggestion when it was needed. I can honestly say I now get excited about enzymes and enantiodivergence. Something I never would have thought possible when I started this project four years ago. We were all so devastated to lose you too soon. Thank you to my new advisor, Professor Alan Kennan, for all of the advice and helping me get to the end of my graduate journey. And a special shoutout to my favorite Luther professors, Molly Wilker and Olga Michels, for inspiring me to go to graduate school. You taught me so much and I wouldn't be where I am without you.

A huge thank you to all of the Williams group members, both past and present. Jonathan, thank you for always believing in me and offering so much helpful advice. Whether I was attempting a complex reaction or trying to fix a vacuum pump, you always went out of your way to help. Maggi, I would not have survived teaching without you. Teaching 245 with you was the most hilarious disaster I could have asked for. Thank you for your support both as a friend and coworker. Morgan, we survived this project together. I'm not sure how, but we did it. We had a lot of long days analyzing NMRs and working out mechanisms. Thank you for being such a great collaborator and such an amazing friend.

Thank you to my parents, who helped me become the person I am today. You have been there to support me every step of the way, and I owe so much of my success to you. You've always made sure I could pursue everything I have wanted to do. While you don't always know

what I'm talking about, you've always been there to listen whenever I need you. I will never be able to find all the words to thank you for how much you've done for me.

John. Love. Husband. I do not know how to even begin to thank you. From coworker, to friend, to husband, you have been there for me all along. Your love and support have meant everything to me. The long hours writing, the longer hours in lab, and so many nights without enough sleep. We've been through so much together, and now we're finally at the end. I am so lucky to have found you, and even luckier that we share this passion. Even when we swear we hate chemistry, we both know it's shaped so much of our lives and we (well, you at least) love it. I'm so happy you've been here to share this journey with me, and that I've gotten to share yours. I will never be able to thank you enough for everything you've done for me. And I do promise to repay you for the extra support you've given me over the past few weeks (including reading this dissertation). Your turn is coming so soon, and I'm so excited for it. I love you so much. I can't wait for the rest of our lives.

DEDICATION

To Yoshi, for the unconditional love and support.

TABLE OF CONTENTS

Chapter 1: Prenylated Indole Alkaloids

I. Introduction

The Stephacidins, Paraherquamides, Brevianamides, Malbrancheamides, and Notoamides are all secondary metabolites that are part of the prenylated indole alkaloid family. These alkaloids are produced by various fungal species in the *Aspergillus*, *Penicillium*, and *Malbranchea* genera.[1–3] These alkaloids contain interesting structural moieties, including a unique bicyclo[2.2.2]diazaoctane core and a heavily functionalized indole derivative. These distinct features have prompted questions about the biogenesis of these compounds, which has been studied extensively by the Williams group.[3–5]

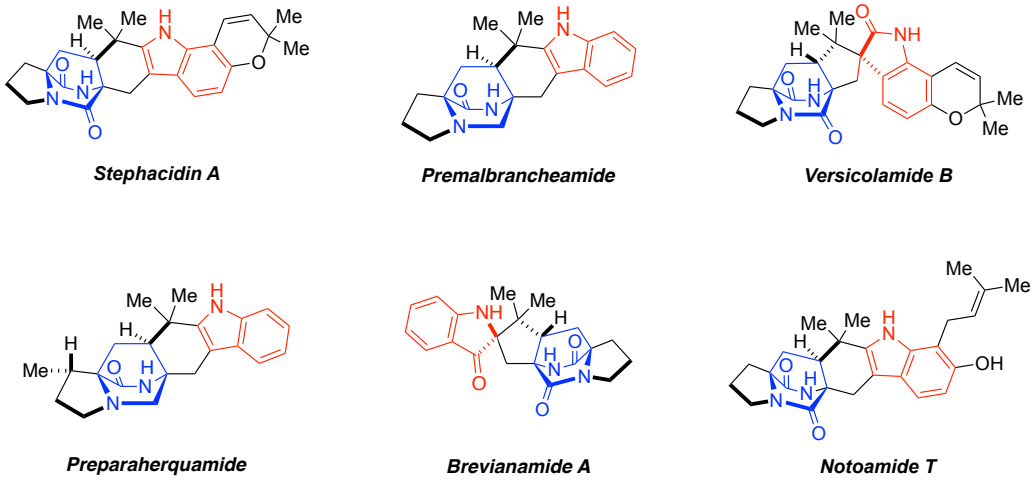

Figure 1.1. Various prenylated indole alkaloids. The bicyclo[2.2.2]diazaoctane core is shown in blue and the indole-based moiety is in red.

In addition to the intriguing origin of these compounds, many prenylated indole alkaloids display a variety of bioactivities including anthelmintic[6–10], anti-tumor[11–13], anti-fungal[14], and antibacterial[14,15]. While both the synthesis and biosynthesis of these compounds have been

investigated for years, there is still much to learn about the formation of these remarkable secondary metabolites.

i. Formation of Bicyclo[2.2.2]diazaoctane core

The unique bicyclo[2.2.2]diazaoctane core sparked investigation into the biosynthetic mechanism of its construction. After the isolation of Brevianamide A (seen in **Figure 1.1**), the first mechanistic proposal for the formation of the bicyclic core was made by Sammes in 1970. He suggested an intramolecular Diels-Alder (IMDA) reaction proceeding through the azadiene species shown in **Figure 1.2**.[16] Conversely, in 1971, Birch proposed an epidithiapiperazinedione intermediate which would form the diazaoctane ring via the loss of S_2.[17,18]

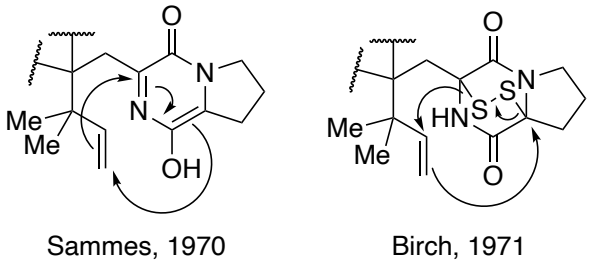

Figure 1.2. Sammes and Birch proposed mechanisms for bicyclo[2.2.2]diazaoctane ring bioformation.[16,18]

Sammes' hypothesized mechanism proved correct—the core does arise through an IMDA reaction. After identification of the Notoamide gene cluster (see Chapter 1, section IV) and numerous incorporation studies of possible IMDA precursors, our understanding of the bicyclic core formation has grown substantially.[19] However, the complexity of these transformations goes well beyond the already unique mechanism. Different organisms utilize distinct substrates and enzymes to form the bicycle, and each identified alkaloid raises new questions about the biosyntheses in the producing organism.

While various substrates are utilized in each fungus to form the bicyclo[2.2.2]diazaoctane ring system, the basic mechanistic strategy is still the same. The oxopiperazine unit undergoes a net 2 electron oxidation and two new C-C bonds are formed through IMDA with the reverse-prenyl moiety.[3] This can occur in one of four distinct stereochemical transition states and results in either *syn* or *anti* relationships between the bridged amide and the diastereotopic proton (position 6, numbering system depicted in **Figure 1.3**).

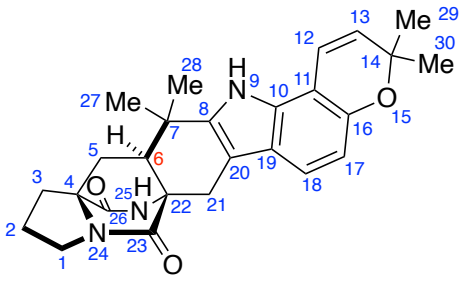

Figure 1.3. General numbering system used in this dissertation, diastereotopic 6-position highlighted in red. However, this numbering system will not be used in reference to indole positions, where the colloquial system will be used instead.

If the proton and amide are on the same side of the molecule, the compound is *syn*. If they are opposite, the compound is *anti*. Each of these diastereomers also has an enantiomer that results from the reaction proceeding from the opposite face. These various stereochemical outcomes can be seen in **Figure 1.4**, beginning with Notoamide S.[20] Both enantiomers of Notoamide T (*syn*) and 6-*epi*-Notoamide T (*anti*) are made through suspected intermediate achiral azadiene **1** that results from the tautomerization of Notoamide S. In this figure, the diastereotopic proton and bridged amide are shown in red for clarity.

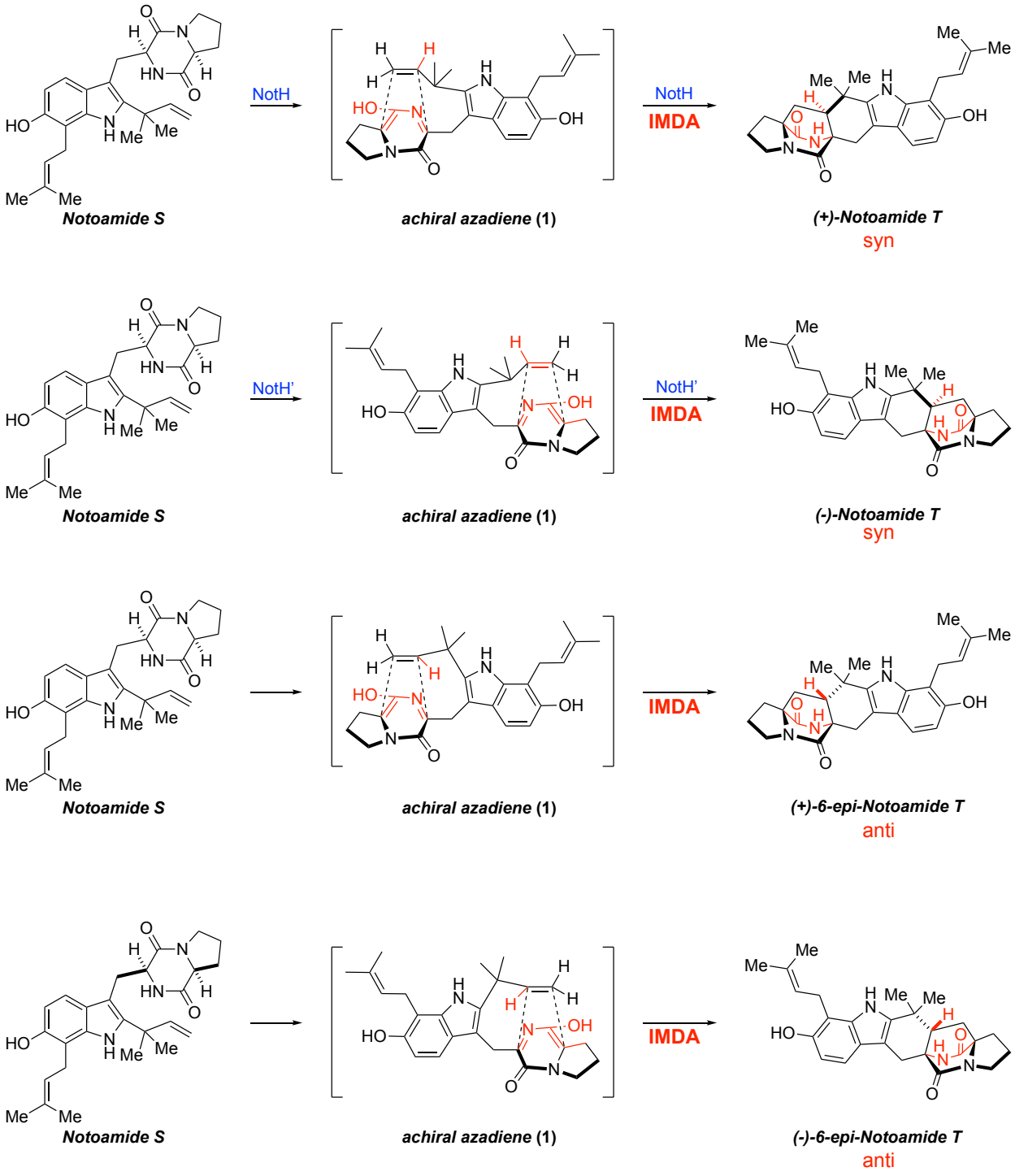

Figure 1.4. Stereochemical outcomes of Notoamide T after IMDA reaction of achiral azadiene **1**. Both the diastereotopic proton and bridged amide are shown in red.[20]

Due to the unique nature of enantio- and diastereo-divergence and congruence in the biosynthetic pathways of these correlating fungi, it has been proposed, and in many cases found, that enzymes are responsible for aiding the Diels-Alder cycloaddition as well as other steps in the biosynthetic pathway.[3,21] Our preparation of these natural products aims to follow biomimetic total syntheses, thereby accessing potential biosynthetic intermediates in the pathways. These intermediates can, in turn, be used to learn more about the biogenesis of these unique natural products.

II. Biosynthetic Diels-Alder Pathways

The prenylated indole alkaloids are classified into two main families: dioxopiperazines and monooxopiperazines. The dioxopiperazines contain two amides, such as Stephacidin A, Versicolamide B, and Notoamide T. The monooxopiperazines have only one amide, like Preparaherquamide and Premalbrancheamide (**Figure 1.1**). Despite this small difference, there are disparate biosynthetic pathways for each, as well as different paths for each producing fungus. This is remarkable from an evolutionary perspective, and studying these processes provide great insight to how natural selection has shaped these pathways leading to the diversity of compounds produced in different species.

It had long been theorized that the intramolecular Diels-Alder responsible for forming the bicyclo[2.2.2]diazaoctane ring system is mediated by a "Diels-Alderase" enzyme. This has been found to be true for many of the prenylated indole alkaloids, and the discovery of these enzymes adds to a very short list of currently known Diels-Alderases; only a few have been reported in the past decade.[22–25] The Diels-Alder reaction is incredibly important in the synthesis of pharmaceuticals, as it avoids charged intermediates, rapidly builds complex moieties, and allows for controlled, stereoselective reactions. It can be used in the synthesis of polymers,

bioconjugates, functionalization of surfaces, assembly of nanomaterials, and the preparation of hydrogels for drug delivery.[26–31] With this versatility, the isolated Diels-Alderases responsible for the bicyclo[2.2.2]diazaoctane ring system can be incredibly valuable in the pharmaceutical industry.

At this point, three separate biosynthetic pathways that create this unique bicyclic core have been found in producing fungi. The first concerns the monooxopiperazines: NADPH-dependent bifunctional reductases/Diels-Alderase. This enzyme reduces a zwitterion to an achiral azadiene in the presence of NADPH and also catalyzes an enantiospecific IMDA to form the bicyclo[2.2.2]diazaoctane ring system. An example of this can be seen in **Figure 1.5**, where MalC aids in the biogenesis of premalbrancheamide.[21]

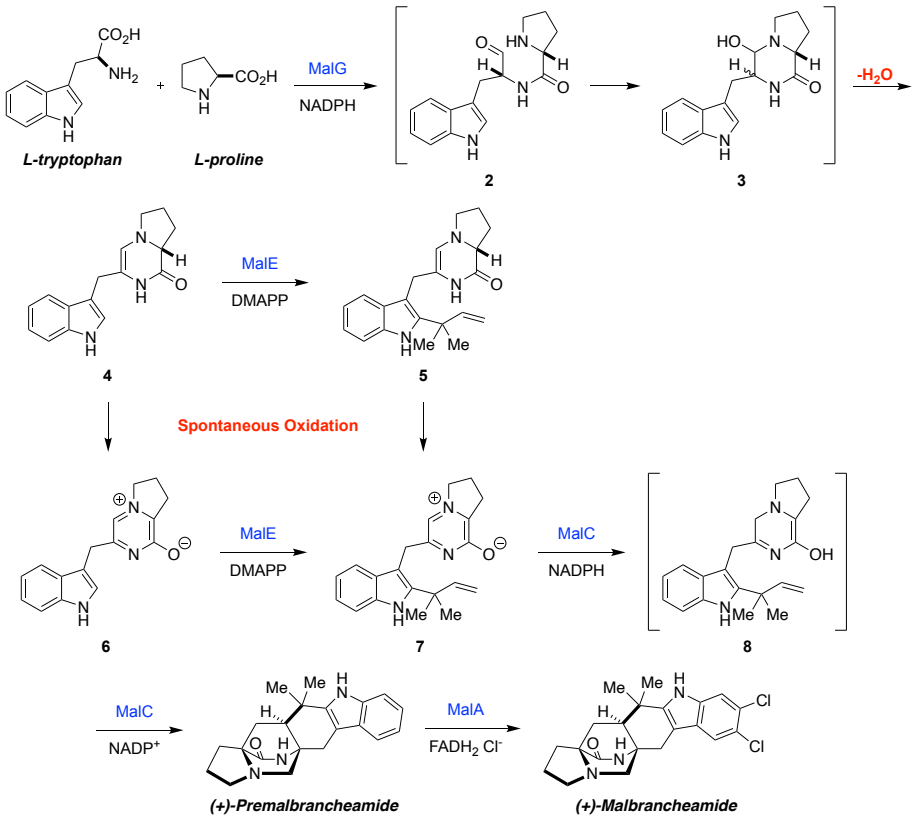

Figure 1.5. Biosynthesis of Malbrancheamide: the first Diels-Alder strategy. MalC is a bifunctional reductase/Diels-Alderase.

To form Malbrancheamide, proline and tryptophan are first coupled with MalG, a non-ribosomal peptide synthetase, forming aldehyde **2**. Spontaneous cyclization and dehydration give dienamine **5**, which is reverse-prenylated by MalE. Spontaneous oxidation yields zwitterion **7**, the substrate for the IMDA. MalC reduces the zwitterion and facilitates the stereoselective IMDA, forming Premalbrancheamide. Finally, halogenase MalA generates Malbrancheamide.[21]

MalC was the first Diels-Alderase to be discovered. It derives its cycloaddition selectivity from NADPH—while NADPH and NADH are both effective cofactors, NADPH offers complete stereocontrol of the IMDA while NADH resulted in a mixture of 63:37 (+) to (-)-premalbrancheamide.[21] Other Diels-Alderases in this category have also been identified, such as PhqE. Homologous proteins for the Citrinalin (CitL, *Penicillium citrinum* F53) and Citrinadin (CtnO, *Penicillium citrinum* IBT 29821) pathways have also been discovered by the Sherman group.[21] These proteins could catalyze the construction of the bicyclic core for these families, and in this case be selective for the *anti*-configuration.

A second strategy for assembly of the bicyclic core of these compounds is in the Brevianamide pathways. In this family, formation of the core requires a cofactor-independent pinacolase followed by a spontaneous intramolecular Diels-Alder reaction.[32] The pinacolase involved is directing, so the ring system is still built enantioselectively, but not enantiospecifically. Biosynthetic pathways that include a pinacol rearrangement are quite rare, and all known cases of pinacolases are cofactor dependent. The pinacolase identified in the biogenesis of Brevianamide A and B seems to be the first known cofactor-independent case.[32]

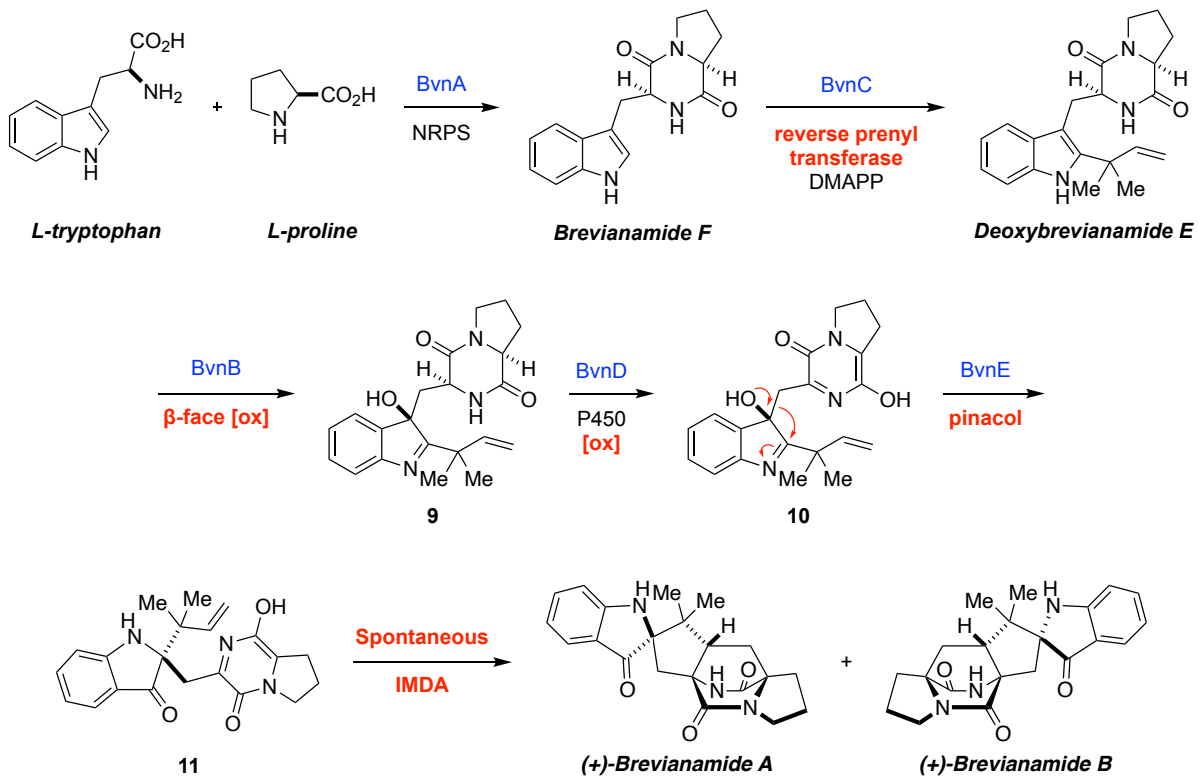

Figure 1.6. Biogenesis of the Brevianamides. BvnE catalyzes a pinacol rearrangement which is followed by a spontaneous IMDA transformation.

In the biosynthesis of Brevianamides A and B, L-tryptophan and L-proline is coupled by BvnA (a nonribosomal peptide-synthetase), forming Brevianamide F (**Figure 1.6**).[19,33] This compound is then reverse-prenylated by BvnC to form Deoxybrevianamide E, followed by *β*-face oxidation by flavoenzyme BvnB which gives hydroxyindolenine **9**.[34] This compound is then oxidized to the azadiene **10** by cytochrome P450 enzyme BvnD. Finally, the cofactor-independent pinacolase BvnE promotes the pinacol rearrangement to form indoxyl **11** which undergoes spontaneous IMDA to give Brevianamide A in excess, a 10:1 ratio to Brevianamide B.[32] Because the Diels-Alder is non-enzyme mediated, it is not stereospecific as seen in the monooxopiperazines.

The last strategy is that of the dioxopiperazines, is the biosynthetic pathway for construction of the Notoamides, Stephacidins, and Versicolamide B, which will be the focus of this dissertation. This pathway is incredibly unique due to the enantiodivergence found between species forming the same natural products. All current evidence supports this divergence originating at the enzyme-mediated IMDA reaction. This pathway is thoroughly discussed in section V.

III. Aspergillus

While prenylated indole alkaloids from this large family have been found in the *Aspergillus*, *Penicillium*, and *Malbranchea* genera, this work will focus heavily on those found in the *Aspergillus* species. In 2008, five prenylated indole alkaloids were isolated by Gloer and coworkers from *Aspergillus amoenus*, a terrestrial derived fungus obtained from a basidiocarp of *Gandoderma australe* collected in a Hawaiian forest.[35] Brevianamide F, (-)-Stephacidin A, Norgeamide D, (+)-Notoamide B, and (+)-Versicolamide B were extracted and their structures determined by NMR and mass spectroscopy. It was also determined through circular dichroism (CD) spectroscopy that both Notoamide B and Versicolamide B possessed a 3*S* configuration at the spiro-oxindole center.[35] Versicolamide B was also the first non-Brevianamide compound discovered to have an *anti*-configuration for its bicyclic core.

Separately, the marine fungus *Aspergillus protuberus* was isolated by the Tsukamoto group from the *Mytilus edulis galloprovincialis* mussel found off the coast of the Noto peninsula in Japan. Stephacidin A, Versicolamide B, and Notoamide B were also isolated from this fungus, but Stephacidin A and Notoamide B having the opposite absolute configuration as those isolated from the terrestrial *Aspergillus amoenus* (**Figure 1.7**).[36]

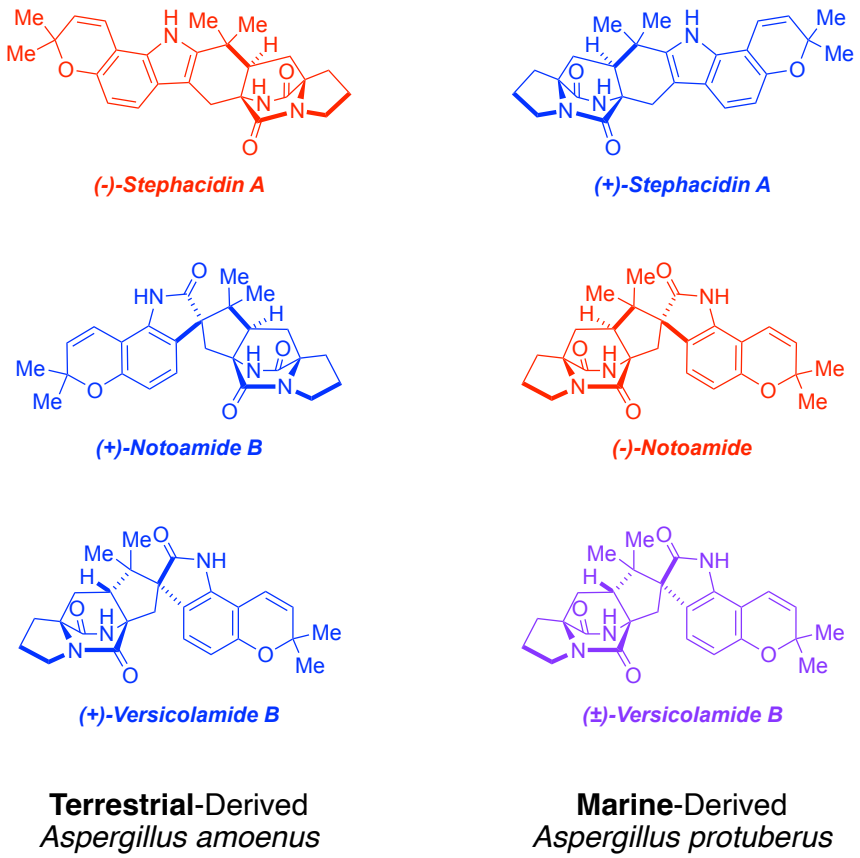

Figure 1.7. Structures of antipodal metabolites from terrestrial-derived *Aspergillus versicolor* and marine-derived *Aspergillus protuberus*.

The difference in these enantiomeric metabolites increased interest in the biogenesis of these compounds. Evidence has strongly suggested that the intramolecular Diels-Alder (IMDA) reaction forms the bicyclo[2.2.2]diazaoctane core and is therefore responsible for the enantio-divergence between the two *Aspergillus* species. These two species follow equivalent pathways to synthesize these metabolites, differing only in the stereogenic formation of the bicyclic core.

When first examining the biosynthetic pathway towards Stephacidin A (**Figure 1.8**), Notoamide E was initially thought to be the precursor to Notoamide T, and eventually Stephacidin A. Notoamide E was found to be a key intermediate in *A. protuberus* and it was

assumed that Notoamide E was converted into more advanced metabolites further down the biosynthetic pathway. [37,38] Feeding studies with [^{13}C]$_2$-Notoamide E were performed on *A. protuberus* and produced Notoamides C and D, as well as new products 3-*epi*-Notoamide C and Notoamides E2-E4.[37,39] However, none of these products contain the bicyclic core and most notably, the labeled Notoamide E was not incorporated into Stephacidin A. The results of these incorporation studies suggested possible intermediates for Stephacidin A (and other natural IMDA products) might include Deoxybrevianamide E, 6-Hydroxy-deoxybrevianamide E, and Notoamide S. From Deoxybrevianamide E to Stephacidin A, four main steps must occur: the IMDA, oxidation of C-6, prenylation, and oxidation/cyclization to form the pyran ring.[40]

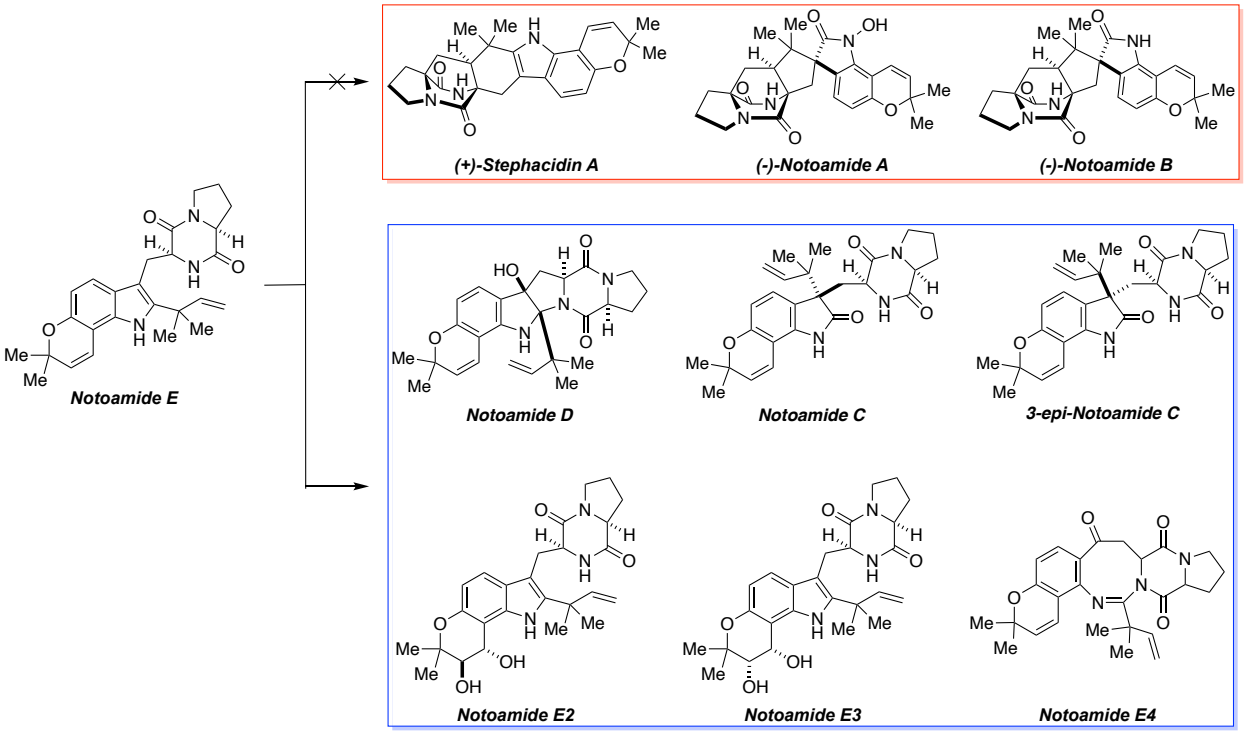

Figure 1.8. Resulting products from feeding study of Notoamide E.

[^{13}C]$_2$-[^{15}N]-Deoxybrevianamide E and [^{13}C]$_2$-[^{15}N]-6-Hydroxy-deoxybrevianamide E were fed to *A. protuberus* but did not result in the formation of Stephacidin A, nor Notoamides A

and B.[41,42] These studies only afforded Notoamides C and D. Next, [^{13}C]$_2$-[^{15}N]-Notoamide S was integrated into *A. amoenus* and was found to be incorporated into (-)-Stephacidin A, (+)-Versicolamide B, (+)-Notoamide B, along with Notoamides C and D.[34] These results show that Notoamide S is the most likely common intermediate for many of the IMDA natural products. It is proposed that Notoamide S undergoes oxidation to form achiral azadiene **1** and subsequently goes through the IMDA reaction to form Notoamide T and 6-*epi*-Notoamide T. These products would then be oxidized and cyclized to form the pyran ring, giving Stephacidin A and 6-*epi*-Stephacidin A, respectively. Stephacidin A can be further oxidized to give Notoamide B after pinacol rearrangement while 6-*epi*-Stephacidin A undergoes the same modifications to form Versicolamide B (**Figure 1.9**). Notoamide S was also recently identified as a minor metabolite in *A. amoenus*, further confirming this conclusion.[20]

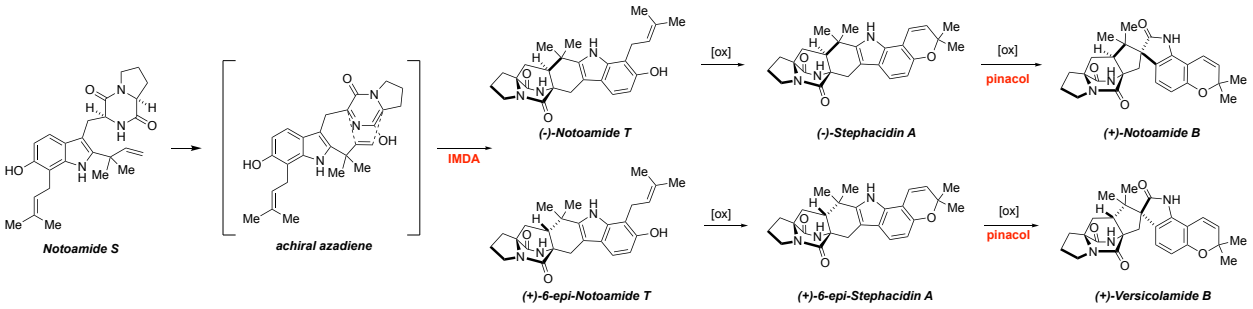

Figure 1.9. Biogenesis of (+)-Notoamide B and (+)-Versicolamide B through Stephacidin A and 6-*epi*-Stephacidin A.

IV. Genome Sequencing

The genomes of ten fungi known to produce the Stephacidins and Notoamides were sequenced to gain insight into the complex enantio- and diastereoselectivity found in the biogenesis of these compounds. Relevant biosynthetic gene clusters have been identified in these genomes, the first being *ftmA*, a NRPS (non-ribosomal peptide synthetase) gene from *Aspergillus*

fumigatus mined in 2006 by Turner *et al*.[43] This gene was heterologously expressed and produced Brevianamide F. As Brevianamide F plays a critical role in the biogenesis of a broad range of prenylated indoles, it was assumed that the *ftmA* gene (or a homolog) would be found in *A. protuberus*, participating in the early steps of its biosynthetic pathways. Rouche 454LX technology was used in tandem with *ftmA* to search for homologous genes in *A. protuberus*, which lead to the discovery of *notE*, an analogous NRPS module sharing 47% nucleotide identity with *ftmA*.[19] This and the other identified gene clusters for producing the Notoamides can be seen in **Figure 1.10**.

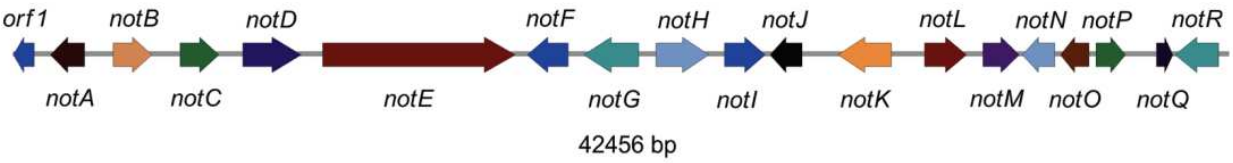

Figure 1.10. The Notoamide biosynthetic gene cluster derived from complete sequencing and bioinformatic mining of *A. protuberus* genome.[19]

With this new information about *A. protuberus*, new conclusions could be drawn about the genetic similarities between these fungi that produce opposite enantiomers of Stephacidin A and Notoamide B. The gene clusters, and by extension, the organisms, are orthologous based on the structure and directionality of the open-reading frames of the genes within the gene clusters.

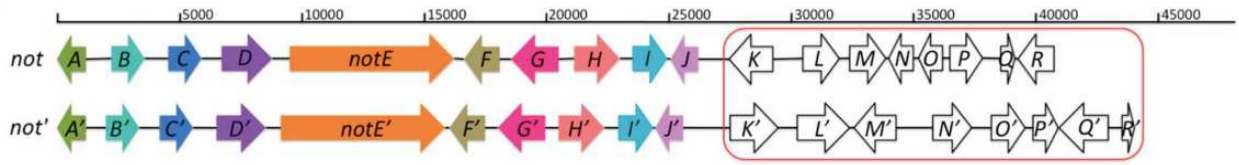

Figure 1.11. (+)-Notoamide gene cluster in *A. amoenus* and (-)-Notoamide cluster in *A. protuberus* have 70.8% nucleotide identity overall.[44]

As seen in **Table 1.1**, orthologous gene clusters have been identified with their respective functions, with some gene clusters showing up to 95% amino acid homology (NotC). For each protein, those marked with the prime indication are from *A. amoenus*, while those without are found in *A. protuberus*. Overall, the gene clusters display almost 71% nucleotide identity (**Figure 1.11**). Some of these enzymes have been cloned and functionally expressed, such as NotC, NotD, NotD', NotF, NotG, NotI, and NotI'.[19] NotH/NotH' is a membrane-bound cytochrome P450 that has so far resisted expression in a heterologous host. As this protein is suspected to cause the key enantiodivergence in the biosynthetic pathway, considerable efforts are being made to functionally express this vital protein.

Table 1.1. Comparison of the Notoamide gene clusters in *A. protuberus* and *A. amoenus*. AA ID/Sim: homology with respect to amino acid identity/similarity.[3]

Protein	Function	Protein	Function	AA ID/Sim
Orf1	Polysaccharide synthase	**Orf1'**	Polysaccharide synthase	Unknown
NotA	Negative regulator	**NotA'**	Negative regulator	70%/77%
NotB	FAD binding domain protein	**NotB'**	FAD binding domain protein	88%/94%
NotC	Prenyl-transferase	**NotC'**	Prenyl-transferase	87%/95%
NotD	Oxidoreductase	**NotD'**	Oxidoreductase	80%/86%
NotE	NRPS	**NotE'**	NRPS	79%/86%
NotF	Prenyl-transferase	**NotF'**	Prenyl-transferase	79%/85%
NotG	P450	**NotG'**	P450	87%/92%
NotH	P450	**NotH'**	P450	84%/92%
NotI	FAD binding domain protein	**NotI'**	FAD binding domain protein	85%/90%
NotJ	Unknown	**NotJ'**	Unknown	80%/84%
NotK	Efflux pump	**NotK'**	Nucleoside transporter	14%/28%
NotL	Transcriptional activator	**NotL'**	Transcriptional factor	15%/22%
NotM	Unknown	**NotM'**	Unknown	-
NotN	Dehydrogenase	**NotN'**	Unknown	-
NotO	Short-chain dehydrogenase	**NotO'**	Unknown	-
NotP	Unknown	**NotP'**	Unknown	-
NotQ	Unknown	**NotQ'**	Transcriptional factor	12%/21% (NotL)
NotR	Transcriptional co-activator	**NotR'**	Unknown	-

The remarkable similarity between these gene clusters highlights the strong resemblance between the different *Aspergillus* species. These gene clusters shed some light about the parallel biosynthetic pathways resulting in separate enantiomers, but there is yet more to uncover. Functional expression of NotH/NotH' will potentially tell us a great deal about the divergence between these two species.

V. Biosynthetic Pathway of the Dioxopiperazines

The dioxopiperazine biosynthesis starts with L-proline and L-tryptophan coupling by nonribosomal peptide-synthetase (NRPS) NotE/NotE', affording Brevianamide F (**Figure 1.12**).[45] This is followed with reverse prenylation at C-2 by NotF, then oxidation of C-6 by NotG, a cytochrome P450 oxidase. This gives 6-hydroxydeoxybrevianamide E which is then prenylated at C-7 to yield Notoamide S.[19]

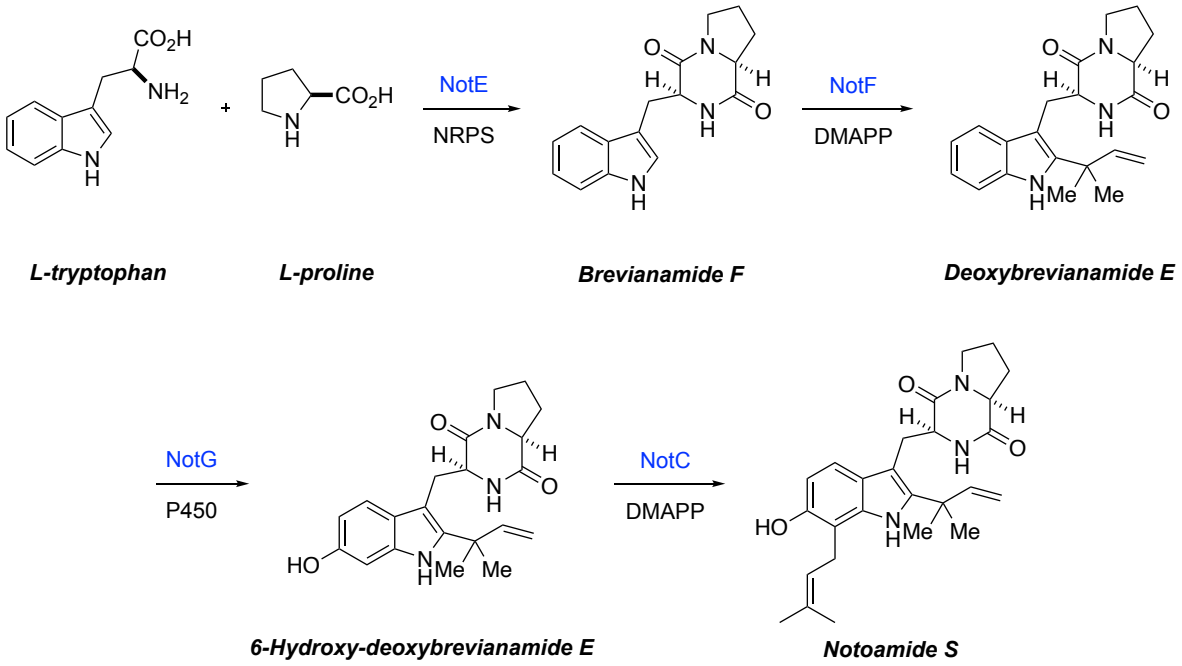

Figure 1.12. The first stage of the dioxopiperazine biosynthesis. Notoamide S is the substrate for the IMDA reaction.

The key enantiodivergent IMDA step in the biosynthetic pathway is most likely mediated by NotH/NotH'.[46] While this protein is membrane-bound and resistant to heterologous expression, all current evidence supports this theory: each version of NotH would oxidize Notoamide S (net 2 electrons) to the achiral azadiene intermediate and direct the subsequent IMDA reaction to form (+)-Notoamide T, (-)-Notoamide T, or (+)-6-*epi*-Notoamide T.

In *A. protuberus*, NotH presumably mediates this reaction to form (+)-Notoamide T as the highly major product, while (+)-6-epi-Notoamide T is formed as a minor metabolite. In *A. amoenus*, it seems NotH' forms (-)-Notoamide T in high majority, and again (+)-6-epi-Notoamide T appears as a minor metabolite. So, in both species, the *syn* diastereomer is predominant.[3] Meanwhile, in *A. taichungensis*, the *anti*-diastereomer, (+)-6-epi-Notoamide T, is likely formed in great majority.[47,48]

Neither enantiomer of 6-*epi*-Notoamide T nor Notoamide T have been isolated directly from these species. However, ^{13}C labeling studies have demonstrated conversion of (±)-[$^{13}C_2$]-Notoamide T to (+)-[$^{13}C_2$]-Stephacidin A and (+)-Notoamide B in *A. amoenus* (**Figure 1.13**).[49] This could be the result of a promiscuous oxidase (NotD') that accepts either enantiomer of Notoamide T to construct the pyran moiety of Stephacidin A, rather than only the natural (+)-enantiomer. This would then result in the natural (-)-Stephacidin A to be further transformed into (+)-Notoamide B through the NotI' monooxygenase.[49]

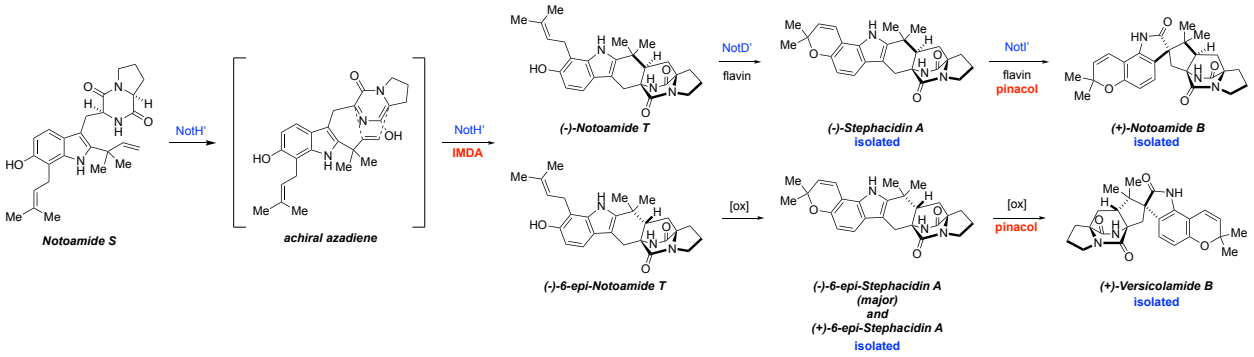

Figure 1.13. It is theorized that NotH' oxidizes Notoamide S into the achiral azadiene, which then undergoes the IMDA transformation; the third Diels-Alder strategy taking place in *A. amoenus*.

When (±)-[$^{13}C_2$]-Notoamide T was incorporated into *A. protuberus*, both (±)-[$^{13}C_2$]-Stephacidin A and (±)-[$^{13}C_2$]-Notoamide B were produced. However, only (+)-Stephacidin A and (-)-Notoamide B have found to be naturally produced in *A. protuberus*.[49] It is presumed that in *A. protuberus*, NotD and NotI are homologous to NotD' and NotI'. NotD catalyzes the oxidation of the prenyl group to the pyran ring, and NotI oxidizes (+)-Stephacidin A which results in pinacol rearrangement to form (-)-Notoamide B (**Figure 1.14**).[46,49]

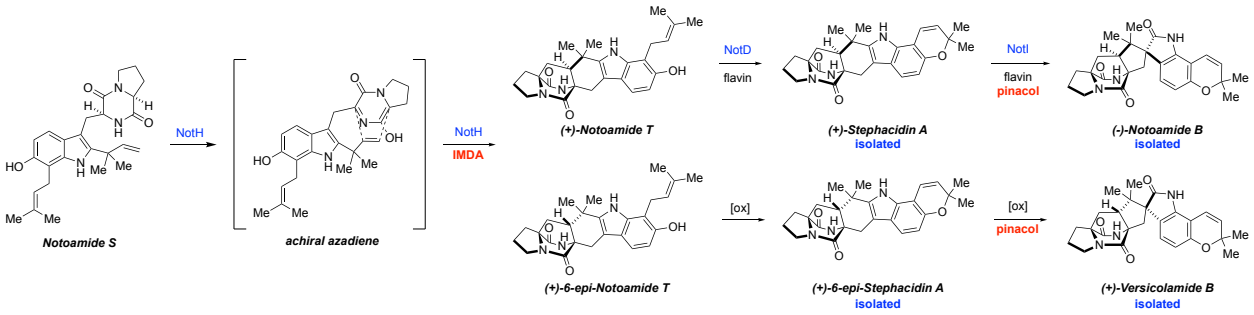

Figure 1.14. It is theorized that NotH oxidizes Notoamide S into the achiral azadiene, which then undergoes the IMDA transformation; the third Diels-Alder strategy taking place in *A. protuberus*.

Of course, 6-*epi*-Notoamide T must be considered in each of these species as well. (+)-Versicolamide B has been found in both *A. amoenus* and *A. protuberus* while (-)-Versicolamide B has only been found in *A. protuberus*.[35,50] (+)-6-*epi*-Stephacidin A is assumed to be the precursor to (+)-Versicolamide B and has been found in *A. protuberus*. However, in *A. amoenus*, both enantiomers of 6-*epi*-Stephacidin A have been detected, with the (-)-isomer being predominant in a 2.4:1 ratio.[20] Only the (+)-enantiomer was converted into (+)-Versicolamide B, which suggests that the oxidase found in *A. amoenus* (NotI') is highly enantio-specific; it does not seem to accept the (-)-enantiomer of 6-*epi*-Stephacidin A.[46] The reasoning for the lack of enantio-purity for 6-*epi*-Stephacidin A in this species is unique to these alkaloids and requires further investigation. Studies of 6-*epi*-Notoamide T in *A. protuberus* are outlined in Chapter 3.

VI. History and Isolation of the Stephacidins and Notoamides

After the isolation of the Brevianamides[45,51,52] and paraherquamides[10,53–56], the late 1990s and 2000s brought the discovery of a new family of indole alkaloids: the Stephacidins and Notoamides. The first compound discovered from this family was Sclerotiamide in 1996 from *Aspergillus scierotiorum* (**Figure 1.15**).[57] It was originally classified as part of the paraherquamide family since it had the bicyclo[2.2.2]diazaoctane core, spiro-oxindole, pyran ring, and unsubstituted proline moiety. Sclerotiamide was thought to be a biosynthetic precursor to some of the paraherquamides. The presence of the unreduced diketopiperazine unit made it different from the paraherquamides, however, and after the discovery of more alkaloids in the family, it was reclassified.

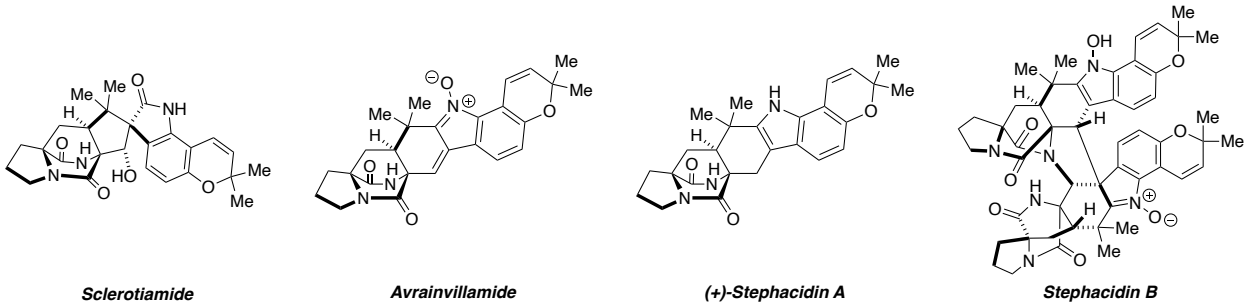

Figure 1.15. First isolated products of the Stephacidin and Notoamide families.

In 1999, structurally related alkaloids (+)-Stephacidin A, Avrainvillamide, and Stephacidin B were isolated from terrestrial fungus *Aspergillus ochraceus* (**Figure 1.15**).[58] Avrainvillamide was initially isolated from marine fungus *Aspergillus* sp. CNC358 by the Fenical group but was also isolated 2 years later from *Aspergillus ochraceus*.[59] These were found to be related because of their bicyclic core and unreduced diketopiperazine moiety. Biochemically, it was thought that (+)-Stephacidin A would be oxidized to Avrainvillamide, giving the imine oxide, which would then dimerize to give Stephacidin B (**Figure 1.16**).[58] In attempt to confirm this suspicion, Myers *et al*. was the first to synthesize Avrainvillamide, which readily dimerized to Stephacidin B under mildly basic conditions.[60] Further, both Williams and Baran independently synthesized Stephacidin A which was biomimetically converted to Stephacidin B.[61,62]

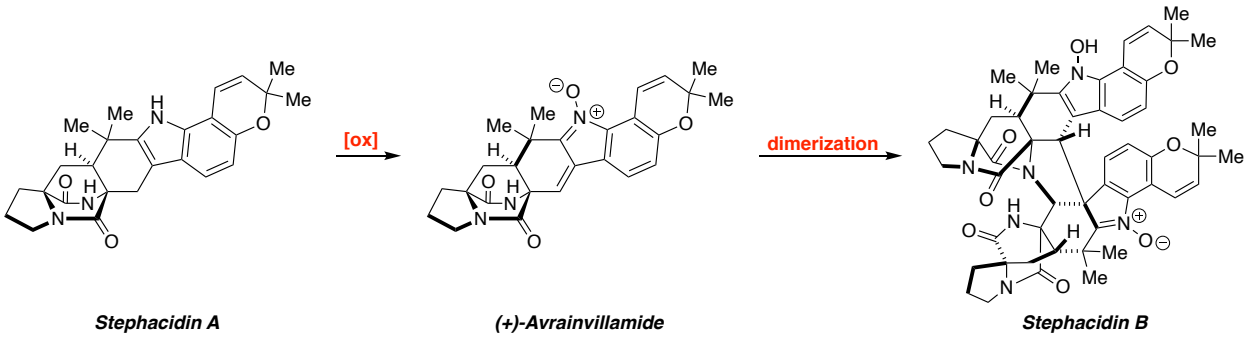

Figure 1.16. Initially proposed biosynthetic pathway to Stephacidin B.

Tsukamoto then isolated Notoamides A-D in 2007 from the fungus *Aspergillus protuberus*, found growing on the mussel *Mytilus edulis* (**Figure 1.17**). This mussel was found off the Noto Peninsula in the Sea of Japan. In addition to the new alkaloids, known compounds Sclerotiamide, (+)-Stephacidin A, and Deoxybrevianamide E were also isolated from the fungus (**Figure 1.17**). Notoamides A-D were structurally similar to the known Stephacidins, also containing the bicyclo[2.2.2]diazaoctane core, unreduced diketopiperazine, and pyranoindole system.[36]

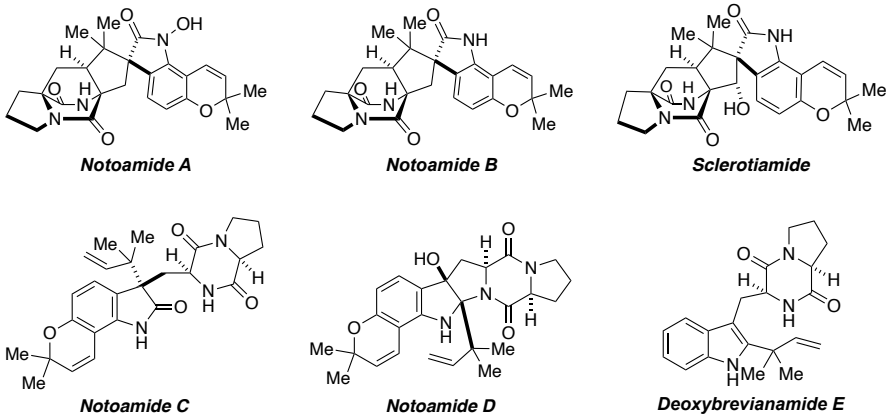

Figure 1.17. Metabolites isolated from *Aspergillus protuberus*.

The Norgeamides were isolated from a cold-water *Aspergillus protuberus* in 2005 by the Hans-Knöll institute (**Figure 1.18**). Norgeamides A, B, and D were closely related to Notoamides C and D and thought to be potential metabolites on the biosynthetic pathway to the more complex metabolites Stephacidin A, Notoamide A, and Notoamide B. Continuing isolation of Notoamides from *Aspergillus protuberus* has occurred, and Notoamides E-R as well as T3-12 are now known natural products (see Chapter 4).[20,37,50,63,64] Notoamides S and T are potential biosynthetic intermediates, where Notoamide S has been isolated from *Aspergillus amoenus*[20] but Notoamide T has yet to be isolated; this will be further discussed in Chapter 2.

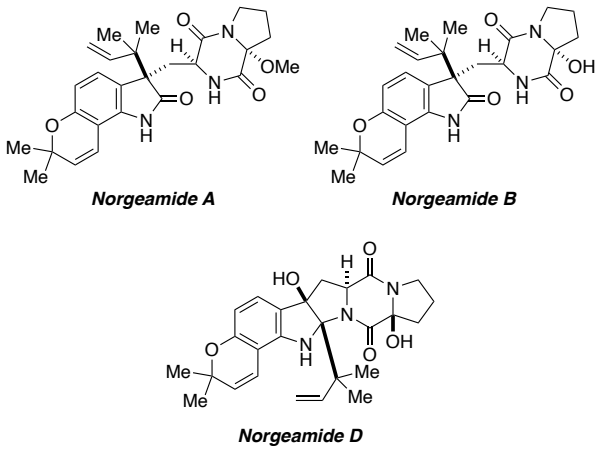

Figure 1.18. Norgeamides isolated from *A. protuberus*.

In terrestrial fungus *Aspergillus amoenus*, new metabolite Versicolamide B was isolated along with known alkaloids Stephacidins A and B.[35] Versicolamide B is unique in that it is the first compound found outside of the Brevianamide family to have the *anti*-configuration. After its discovery from *Aspergillus amoenus*, it was also found to be produced by *Aspergillus protuberus*, where both enantiomers were isolated.[50,65] More in-depth analysis of the compounds produced by each of these *Aspergillus* species revealed that *Aspergillus protuberus* produces (+)-Stephacidin A, (-)-Notoamide B, (-)-Versicolamide B, and (+)-Versicolamide B whereas *Aspergillus amoenus* produces (-)-Stephacidin A, (+)-Notoamide B, and (+)-Versicolamide B (**Figure 1.7**). The enantiomeric divergence between these two species is unprecedented.

In addition to the unique biosynthesis and enantiodivergence of these families, some of the compounds have displayed various bioactivities that could be useful as pharmaceuticals. Of the Stephacidin family, Sclerotiamide, Avrainvillamide, Stephacidin A, and Stephacidin B have exhibited the greatest bioactivity as insecticidal[57], anti-bacterial[59], and anti-tumor agents[58]. The Notoamides display RANKL-induced osteoclast inhibition (see Chapter 2, section I).[66]

Sclerotiamide demonstrates potent activity against first instar larvae of the corn earworm *Helicoverpa zea*. When Sclerotiamide is fed in a 200 ppm standard test diet, *H. zea* had a 46% mortality rate, as well as a 98% reduction in growth rate in survivors, relative to controls. Sclerotiamide was also found to be effective against the beetle *Carpophilus hemipterus*, both larvae and adults, when fed at a 100 ppm dietary level. This resulted in a 44% and 40% reduction in feeding rates among the larvae and adults, respectively.[57]

Avrainvillamide has been shown to be an effective antibiotic that inhibits growth of *Staphylococcus aureus, Staphylococcus pyogenes,* and *Enterococcus faecalis*, all of which are multi-drug resistant organisms (MDRO). The minimum inhibitory concentration (MIC) for these are 12.5, 12.5, and 25 μg/mL, respectively. Avrainvillamide has also shown antitumor activity against various cell lines including human colon HCT116 cells, melanoma MALME-3M cells, and breast cancer cells βT-549 and T-47D.[59]

Stephacidins A and B also display cytotoxicity to a variety of tumor cell lines. Stephacidin B has proven to be far more potent, especially against testosterone-dependent LNCaP cells.[58]

This expansive family of compounds has great potential for its biological activity in addition to its curious biosynthetic pathway. As a result, substantial effort has been made to synthesize many of these natural products. Previous syntheses relative to the current work of this dissertation are outlined in the next section.

VII. Previous Syntheses

i. Synthesis of Notoamide J

Notoamide J was isolated by the Tsukamoto group off the coast of the Noto Peninsula in the Sea of Japan.[63] Initially thought to be a precursor to significant spiro-oxindoles in the Stephacidin and Notoamide families, Notoamide J was synthesized to test its identity as an advanced intermediate for such compounds. As it does not contain the bicyclo[2.2.2]diazaoctane core, Notoamide J was a possible late-stage intermediate to the spiro-oxindole compounds that had undergone the suspected IMDA to form the bicyclic core. It should also be noted that Notoamide J does not contain the pyranoindole complex found in the Stephacidins and some Notoamides but does have a hydroxy substituent at the 6-position on the indole, giving it the possibility of forming one. These moieties present in Notoamide J provided provocative hints that it could be the precursor to Notoamide B and/or Versicolamide B.

To further investigate this hypothesis, the Williams group set out to synthesize Notoamide J in a way that would allow for incorporation of isotopic elements.[67] It was thought that Notoamide J could be procured from oxidation and pinacol rearrangement of **12**, which could be made after coupling **13** to L-proline. Hydroxyindole **14** could arise from **15** by following the Leimgruber-Batcho protocol (**Figure 1.19**).

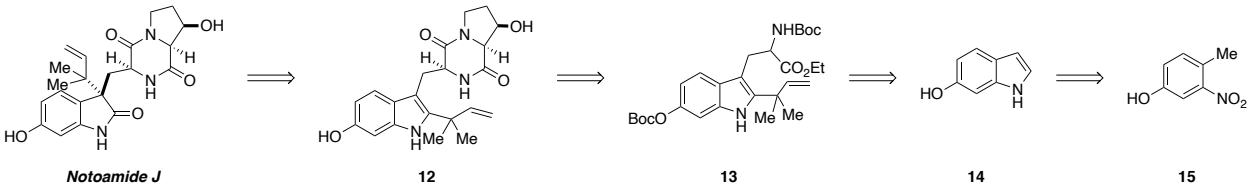

Figure 1.19. Planned retrosynthesis for synthesis of Notoamide J.

Following a modified Leimgruber-Batcho protocol, commercially available nitrophenol **15** was first benzylated to **16** (**Figure 1.20**). Condensation with dimethylformamide dimethylacetal and pyrrolidine provided enamine **17**, both in high yields. Reduction of the nitro group, resulting cyclization, and benzylic deprotection using Pd/C and hydrogen gas afforded hydroxyindole **14**. Boc protection of the indole and subsequent chlorination of the C-3 position resulted in chlorinated indole **19** which was then reverse-prenylated at the C-2 position using the procedure established by Danishefsky and coworkers.[68] This method was done by exposure to prenyl-9BBN and triethylamine and resulted in **21** in a 48% yield.[67]

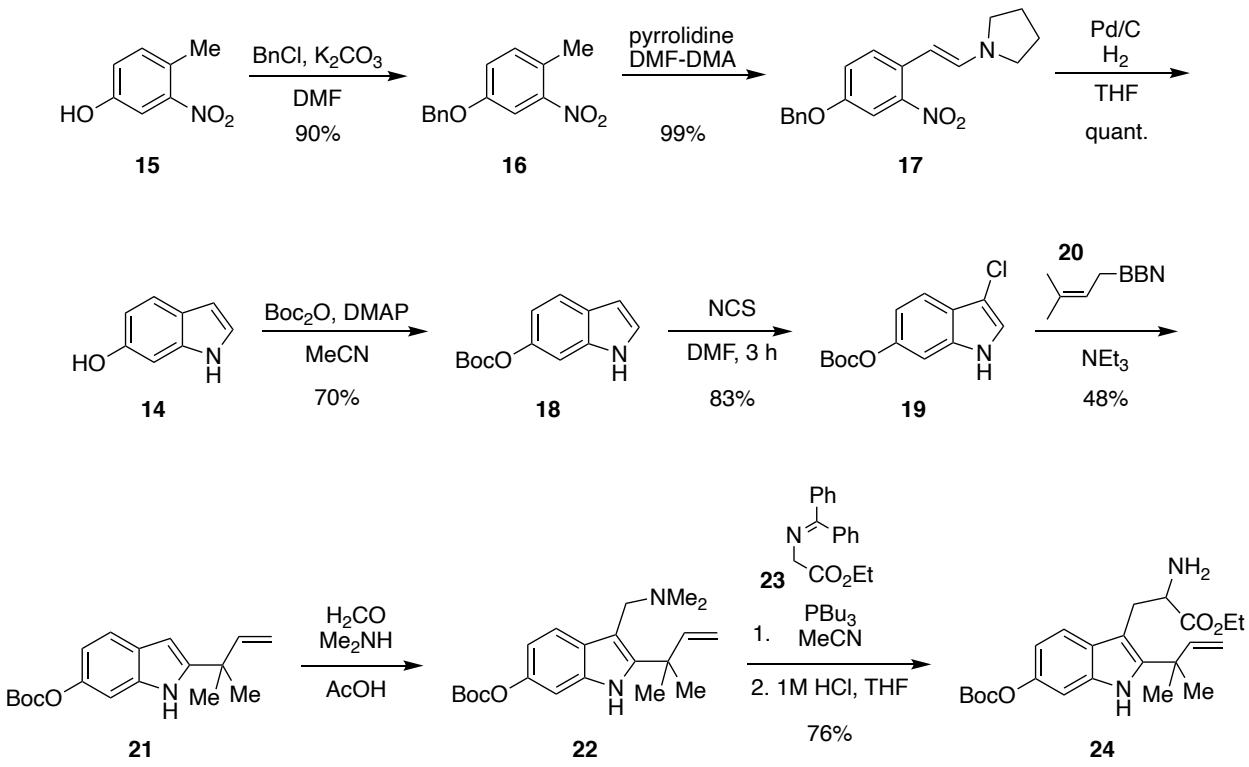

Figure 1.20. Leimgruber-Batcho protocol and continuation to tryptophan derivative.

Gramine **22** was formed from this product via Mannich reaction in an 84% yield; it was then coupled with the benzophenone imine derivative of glycine using a modified Somei-Kametani coupling. The crude imine was carried forward for hydrolysis, resulting in tryptophan

24 in a 76% yield. The free amine was then Boc protected in a near quantitative yield and coupled with L-proline ethyl ester with HATU to give amide **26** (**Figure 1.21**). Treatment with TFA removed the Boc groups, affording the free amine. The resulting dipeptide was cyclized in the presence of 2-hydroxypyridine to provide both *cis* and *trans* diketopiperazines in a 1:1 ratio and 53% yield (over 2 steps), which were separable by column chromatography. The *cis* diastereomer was carried forward and the synthesis was completed by use of Davis Oxaziridine to perform the oxidation and subsequent pinacol rearrangement, giving Notoamide J and 3-*epi*-Notoamide J in a 2:1 ratio and 47% total yield.[67]

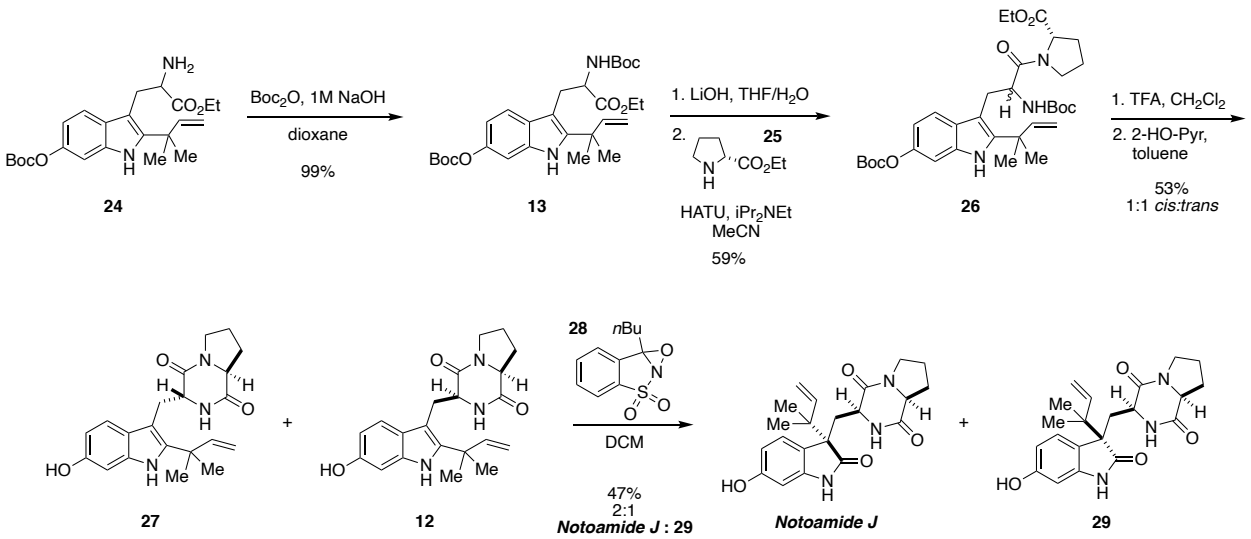

Figure 1.21. Assembly of Notoamide J.

This synthesis is used as the basis to many natural products that contain both the bicyclo[2.2.2]diazaoctane core and the 6-hydroxy indole moiety. Some steps are modified, but this synthesis has been very influential to many others discussed in later sections.

ii. Synthesis of Notoamide S

McAfoos *et al*. completed the first synthesis of Notoamide S in 2010. [40] It was proposed that Notoamide S could be made by coupling Fmoc-protected proline **31** with the prenylated

hydroxytryptophan derivative **30** (**Figure 1.22**). It was thought this tryptophan derivative could be made from known prenylated indole **32**.

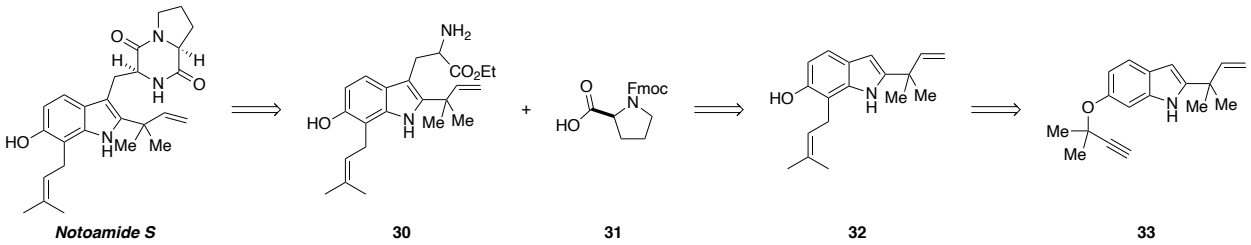

Figure 1.22. Planned retrosynthesis for synthesis of Notoamide S.

As seen in **Figure 1.23**, treatment of propargyl ether **33** with Lindlar's catalyst in a hydrogen atmosphere resulted in partial reduction of the alkyne and the resulting alkene was heated in a microwave to trigger the Claisen rearrangement, giving prenylated indole **32**. This Claisen product was treated with formaldehyde and dimethylamine to give gramine **34** in a low 20% yield.[40]

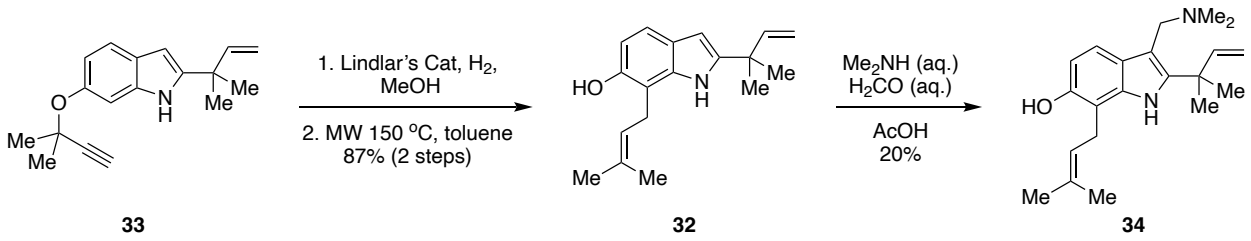

Figure 1.23 Formation of gramine **36** from the propargyl ether **34**.

In attempt to improve the poor yield of this step, the initial order of the synthesis was reversed and alkyne **33** was transformed to gramine **34** using the same conditions, this time having a high yield of 95% (**Figure 1.24**). Again, Lindlar's catalyst and microwave conditions were used to perform the Claisen rearrangement and **34** was accomplished in a 75% overall yield. However, when the gramine was converted to the tryptophan derivative using

benzophenone imine in a Somei-Kametani type coupling followed by hydrolysis, only a 10% yield was achieved. It was theorized that the acidity of the proton on the free phenol was interfering with the reaction. A new approach was then tested, using the propargyl group on **35** as a protecting group while the tryptophan derivative was formed.[40]

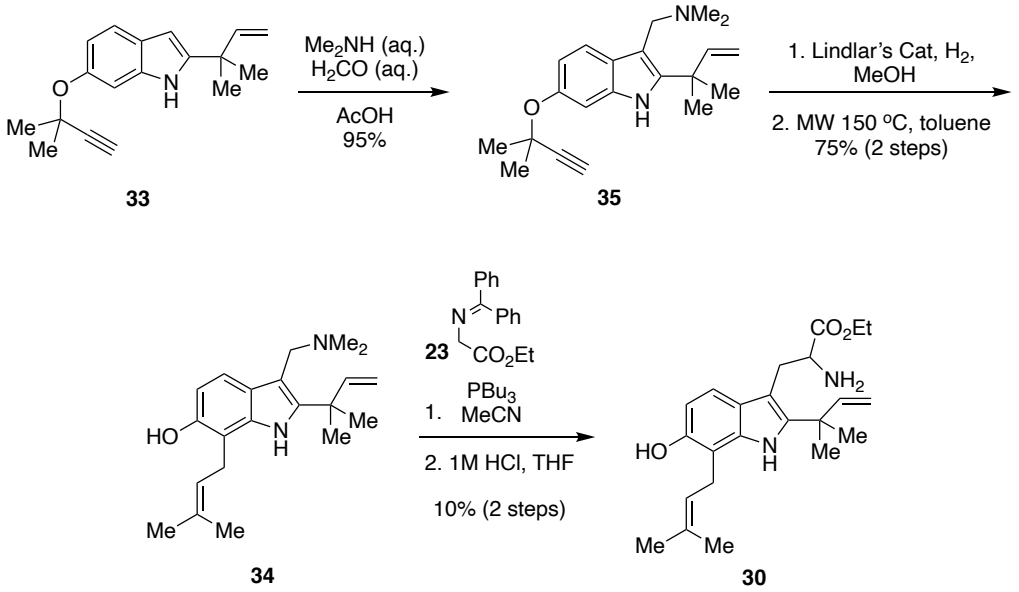

Figure 1.24. Synthesis of tryptophan derivative **30** from propargyl alcohol **33**.

As seen in **Figure 1.25** Somei-Kametani conditions were again used (on **35**) to create the desired tryptophan derivative and subsequent hydrolysis yielded the free amine in 80% over 2 steps. Tryptophan **36** was then coupled to Fmoc proline **31** in the presence of HATU and DIPEA with a successful 85% yield. However, deprotection of the Fmoc group and resulting cyclization to the diketopiperazine was accompanied by undesired pyran ring formation to give natural product Notoamide E and 6-*epi*-Notoamide E. The serendipitous formation of this natural product was 3 steps shorter than the previously reported synthesis.[40]

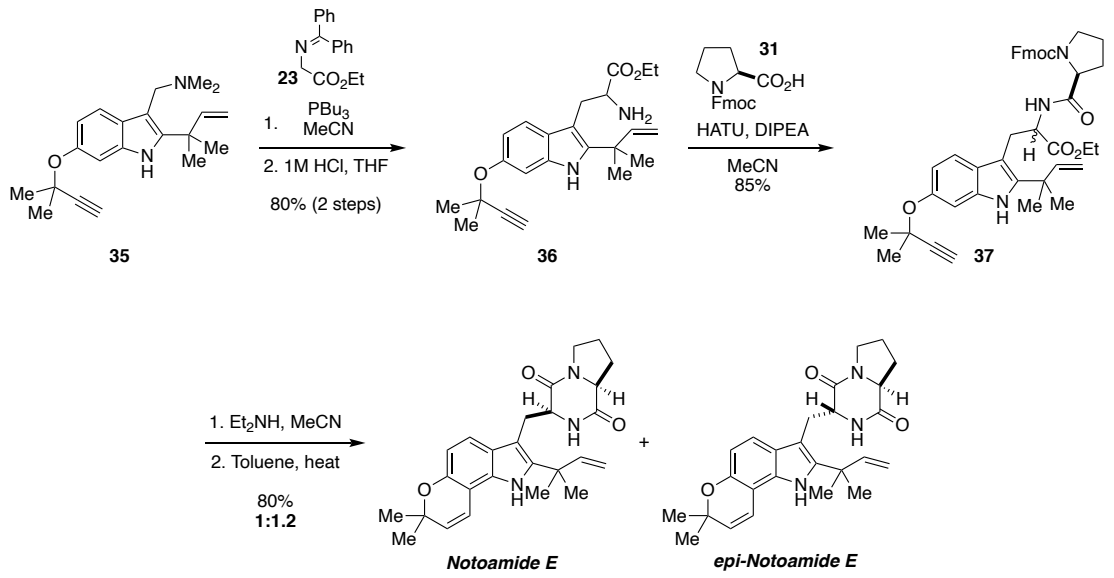

Figure 1.25. Final steps to synthesize Notoamide E and 6-*epi*-Notoamide E.

To remedy the pyran ring formation, Lindlar's catalyst was used to reduce the alkyne before cyclization (**Figure 1.26**). Exposure to diethylamine and heat resulted in cyclization and desired Notoamide S was formed in modest yield (18%). Unexpectedly, along with *epi*-Notoamide S, Notoamide E and *epi*-Notoamide E were also found in the reaction mixture. It was concluded that some pyran ring formation was occurring during the Somei-Kametani coupling and the inseparable by-products had been carried through the rest of the synthesis. The temperature for the reaction was lowered below reflux and Notoamide S was then obtained in a 29% yield. Side products *epi*-Notoamide S, Notoamide E, and *epi*-Notoamide E were obtained in 20, 8, and 5% yields, respectively. In this synthesis of Notoamide S, a 19% overall yield was achieved in seven steps from indole **33**.[40]

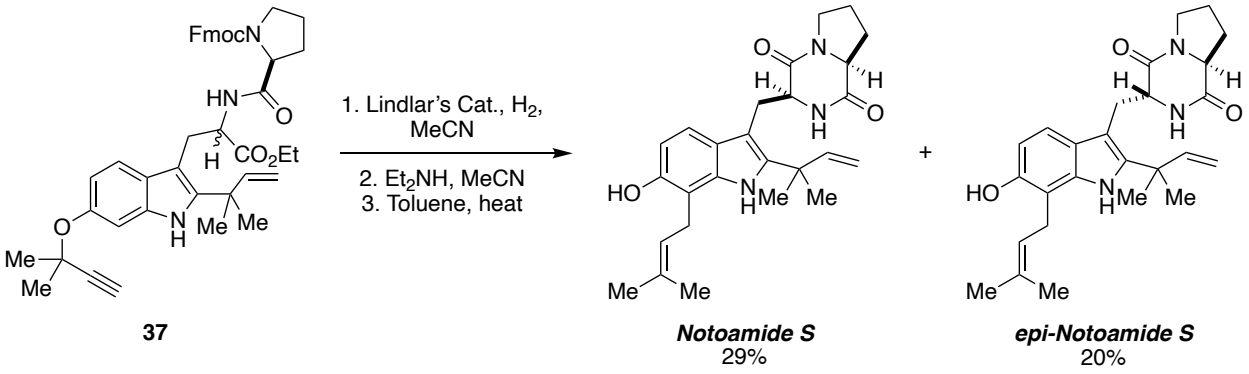

Figure 1.26. Final steps to form Notoamide S: reduction of alkyne, deprotection of Fmoc group, cyclization to form diketopiperazine ring, and Claisen rearrangement.

iii. Synthesis of Stephacidin A: Greshock 2007

Greshock's synthesis of Stephacidin A in 2007 is often referenced for the synthesis of pyranodiketopiperazine **41**.[62] The synthesis began with **38**, whose synthesis was completed by Grubbs *et al*. in 2005.[69] The compound was coupled with hydroxyproline derivative **39** with the aid of BOPCl and DIPEA, yielding **40** in a 54% yield (**Figure 1.27**). Next, morpholine was used for removal of the Fmoc group, which then resulted in cyclization to afford diketopiperazine **41** in 95% yield. The alcohol was removed with a Mitsunobu-type elimination and the lactim ether was formed with Me_3OBF_4 and Cs_sCO_3, giving **42** with a yield of 81%. Then, **42** was treated with 20% aqueous KOH and methanol to promote the tautomerization to achiral azadiene **43** and subsequent IMDA, giving **44** (25% yield) and **45** (61% yield) with a d.r. of 2.4:1, respectively. The achiral azadiene seemed to be metastable and could be observed both on TLC and in ^{1}H NMR (when treated with KOD in CD_3OD/D_2O). Unsurprisingly, the IMDA favored the *syn* diastereomer. [62]

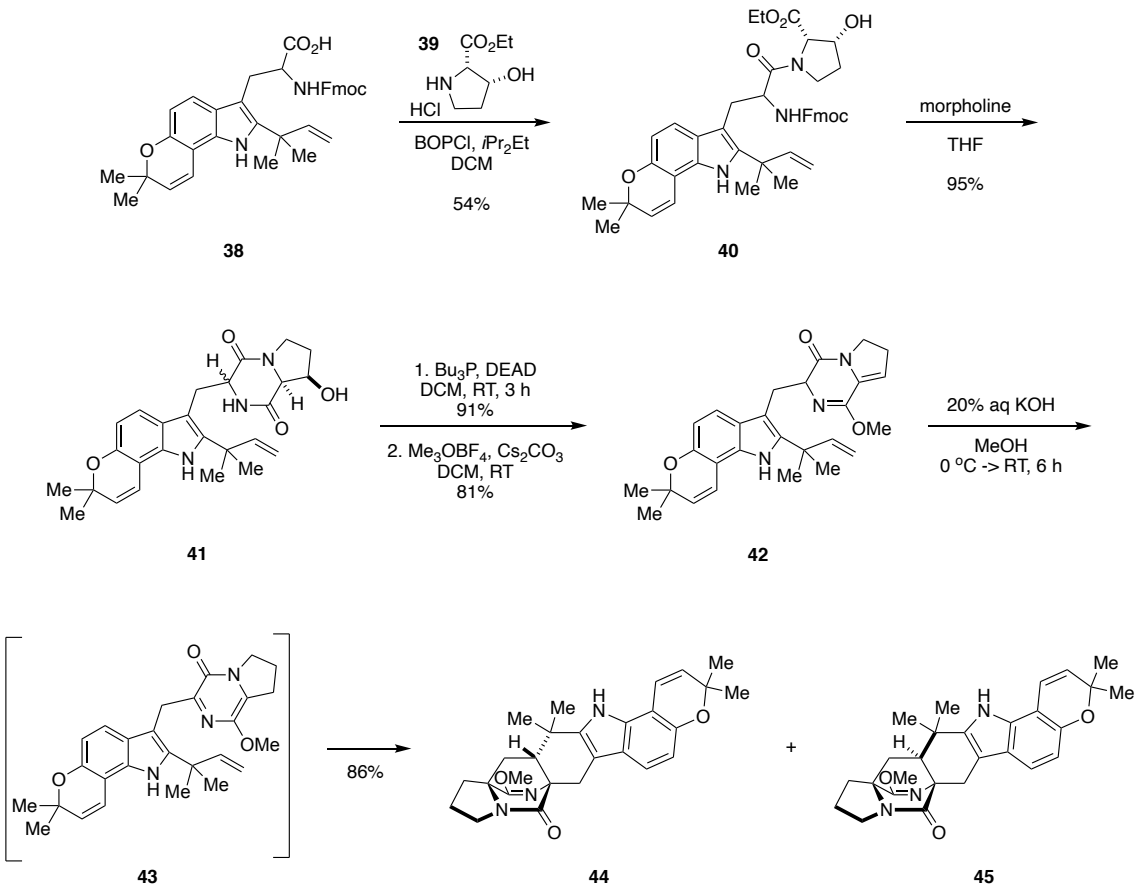

Figure 1.27. Synthesis of bicyclic lactim ethers **44** and **45**, starting from tryptophan derivative **38**.

The lactim ether was then cleaved with HCl, and the bicyclic ring reformed after treatment with sodium bicarbonate, giving Stephacidin A in 96% yield (**Figure 1.28**). Exposure to Davis Oxaziridine then resulted in a 73% yield of exclusively Notoamide B as a single diastereomer. This can be justified as the epoxidation occurred on the less-hindered alpha face, which after ring opening and [1,5]-sigmatropic shift, ended with Notoamide B as the sole product.[62]

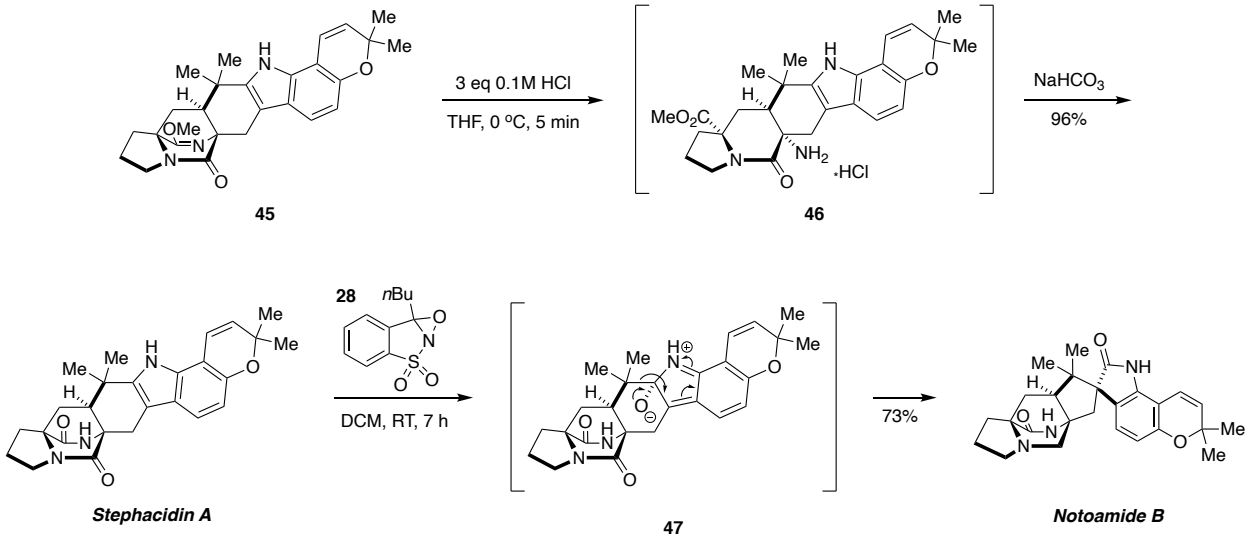

Figure 1.28. Synthesis of Stephacidin A and Notoamide B.

iv. Synthesis of Versicolamide B: Greshock 2008

Versicolamide B was isolated from *Aspergillus protuberus* by the Tsukamoto group. This natural product is found in the biosynthetic pathway of 6-*epi*-Notoamide T, after 6-*epi*-Stephacidin A. The synthesis of Versicolamide B sets precedent for formation of the spiro-oxindole moiety.

The first synthesis of Versicolamide B utilized diketopiperazine **41**, prepared in a synthesis of Stephacidin A done by Greshock *et al*. in 2007 (**Figure 1.27**).[62,69] This synthesis is similar to the one discussed in the previous section, with a slight rearrangement of steps. Starting with diketopiperazine **41**, the alcohol was eliminated using Mitsunobu-type conditions in good yield (**Figure 1.27**). The lactim ether was then formed using Me_3OBF_4 and Cs_2CO_3, giving **42**. Next, KOH and methanol were used to perform the intramolecular Diels-Alder, through intermediate achiral azadiene **43**, resulting in a 61% yield of the *syn* diastereomer and 25% of the *anti* (2.4:1 d.r.). Both compounds were separated and exposed to Davis Oxaziridine, causing the

pinacol-type rearrangement (**Figure 1.29**). After deprotection of the lactim ether, the *syn* compound formed Notoamide B while the *anti* formed Versicolamide B.[35]

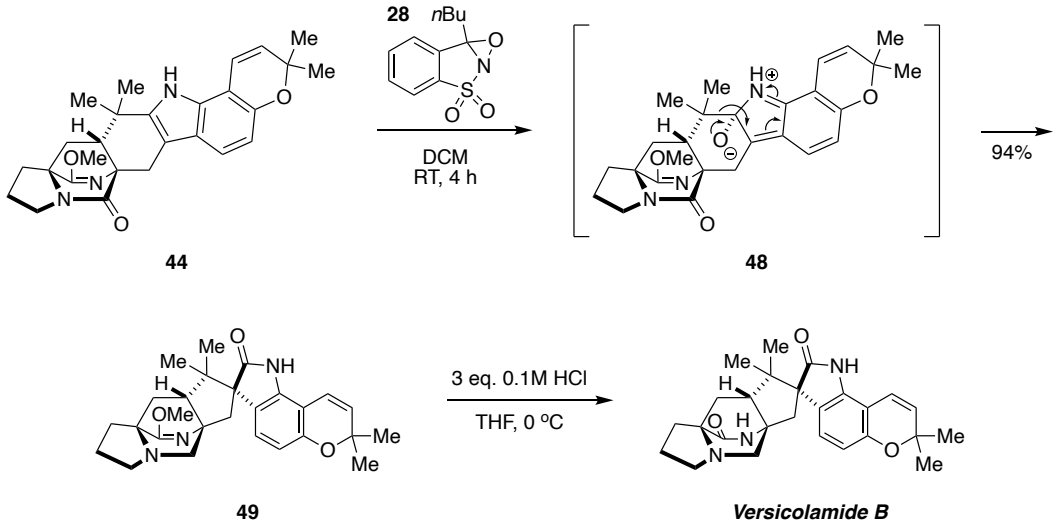

Figure 1.29. Synthesis of Versicolamide B.

v. Synthesis of Versicolamide B: Miller 2009

Miller *et al*.'s synthesis of Versicolamide B begins with prenylated tryptophan derivative **38** as made in by Grubbs *et al*. in 2005.[69] It was coupled with L-hydroxyproline **39** with HATU in 87% yield (**Figure 1.30**). Resulting compound **40** was then Fmoc-deprotected with exposure to diethylamine, which led to cyclization to form the diketopiperazine diastereomers. These diastereomers were separated before treatment with Davis Oxaziridine to epoxidate the C2-C3 position of the indole. This spurred a pinacol rearrangement to afford four spiro-oxindole diastereomers.[70]

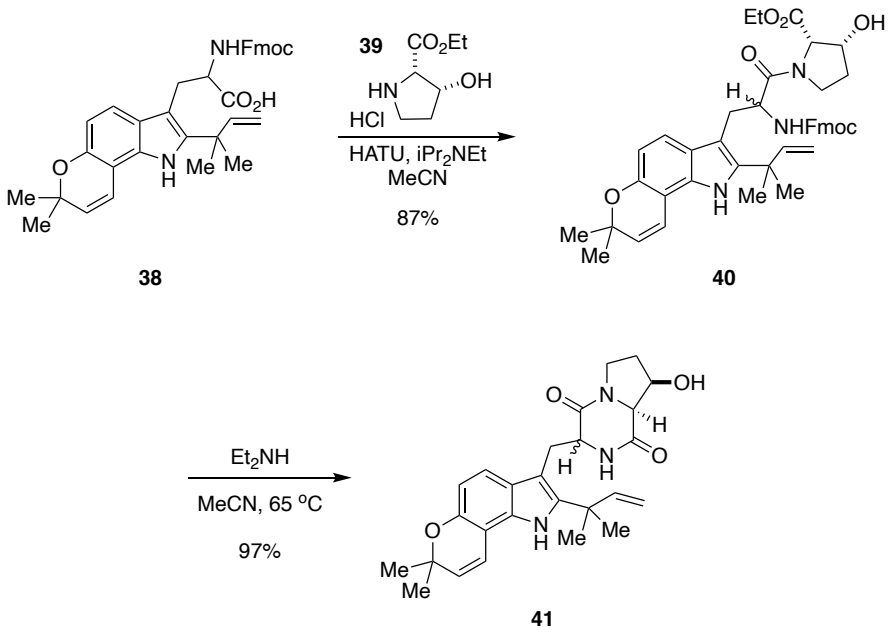

Figure 1.30. Synthesis of diketopiperazine from tryptophan derivative **38**.[70]

The *cis* diketopiperazine yielded the *S* and *R* diastereomers in an 80% yield, with a 3:1 diastereomeric ratio, respectively (**Figure 1.31**). The *trans* diketopiperazine also gave an 80% yield but with a 1:1 ratio of diastereomers. Each compound was separately treated with DEAD and PBu_3 to eliminate the alcohol in preparation for the azadiene tautomerization.[70]

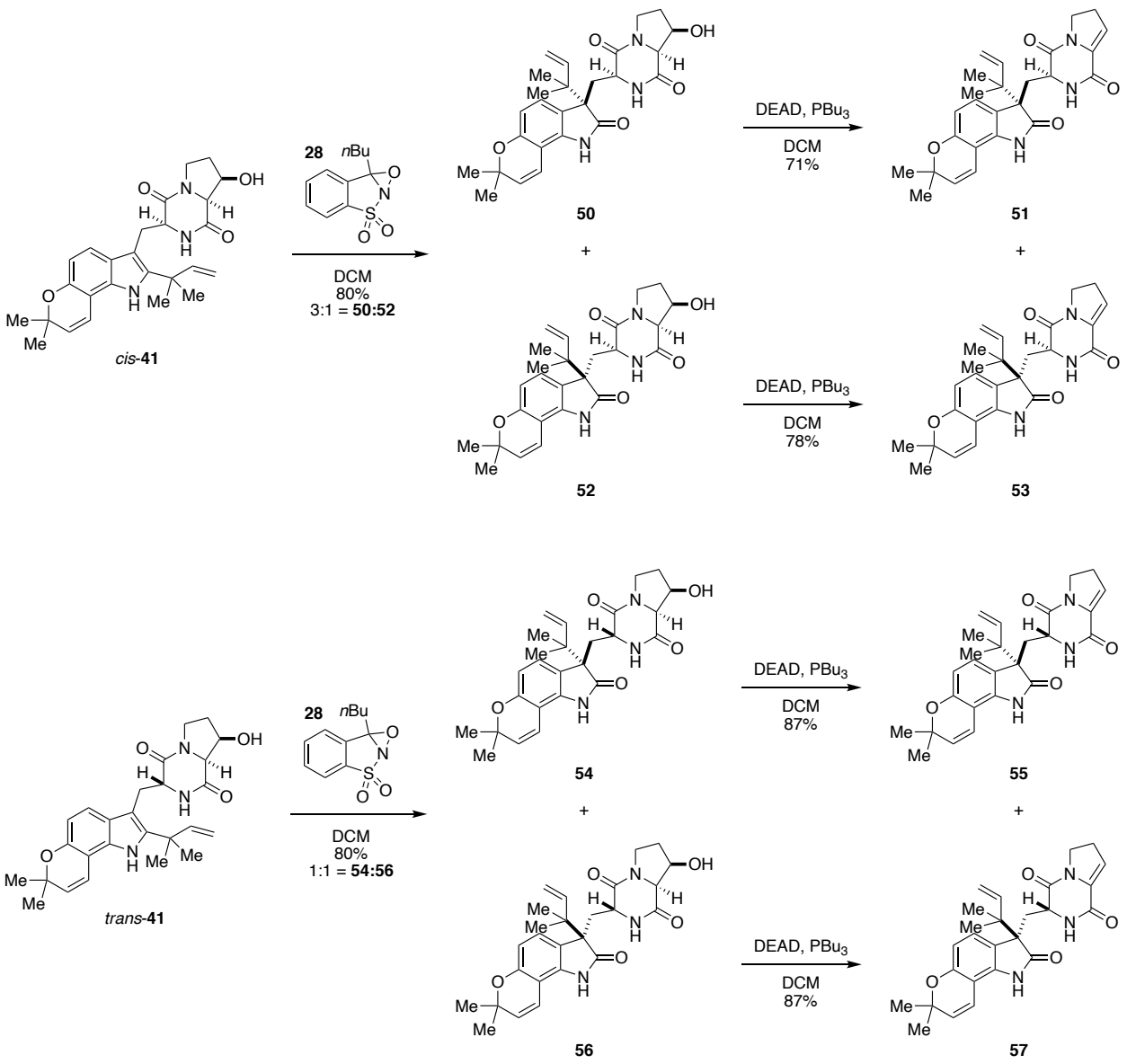

Figure 1.31. Formation of spiro-oxindoles from diketopiperazine diastereomers.[70]

As seen in **Figure 1.32**, the *S* and *R* diastereomers were combined, as stereochemistry at the diketopiperazine would be lost in the tautomerization. Each set was treated with 20% KOH in methanol to promote the tautomerization and the IMDA reaction proceeded spontaneously afterword.[70] Each set resulted in exclusively *anti* configurations at the bicyclic core, aligning with what was seen in theoretical calculations done by Domingo *et al*. in 2003 (**Figure 1.33**).[71]

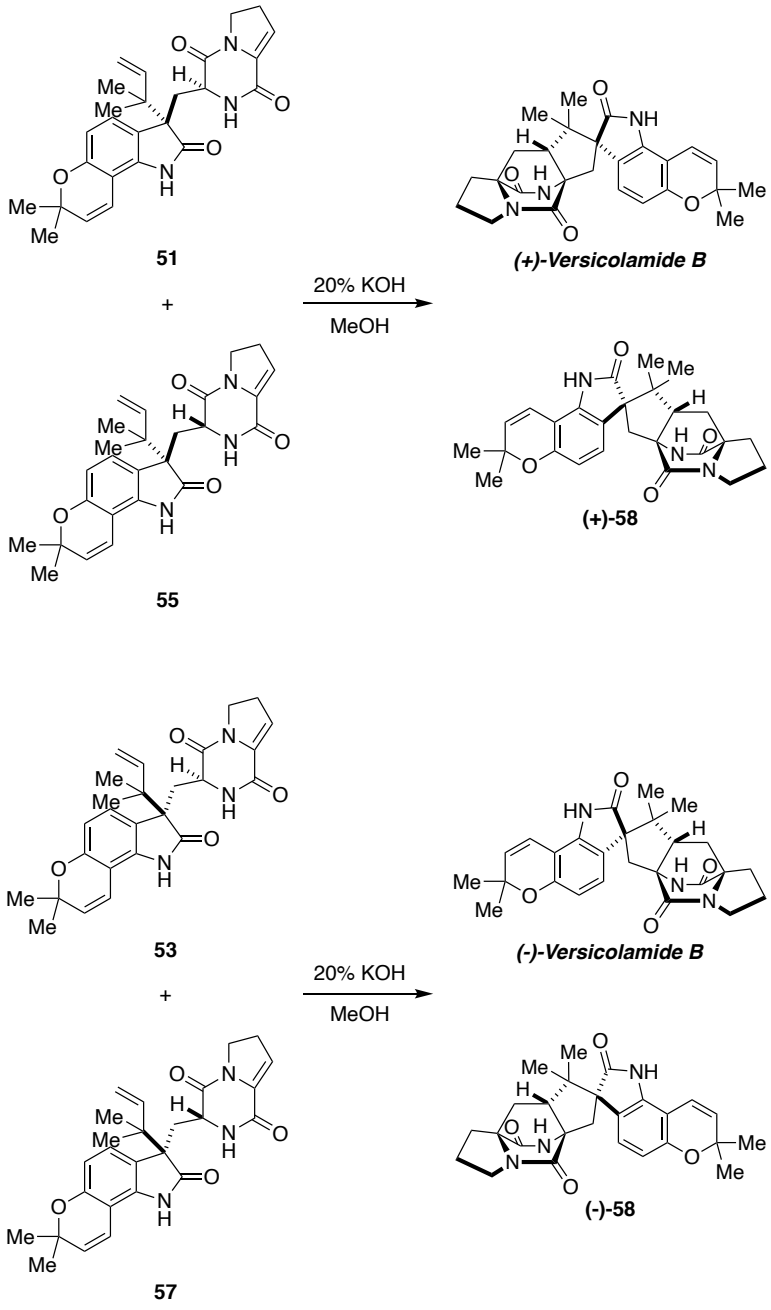

Figure 1.32. IMDA of spiro-oxindoles to make Versicolamide B enantiomers.[70]

Thus, each enantiomer of Versicolamide B was synthesized in this synthesis. The formation of exclusively *anti* cycloadducts in this synthesis is conflicting with the *syn* confirmation preference seen in the Diels-Alder reactions performed on indole-based

compounds. Knowledge that the *anti* bicyclic confirmation is preferred when the oxindole substrate is used can be very useful information in future syntheses.[70]

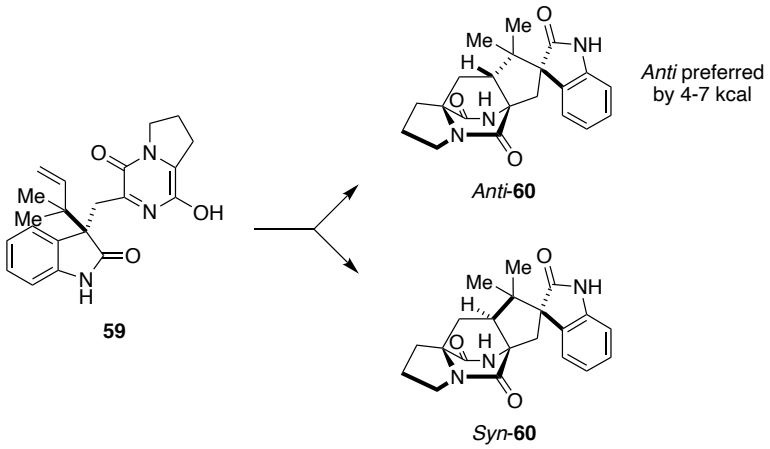

Figure 1.33. *Ab initio* calculations by Domingo and coworkers show a strong preference for *anti* transition state on model system **59**.[70,71]

Chapter 2: Total Synthesis of 6-*epi*-Notoamide T and Notoamide T2

I. Biological Activity

While the synthesis of 6-epi-Notoamide T is of great importance for elucidation of the biosyntheses of the *Aspergillus* compounds, it also shows strong inhibition of receptor activator of nuclear factor-κB ligand (RANKL)-induced osteoclastogenic differentiation in murine RAW264 cells.[66] Osteoporosis is connected to the deregulation of osteoclast function, so compounds that affect the production of osteoclasts are of great interest to treatment of this disease. RANKL inhibition limits osteoclast genesis and suppresses bone resorption, therefore decreasing bone loss.[13,72–75]

Since the dioxopiperazines, specifically the Notoamides, Stephacidins, and Versicolamide B, are found as opposite enantiomers in different species of *Aspergillus*, it's been questioned whether these compounds display enantiomer-specific biological activities. Notoamides A-D, Notoamide T, 6-*epi*-Notoamide T, Versicolamide B and C, Stephacidin A, and 6-*epi*-Stephacidin A were tested for inhibition of osteogenesis, detected by tartrate-resistant acid phosphatase (TRAP) assay.[66] With respect to Notoamide A, Notoamide B, and Stephacidin A, the (-)-enantiomer inhibited osteogenesis more than their (+)-enantiomer counterparts (**Figure 2.1**). Neither enantiomer of Notoamide T showed inhibition, but (+)-6-*epi*-Notoamide T demonstrated complete inhibition at the same concentration (10 μg/mL), while (-)-6-*epi*-Notoamide T showed complete inhibition at only 5 μg/mL. The racemic mixture was resolved and the (+)-enantiomer exhibited inhibition with IC_{50} values of 4.4 μM while the (-)-enantiomer displayed a value of 1.7 μM.[66]

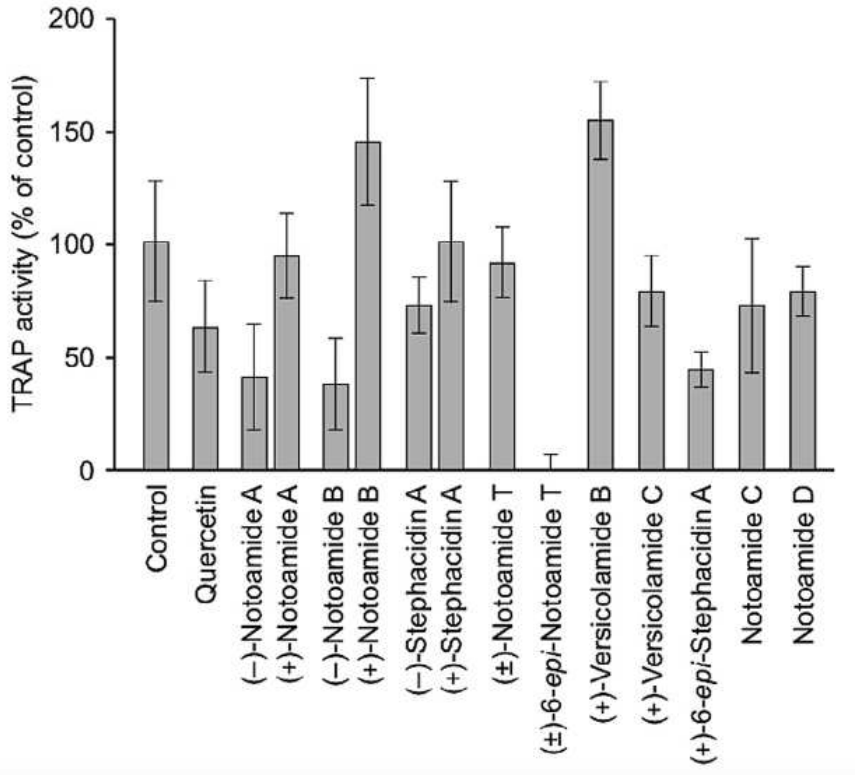

Figure 2.1. Inhibitory activities of compounds against RANKL-induced TRAP activity. RAW264 cells were treated with 250 ng/mL in the presence of 10 μg/mL of each compound. Quercetin was used as a positive control at 3.1 10 μg/mL.[66]

While the mechanism of action for this inhibition is still unclear, (-)-6-*epi*-Notoamide T shows clear bioactivity through RANKL inhibition that could be beneficial to the treatment of osteoporosis.

II. Improved Synthesis of 6-*epi*-Notoamide T

i. Following Previously Reported Synthesis

As discussed in Chapter 1, Notoamide T and 6-*epi*-Notoamide T are suspected intermediates in the *Aspergillus protuberus* and *amoenus* biosynthetic pathways. These compounds are thought to result from the intramolecular Diels-Alder, the key enantiodivergent

step for the dioxopiperazine families. Additionally, [^{13}C]$_2$-(±)-6-*epi*-Notoamide T was incorporated into *A. protuberus* which resulted in the discovery of eleven new metabolites (discussed further in Chapter 3).[65] These metabolites had not been isolated from the fungus before and all were isolated as racemic mixtures. Consequently, enantiomerically pure 6-*epi*-Notoamide T was needed to determine if an unnatural enantiomer triggered the new metabolite profile. To do so, it was first necessary to complete the synthesis of 6-*epi*-Notoamide T and obtain large quantities enantiomerically pure material.

Originally, the synthesis reported previously by Sunderhaus *et al.* for Notoamide T (and 6-*epi*-Notoamide T) was followed.[49] As per the literature precedent, a modified Leimgruber-Batcho synthesis was employed to make Boc-protected 6-hydroxyindole **14** (**Figure 2.2**). 4-Methyl-3-nitrophenol **15** was protected with a benzyl group and then alkylated with *N,N*-dimethylformamide dimethyl acetal and pyrrolidine to afford **17**. Reductive cyclization and benzylic deprotection then gave the 6-hydroxy indole **14**. This method was quite limited in scale; only 5 grams could be used in order to achieve a moderate yield. More than that and the yield decreased drastically. Unfortunately, it also produced an insoluble substance as a byproduct. When first pursuing the synthesis, the hydroxyindole was Boc-protected, giving **18**.

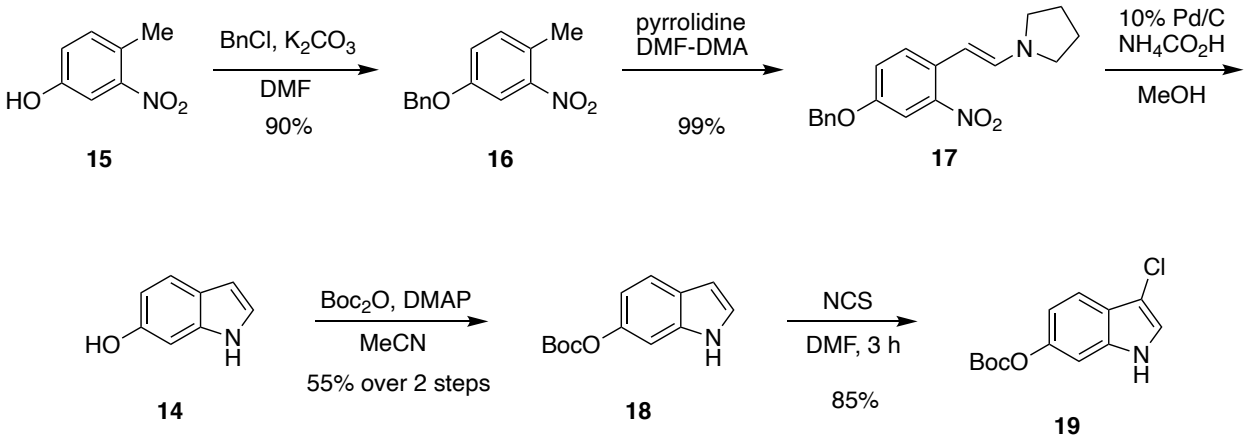

Figure 2.2. Synthesis of chloroindole **19**.

Next, the reverse-prenylation method established by Danishefsky *et al.* was used.[68] Indole **18** was chlorinated at the C-3 position with NCS to give **19** (**Figure 2.2**). Before the chloroindole could be reverse-prenylated, prenyl-9-BBN had to be synthesized. This is shown in **Figure 2.3** and described below.

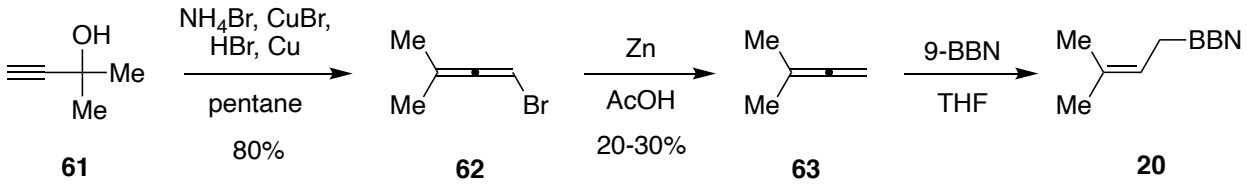

Figure 2.3. Synthesis of BBN complex used for prenylation of chlorinated indole **19**.

First, bromoallene **62** was formed following literature procedure.[76] Next, reduction of **62** with zinc in acetic acid gives the dimethyl allene complex **63**. This reaction has historically been low yielding and unreliable. The dimethyl allene product is extremely volatile with a boiling point of only 40-41 ^{o}C.

As seen in **Figure 2.4**, allene was then reacted with 9-BBN in THF *in situ*, producing **20**. This, combined with exposure to triethyl amine, gave the reverse-prenylated indole **21**. Gramine was then formed via Mannich reaction from **21** using dimethylamine and formaldehyde which was then coupled to the benzophenone imine of glycine **23** using a modification of the Somei-Kametani coupling procedure.[77,78] Hydrolysis of the resulting imine resulted in tryptophan derivative **24.** Coupling of **24** with Fmoc-protected hydroxy proline **65** gave dipeptide **66** with a 75% yield.

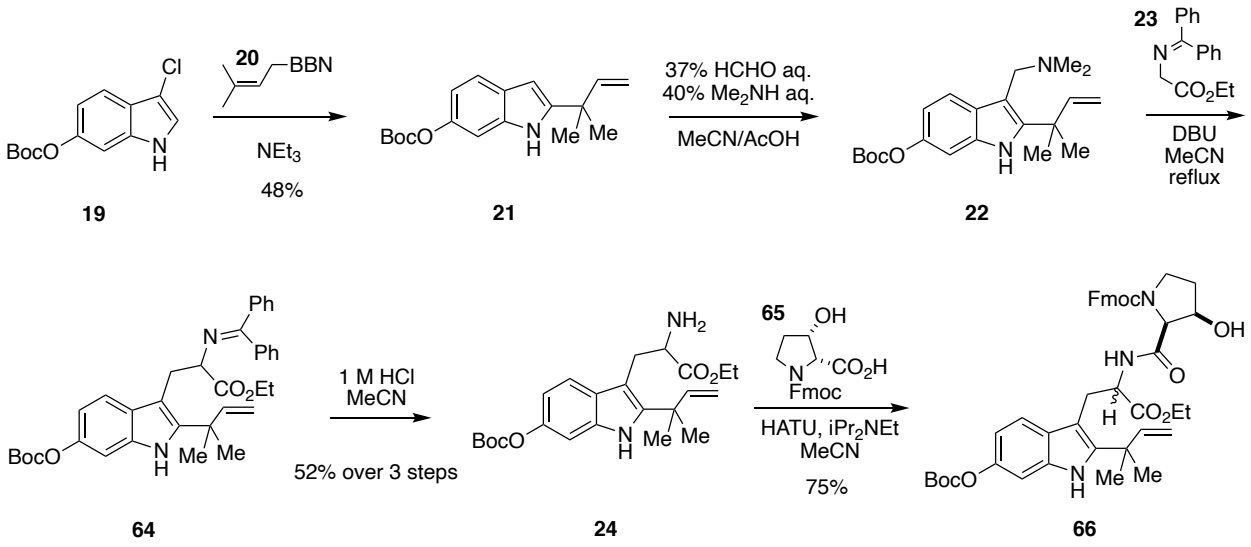

Figure 2.4. Steps 6-10 of following the original 6-*epi*-Notoamide T synthesis.[49]

The dipeptide was then deprotected and cyclized with triethylamine and 2-hydroxypyridine in acetonitrile to give the diketopiperazine **67** in moderate yield (**Figure 2.5**). Next, the diketopiperazine was treated with TFA to remove the Boc group (**68**), leaving the phenol unprotected for installation of the second reverse-prenyl group via Pd-catalyzed alkylation (**70**). The remaining alcohol on **70** was mesylated, which was then treated with 1 M KOH in MeOH. This should have resulted in the elimination, tautomerization, IMDA, and Claisen rearrangement to give Notoamide T and its epimer 6-*epi*-Notoamide T in a 1.3:1 ratio.[49] Instead, following the established procedure only resulted in degradation of the starting material. After numerous attempts, my colleague Poramate Songthammawat tried to carry out the procedure, but the reaction failed in his hands as well. Although the conditions were attempted multiple times, the reaction only resulted in degradation. At this point, the focus turned to exploring new routes to perform the elimination and tautomerization/IMDA reactions.

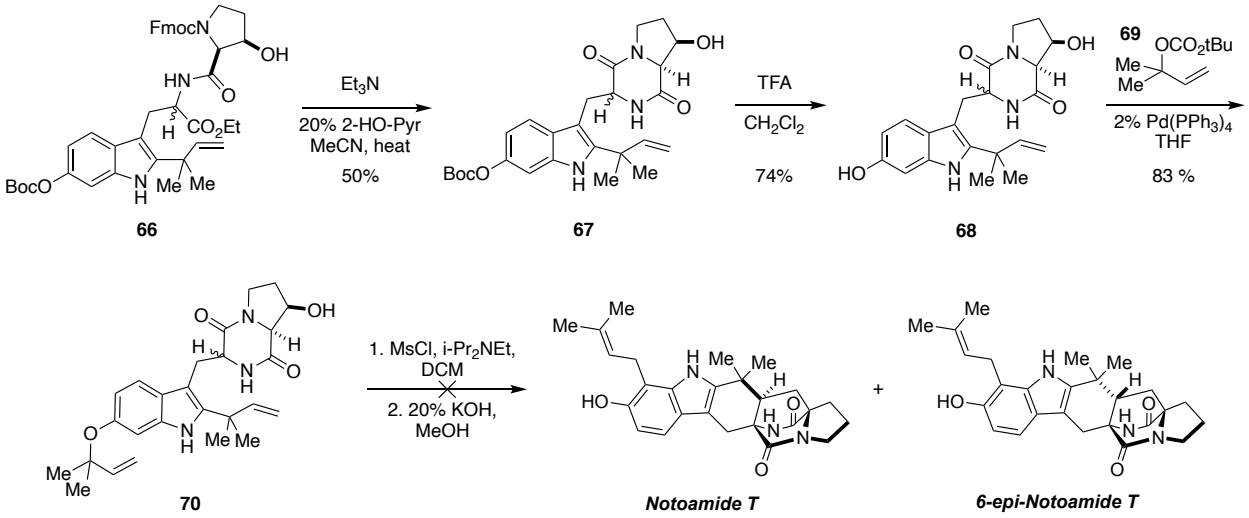

Figure 2.5. Final steps of the 6-*epi*-Notoamide T synthesis. The final IMDA step was not reproducible in our hands.

ii. Intramolecular Diels-Alder Conditions

After execution of the mesylation, 1 M KOH in MeOH was used for the IMDA reaction. This reaction was run at various temperatures (see **Table 2.1**), all of which resulted in various levels of decomposition, leaving **71** as the only recognizable product in low yields.

Table 2.1. IMDA attempts using mesylation and 1M KOH as base.

Base	Solvent	Temp	Time	Product
1M KOH	MeOH	60 °C	42 h	**71**, Decomposition
1M KOH	MeOH	75 °C	18 h	**71**, Decomposition
1M KOH	MeOH	75 °C	4 h	**71**, Decomposition

In place of mesylation, a Mitsunobu-type reaction was utilized for elimination of the alcohol to ensure pure starting material to test IMDA conditions (**Figure 2.6**). With eliminated product **71** in hand, various conditions were screened to perform the IMDA transformation (**Table 2.2**).

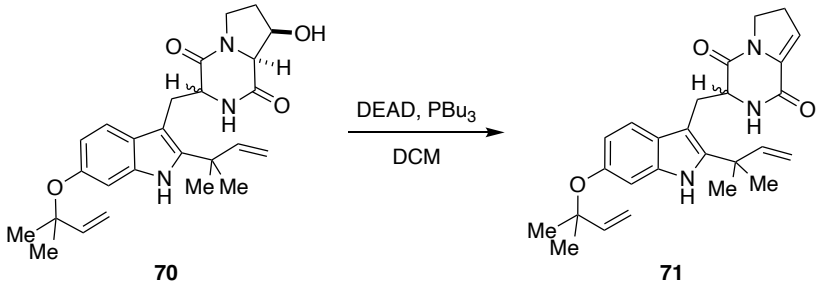

Figure 2.6. Use of Mitsunobu-type conditions for alcohol elimination.

Standard 1 M KOH in MeOH conditions resulted in recovery of Mitsunobu product and decomposition. As many other IMDA reactions from the Williams group have used 20% KOH in place of 1 M, these conditions were attempted on the substrate. It was thought that by using a higher concentration of base, lower temperatures could be used. This might allow for consumption of starting material while preventing degradation. Using 20% KOH, the reaction was performed at 0 °C which resulted in a mixture of **71** and **72**. When started at 0 °C followed by warming to room temperature, only **72** was observed.

Table 2.2. IMDA conditions after elimination via Mitsunobu.

71 **72**

Base	Solvent	Temp	Time	Product
DBU	DCM	RT	18 h	**71, 72** (trace)
1 M KOH	MeOH	0 °C	48 h	**71, 72,** Decomposition
1 M KOH	MeOH	0 °C → RT	18 h	**71, 72,** Decomposition
20% KOH	MeOH	0 °C	18 h	**71, 72**
20% KOH	MeOH	0 °C → RT	48 h	**72**
20% KOH	MeOH	65 °C	24 h	**72**, Decomposition
20% KOH	THF	RT	48 h	**71**
20% KOH	THF	65 °C	18 h	**71**
1M LiOH	H_2O	RT	1 h	**72**

In an effort to vary the substrate of the IMDA reaction, conditions were also tested on substrates **67** and **68** which resulted in decomposition or lack of reaction (**Table 2.3**).

Table 2.3. Mitsunobu and IMDA conditions on hydroxy and Boc-protected hydroxyindoles.

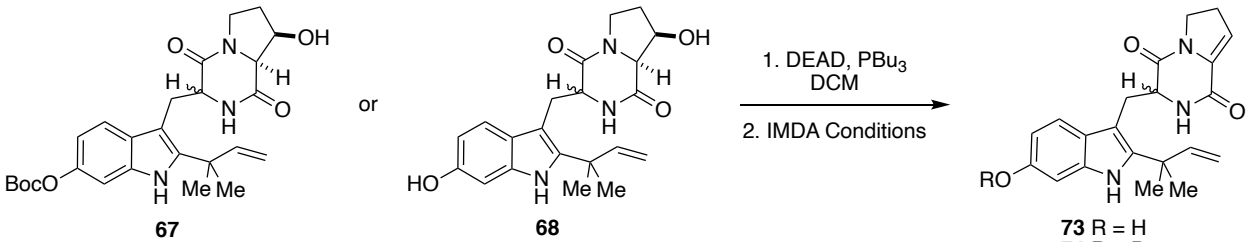

67 **68** **73** R = H, **74** R = Boc

Substrate	Base/solvent	Solvent	Temp	Time	Product
67	20% KOH	MeOH	0 °C	18 h	**73**
67	20% KOH	MeOH	0 °C → RT	18 h	**73**
68	20% KOH	MeOH	RT	48 h	Decomposition

Previously, methyl lactim ethers have been used prior to IMDA reactions.[35] The ethyl lactim ether was made and tested with various reaction times for the usual conditions (**Table 2.4**), however, no Diels-Alder product was isolated. It is possible that the ethyl ether was displaced and reformed the original diketopiperazine **70** before the IMDA had a chance to proceed, rendering it useless.

Table 2.4. IMDA conditions after elimination with Mitsunobu conditions and formation of ethyl lactim ether.

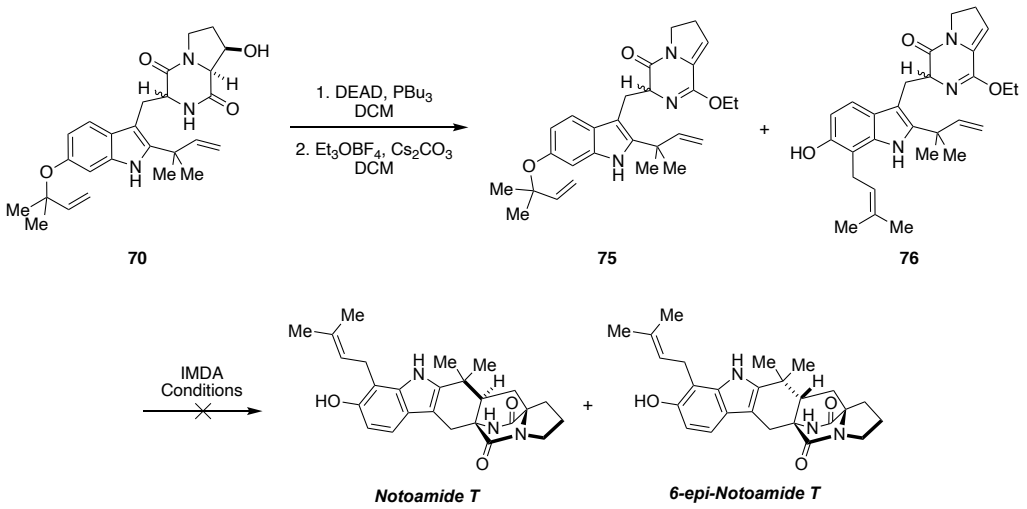

Base/solvent	Solvent	Temp	Time	Product
20% KOH	MeOH	0 ºC	6 h	**76**
20% KOH	MeOH	0 ºC	18 h	Decomposition
20% KOH	MeOH	0 ºC	48 h	Decomposition

It was thought that the polar protic nature of the methanol was assisting the decomposition. Consequently, methanol was replaced with THF in the reaction. However, running the reaction at both room temperature and at reflux only resulted in the recovery of starting material. This led to the suspicion that while the polar protic solvent may be causing

decomposition, it is still necessary for the IMDA reaction to occur, likely aiding in tautomerization.

iii. Improved Synthesis of 6-epi-Notoamide T

During the efforts to improve the IMDA conditions, improvements were in progress for the synthetic route. It simply could not be performed on an adequate scale to generate the amount of material necessary. The poor yield and limited scalability in synthesizing protected hydroxyindole **18** created a bottleneck quite early in the synthesis. When using 10% Pd/C and H_2 in MeOH, the reaction yielded 44% after subsequent Boc protection. When ammonia formate was used in place of hydrogen, the yield increased to a mediocre 55% over the two steps. To remedy this, instead of using the modified Leimgruber-Batcho synthesis which hydrogenates the benzyl group from enamine **17**, Raney Nickel and hydrazine hydrate were employed to cyclize to the indole while leaving the benzyl group intact.[79] This reaction could be carried out at a 100 gram scale with an 85% yield. At a lower scale of 50 grams or less, the yield increased to 93%. A comparison of the routes used for the protected hydroxyindole synthesis can be seen in **Figure 2.7**. This allowed for far more material to be carried through the synthesis, making it much more efficient.

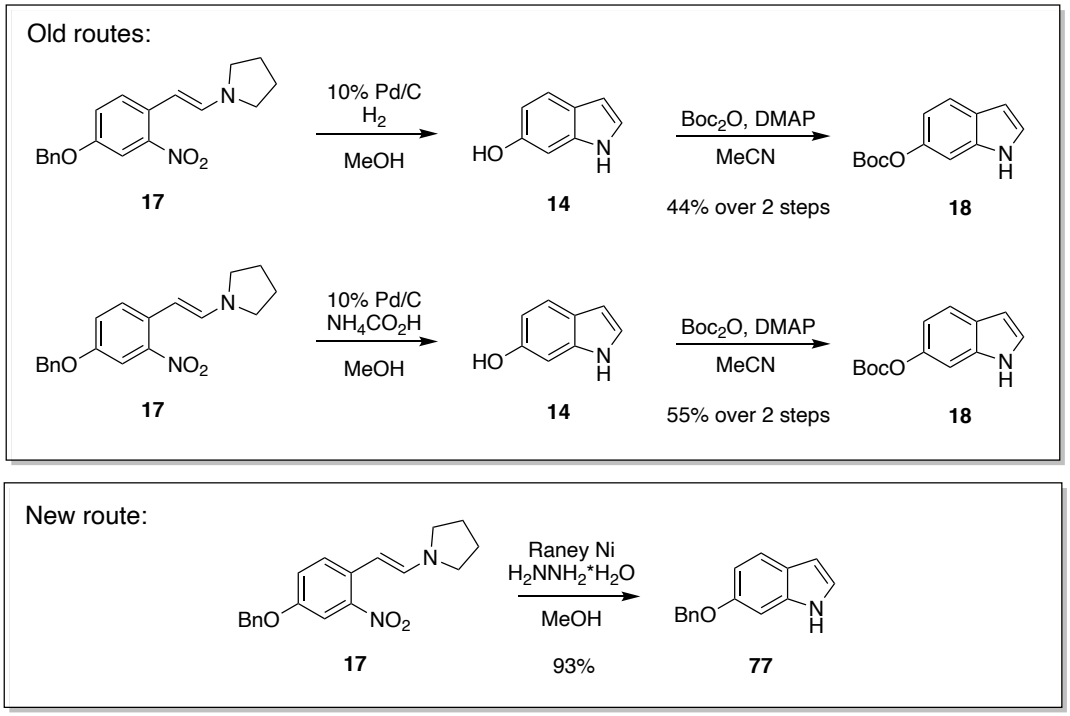

Figure 2.7. New method of synthesizing the protected hydroxyindole has a higher yield over fewer steps and can be run on a much larger scale than previous routes.

The low-yielding dimethylallene synthesis was also a complication. The synthesis was incredibly time-consuming when only a few grams could be made at a time. It was found that if the scale of the reaction was decreased slightly (from 90g of **62** to 70g) and the equivalence of zinc catalyst was increased from 1.2 to 1.4, the yield improved (**Figure 2.8**). The yield was further improved when the previously used zinc mesh was replaced with zinc dust to increase catalyst surface area. This increased the yield from 20-30% to 89%—a substantial increase.

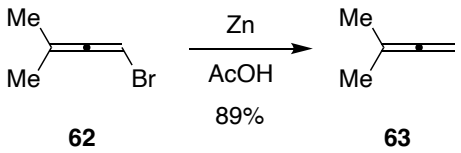

Figure 2.8. Improved synthesis of dimethylallene.

The synthesis could then be carried forward in the same manner as the original synthesis until diketopiperazine product **84** with similar or higher yields (**Figure 2.9**). Since the benzyl protecting group is most easily removed by hydrogenation, it was necessary to carry out the IMDA before deprotecting, unlike the original synthesis.

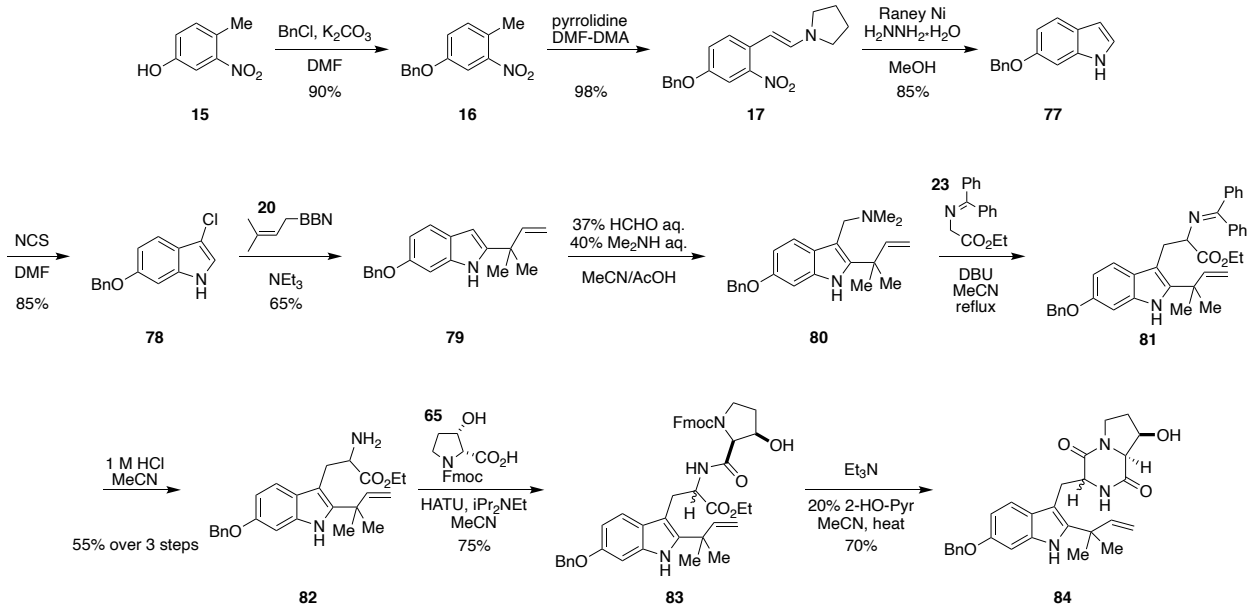

Figure 2.9. Improved synthesis of 6-*epi*-Notoamide T from starting material nitrophenol **15** to diketopiperazine **84**.

In previous attempts at the IMDA, it seemed that a polar protic solvent was necessary for the reaction to occur, but that it may also be causing decomposition. Considering this, a mixture of THF and MeOH was used to solvate 1M KOH on diketopiperazine **84**, resulting in a successful intramolecular Diels-Alder reaction. Conditions were varied until it was found that a ratio of 2:1 THF/MeOH and 20% KOH was most successful, resulting in a reliable 56% yield with a diastereomeric ratio of 1.1:1 of the *syn* and *anti*-products (**Figure 2.10**).

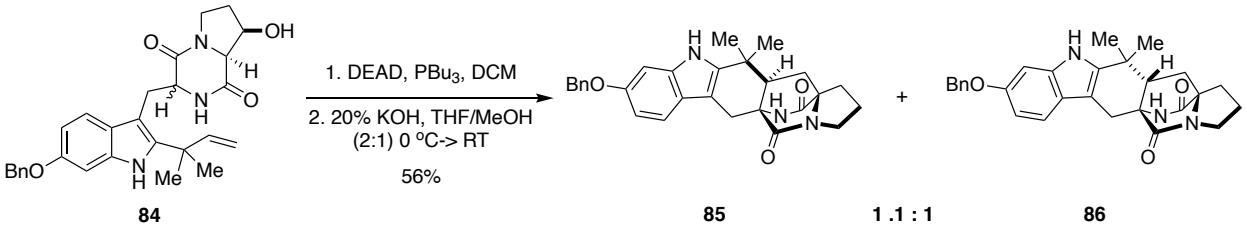

Figure 2.10. Successful synthesis of the bicyclo[2.2.2]diazaoctane core.

With the bicyclo[2.2.2]diazaoctane core established, the alcohol could then be deprotected in quantitative yield (**Figure 2.11**). Next, the free phenol is alkylated and the Claisen rearrangement occurs, resulting in the prenyl group on the C-7 position of the indole, giving 6-*epi*-Notoamide T and Notoamide T.

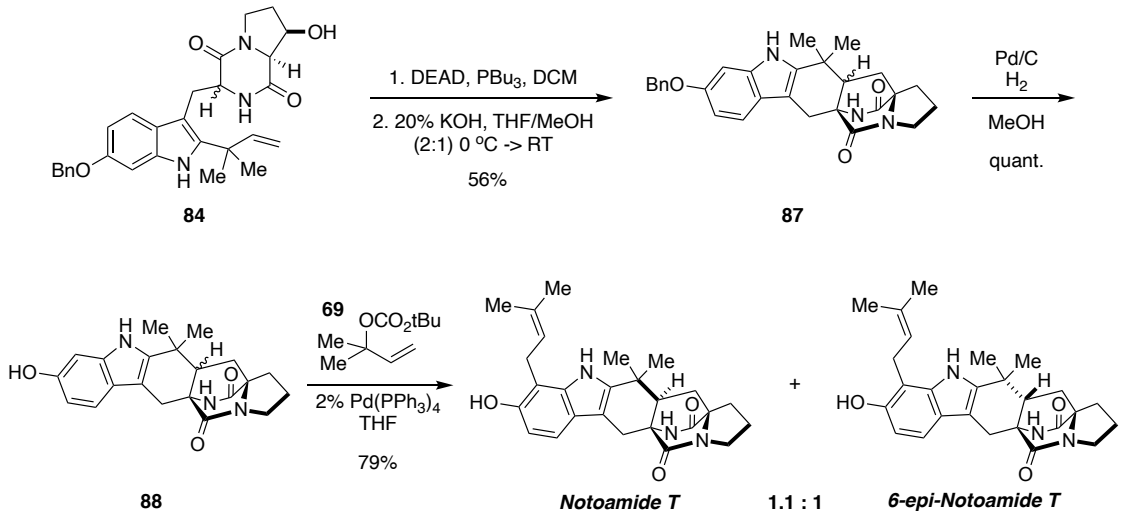

Figure 2.11. Final steps of improved 6-*epi*-Notoamide T synthesis. Intramolecular Diels-Alder, deprotection of benzyl group, and addition of prenyl group to C-7 of the indole.

This synthesis is one step shorter than the previous, scales better, and has a more reliable and higher yielding intramolecular Diels-Alder reaction. This synthesis can be used to make other products in the 6-*epi*-Notoamide T family such as 6-*epi*-Notoamide T3-12 isolated from *Aspergillus protuberus*. Additionally, an interesting new natural product was unexpectedly

isolated from *A. protuberus* from a feeding study using [^{13}C]$_2$-(±)-Notoamide T. This synthesis could be applied to this new product as well.

III. Total Synthesis of Notoamide T2

i. Biosynthetic Significance

While the bioconversion of Notoamide T to Stephacidin A had long been suspected, Sunderhaus *et al.*'s synthesis of Notoamide T unlocked the ability to produce doubly ^{13}C-labeled Notoamide T.[49] A racemic mixture of [^{13}C]$_2$-(±)-Notoamide T was offered to both *A. protuberus* and *A. amoenus* and the resulting fungal extracts were analyzed with LC-MS and ^{13}C NMR. This analysis determined that Notoamide T was incorporated into advanced secondary metabolites. In *A. amoenus*, (+)-Stephacidin A and (+)-Notoamide B were isolated with 4.7% and 0.6% ^{13}C incorporation, respectively (**Figure 2.12**).[49] As the natural (-)-enantiomer of Stephacidin A was not recovered, it's presumed that it was produced but subsequently transformed into (+)-Notoamide B. This theory aligns with the proposed biosynthetic pathway of *A. amoenus*, discussed in Chapter 1. This also suggests that the oxidase responsible for construction of the pyran ring (NotD') promiscuously accepts both enantiomers of Notoamide T, while pinacolase NotI' only tolerates the natural (-)-enantiomer of Stephacidin A.

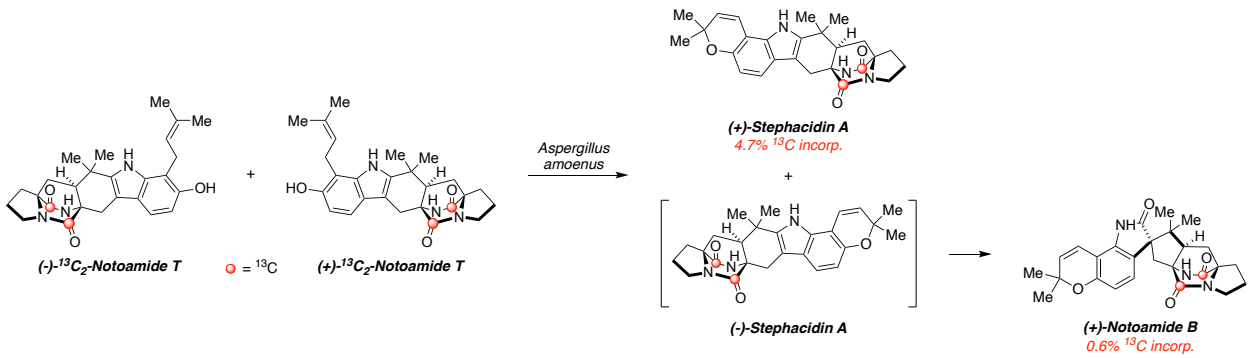

Figure 2.12. Incorporation of [^{13}C]$_2$-(±)-Notoamide T in *A. amoenus*, resulting in [^{13}C]$_2$-(+)-Stephacidin A (4.7% ^{13}C incorporation) and [^{13}C]$_2$-(+)-Notoamide B (0.6% ^{13}C incorporation).[49]

While only specific enantiomers were isolated from incorporation studies with *A. amoenus*, incorporation of [^{13}C]$_2$-(±)-Notoamide T in *A. protuberus* resulted in isolation of exclusively racemic products. When doubly labeled racemic Notoamide T was fed to *A. protuberus*, natural metabolites Stephacidin A, Notoamide B, Notoamide F, and Notoamide R were all isolated as racemates. Incorporation percentages can be seen in **Figure 2.13**. Interestingly, new natural product Notoamide T2 was also isolated.[49]

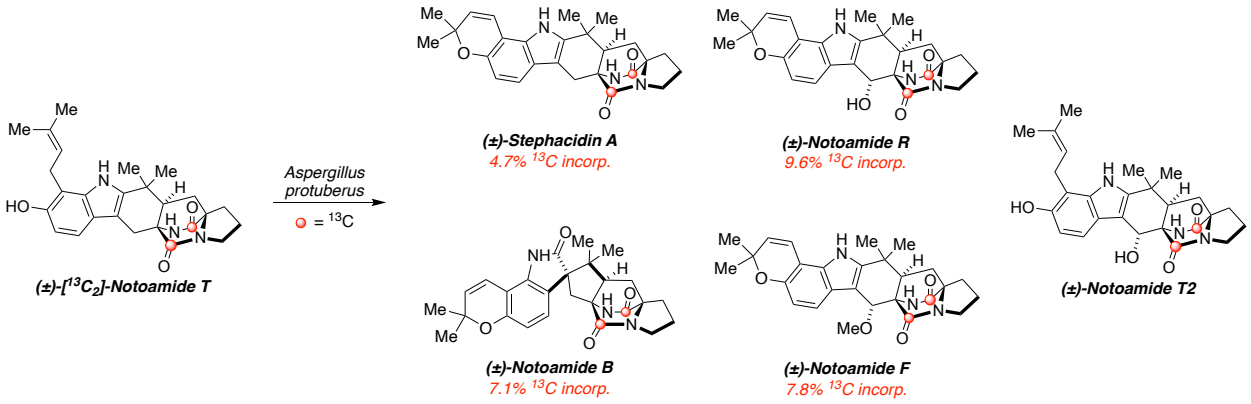

Figure 2.13. Incorporation of [^{13}C]$_2$-(±)-Notoamide T in *A. protuberus*, resulting in isolation of racemic known products Stephacidin A, Notoamide B, Notoamide F, and Notoamide R, as well as new natural product Notoamide T2.[49]

This study suggests the enzymes responsible for conversion of Notoamide T and Stephacidin A into more advanced metabolites (including NotD and NotI) do not distinguish between enantiomers of these products. It also suggests that another, unknown, pathway exists in the fungus to create Notoamide T2. Or, that the enzyme responsible for conversion of Stephacidin A to Notoamide R also accepts Notoamide T. These questions have not yet been answered, but synthesis of Notoamide T2 may be helpful in this investigation. Synthesis of ^{13}C-labeled Notoamide T2 could help elucidate whether more advanced metabolites are produced from this product, or possibly whether it can be accepted and converted in *A. amoenus*.

ii. Synthesis of Notoamide T2

The work in this section was done with the help of John Manganaro. The first total synthesis of Notoamide T2 began with *syn* cycloadduct **85**, found in the improved synthesis of Notoamide T reported in section I. Literature precedent showed that the methyne on C-3 could be oxidized to a ketone using just over 2 equivalents of DDQ.[80–82] It was reasoned that using 1 equivalent of DDQ might stop oxidation at the alcohol, rather than proceeding to the ketone. This proved true, and the compound was oxidized with DDQ in the presence of water to yield alcohol **89** as a single diastereomer with an impressive 87% yield (**Figure 2.14**). From here, the benzyl protecting group was hydrogenated to give phenol **90**, which was carried forward without further purification. Alkylation of **90** with carbonate **28** and catalytic palladium tetrakistriphenylphosphine yielded **91**, which was subjected to chemical microwave. This instigated the Claisen rearrangement, resulting in Notoamide T2.

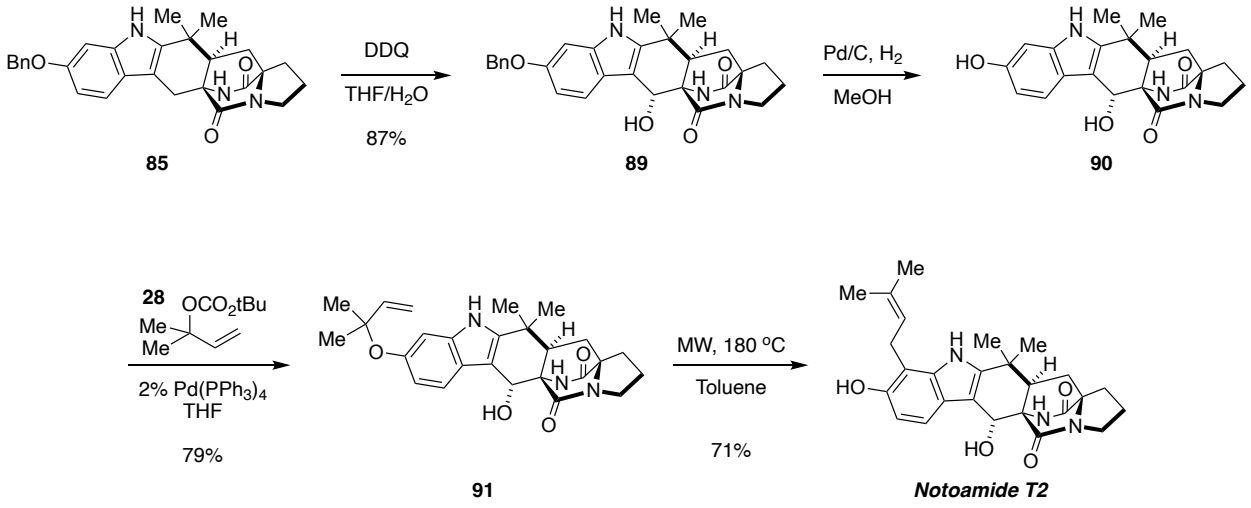

Figure 2.14. The first total synthesis of Notoamide T2.

iii. Conclusions

The synthesis of this compound will help us learn more about the seemingly endless biosynthetic pathways of the *Aspergillus* species. If this compound is ^{13}C labeled, it can be fed to

A. amoenus or *A. protuberus* to see whether it is incorporated into any new metabolites, signifying the awakening of dormant tailoring genes in the fungus. If new products are found, it would signify the existence of a previously unknown biosynthetic path in these fungi. If none are found, it would confirm that Notoamide T2 is likely a shunt metabolite: it is not incorporated into more advanced metabolites. ^{13}C labeling for the bicyclic substrates has been well established in the Williams group (**Figure 2.15**).[42,49,65,83]

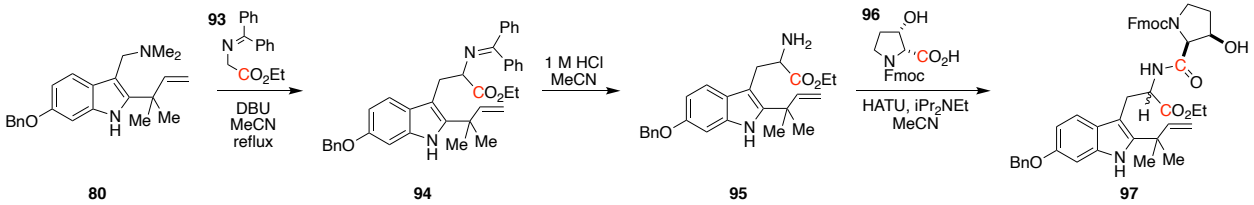

Figure 2.15. Proposed synthetic scheme to label Notoamide T2 and related compounds in this dissertation, where C = ^{13}C.

This scheme can be used to label Notoamide T2 for incorporation studies by incorporating these steps into the Notoamide T synthesis and simply replacing compound **81** with its ^{13}C labeled counterpart. This compound could then be incorporated into both *Aspergillus* species mentioned above to glean more about their respective biosynthetic pathways. It is particularly interesting that this compound was isolated from *A. protuberus* and not *A. amoenus*. The species generally follow similar biogenesis pathways, but more pathways are known in *A. protuberus* than *A. amoenus* at this point. Further knowledge could be gained about these unique species from an incorporation study with Notoamide T2.

Chapter 3: Towards the Total Synthesis of 6-*epi*-Notoamide T9 and Notoamide TI

I. 6-*epi*-Notoamide T9

i. Isolation and Biosynthetic Insights

As discussed in Chapter 1, it has been speculated that Notoamide S is a precursor to Stephacidin A, Notoamide B, 6-*epi*-Stephacidin A, and Versicolamide B. Notoamide S would be converted to Stephacidin A and successively Notoamide B through intermediate Notoamide T. Or, it could be converted to 6-*epi*-Notoamide T which would then form 6-*epi*-Stephacidin A followed by Versicolamide B. Evidence of the bioconversions of Stephacidin A into Notoamide B and Notoamide T into each has been reported by the group in 2011 and 2013, respectively.[49,84] While this pathway has been established, the Versicolamide B pathway had not. To verify the proposed intermediates, the Tsukamoto group performed feeding studies with *Aspergillus protuberus* to show the bioconversion of 6-*epi*-Notoamide T to 6-*epi*-Stephacidin A to Versicolamide B (2014).[65]

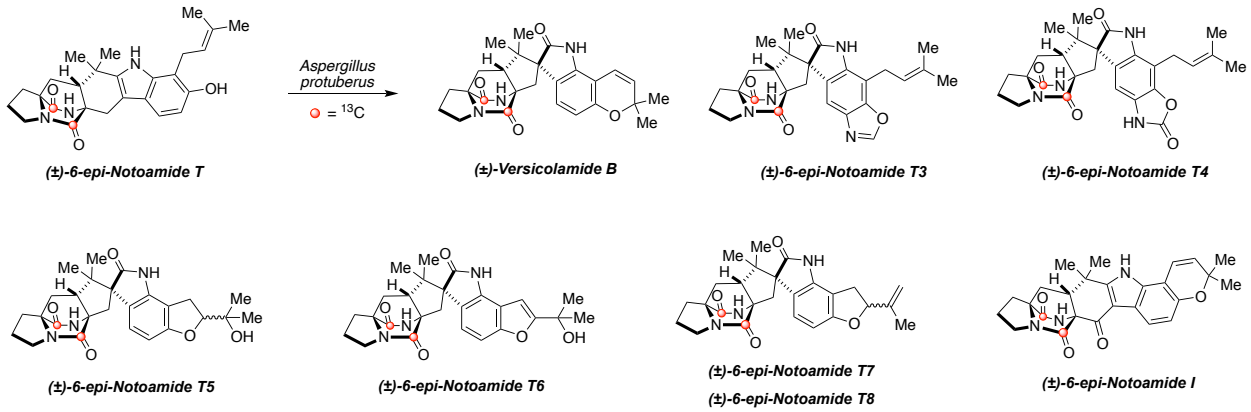

Figure 3.1. Novel compounds T3-8 and Notoamide I isolated along with Versicolamide B after [13C]$_2$-(±)-6-*epi*-Notoamide T incorporation.[65]

A precursor incorporation experiment used [^{13}C]$_2$-(±)-6-*epi*-Notoamide T in *Aspergillus protuberus*, incubating the fungal cells in a trace element solution (using a liquid medium of seawater, malt extract, and peptone) containing the proposed metabolite. The culture was extracted with *n*-BuOH after 14 days and purified by column chromatography and HPLC, affording [^{13}C]$_2$-Versicolamide B and seven new metabolites, 6-*epi*-Notoamide T3-T8 and 6-*epi*-Notoamide I (**Figure 3.1**). Another precursor experiment was done using non-labeled 6-*epi*-Notoamide T where after 16 days, the culture was extracted and purified, yielding 4 novel metabolites 6-*epi*-Notoamides T9-T12 (**Figure 3.2**). All new metabolites discovered were racemates, presumably because racemic precursor was used in the incorporation studies. This indicates the enzymes involved in the transformations to these new metabolites are likely plastic enough to accept both enantiomers of 6-*epi*-Notoamide T.[65]

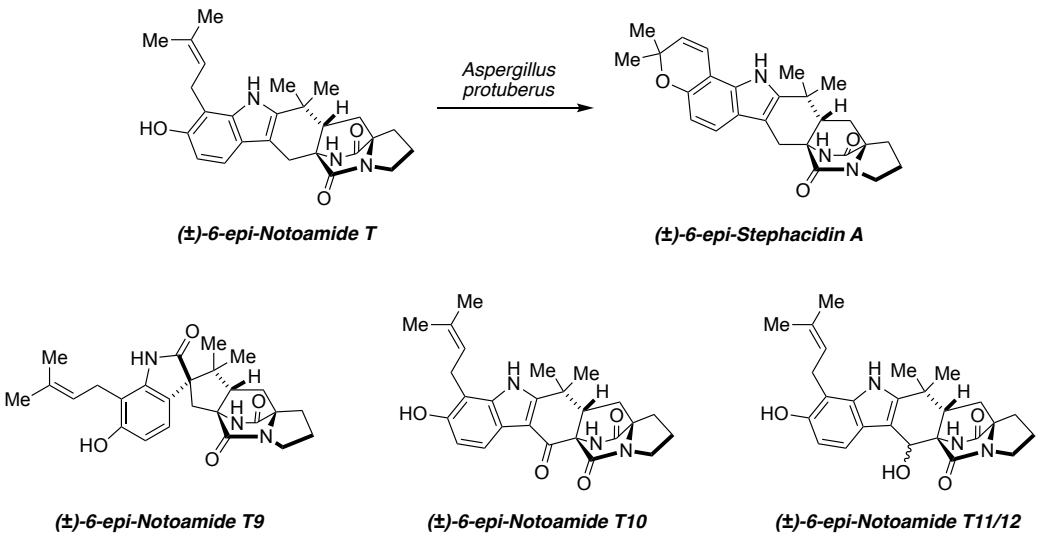

Figure 3.2. 6-*epi*-Stephacidin A and novel products 6-*epi*-Notoamides 9-12 resulting from 6-*epi*-Notoamide T feeding study.

When normal culture conditions were tested, 6-*epi*-Notoamides T3-T12 and 6-*epi*-Notoamide I were not produced to any detectable extent.[65] These results indicate that the presumably natural metabolite expanded the metabolic breadth of the organism by awakening dormant tailoring genes. While 6-*epi*-Notoamide T is believed to be an endogenous metabolite to the organism, the precursor study used a racemic, labeled substance. Further investigations into these interesting outcomes require sufficient quantities of optically pure enantiomers to probe whether the alteration in metabolic profile is triggered by an enantiomer unnatural to the producing organism.

Of particular interest from these newly discovered metabolites, 6-*epi*-Notoamide T3 and T4 contain incredibly rare moieties.[65] The benzene of the tryptophan moiety now is fused to an oxazole and 2-oxazolone component, respectively. Oxidative amination of an aromatic ring may be an unprecedented biochemical transformation. The oxidative amination is suspected to go through the mechanism suggested in **Figure 3.3**, starting with oxidation and consequent pinacol

rearrangement of [^{13}C]$_2$-(±)-6-*epi*-Notoamide T. This is hypothesized to form the spiro-oxindole, [^{13}C]$_2$-(±)-6-*epi*-Notoamide T9. Subsequent oxidation and integration of glycine could then give imine **100**. Then, decarboxylation results in **101** which will then cyclize to **102**. This compound is then oxidized to oxazole 6-*epi*-Notoamide T3, which can be further oxidized to oxazolone 6-*epi*-Notoamide T4.[65]

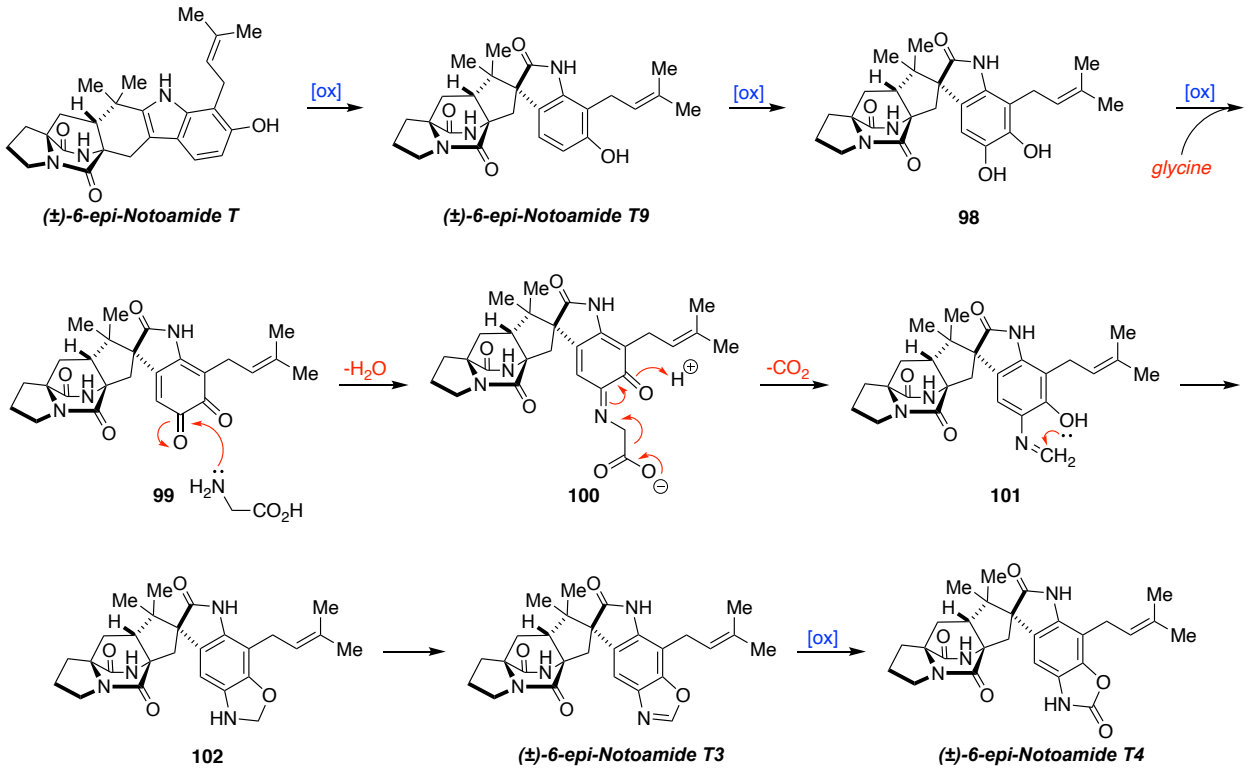

Figure 3.3. Proposed biosynthetic pathway to (±)-6-*epi*-Notoamide T3 and T4 from (±)-6-*epi*-Notoamide T.[65]

NotI has been shown to catalyze the semi-pinacol rearrangement in many *Aspergillus* substrates.[46] There are likely at least six enzymes responsible for the remaining transformations to T4: (1) a hydroxylase to form **98** from T9, (2) a catechol oxidase to **99**, (3) a glycine aminotransferase to **100**, (4) a decarboxylase/cyclase to **102**, (5) an oxazolidine oxidase to T3, and (6) an oxazolidinone oxidase to T4.[65] These complex transformations could signify that

multiple dormant tailoring genes in the organism were triggered by the presence of one (or both) enantiomers of 6-*epi*-Notoamide T.

Since 6-*epi*-Notoamide T9 is thought to be the precursor to 6-*epi*-Notoamide T3 and T4, it was prudent to synthesize 6-*epi*-Notoamide T9 before attempting T3 and T4. Additionally, this compound could be used to probe for the unprecedented enzymes responsible for the unique transformations to 6-*epi*-Notoamides T3 and T4.

ii. Synthetic Efforts Towards 6-epi-Notoamide T9

The initial route proposed to do this was to mimic the syntheses of Versicolamide B and Notoamide B (**Figure 3.4**). These compounds were made using Davis Oxaziridine to promote the pinacol-type rearrangement to the spiro-oxindole. The spiro-oxindole is formed via epoxidation of the 2,3-disubstitued indole on the less hindered face, followed by opening of the epoxide (**Figure 3.5**).

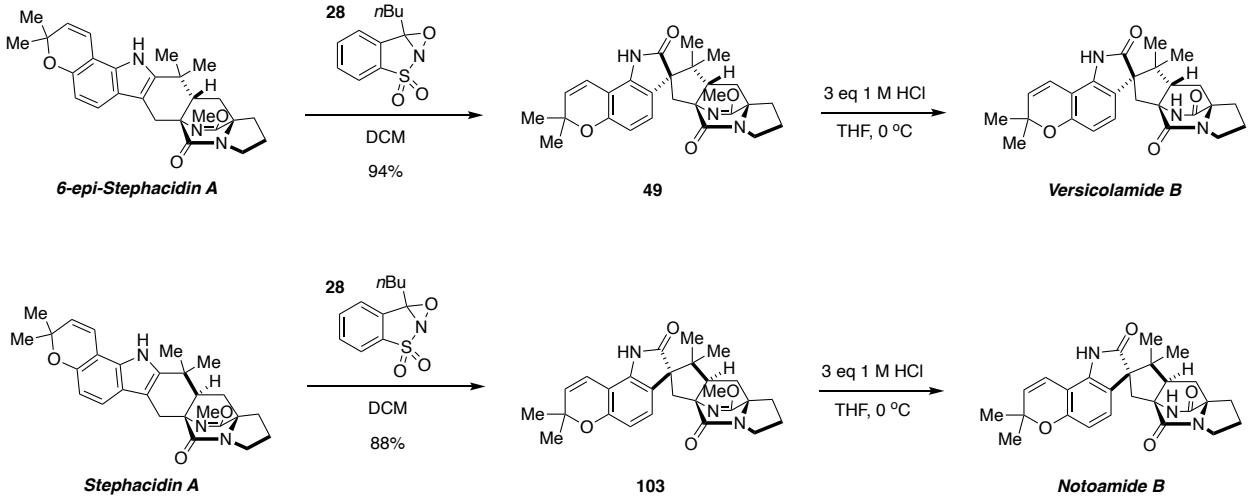

Figure 3.4. Precedent for use of Davis Oxaziridine to do pinacol-type rearrangement on 6-*epi*-Notoamide T to form 6-*epi*-Notoamide T9.

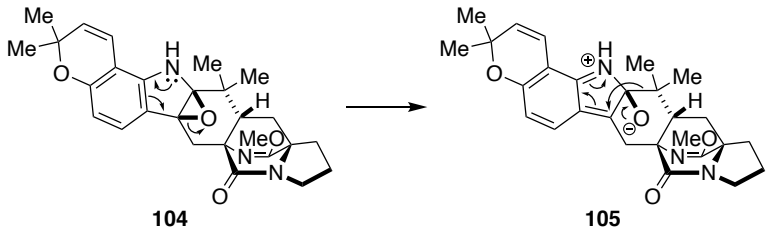

Figure 3.5. Davis Oxaziridine epoxidates of the 2,3-disubstitued indole. This is then opened in a pinacol-type rearrangement to form the spiro-oxindole compound.

Thus, the first synthesis of 6-*epi*-Notoamide T9 was proposed, shown in **Figure 3.6**. In this synthesis, the protected Diels-Alder product **86** would be rearranged to the spiro-oxindole **106** using Davis Oxaziridine. The resulting compound would be deprotected via hydrogenation, then alkylated with tetrakis(triphenylphosphine)palladium(0) and carbonate **69**. This step should also produce the subsequent Claisen rearrangement, forming 6-*epi*-Notoamide T9.

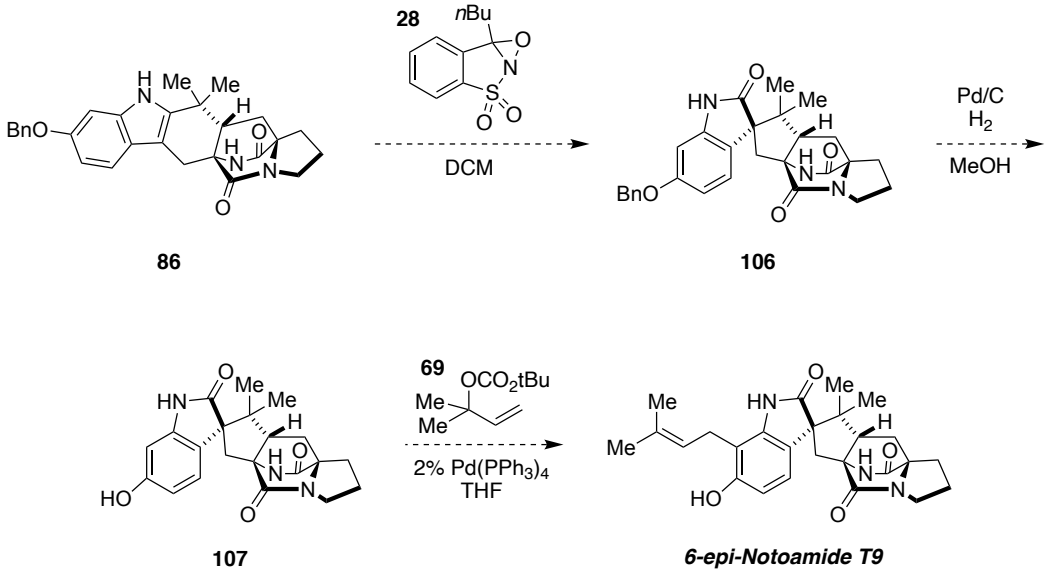

Figure 3.6. First proposed synthesis of 6-*epi*-Notoamide T9. Compound **86** from improved 6-*epi*-Notoamide T synthesis (see **Figure 2.9**).

In order to test this synthesis, the *syn* diastereomer of the bicyclic compound (**85**) was used as much more was available (**Figure 3.7**). The reaction worked easily, resulting in the

spiro-oxindole as planned. The spiro-oxindole compounds have a signature shift of 180-185 ppm for the new carbonyl and a new peak at 182 ppm was seen in the ^{13}C NMR. The conformation of the spiro-oxindole stereocenter was confirmed by determining the peaks of H_a and H_b (C-4 and C-10, respectively) and finding ROESY correlation between them. The other proton on C-10 did not show a correlation with H_a.

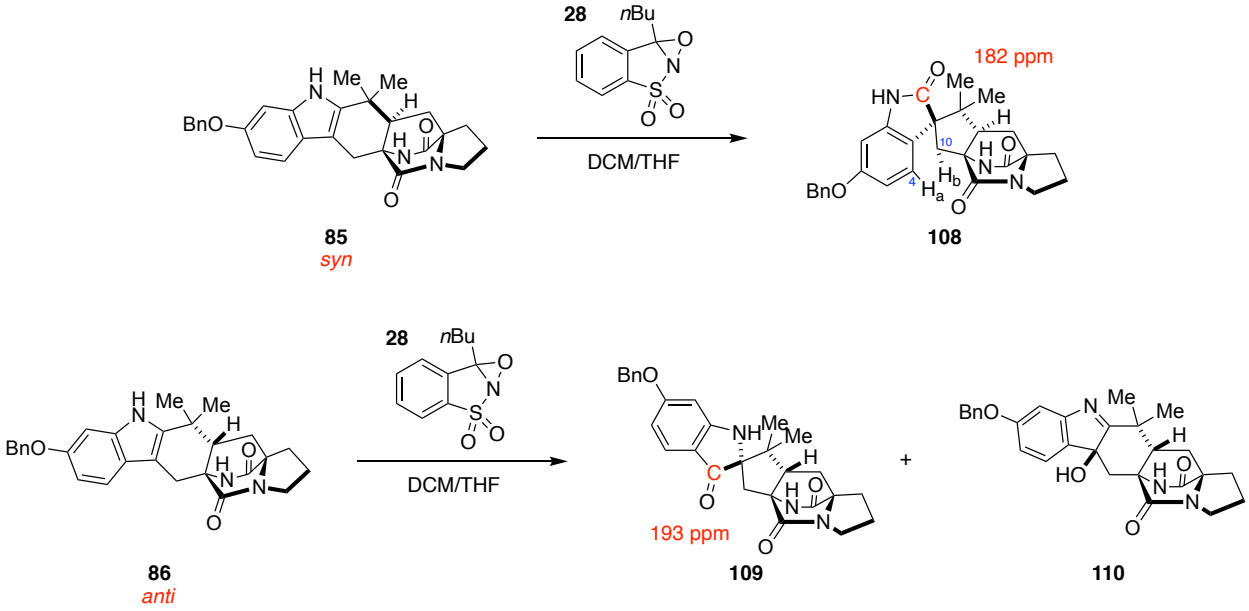

Figure 3.7. Results from using Davis Oxaziridine for pinacol rearrangement. Oxindole was achieved from the *syn* IMDA compound **85**, but the indoxyl and hydroxyindolenine from *anti* IMDA **86**.

After this success, **86** was exposed to Davis Oxaziridine with high hopes. However, instead of yielding the oxindole, indoxyl **109** and hydroxyindolenine **110** were found instead. Contrary to the oxindole's carbonyl peak around 180-184 ppm, the indoxyl peak appears over 190 ppm (193 ppm was observed). The hydroxy carbon of the indolenine produces a peak around 80 ppm (82.7 ppm observed).

While the indoxyl cannot be rearranged to the oxindole, the hydroxyindolenine has been shown on numerous occasions to rearrange to the oxindole in the presence of acid. Following conditions used by Greshock[85], 2M HCl was employed to promote the rearrangement of **110** into the oxindole (**Figure 3.8**). This, however, did not work, and only starting material was recovered. It was theorized that the hydroxyindolenine is too stable to rearrange, possibly due to effects from the oxygen on the 6-position of the indole.

To remedy this, the approach was changed to form the chloroindolenine, which should be less stable than the hydroxyindolenine (**Figure 3.8**). This proved true when **86** was exposed to tert-butyl hypochlorite and triethylamine in DCM and subsequently, 2M HCl. The spiro-oxindole was indeed formed, but it was the wrong diastereomer. This was determined due to ROESY correlation between H_a on C-4 and H_b on C-10.

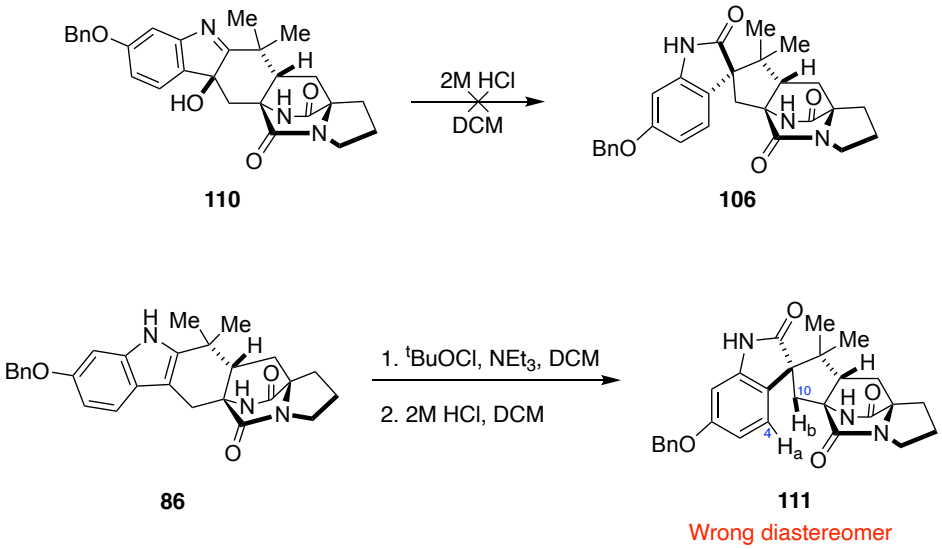

Figure 3.8. The attempt to rearrange hydroxyindolenine **110** to the oxindole using 2M HCl was unsuccessful. ^{t}BuOCl was used instead to form the chloroindolenine intermediate, but this resulted in the wrong diastereomer after rearrangement with 2M HCl.

After finding the chloroindolenine route to be unsuccessful, attention was turned back to the hydroxyindolenine intermediate. A variety of conditions were used in attempt to promote the rearrangement into the oxindole, as outlined in **Table 3.1**. First, methanol was tried in place of DCM to see if a homogenous solution (and polar protic solvent) was more effective than the typical biphasic conditions, however only starting material was achieved. Alternative acids were also considered, and both tosylic acid and sulfuric acid were tested. Hydroxyindolenine **110** was exposed to sulfuric acid (10%) at room temperature for 18 hours, also resulting in starting material. Harsher conditions were explored at this point, and **110** was refluxed with tosylic acid for 20 minutes as per the conditions of Cushing *et al*.[86] When this still resulted in starting material, the reaction was run overnight (after monitoring by TLC throughout the day), which resulted in decomposition.

Table 3.1. Conditions to rearrange hydroxyindolenine to oxindole. All were unsuccessful, either resulting in starting material or decomposition.

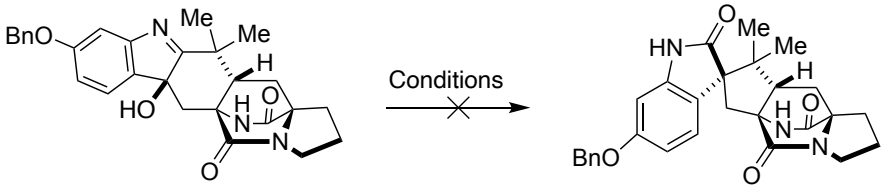

110 **106**

Reagent	Solvent	Temp	Time	Product
2M HCl	DCM	RT	4 h	Decomposition
2M HCl	MeOH	RT	4 h	Decomposition
10% H_2SO_4	MeOH	RT	4 h	Decomposition
TsOH	THF/H_2O (10:1)	Reflux	4 h	**110**
TsOH	THF/H_2O (10:1)	Reflux	Overnight	Decomposition
$Sc(OTf)_3$	Toluene	110 °C	5 h	Decomposition

At this point it was determined that the hydroxyindolenine product was possibly too stable to rearrange and an alternative route was planned (**Figure 3.9**). Attempting the pinacol rearrangement on the diketopiperazine product (before performing the Diels-Alder reaction) would make a far less stable intermediate that might be more prone to rearrangement. Compound **68** was subjected to alkylation using the palladium catalyst and **69** to form **70**. Once the reverse-prenyl group was successfully installed, **70** was subjected to Davis Oxaziridine in DCM and THF (1:1). THF was used in this case to increase solubility of **70**, as it was not soluble in DCM alone. Oxindole **112** was achieved in a modest yield of 50% from this reaction. The Davis Oxaziridine pinacol reaction had previously been attempted on **68**, though MeOH needed to be added as a solvent due to poor solubility and a low yield of 3% resulted. It is thought that both the polar protic solvent and free phenol kept the Davis Oxaziridine from coordinating with the indole nitrogen and the new route was chosen to mitigate those concerns.

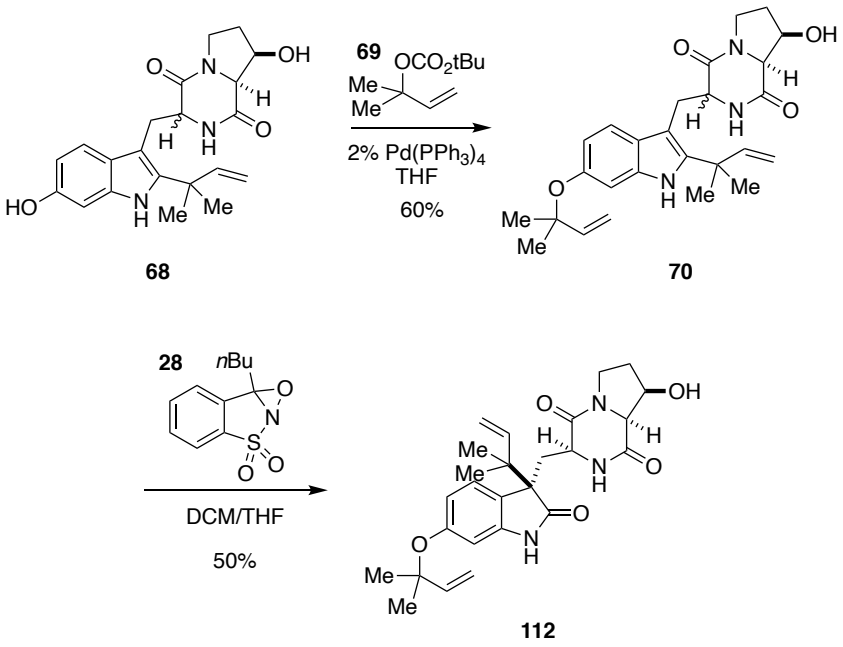

Figure 3.9. Successful new route to spiro-oxindole product, starting from diketopiperazine **68**.

With oxindole **112** in hand, the IMDA reaction needed to be performed, following the mesylation of the alcohol. As seen in **Table 3.2**, conditions of 20% KOH in 2:3 MeOH/THF at 0 ^{o}C for 4 hours was attempted first for the Diels-Alder reaction, which resulted in decomposition. Seeing this, the conditions from the improved 6-*epi*-Notoamide T synthesis (**Figures 2.10** and **2.11**) were used next, though the reaction was kept at 0 ^{o}C instead of warming to room temperature. Though it was hoped that the dilution of polar protic solvent (from 2:3 MeOH/THF to 1:2) would decrease decomposition, it did not, and no identifiable material was recovered from the reaction. Next, the concentration of KOH was lowered to 1M, which still resulted in decomposition. The temperature was then lowered to -20 ^{o}C, and after monitoring the reaction overnight, starting material was still the only product. Thinking that -10 ^{o}C might be a suitable intermediate temperature, the reaction was ran as such, but the material decomposed.

This project was ultimately terminated at this point, as it was difficult to bring up enough starting material for these reactions and other projects were proving more fruitful. If this project were to be continued, it would be interesting to try further dilutions of the MeOH in THF—possibly trying 1:3 MeOH/THF, 1:4, etc. In addition, non-ionic bases could be tested, such as DBU or DIPEA.

Table 3.2. Attempts to do IMDA reaction on **112** to form 6-*epi*-Notoamide T9. All were unsuccessful, either resulting in decomposition or starting material.

112 ***6-epi-Notoamide T9***

Base	MeOH/THF Ratio	Temp	Time	Product
20% KOH	2:3	0 ºC	4 h	Decomposition
20% KOH	1:2	0 ºC	4 h	Decomposition
1M KOH	1:2	0 ºC	4 h	Decomposition
1M KOH	1:2	-20 ºC	Overnight	Starting Material
1M KOH	1:2	-10 ºC	4 h	Decomposition

iii. Future Directions: Synthesis of 6-epi-Notoamides T3 and T4

If 6-*epi*-Notoamide T9 is synthesized, this paves the way to synthesize 6-*epi*-Notoamide T3 and T4. A potential route for this synthesis is proposed in **Figure 3.10**. Acylation of 6-*epi*-Notoamide T9 with chlorosulfonyl isocyanate should give carbamate **113**.[87] The next step would be a Rh(II)-catalyzed intramolecular aromatic C(sp^2)-H amination/nitrenoid insertion to give benzoxazolone 6-*epi*-Notoamide T4. Parameshwar *et al*. found that a prominent electronic effect was seen in substrates with donating substituents. These substrates provided the desired products in good to excellent yields, allowing more varied substrates than what may be possible using traditional methods.[88]

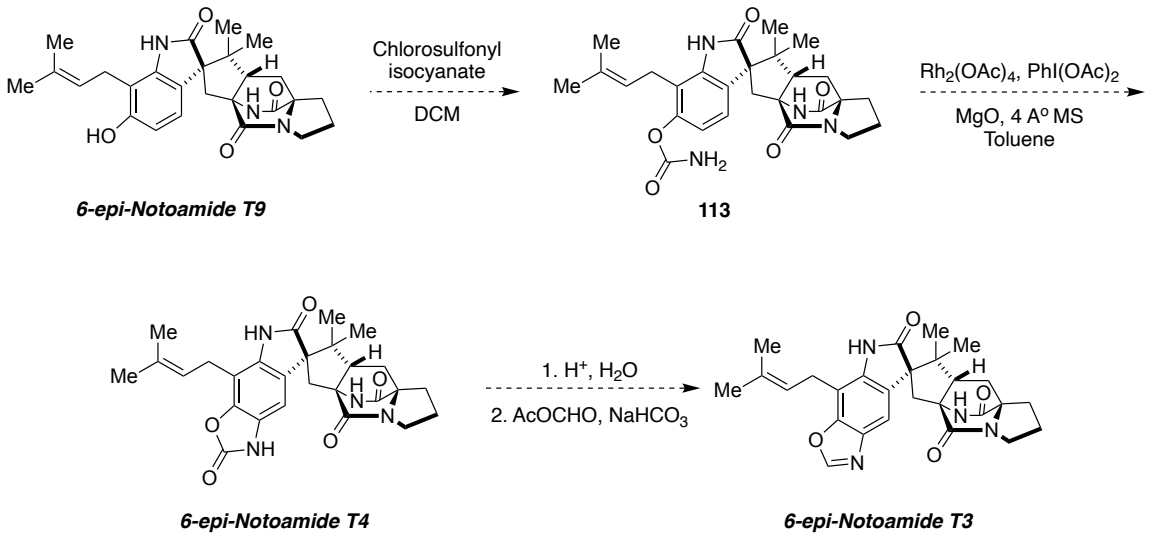

Figure 3.10. Proposed synthesis of 6-*epi*-Notoamide T3 and T4.

Alternatively, the route in **Figure 3.11** could potentially be used to get to 6-*epi*-Notoamide T3 through T4. First, the nitrogen in the benzoxazolone is Boc-protected with di-tert-butyl dicarbonate and DMAP. Next, methylmagnesium bromide is used to cleave the cyclic carbamate, leaving carbanion intermediate **115**. Addition of **115** to triethyl orthoformate and trifluoroacetic acid then gives oxazole 6-*epi*-Notoamide T3.[89]

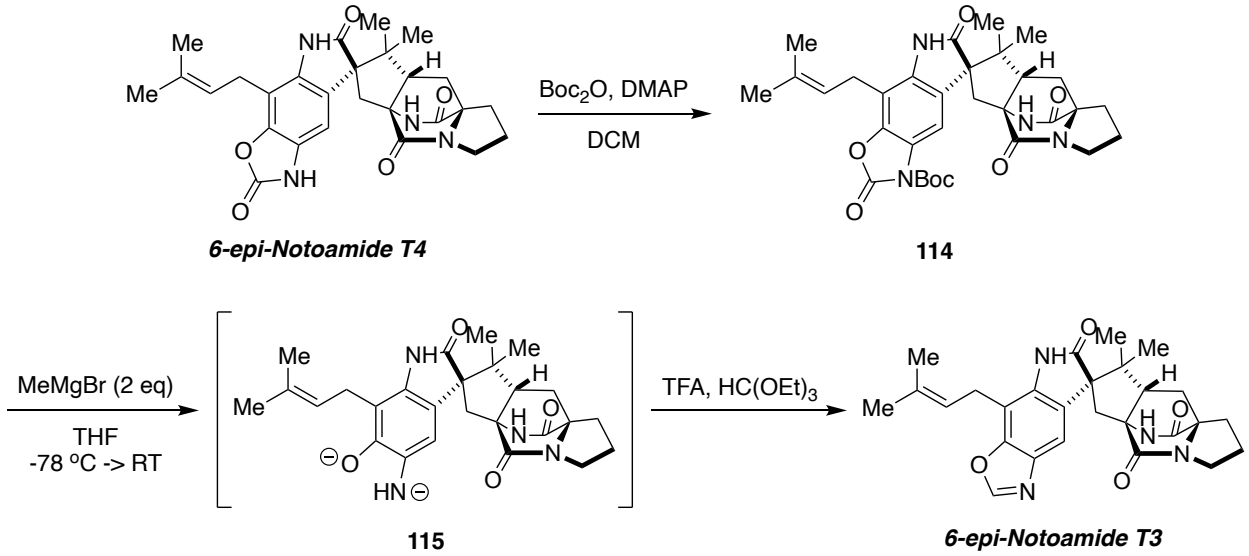

Figure 3.11. Alternative route to 6-*epi*-Notoamide T3.

Synthesis of 6-*epi*-Notoamide T9 will aid in studying the biosynthetic transformations that lead to 6-*epi*-Notoamides T3 and T4, as well as the rest of the metabolites in this new family. This compound could also be ^{13}C labeled, using the method discussed in Chapter 2. This could be used for incorporation studies in *A. protuberus* to determine whether 6-*epi*-Notoamide T9 is indeed an intermediate for T3 and T4. Once this is established, genome mining and heterologous expression, combined with gene knockout studies, could lead to the isolation of new enzymes from this species. If there is an enzyme responsible for oxidative amination of the aromatic ring, this could be an unprecedented discovery.

Uncovering these new metabolites imply that the biosynthesis of secondary metabolites in fungi is much more malleable than originally thought. Considerable effort is being made to elucidate the full functionality of these astonishing fungi.

II. Notoamide TI

i. Biosynthetic Significance

In addition to 6-*epi*-Notoamide T9, there are many prenylated indole alkaloids that contain the spiro-oxindole moiety. In the case of the Notoamides, NotI and NotI' are responsible for the transformation to the spiro-oxindole compounds via epoxidation of the indole (C-2,3) followed by a semi-pinacol rearrangement.[46] While much is known about the biosynthetic pathway of the Notoamides, the enzyme responsible for the IMDA has not yet been heterologously expressed, and thus its role in the pathway cannot be confirmed. While it is suspected that the Diels-Alderase instigates the enantio-divergence in the Notoamide biosynthesis, more investigation needs to be done. To confirm the current hypothesis, the Sherman group utilized these flavin-dependent monooxygenases to determine if NotI/NotI' causes the enantio-divergence between *Aspergillus* species.

(+) and (-)-Stephacidin A were incubated separately with both NotI and NotI' (**Figure 3.12**). Each showed conversion in both enzymes, with (+)-Stephacidin A converting to (-)-Notoamide B and (-)-Stephacidin A forming (+)-Notoamide B. Additionally, each oxidase converted (+)-6-*epi*-Stephacidin A to (+)-Versicolamide B, but neither reacted with (-)-6-*epi*-Stephacidin A.[46] This, coupled with the fact that (-)-Versicolamide B has not been isolated from *A. amoenus*, supports the hypothesis that (-)-6-*epi*-Stephacidin A is produced as a shunt metabolite in this species. This portion of the study shows that while NotI/NotI' is flexible regarding their enantiomeric substrates, the facial selectivity of the oxidation appears to be extremely diastereoselective, with the least-hindered face of the 2,3-disubstituted indole being epoxidized. This supports the hypothesis that NotI/NotI' are not responsible for the enantio-divergence seen between *Aspergillus* species, and this instead occurs earlier in the biosynthetic pathway.

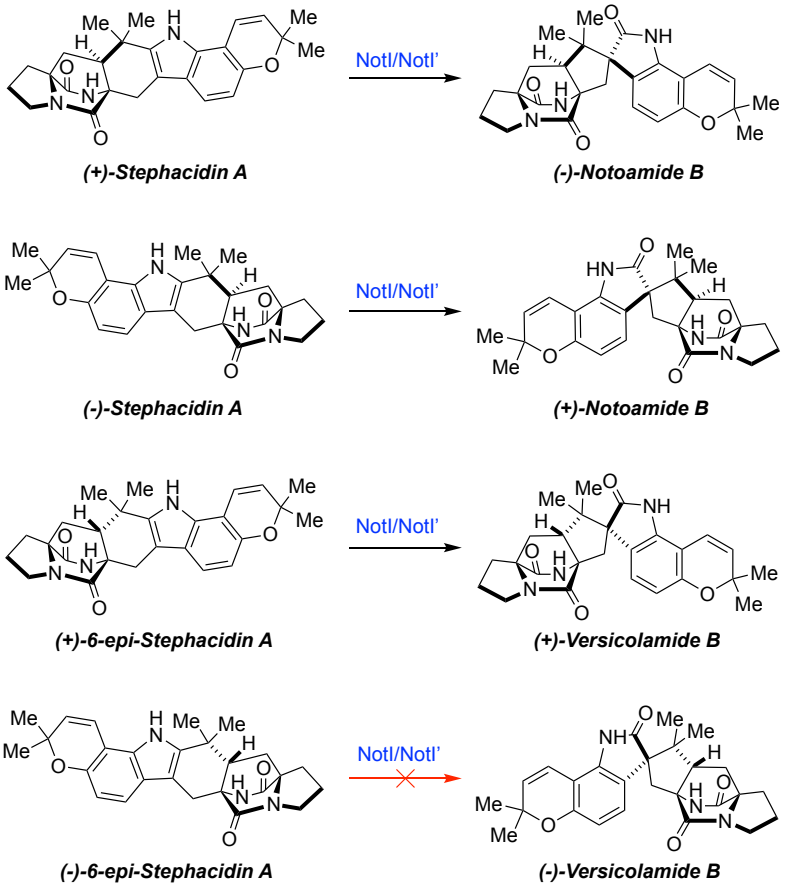

Figure 3.12. Reactions catalyzed by NotI/NotI'.

The Sherman group also sought to confirm the timing of this oxidation/semi-pinacol rearrangement. This was done by using pre-IMDA substrates Brevianamide F, Deoxybrevianamide E, 6-Hydroxydeoxybrevianamide E, Notoamide S, and Notoamide E. Notoamide T, a post-IMDA metabolite, was also used as a substrate. The oxidases proved malleable, showing great substrate tolerance. New products were produced with masses indicative of oxidization. However, they demonstrated poor control, with multiple products produced in many cases—either due to loss of stereocontrol or alternatively oxidized products.[46]

A novel metabolite was discovered upon exposing Notoamide T to NotI/NotI' (**Figure 3.13**). This product was named Notoamide TI, and its structure was determined through NMR

spectroscopy, though the spiro-oxindole stereocenter was not reported.[46] The production of this compound suggests that there may be parallel pathways for the formation of Notoamide B through Notoamide T. Although, precursor incorporation studies do indicate that the pyran ring formation occurs before the pinacol rearrangement, meaning this is plausibly the preferred route.[84] Further studies are needed to learn more about a potential alternative biosynthetic pathway.

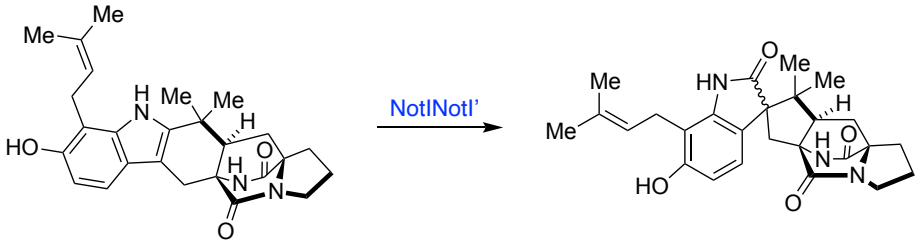

Notoamide T ***Notoamide TI***

Figure 3.13. Formation of novel product Notoamide TI through oxidation/semi-pinacol catalysis of Notoamide T by NotI/NotI'.

ii. Current Work Towards Notoamide TI

As the synthesis of Notoamide TI could potentially be useful in determining the existence of an alternate route to Notoamide B, a route was proposed to synthesize this compound. While the stereochemistry of Notoamide TI was not reported, it was hypothesized that the compound had to contain the *syn* cycloadduct, as oxidation and semi-pinacol rearrangement should not affect the bicyclic core of the compound. Additionally, it would be plausible that the spiro-center connectivity would be the same as Notoamide B, a more advanced metabolite found in the same pathway formed when Stephacidin A reacts with NotI.

Since Notoamide B can be made synthetically from Stephacidin A with Davis Oxaziridine[35,62], it was theorized that Notoamide TI could be produced from Notoamide T in the

same fashion. As discussed earlier in this chapter, Davis Oxaziridine showed poor conversion to the oxindole when in the presence of a free-phenol. With this in mind, and with compound **116** on hand, the semi-pinacol was promoted with Davis Oxaziridine, and the spiro-oxindole was produced in a respectable yield of 78% (**Figure 3.14**). The consistency of stereochemistry with Notoamide TI at the spiro-center was not able to be confirmed yet, as a NOESY was not reported for TI. It was thought that ^{1}H and ^{13}C NMR peaks (and 2D data available) could be compared to those reported in literature once the Claisen rearrangement had occurred.

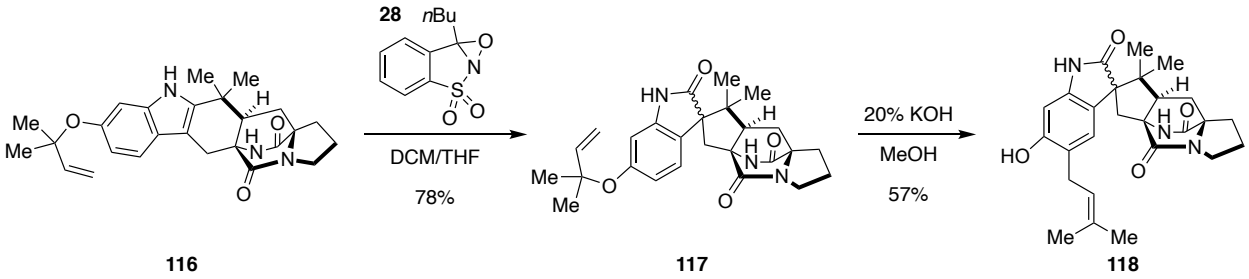

Figure 3.14. Semi-pinacol rearrangement of **116**, followed by exposure to KOH in methanol to promote Claisen rearrangement to **118**.

The Claisen rearrangement was stimulated by 20% KOH in methanol, and prenylation of the C-7 position of the oxindole was expected, as this was the exclusive regioselectivity of related indole substrates. Instead, the Claisen seemed to prefer the C-5 position in a 57% yield, with the recovered starting material. This was evident from the aromatic singlets seen in ^{1}H NMR, rather than the expected doublets. There was also a lack of correlation between these aromatic peaks in COSY NMR. The preference for C-5 in the oxindole substrate could be due to less electron donation from the nitrogen adjacent to the phenyl ring. It has been shown in both theoretical calculations and experimentation that the C-7 position is normally favored in a Claisen rearrangement from 6-hydroxyindole, but this preference decreases with less electron donation from the meta substituent.[90] In a final effort to direct the Claisen to the C-7 position on

this substrate, the remaining starting material (about 3 mg) was microwaved in toluene for one hour (**Figure 3.15**).

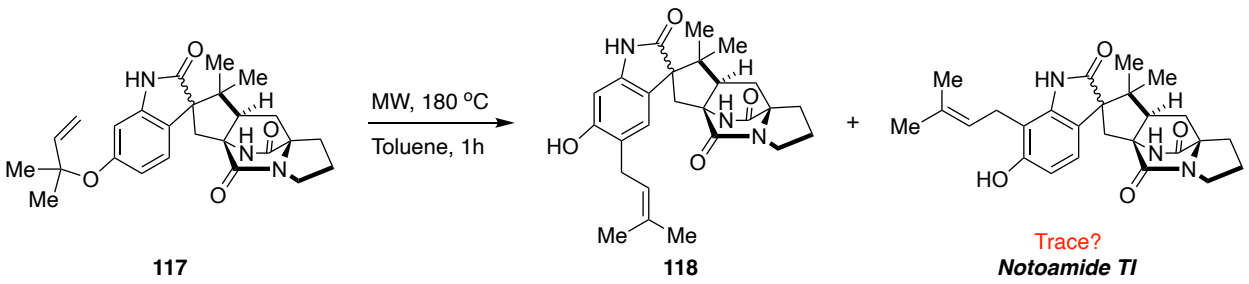

117 118

Figure 3.15. Substrate **117** was microwaved to promote a Claisen rearrangement.

After purification of this reaction, compound **118** was again isolated as a product. Trace amount of another product was isolated, which showed two doublets in the aromatic region, but there was not sufficient material to completely elucidate the structure of the compound.

iii. Future Directions and Conclusions

To remedy this incorrect regioselectivity, an alternative route was proposed in **Figure 3.16** where pinacol follows the Claisen-rearrangement. This route starts with compound **85**, made in the improved 6-*epi*-Notoamide T synthesis. This compound is hydrogenated to remove the benzyl group, exposing the phenol. The phenol is then alkylated with carbonate **69**, forming the reverse prenyl ether. This reaction results in Claisen rearrangement to the C-7 position. If this does not occur, or does not completely occur, the Claisen can be stimulated with use of the microwave or base. When executed on related indole substrates, the regioselectivity has always favored the C-7 position. Last, the pinacol rearrangement will be executed using Davis Oxaziridine. This may result in low yield due to the unprotected phenol but has been proven to work in the presence of one before. However, the phenol could be Boc-protected before the rearrangement, if necessary.

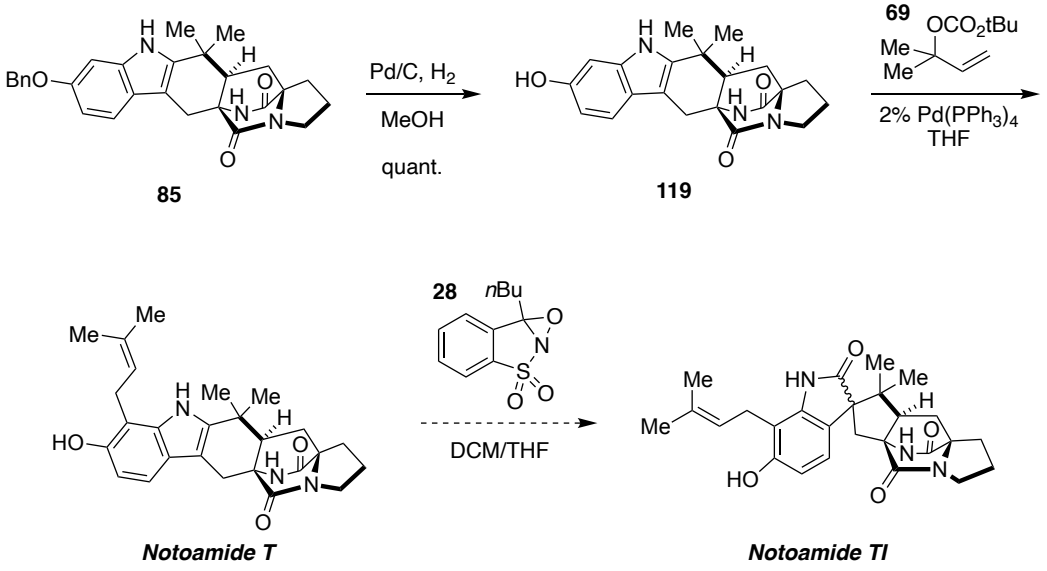

Figure 3.16. Alternative route to Notoamide TI, performing the Claisen rearrangement before the semi-pinacol.

If Davis Oxaziridine does not produce the correct diastereomer for Notoamide TI, other conditions for the pinacol rearrangement could be explored. One possibility are conditions used by Glinka *et al.* when studying the regioselectivity of indole oxidation on Paraherquamide, seen in **Figure 3.17**.[91] These conditions produced the *R* diastereomer at the spiro-center, opposite from the *S* diastereomer of Notoamide B (synthesized using Davis Oxaziridine).

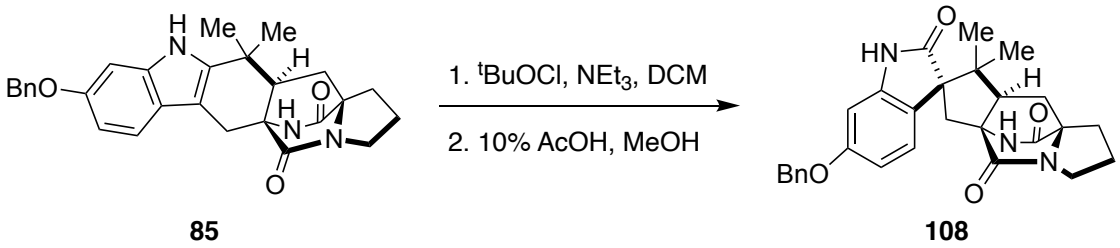

Figure 3.17. Alternative conditions for the semi-pinacol rearrangement using *tert*-butyl hypochlorite.

Synthesis of this metabolite could unlock knew knowledge about the biosynthetic pathways in the *Aspergillus* species. This synthesis could be adapted to label the molecule with ^{13}C using previously established methods, discussed in Chapter 2.[1] This could be incorporated into *A. protuberus* and *A. amoenus* to see if any new natural products are produced. Novel metabolites would signal an alternative oxidative pathway in the fungi. Alternatively, incorporation into Versicolamide B would indicate that the pyran ring formation from NotD/NotD' and pinacol rearrangement by NotI/NotI' are interchangeable, or that an alternate oxidase can catalyze the pyran ring formation on Notoamide TI. Synthesis of Notoamide TI will further elucidate the biogenesis of the Notoamides and related compounds.

Chapter 4: Total Synthesis of 6-epi-Notoamides T10-T12

I. Isolation and Biosynthetic Significance

As discussed in the previous chapter (Chapter 3), racemic [^{13}C]$_2$-6-*epi*-Notoamide T was used in precursor incorporation experiments with *Aspergillus protuberus*.[65] It was expected that both 6-*epi*-Stephacidin A and Versicolamide B would be isolated from the culture as per the biosynthetic route: (+)-6-*epi*-Notoamide T is oxidized and cyclized by NotD' to 6-*epi*-Stephacidin A, followed by oxidation and pinacol rearrangement by NotI' to form Versicolamide B (**Figure 4.1**).

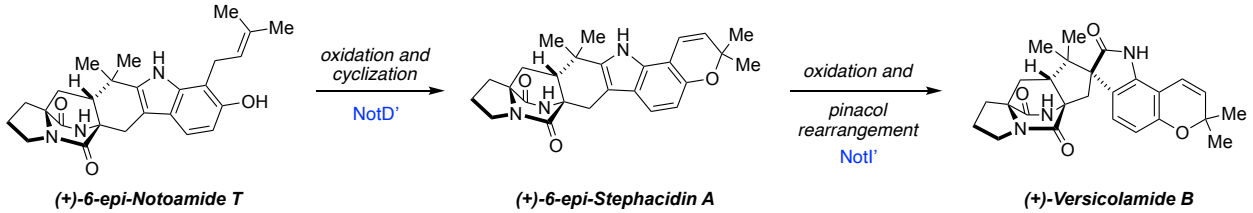

Figure 4.1. Biogenesis of Versicolamide B through 6-*epi*-Notoamide T then 6-*epi*-Stephacidin A.

As seen in **Figure 4.2**, 6-*epi*-Stephacidin A was not observed as one of the compounds isolated after the precursor study, though Versicolamide B was found (along with the new metabolites, see Chapter 3).[65] While 6-*epi*-Stephacidin A was not observed in the ^{13}C study, it could have initially been produced and later converted into Versicolamide B. Indeed, when the fungus was cultured on normal agar medium, ^{1}H NMR revealed that 6-*epi*-Stephacidin A only appeared in the culture after 6 days of incubation then disappeared.[65]

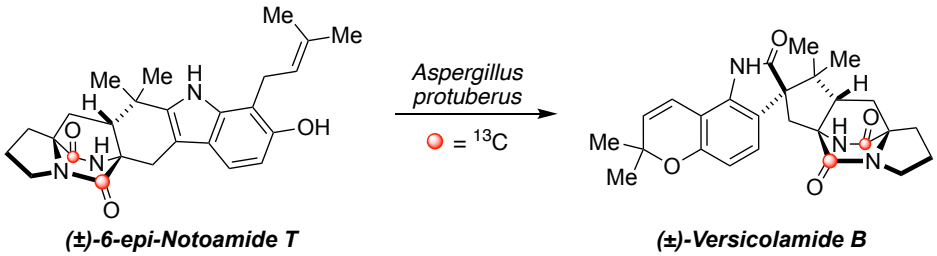

Figure 4.2. Precursor incorporation of [^{13}C]$_2$-6-*epi*-Notoamide T in *Aspergillus protuberus* produced [^{13}C]$_2$-Versicolamide B (along with 7 novel metabolites – see **Figure 3.1**).

In effort to show conversion of 6-*epi*-Notoamide T to 6-*epi*-Stephacidin A, non-labeled (±)-6-*epi*-Notoamide T was used in precursor incorporation experiments on minimal media agar plates (**Figure 4.3**). After 16 days, extraction yielded (±)-6-*epi*-Stephacidin A and four new (±)-6-*epi*-Notoamides T9-12.[65] These two incorporation studies confirm that 6-*epi*-Notoamide T is a precursor to both 6-*epi*-Stephacidin A and Versicolamide. 6-*epi*-Notoamide T is also a precursor to the new metabolites discovered, including the oxidized compounds 6-*epi*-Notoamide T10-12.

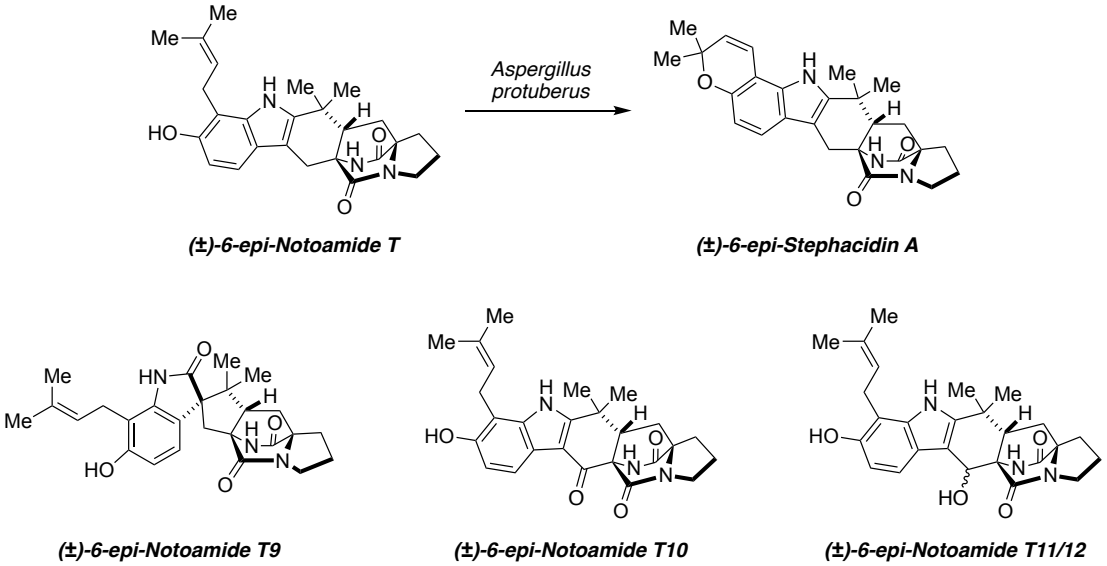

Figure 4.3. Resulting products from *Aspergillus protuberus* incorporation study using unlabeled, racemic 6-*epi*-Notoamide T: (±)-6-epi-Stephacidin A and (±)-6-*epi*-Notoamides T9-12.

It's of interest to see how exactly 6-*epi*-Notoamide T is transformed into 6-*epi*-Notoamide T10-12, as these are not produced by the fungus under natural conditions. This likely means dormant tailoring genes have been activated by the presence of an unnatural enantiomer of 6-*epi*-Notoamide T, and we could discover more about the biosynthetic pathway of these compounds via incorporation studies of these new metabolites in *Aspergillus protuberus*. It could be possible that T10 is a precursor to T11/12 or vice versa. We could also elucidate the enzymes catalyzing these transformations and determine if these are shunt metabolites or have a purpose in the fungus.

II. Synthesis of 6-*epi*-Notoamide T10-12

For these reasons, I set out to synthesize 6-*epi*-Notoamides T10-12. The initial route proposed for the synthesis of these compounds can be seen in **Figure 4.4**. The *anti*-diastereomer **86** would be oxidized with DDQ. This should be selective for the methylene on C-3 of the indole, as seen in precedent set by Fujimori *et al.*, Sissouma *et al.*, and Gautam *et al.*[80,81,92] Next, hydrogenation of the benzyl protecting group will take place as before, using Pd/C and hydrogen gas. Then, the alkylation of the phenol will be catalyzed with palladium, which should be followed by the Claisen rearrangement, forming 6-*epi*-Notoamide T10. The newly formed ketone should be able to be selectively reduced with $NaBH_4$, leaving the amides unaffected, resulting in 6-*epi*-Notoamide T11/12. This is following precedent set by Dilek *et al.* and Stahl *et al.*[82,93]

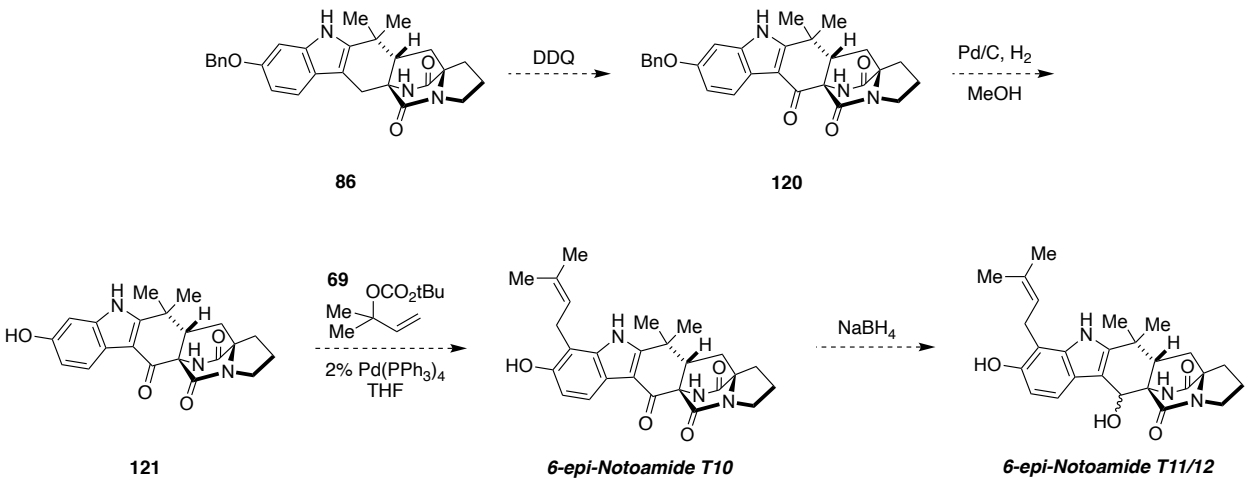

Figure 4.4. Proposed route for synthesis of 6-*epi*-Notoamide T10 and 6-*epi*-Notoamide T11/12

Sufficient quantities of *syn* diastereomer **85** was on hand, due to separation of the diastereomers after the IMDA reaction when synthesizing 6-*epi*-Notoamide T. It was decided that this compound could be put to good use in a trial run of the route planned to synthesize 6-*epi*-Notoamide T10 (**Figure 4.5**). The oxidation of the methylene off C-3 with DDQ went as planned, forming **89**. This was confirmed by the appearance of a peak on the ^{13}C NMR at 181.04 ppm, well within the position of a carbonyl and incredibly close to the reported position of that carbon on 6-*epi*-Notoamide T10 (181.2 ppm in DMSO). Additionally, the ^{1}H NMR showed disappearance of the doublets produced by H_a and H_b, normally at 3.68 ppm and 2.76 ppm. Deprotection of the benzyl group was also successful, with disappearance of the aromatic protons (between 6.95 and 7.80 ppm) and methylene (5.25 ppm) in the ^{1}H NMR of **90**. The last step was not tested due to the robust nature of the reaction.

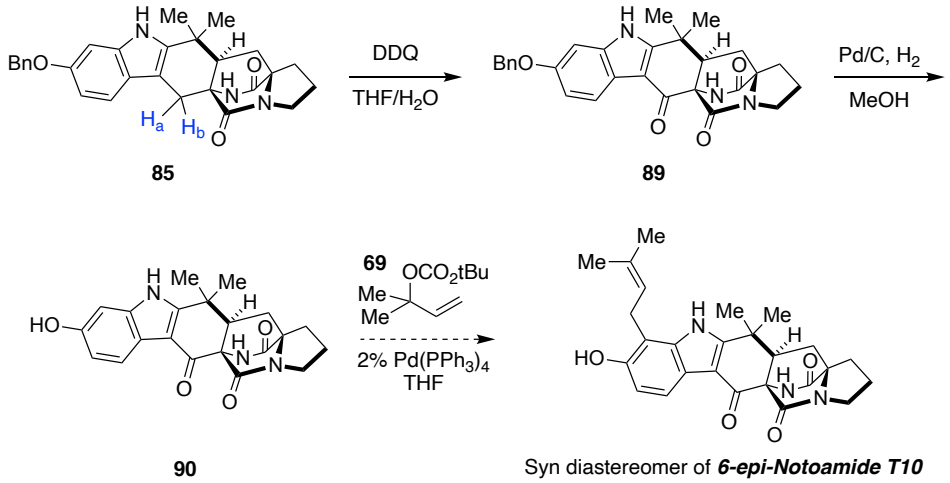

Figure 4.5. Partial synthesis of the *syn* diastereomer of 6-*epi*-Notoamide T10 to test oxidation of the cyclohexane methylene and hydrogenation of the benzyl group.

As seen in **Figure 4.6**, the analogous synthesis of 6-*epi*-Notoamide T10 went smoothly. DDQ was used for the oxidation off of C-3 resulting in a 70% yield of **86**. Again, this was confirmed by loss of H_a and H_b doublets. Hydrogenation of the benzyl group was incredibly clean with a near quantitative yield. The benzyl protons (7.26-7.55 ppm and 5.12 ppm) are not present in the proton NMR of **121**, and the ^{13}C NMR still shows the ketone peak at 183.64 ppm. With **121** in hand, there was only one more step to 6-*epi*-Notoamide T10. The alkylation produced both the ether product (**122**) as well as 6-*epi*-Notoamide T10, with a modest combined yield of 31%. KOH in MeOH could catalyze the Claisen rearrangement, converting 38% of the remaining ether product to the natural product. A broad triplet could be seen at 5.25 ppm, signifying the methyne proton on the prenyl tail, confirming the Claisen. New methyl peaks from the prenyl group could also be seen at 1.68 and 1.81 ppm.

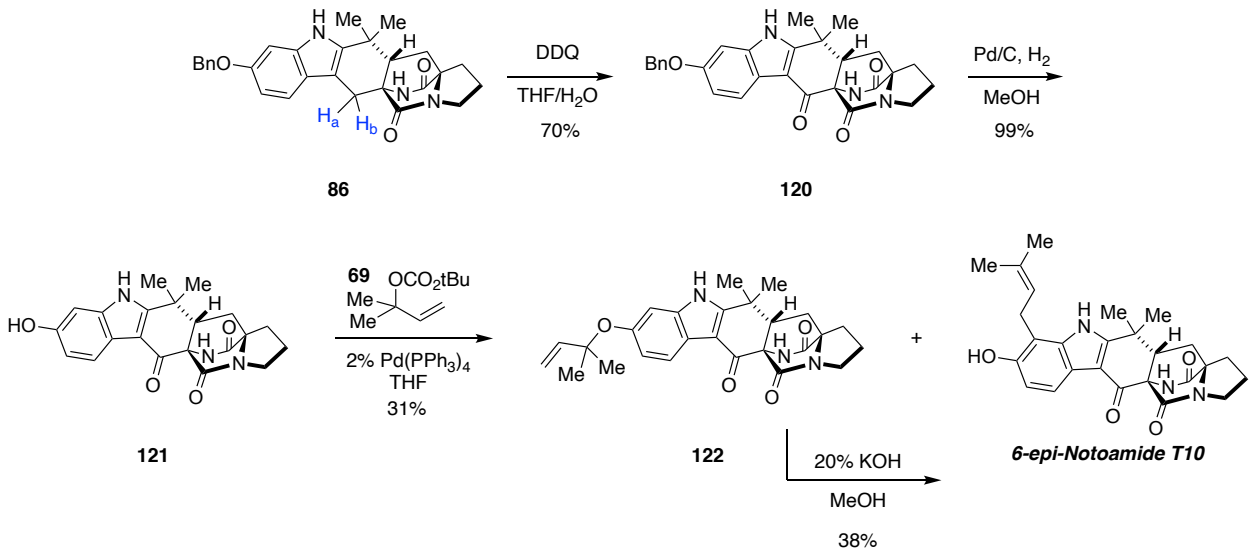

Figure 4.6. Synthesis of 6-*epi*-Notoamide T10.

It was also found that 6-*epi*-Notoamide T10 could be made directly from 6-*epi*-Notoamide T, though with a lower yielding oxidation reaction (**Figure 4.7**). Though the overall yield would be lower, this route might be optimal if 6-*epi*-Notoamide T could isolated from fungi in the future.

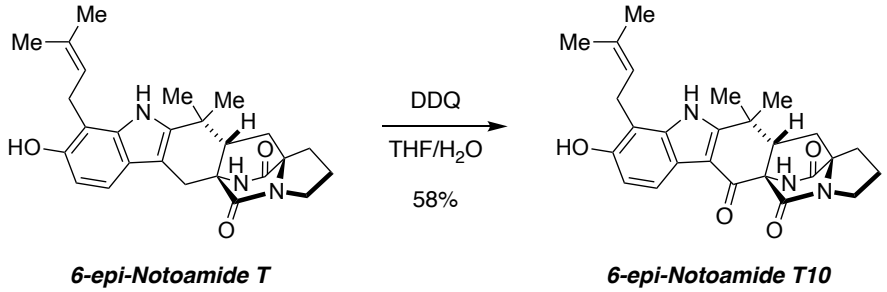

Figure 4.7. 6-*epi*-Notoamide T10 can also be made directly from 6-*epi*-Notoamide T using DDQ.

The synthesis of 6-*epi*-Notoamide T11/12 was done by reducing the newly installed ketone on 6-*epi*-Notoamide T10 to an alcohol (**Figure 4.8**). As T11 and T12 are diastereomers at

the alcohol carbon, this reaction did not need to be stereoselective. Sodium borohydride was selected to reduce the ketone, as it should do so without disturbing the amides or prenyl group.

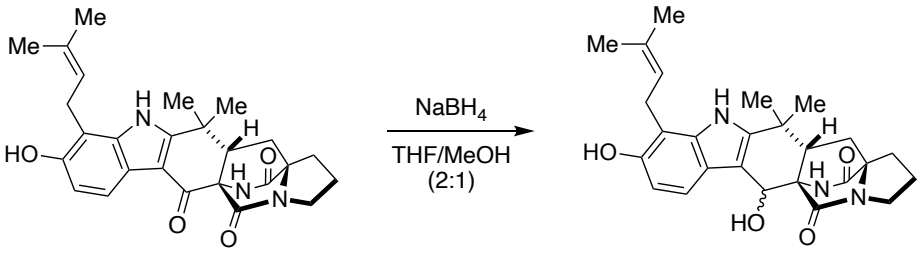

6-epi-Notoamide T10 ***6-epi-Notoamide T11/12* (123)**

Figure 4.8. Synthesis of 6-*epi*-Notoamide T11/12.

This reaction was carried out on less than a 3 milligram scale. Corresponding TLC is shown in **Figure 4.9**. After purification of the reaction, sub-milligram quantities were isolated from a preparative TLC plate. Due to the precision of the balances available, a confident yield of this reaction is not available.

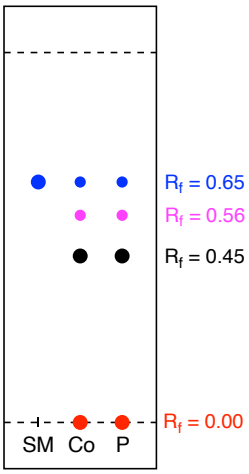

Figure 4.9. TLC of reaction shown in **Figure 4.8**. Lane 1: starting material 6-*epi*-Notoamide T10, Lane 2: Co-spot, Lane 3: product.

By PTLC in 15% MeOH/DCM, the reaction appeared to have yielded product, though there was not complete consumption of starting material. The product lane showed a strong spot

with an R_f of 0.45 (referred to as product **123a**), a faint spot at 0.56 (referred to as product **123b**), and a faint spot of starting material at 0.65 (along with degraded material on the baseline). If 6-*epi*-Notoamide T11/12 had indeed been formed, these spots would make sense, as the alcohol product should be more polar on silica than the starting ketone. The products may have separated into both spots (one at 0.56 and one at 0.45), or both products could be in one spot.

Mass spectra was taken for both products, with the expected exact mass being 472.2212 amu. Product **123a** exhibited a matching mass of 472.2210 amu, which is a mass error of -0.4235 ppm. Product **123b** did not produce a matching mass.

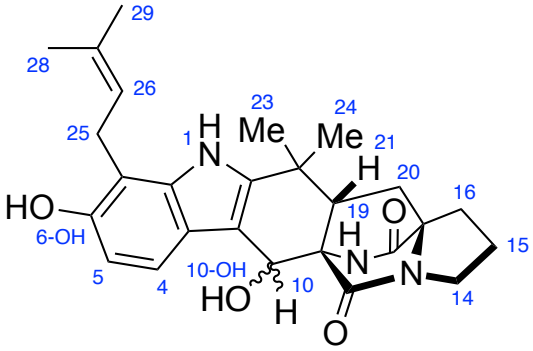

6-epi-Notoamide T11/12

Figure 4.10. Numbering system for 6-*epi*-Notoamide T11/12.

Proton NMR spectra were also collected for both **123a** and **123b** (see numbering system in **Figure 4.10**). Product **123b** was clearly not either of the desired products. Identifying product **123a** was a bit more complex. The proton NMR (in DMSO) clearly had many of the peaks expected of T11 and/or T12. The doublets for 4 and 5 produced the expected J-values of 8.3 Hz, though the shifts were different than expected. While T11 produces doublets at 6.56 and 7.08 ppm, and T12 produces these peaks at 6.54 and 7.28 ppm, **123a** has doublets at 6.75 and 7.66

ppm. For 26, the expected values from T11/12 were broad triplets of 5.24 ppm (J = 6.9 Hz)/5.22 ppm (J = 6.7 Hz), respectively. **123a** produced a matching broad triplet at 5.21 ppm (J = 6.8 Hz).

The diagnostic signals for this molecule are 10-H and 10-OH. In T11, 10-H exhibits at 5.17 ppm (s) and 10-OH at 5.86 ppm (s). In T12, these peaks appear as doublets, where 10-H shifts at 5.72 ppm (9.0) and 10-OH appears at 4.87 (9.0). The NMR of **123a** has a few peaks that may represent these, though it is not clear. There are clear peaks at 6.87 (s), 6.63 (d, 2.3), 6.58 (s), and 4.08 (d, 9.0) ppm. While there are 2 singlets and 2 doublets, the shifts are off, and one doublet doesn't have a similar J value. That being said, the J-value for the doublet at 4.08 ppm is promising. It's also possible that the other doublet is under the DCM peak at 5.74 ppm. Additionally, hydrogen bonding could be affecting the peaks, and the discrepancy in shift could be due to a concentration dependency.

Of course, a COSY or NOESY would be quite helpful in determining the structure, but these were not obtained before the compound was lost to decomposition.

Due to the extremely accurate match in mass spectra and general similarity of the proton NMR, it is likely that 6-*epi*-Notoamide T11, T12, or both have been synthesized. But currently, without further data, it is not possible to be certain of this synthesis.

Chapter 5: Towards the Total Synthesis of Citrinalin C

I. Biosynthetic Significance

The Citrinalins are a newly discovered family of the prenylated indole alkaloids. Citrinalin A and B were isolated from *Penicillium citrinum* in 2010 by the Berlinck group (**Figure 5.1**).[94] These compounds are part of the decarbonylated alkaloids—named for alkaloids that do not contain a bicyclic core, likely as a result of decarbonylation of the core.[95] This family is also comprised of the Citrinadins[95–99], PF1270's[100], Cyclopiamines[101–103] and Penicimutamides[104,105] (**Figure 5.1**).

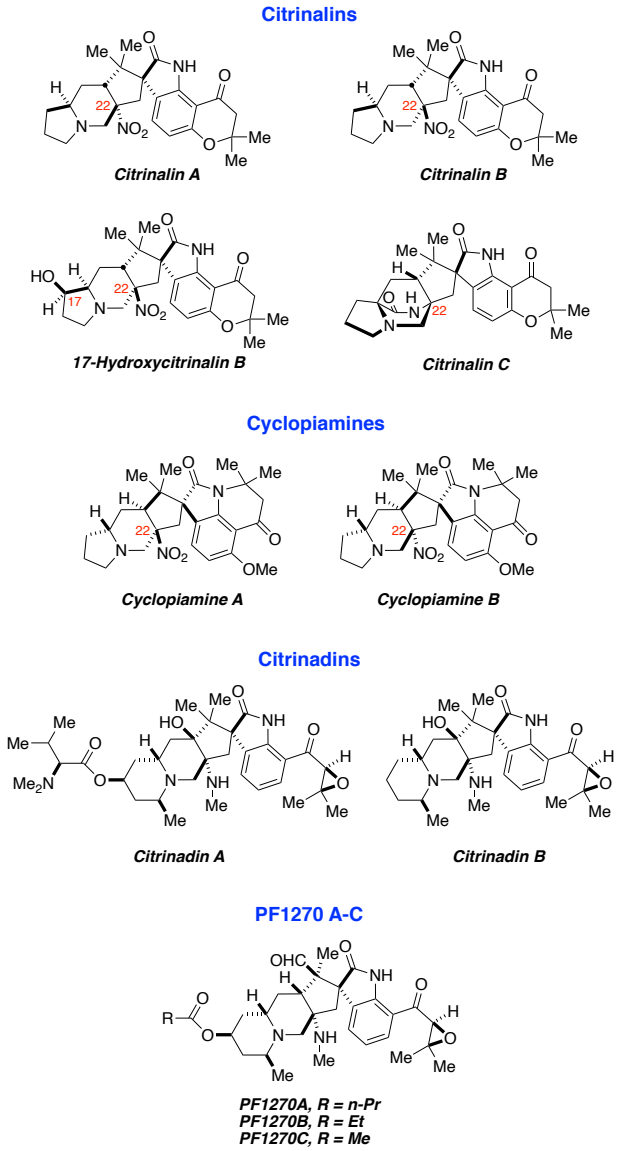

Figure 5.1. Decarbonylated prenylated indole alkaloids.

In 2014, Berlinck and coworkers performed isolation studies with *P. citrinum* F53.[101] Through these initial studies, 17-hydroxycitrinalin B and Citrinalin C were isolated. In further studies, it was found that [1-^{13}C]glucose, [U-^{13}C]anthranilic acid, and [U-^{13}C]ornithine were incorporated into Citrinalin A, Citrinalin B, and 17-Hydroxycitrinalin B (**Figure 5.2**).[101] While there have been no incorporation studies before Berlinck's on the decarbonylated alkaloids reported here, studies on similar prenylated indole alkaloids all suggest tryptophan, proline, and

two isoprene units as biosynthetic precursors. As ornithine is a known biosynthetic precursor to proline, these studies support an analogous biosynthesis for these compounds.[101]

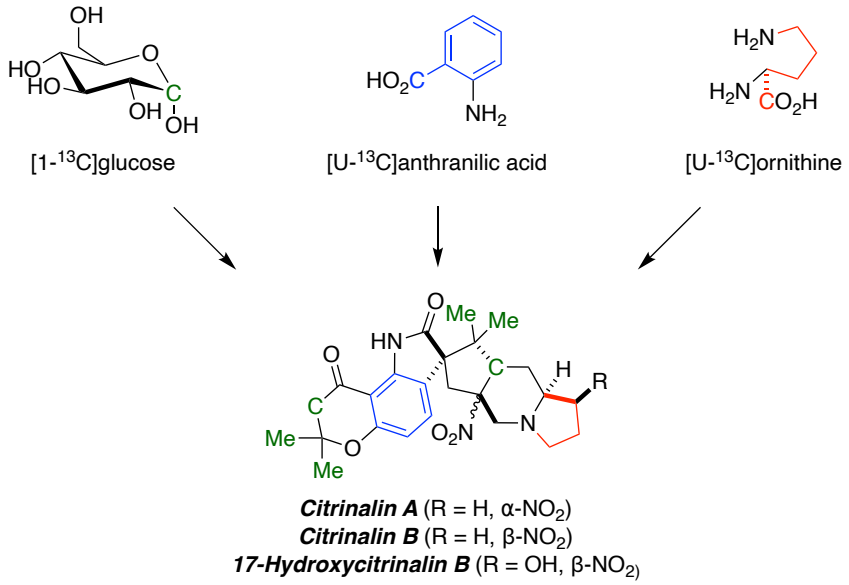

Figure 5.2. ^{13}C incorporation studies of *P. citrinum* F53 reveal that glucose (green), anthranilic acid (blue) and ornithine (red) are biosynthetic precursors to the Citrinalins.

Isolation of new metabolite Citrinalin C led to the current theory that Citrinalins A, B, and the rest of the decarbonylated alkaloids arise from decarbonylated deconstruction of a precursor with a bicyclic core. The loss of CO from the bicyclo[2.2.2]diazaoctane ring is a rare, if not unprecedented biological transformation.

There have been two different proposals for the arisal of Citrinalins A and B through Citrinalin C. The first being that the amide bridge on Citrinalin C is hydrolyzed and followed by decarboxylation (**Figure 5.3**). Then, the amino-group is oxidized to a nitro group, resulting in Citrinalin A. Citrinalin B could then arise from a nitronate iminium intermediate (**124**).[101] This is similar to the proposed biosynthesis of Cyclopiamine B, which has a similar structure.[95]

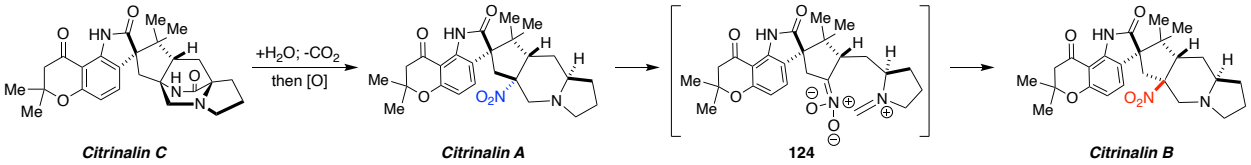

Figure 5.3. First proposed biosynthetic pathway to form Citrinalins A and B.

Alternatively, since Citrinalin A and B only differ in stereochemistry at C-22, Williams has suggested that they both arise from a common planar intermediate formed by the loss of CO (**Figure 5.4**). There are two mechanisms proposed regarding the formation of a planar intermediate. The first mechanism suggested is an enzymatic ring-opening of the bicyclo[2.2.2]diazaoctane core followed by iminium ion formation, CO loss, and hydride reduction. The second possibility is a radical-based decarbonylative process which would be quenched by an H atom on either the α or β face.

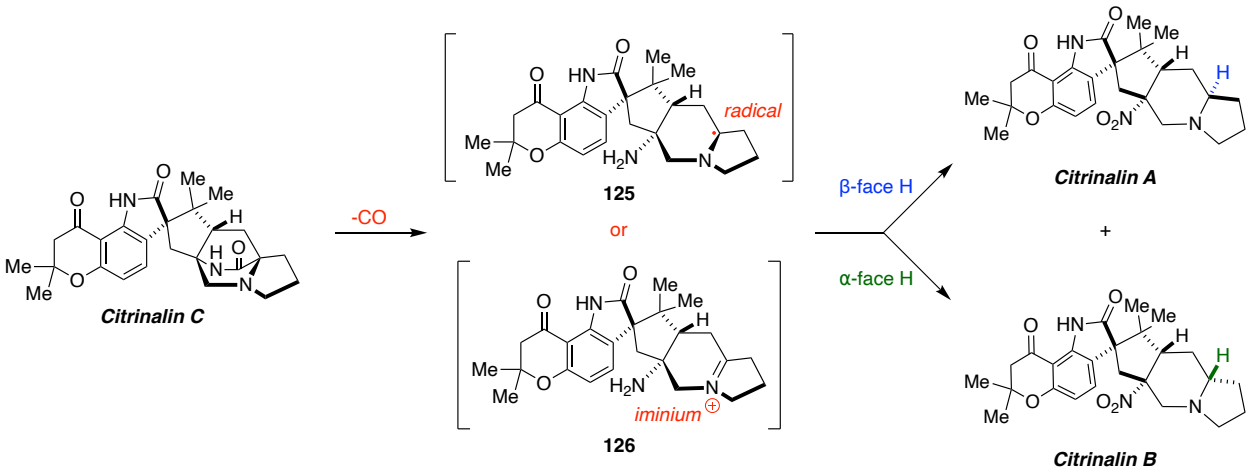

Figure 5.4. Possible biosynthetic pathway from Citrinalin C to Citrinalins A and B through a common planar intermediate.

Given that this decarbonylation is an exceptionally unique biochemical transformation, it is of great interest to elucidate the mechanism of how this occurs. It is also intriguing that the amine is oxidized by a net 8 electrons to the nitro group, a rare occurrence in natural products.

This oxidation seems to be mediated by a unique flavoenzyme encoded by *citF* which has been discovered in a biosynthetic gene cluster.[101] Synthesis of Citrinalin C could confirm one of the hypothesized biosyntheses for this family of compounds and could help identify the enzymes that mediate these novel and intriguing transformations.

II. Previous Syntheses

While Sarpong and coworkers reported the synthesis of *ent*-Citrinalin B in 2014[101], Citrinalin B does not have the bicyclic core formed by the IMDA so this was not a plausible route for the synthesis of Citrinalin C. Still, this route establishes conditions for oxidation of the pyran ring to the chromanone moiety found on the Citrinalins. This oxidation will be employed in the route to Citrinalin C. The route proposed in this chapter more closely follows Greshock's 2008 synthesis of Versicolamide B[35], which is overviewed in Chapter 1, section VII-ix.

III. Towards the Total Synthesis of Citrinalin C

Initially, it was proposed that bicyclic compound **88** could be used for the synthesis of Citrinalin C, as this compound was on hand from the 6-*epi*-Notoamide T synthesis (**Figure 2.11**). It was thought that starting with this compound could eliminate the need to start from early material and instead the free phenol could be alkylated with carbonate **127** (**Figure 5.5**). The compound could then undergo a Claisen rearrangement to form 6-*epi*-Stephacidin A. Once 6-*epi*-Stephacidin A is achieved, DIBAL could be used to selectively reduce the tertiary amide to the tertiary amine.[106] Similar to the synthesis of Versicolamide B, Davis Oxaziridine would be employed to carry out the pinacol rearrangement to form the spiro-oxindole.[35] In this case, there is a tertiary amine that is susceptible to oxidation by the oxaziridine. Similar to Greshock's synthesis of Marcfortine C, PPTS can be used to protect the amine, and has shown to be robust enough to be unaffected by the oxaziridine while not interfering with the sensitive reagent.[106] In

accordance with the synthesis of *ent*-Citrinalin B, a Wacker oxidation can be used to oxidize the pyran ring, completing the synthesis of Citrinalin C.[101]

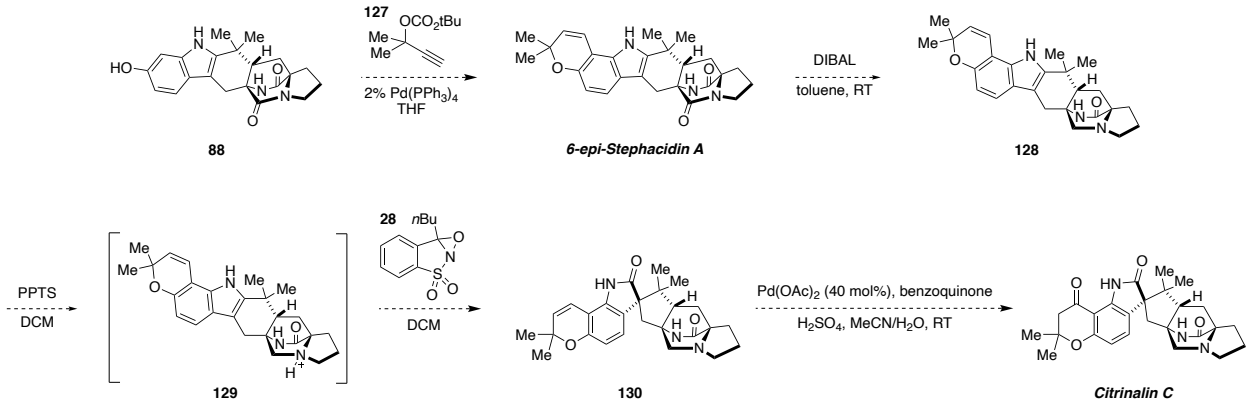

Figure 5.5. First proposed synthesis of Citrinalin C.

Unfortunately, formation of the pyran ring could not be achieved via the palladium catalyzed reaction with carbonate **127** (**Figure 5.6**). Only starting material was recovered from the reaction.

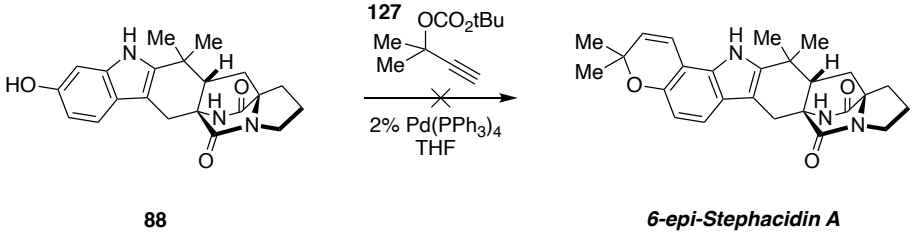

Figure 5.6. Alkylation of phenol catalyzed by tetrakis(triphenylphosphine)palladium(0) was unsuccessful.

As cupric chloride dihydrate was used by Cox *et al.* to form a propargyl ether in pursuit of paraherquamide F[39], an analogous reaction was attempted on **88** (**Figure 5.7**). When this was ineffective, the substrate was changed to the diketopiperazine free-phenol. Both the copper and palladium catalysts were used to no avail. After further reading of past dissertations from the Williams group, it seems that while many attempts have been made to install the pyran ring on

more complex products, they have all resulted in failure. Ultimately, this synthesis was abandoned, and a new synthesis was proposed from scratch.

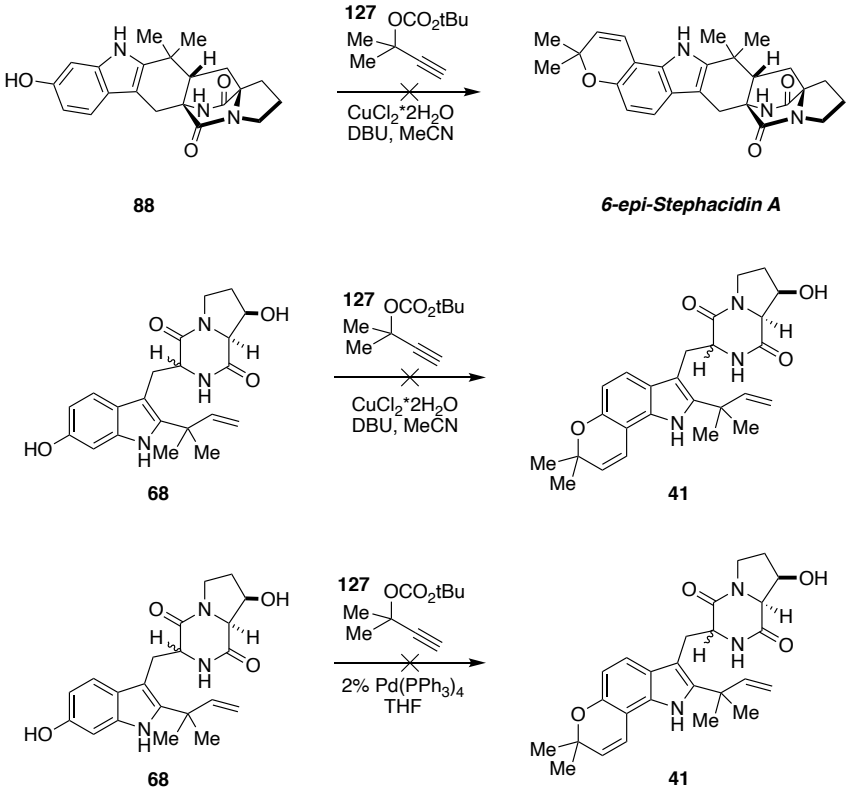

Figure 5.7. Other methods to alkylate phenol were also unsuccessful.

This new synthesis would parallel the 6-*epi*-Notoamide T synthesis from Chapter 2, aside from the addition of the pyran ring earlier in the synthesis. The IMDA reaction to form Stephacidin A (as well as earlier reactions in the synthesis) have shown to be less particular than those of 6-*epi*-Notoamide T, consistently showing higher yields.[85] It was thought that the reactions in the 6-*epi*-Notoamide T synthesis would work as well or better with the pyran ring substituent in place of the protected phenol.

As with the synthesis of 6-*epi*-Notoamide T, nitrophenol **15** was benzyl protected and a Raney nickel and hydrazine hydrate was used to form protected hydroxyindole **16** (**Figure 5.8**).

The indole was then deprotected using Pd/C and hydrogen gas. Cupric chloride dihydrate was then employed to alkylate the free phenol, forming the propargyl ether.

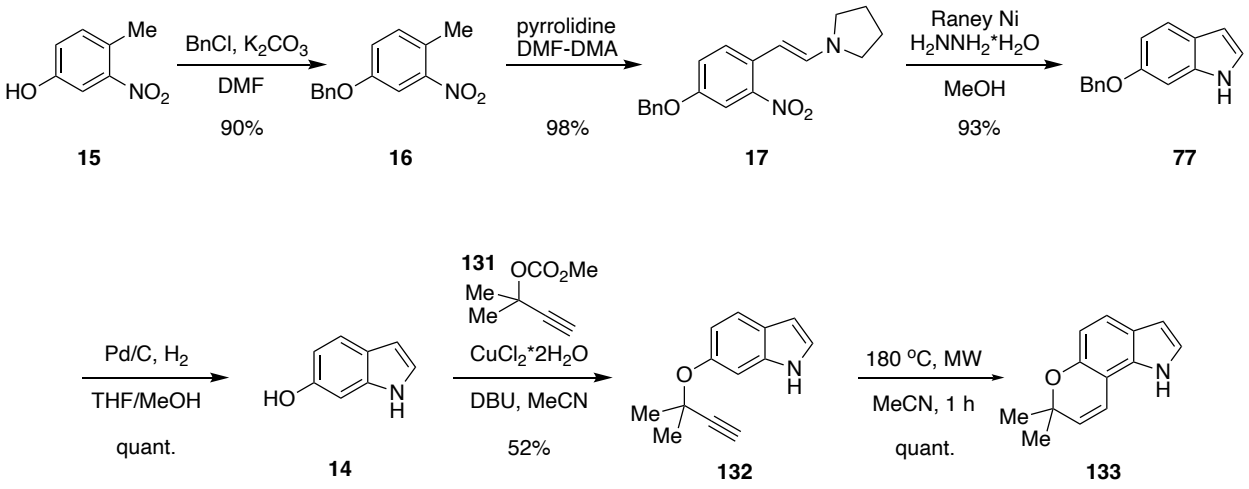

Figure 5.8. Synthesis of pyranoindole **133**.

While some previous routes have formed the pyran ring using 3-chloro-3-methyl-1-butyne,[69] these routes resulted in much poorer yields than Guerrero *et al.*, who reported a yield of 71% using carbonate **131**.[107] Carbonate **131** was on hand, so it was used in the reaction. When literature conditions resulted in poor yields (entry 1, **Table 5.1**), the methyl carbonate counterpart was tested, with similar results. Next, raising the equivalents of both the carbonate and base (DBU) was attempted, resulting in a slightly higher yield of 42%. Raising the amount of carbonate while keeping the DBU constant was also tried, but this resulted in lower yields than the initial conditions. When both the carbonate and DBU equivalents were increased further (to 2 and 2.1, respectively) a 37% yield was achieved. When 3 equivalents of each were tested, a modest yield of 52% was achieved. While this was not optimal, the synthesis was continued at this point.

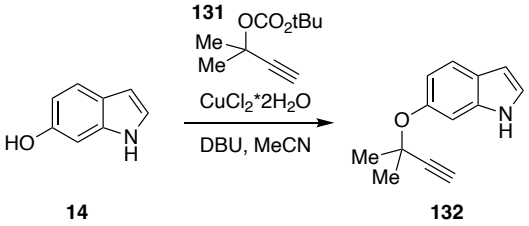

Table 5.1. Conditions tested for propargyl ether.

Entry	Carbonate (eq)	DBU (eq)	Yield
1	1	1.1	29%
2	1.5	1.5	42%
3	2	1.1	28%
4	2	2.1	37%
5	3	3	52%

Next, in **Figure 5.9**, the C-3 position was chlorinated in a 90% yield, again following the Danishefsky procedure for prenylation. Then, chlorinated indole **134** was exposed to BBN complex **18** in the presence of triethylamine, and prenylated indole **135** was formed with a yield of 69%. Gramine derivative **136** was made using formaldehyde and dimethylamine, then coupled with glycine derivative **23** to give imine **137**. Hydrolysis of **137** yielded tryptophan derivative **138** with a 65% yield over the last three steps. This compound was then coupled with Fmoc-protected hydroxyproline **65**, giving **139** in a 78% yield.

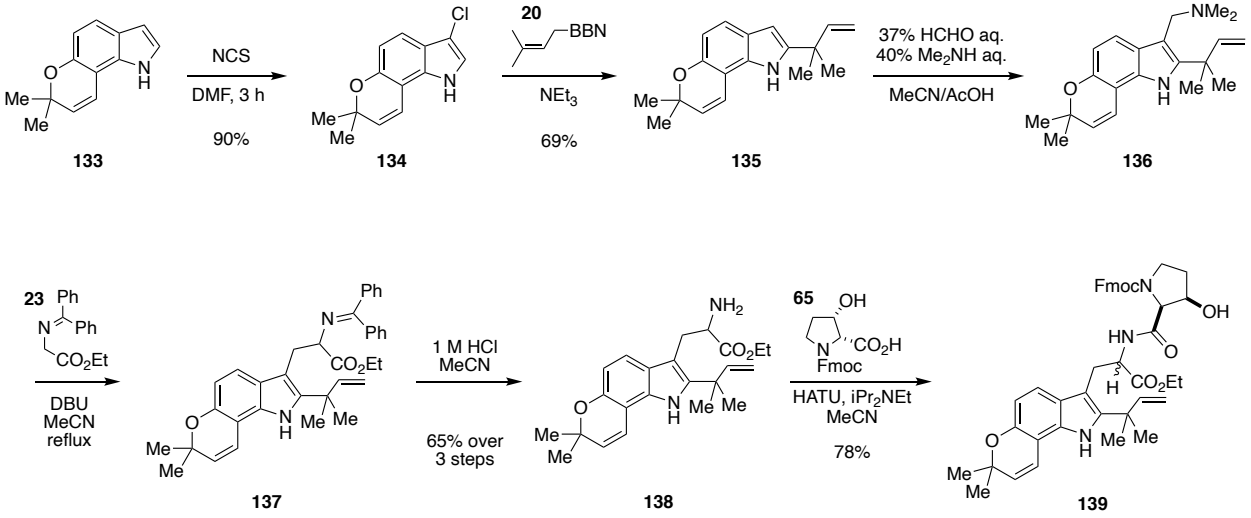

Figure 5.9. Synthesis of Citrinalin C, synthesis from pyranoindole **133** to dipeptide **139**.

However, when the compound was treated with triethylamine in the presence of 2-hydroxypyridine, the compound completely degraded rather than deprotecting and cyclizing into diketopiperazine **41** (**Figure 5.10**). An alternative method would be needed to form the diketopiperazine.

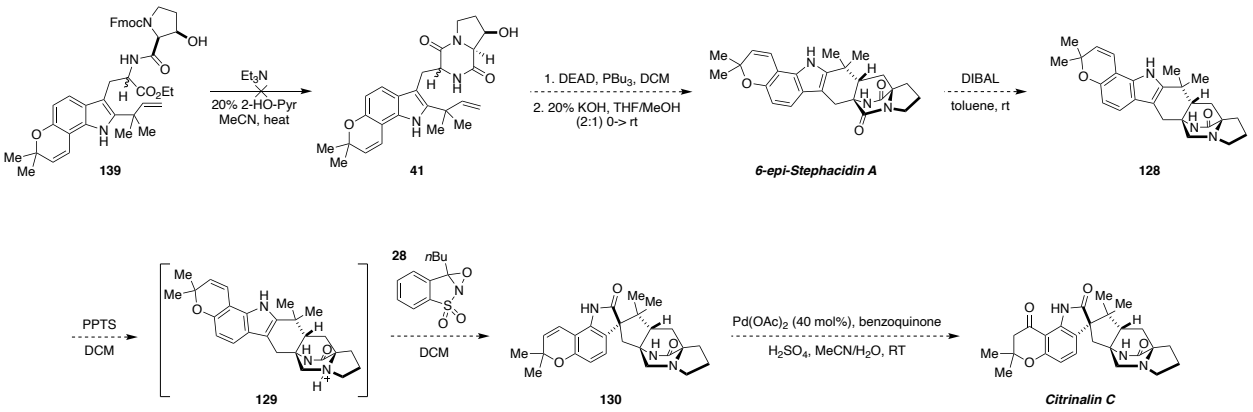

Figure 5.10. Dipeptide product degraded during deprotection and cyclization. Synthesis could not be completed.

IV. Future Directions and Conclusions

As seen in **Figure 5.11**, newly proposed conditions would follow Greshock *et al.*'s work in the synthesis of Stephacidin A and Notoamide B.[62] Morpholine would be used in place of the previous conditions to deprotect the Fmoc group, which should result in the cyclization into the diketopiperazine ring, forming **41**.

From this point, the remaining steps in **Figure 5.10** should be viable. The hydroxy group on the 5 membered ring can be eliminated with Mitsunobu-type conditions, then the intramolecular Diels-Alder reaction can proceed. The IMDA conditions used for 6-*epi*-Notoamide T may be optimal, otherwise, the secondary amide could be treated with Me_3OBF_4 and Cs_2CO_3 to provide the lactim ether. From there, 20% KOH in MeOH should affect the

tautomerization and subsequent IMDA reaction, forming Stephacidin A and 6-*epi*-Stephacidin A. The remaining steps to Citrinalin C are the same as those proposed above.

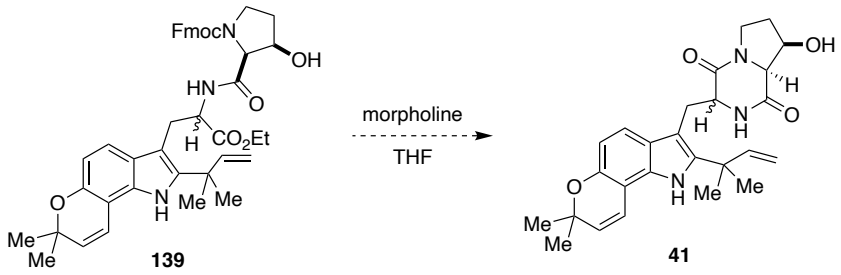

Figure 5.11. Potential conditions to make diketopiperazine **41**.

An alternative route is also proposed in **Figure 5.12**. This route simply rearranges the transformations, performing the pinacol rearrangement with Davis Oxaziridine before the Diels-Alder reaction. The pyranoindole-spiro-diketopiperazine substrate has been shown to favor the *anti*-product in the IMDA reaction, with calculations predicting a 4-7 kcal/mol preference for this product.[71,108] It has also been shown experimentally in the synthesis of Versicolamide B.[70] This would also negate the need to PPTS protect the tertiary amide in **130**, but the reduction of the tertiary amide using DIBAL may also affect the oxindole moiety.

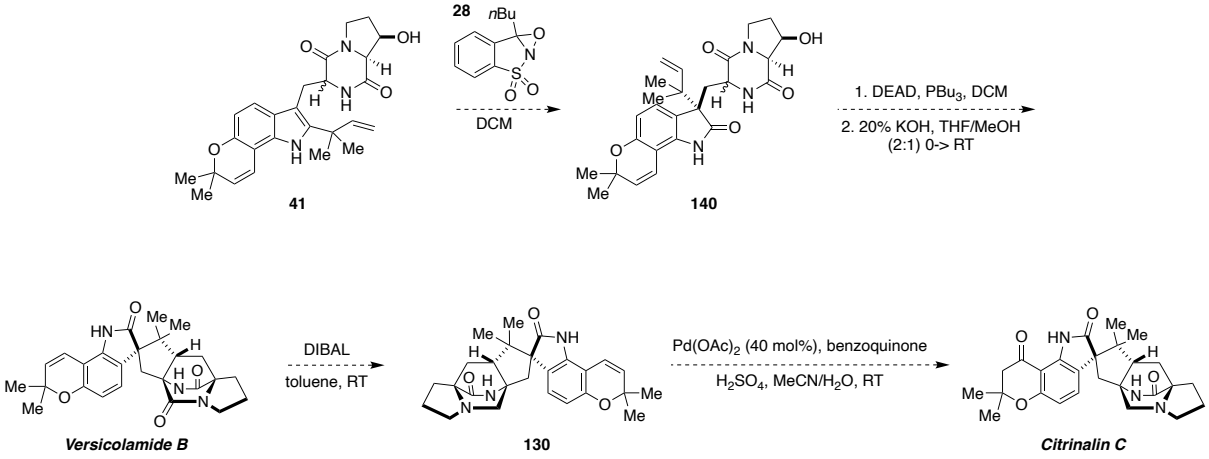

Figure 5.12. Potential steps to the synthesis of Citrinalin C.

This could be remedied by using a lactam ether protecting group for both secondary amides in the molecule but would add additional steps to the synthesis (**Figure 5.13**).

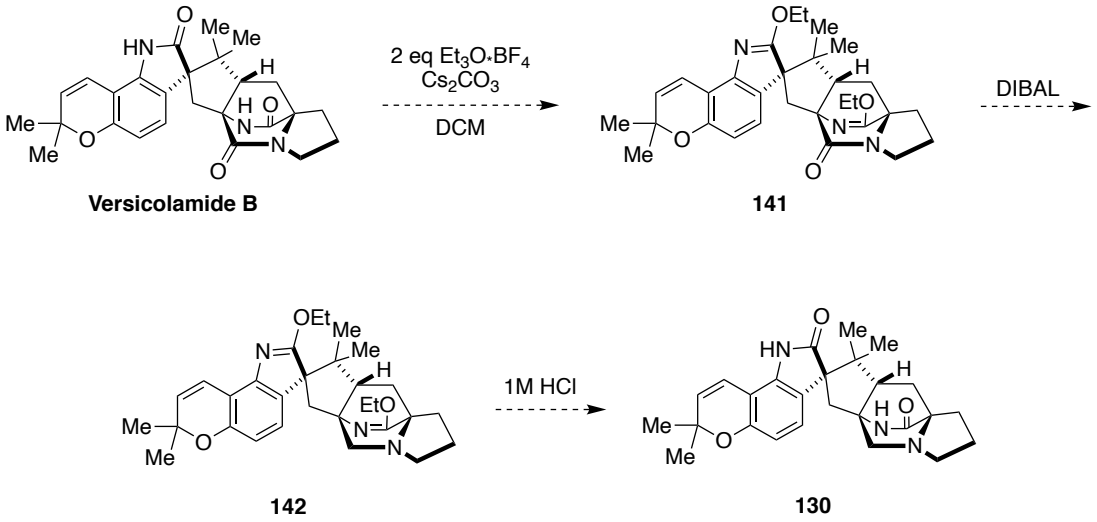

Figure 5.13. Protection of secondary amides with lactam either prior to reduction with DIBAL.

Although the synthesis was not completed, intermediates were sent to our collaborators in the Sherman group for testing. If these intermediates are compatible with any known enzymes in related biosynthetic pathways, these could be possible intermediates for Citrinalins A-C. The synthesis of Citrinalin C will help us unlock new knowledge about the construction of the decarbonylated prenylated indole alkaloids. The decarbonylated alkaloids (Citrinalins, Citrinadins, Cyclopiamines, Penicimutamides, and PF1270's) likely arise from unparalleled reductive decarbonylative deconstruction of precursors containing the bicyclo[2.2.2]diazaoctane core. Biomimetic synthesis will aid in discovery of this unique biogenic pathway.

References

(1) Finefield, J. M.; Frisvad, J. C.; Sherman, D. H.; Williams, R. M. Fungal Origins of the Bicyclo[2.2.2]Diazaoctane Ring System of Prenylated Indole Alkaloids. *J. Nat. Prod.* **2012**, *75* (4), 812–833.

(2) Finefield, J. M.; Sherman, D. H.; Kreitman, M.; Williams, R. M. Enantiomeric Natural Products: Occurrence and Biogenesis. *Angew. Chemie Int. Ed.* **2012**, *51* (20), 4802–4836.

(3) Klas, K. R.; Kato, H.; Frisvad, J. C.; Yu, F.; Newmister, S. A.; Fraley, A. E.; Sherman, D. H.; Tsukamoto, S.; Williams, R. M. Structural and Stereochemical Diversity in Prenylated Indole Alkaloids Containing the Bicyclo[2.2.2]Diazaoctane Ring System from Marine and Terrestrial Fungi. *Nat. Prod. Rep.* **2018**, *35* (6), 532–558.

(4) Williams, R. M. Natural Products Synthesis: Enabling Tools To Penetrate Nature's Secrets of Biogenesis and Biomechanism. *J. Org. Chem.* **2011**, *76* (11), 4221–4259.

(5) Klas, K.; Tsukamoto, S.; Sherman, D. H.; Williams, R. M. Natural Diels–Alderases: Elusive and Irresistable. *J. Org. Chem.* **2015**, *80* (23), 11672–11685.

(6) Polonsky, J.; Merrien, M.-A.; Prangé, T.; Pascard, C.; Moreau, S. Isolation and Structure (X-Ray Analysis) of Marcfortine A, a New Alkaloid from Penicillium Roqueforti. *J. Chem. Soc., Chem. Commun.* **1980**, *0* (13), 601–602.

(7) Prangé, T.; Billion, M.-A.; Vuilhorgne, M.; Pascard, C.; Polonsky, J.; Moreau, S. Structures of Marcfortine B and C (X-Ray Analysis), Alkaloids from Penicilliumroqueforti. *Tetrahedron Lett.* **1981**, *22* (21), 1977–1980.

(8) Paterson, R. R. M.; Simmonds, M. J. S.; Kemmelmeier, C.; Blaney, W. M. Effects of Brevianamide A, Its Photolysis Product Brevianamide D, and Ochratoxin A from Two Penicillium Strains on the Insect Pests Spodoptera Frugiperda and Heliothis Virescens. *Mycol. Res.* **1990**, *94* (4), 538–542.

(9) Blanchflower, S. E.; Banks, R. M.; Everett, J. R.; Manger, B. R.; Reading, C. New Paraherquamide Antibiotics with Anthelmintic Activity. *J. Antibiot. (Tokyo).* **1991**, *44* (5), 492–497.

(10) Banks, R. M.; Blanchflower, S. E.; Everett, J. R.; Manger, B. R.; Reading, C. Novel Anthelmintic Metabolites from an Aspergillus Species; the Aspergillimides. *J. Antibiot. (Tokyo).* **1997**, *50* (10), 840–846.

(11) Jeremy E. Wulff; Seth B. Herzon; Romain Siegrist, and; Myers*, A. G. Evidence for the Rapid Conversion of Stephacidin B into the Electrophilic Monomer Avrainvillamide in Cell Culture. **2007**.

(12) Jeremy E. Wulff; Romain Siegrist, and; Myers*, A. G. The Natural Product Avrainvillamide Binds to the Oncoprotein Nucleophosmin. **2007**.

(13) de Groot, A. F.; Appelman-Dijkstra, N. M.; van der Burg, S. H.; Kroep, J. R. The Anti-Tumor Effect of RANKL Inhibition in Malignant Solid Tumors – A Systematic Review. *Cancer Treat. Rev.* **2018**, *62*, 18–28.

(14) Wang, X.; You, J.; King, J. B.; Powell, D. R.; Cichewicz, R. H. Waikialoid A Suppresses Hyphal Morphogenesis and Inhibits Biofilm Development in Pathogenic *Candida Albicans*. *J. Nat. Prod.* **2012**, *75* (4), 707–715.

(15) Ji, N.-Y.; Liu, X.-H.; Miao, F.-P.; Qiao, M.-F. Aspeverin, a New Alkaloid from an Algicolous Strain of *Aspergillus Versicolor*. *Org. Lett.* **2013**, *15* (10), 2327–2329.

(16) Porter, A. E. A.; Sammes, P. G. A Diels–Alder Reaction of Possible Biosynthetic Importance. *J. Chem. Soc. D* **1970**, *0* (17), 1103a-1103a.

(17) Baldas, J.; Birch, A. J.; Russell, R. A. Studies in Relation to Biosynthesis. Part XLVI. Incorporation of Cyclo-L-Tryptophyl-L-Proline into Brevianamide A. *J. Chem. Soc. Perkin Trans. 1* **1974**, *0* (0), 50.

(18) Birch, A. J. *Terpenoid Compounds of Mixed Biogenetic Origins*; 1971; Vol. 19.

(19) Ding, Y.; Wet, J. R. de; Cavalcoli, J.; Li, S.; Greshock, T. J.; Miller, K. A.; Finefield, J. M.; Sunderhaus, J. D.; McAfoos, T. J.; Tsukamoto, S.; et al. Genome-Based Characterization of Two Prenylation Steps in the Assembly of the Stephacidin and Notoamide Anticancer Agents in a Marine-Derived *Aspergillus* Sp. *J. Am. Chem. Soc.* **2010**, *132* (36), 12733–12740.

(20) Kato, H.; Nakahara, T.; Sugimoto, K.; Matsuo, K.; Kagiyama, I.; Frisvad, J. C.; Sherman, D. H.; Williams, R. M.; Tsukamoto, S. Isolation of Notoamide S and Enantiomeric 6- *Epi* -Stephacidin A from the Fungus *Aspergillus Amoenus* : Biogenetic Implications. *Org. Lett.* **2015**, *17* (3), 700–703.

(21) Dan, Q.; Newmister, S. A.; Klas, K. R.; Fraley, A. E.; Mcafoos, T. J.; Somoza, A. D.; Sunderhaus, J. D.; Ye, Y.; Shende, V. V; Yu, F.; et al. Fungal Indole Alkaloid Biogenesis Through Evolution of a Bifunctional Reductase/Diels-Alderase. *Nat. Chem.* **2019**, *11*, 972–980.

(22) Kim, H. J.; Ruszczycky, M. W.; Choi, S.; Liu, Y.; Liu, H. Enzyme-Catalysed [4+2] Cycloaddition Is a Key Step in the Biosynthesis of Spinosyn A. *Nat. 2011 4737345* **2011**, *473* (7345), 109–112.

(23) Hudson, G. A.; Zhang, Z.; Tietz, J. I.; Mitchell, D. A.; Donk, W. A. van der. In Vitro Biosynthesis of the Core Scaffold of the Thiopeptide Thiomuracin. *J. Am. Chem. Soc.* **2015**, *137* (51), 16012–16015.

(24) Wever, W. J.; Bogart, J. W.; Baccile, J. A.; Chan, A. N.; Schroeder, F. C.; Bowers, A. A. Chemoenzymatic Synthesis of Thiazolyl Peptide Natural Products Featuring an Enzyme-Catalyzed Formal [4 + 2] Cycloaddition. *J. Am. Chem. Soc.* **2015**, *137* (10), 3494–3497.

(25) M, O.; F, L.; Y, H.; M, C.; MC, T.; Z, Y.; M, S.; K, W.; KN, H.; Y, T. SAM-Dependent Enzyme-Catalysed Pericyclic Reactions in Natural Product Biosynthesis. *Nature* **2017**, *549* (7673), 502–506.

(26) McKay, C. S.; Finn, M. G. Click Chemistry in Complex Mixtures: Bioorthogonal Bioconjugation. *Chem. Biol.* **2014**, *21* (9), 1075–1101.

(27) Gregoritza, M.; Brandl, F. P. The Diels–Alder Reaction: A Powerful Tool for the Design of Drug Delivery Systems and Biomaterials. *Eur. J. Pharm. Biopharm.* **2015**, *97*, 438–453.

(28) Lallana, E.; Fernandez-Trillo, F.; Sousa-Herves, A.; Riguera, R.; Fernandez-Megia, E. Click Chemistry with Polymers, Dendrimers, and Hydrogels for Drug Delivery. *Pharm. Res. 2012 294* **2012**, *29* (4), 902–921.

(29) Lallana, E.; Sousa-Herves, A.; Fernandez-Trillo, F.; Riguera, R.; Fernandez-Megia, E.

Click Chemistry for Drug Delivery Nanosystems. *Pharm. Res. 2011 291* **2011**, *29* (1), 1–34.

(30) Nimmo, C. M.; Shoichet, M. S. Regenerative Biomaterials That "Click": Simple, Aqueous-Based Protocols for Hydrogel Synthesis, Surface Immobilization, and 3D Patterning. *Bioconjug. Chem.* **2011**, *22* (11), 2199–2209.

(31) Hein, C. D.; Liu, X.-M.; Wang, D. Click Chemistry, A Powerful Tool for Pharmaceutical Sciences. *Pharm. Res. 2008 2510* **2008**, *25* (10), 2216–2230.

(32) Ye, Y.; Du, L.; Zhang, X.; Newmister, S. A.; McCauley, M.; Alegre-Requena, J. V.; Zhang, W.; Mu, S.; Minami, A.; Fraley, A. E.; et al. Fungal-Derived Brevianamide Assembly by a Stereoselective Semipinacolase. *Nat. Catal.* **2020**, *3* (6), 497–506.

(33) Sanz-Cervera, J. F.; Glinka, T.; Williams, R. M. Biosynthesis of Brevianamides A and B: In Search of the Biosynthetic Diels-Alder Construction. *Tetrahedron* **1993**, *49* (38), 8471–8482.

(34) Li, S.; Finefield, J. M.; Sunderhaus, J. D.; McAfoos, T. J.; Williams, R. M.; Sherman, D. H. Biochemical Characterization of NotB as an FAD-Dependent Oxidase in the Biosynthesis of Notoamide Indole Alkaloids. *J. Am. Chem. Soc.* **2012**, *134* (2), 788–791.

(35) Greshock, T. J.; Grubbs, A. W.; Jiao, P.; Wicklow, D. T.; Gloer, J. B.; Williams, R. M. Isolation, Structure Elucidation, and Biomimetic Total Synthesis of Versicolamide B, and the Isolation of Antipodal (−)-Stephacidin A and (+)-Notoamide B FromAspergillus Versicolor NRRL 35600. *Angew. Chemie Int. Ed.* **2008**, *47* (19), 3573–3577.

(36) Kato, H.; Yoshida, T.; Tokue, T.; Nojiri, Y.; Hirota, H.; Ohta, T.; Williams, R. M.;

Tsukamoto, S. Notoamides A–D: Prenylated Indole Alkaloids Isolated from a Marine-Derived Fungus,Aspergillus Sp. *Angew. Chemie Int. Ed.* **2007**, *46* (13), 2254–2256.

(37) Tsukamoto, S.; Kato, H.; Greshock, T. J.; Hirota, H.; Ohta, T.; Williams, R. M. Isolation of Notoamide E, a Key Precursor in the Biosynthesis of Prenylated Indole Alkaloids in a Marine-Derived Fungus, *Aspergillus* Sp. *J. Am. Chem. Soc.* **2009**, *131* (11), 3834–3835.

(38) Tsukamoto, S.; Kato, H.; Greshock, T. J.; Hirota, H.; Ohta, T.; Williams, R. M. Correction to Isolation of Notoamide E, a Key Precursor in the Biosynthesis of Prenylated Indole Alkaloids in a Marine-Derived Fungus, *Aspergillus* Sp. *J. Am. Chem. Soc.* **2013**, *135* (29), 10878–10878.

(39) Cox, R. J.; Williams, R. M. Synthetic Studies towards Paraherquamide F: Synthesis of the 1,7-Dihydropyrano[2,3-g]Indole Ring System. *Tetrahedron Lett.* **2002**, *43* (12), 2149–2152.

(40) Mcafoos, T. J.; Li, S.; Tsukamoto, S.; Sherman, D. H.; Williams, R. M. Studies on the Biosynthesis of the Stephacidins and Notoamides. Total Synthesis of Notoamide S. *Heterocycles* **2010**, *82* (1), 461–472.

(41) Kato, H.; Nakamura, Y.; Finefield, J. M.; Umaoka, H.; Nakahara, T.; Williams, R. M.; Tsukamoto, S. Study on the Biosynthesis of the Notoamides: Pinacol-Type Rearrangement of the Isoprenyl Unit in Deoxybrevianamide E and 6-Hydroxydeoxybrevianamide E. *Tetrahedron Lett.* **2011**, *52* (51), 6923–6926.

(42) Finefield, J. M.; Sherman, D. H.; Tsukamoto, S.; Williams, R. M. Studies on the Biosynthesis of the Notoamides: Synthesis of an Isotopomer of 6-Hydroxydeoxybrevianamide E and Biosynthetic Incorporation into Notoamide J. *J. Org.*

Chem. **2011**, *76* (15), 5954–5958.

(43) Maiya, S.; Grundmann, A.; Li, S.-M.; Turner, G. The Fumitremorgin Gene Cluster of Aspergillus Fumigatus: Identification of a Gene Encoding Brevianamide F Synthetase. *ChemBioChem* **2006**, *7* (7), 1062–1069.

(44) Li, S.; Anand, K.; Tran, H.; Yu, F.; Finefield, J. M.; Sunderhaus, J. D.; McAfoos, T. J.; Tsukamoto, S.; Williams, R. M.; Sherman, D. H. Comparative Analysis of the Biosynthetic Systems for Fungal Bicyclo[2.2.2]Diazaoctane Indole Alkaloids: The (+)/(-)-Notoamide, Paraherquamide and Malbrancheamide Pathways. *Medchemcomm* **2012**, *3* (8), 987–996.

(45) Birch, A. J.; Wright, J. J. The Brevianamides: A New Class of Fungal Alkaloid. *J. Chem. Soc. D Chem. Commun.* **1969**, *0* (12), 644b.

(46) Fraley, A. E.; Tran, H. T.; Kelly, S. P.; Newmister, S. A.; Tripathi, A.; Kato, H.; Tsukamoto, S.; Du, L.; Li, S.; Williams, R. M.; et al. Flavin-Dependent Monooxygenases NotI and NotI′ Mediate Spiro-Oxindole Formation in Biosynthesis of the Notoamides. *ChemBioChem* **2020**, *21* (17), 2449–2454.

(47) Li, F.; Zhang, Z.; Zhang, G.; Che, Q.; Zhu, T.; Gu, Q.; Li, D. Determination of Taichunamide H and Structural Revision of Taichunamide A. *Org. Lett.* **2018**, *20* (4), 1138–1141.

(48) Kagiyama, I.; Kato, H.; Nehira, T.; Frisvad, J. C.; Sherman, D. H.; Williams, R. M.; Tsukamoto, S. Taichunamides: Prenylated Indole Alkaloids from Aspergillus Taichungensis (IBT 19404). *Angew. Chemie Int. Ed.* **2016**, *55* (3), 1128–1132.

(49) Sunderhaus, J. D.; McAfoos, T. J.; Finefield, J. M.; Kato, H.; Li, S.; Tsukamoto, S.; Sherman, D. H.; Williams, R. M. Synthesis and Bioconversions of Notoamide T: A Biosynthetic Precursor to Stephacidin A and Notoamide B. *Org. Lett.* **2013**, *15* (1), 22–25.

(50) Tsukamoto, S.; Kawabata, T.; Kato, H.; Greshock, T. J.; Hirota, H.; Ohta, T.; Williams, R. M. Isolation of Antipodal (−)-Versicolamide B and Notoamides L−N from a Marine-Derived *Aspergillus* Sp. *Org. Lett.* **2009**, *11* (6), 1297–1300.

(51) Birch, A. J.; Wright, J. J. Studies in Relation to Biosynthesis—XLII: The Structural Elucidation and Some Aspects of the Biosynthesis of the Brevianamides-A and -E. *Tetrahedron* **1970**, *26* (10), 2329–2344.

(52) Birch, A. J.; Russell, R. A. Studies in Relation to Biosynthesis—XLIV : Structural Elucidations of Brevianamides-B, -C, -D and -F. *Tetrahedron* **1972**, *28* (11), 2999–3008.

(53) Yamazaki, M.; Okuyama, E.; Kobayashi, M.; Inoue, H. The Structure of Paraherquamide, a Toxic Metabolite from Penicillium Paraherquei. *Tetrahedron Lett.* **1981**, *22* (2), 135–136.

(54) Liesch, J. M.; Wichmann, C. F. Novel Antinematodal and Antiparasitic Agents from Penicillium Charlesii. II. Structure Determination of Paraherquamides B, C, D, E, F, and G. *J. Antibiot. (Tokyo).* **1990**, *43* (11), 1380–1386.

(55) HAYASHI, H.; TAKIUCHI, K.; MURAO, S.; ARAI, M. Structure and Insecticidal Activity of New Indole Alkaloids, Okaramines A and B, from Penicillium Simplicissimum AK-40. *Agric. Biol. Chem.* **1989**, *53* (2), 461–469.

(56) Blanchflower, S. E.; Banks, R. M.; Everett, J. R.; Reading, C. Further Novel Metabolites

of the Paraherquamide Family. *J. Antibiot. (Tokyo).* **1993**, *46* (9), 1355–1363.

(57) and, A. C. W.; Gloer*, J. B.; And, D. T. W.; Dowd, P. F. Sclerotiamide: A New Member of the Paraherquamide Class with Potent Antiinsectan Activity from the Sclerotia of Aspergillus Sclerotiorum. *J. Nat. Prod.* **1996**, *59*, 1093–1095.

(58) Qian-Cutrone, J.; Huang, S.; Shu, Y.-Z.; Vyas, D.; Fairchild, C.; Menendez, A.; Krampitz, K.; Dalterio, R.; Klohr, S. E.; Gao, Q. Stephacidin A and B: Two Structurally Novel, Selective Inhibitors of the Testosterone-Dependent Prostate LNCaP Cells. *J. Am. Chem. Soc.* **2002**, *124* (49), 14556–14557.

(59) Sugie, Y.; Hirai, H.; Inagaki, T.; Kojima, N. A New Antibiotic CJ-17,665 from Aspergillus Ochraceus. *J. Antibiot. (Tokyo).* **2001**, *54* (11), 911–916.

(60) Herzon, S. B.; Myers*, A. G. Enantioselective Synthesis of Stephacidin B. *J. Am. Chem. Soc.* **2005**, *127* (15), 5342–5344.

(61) Baran, P. S.; Hafensteiner, B. D.; Ambhaikar, N. B.; Guerrero, C. A.; Gallagher, J. D. Enantioselective Total Synthesis of Avrainvillamide and the Stephacidins. **2006**.

(62) Greshock, T. J.; Grubbs, A. W.; Tsukamoto, S.; Williams, R. M. A Concise, Biomimetic Total Synthesis of Stephacidin A and Notoamide B. *Angew. Chemie Int. Ed.* **2007**, *46* (13), 2262–2265.

(63) Tsukamoto, S.; Kato, H.; Samizo, M.; Nojiri, Y.; Onuki, H.; Hirota, H.; Ohta, T. Notoamides F−K, Prenylated Indole Alkaloids Isolated from a Marine-Derived Aspergillus Sp. *J. Nat. Prod.* **2008**, *71* (12), 2064–2067.

(64) Tsukamoto, S.; Umaoka, H.; Yoshikawa, K.; Ikeda, T.; Hirota, H. Notoamide O, a

Structurally Unprecedented Prenylated Indole Alkaloid, and Notoamides P−R from a Marine-Derived Fungus, *Aspergillus* Sp. *J. Nat. Prod.* **2010**, *73* (8), 1438–1440.

(65) Kato, H.; Nakahara, T.; Yamaguchi, M.; Kagiyama, I.; Finefield, J. M.; Sunderhaus, J. D.; Sherman, D. H.; Williams, R. M.; Tsukamoto, S. Bioconversion of 6-Epi-Notoamide T Produces Metabolites of Unprecedented Structures in a Marine-Derived Aspergillus Sp. *Tetrahedron Lett.* **2015**, *56*, 247–251.

(66) Kato, H.; Kai, A.; Kawabata, T.; Sunderhaus, J. D.; McAfoos, T. J.; Finefield, J. M.; Sugimoto, Y.; Williams, R. M.; Tsukamoto, S. Enantioselective Inhibitory Abilities of Enantiomers of Notoamides against RANKL-Induced Formation of Multinuclear Osteoclasts. *Bioorg. Med. Chem. Lett.* **2017**, *27* (22), 4975–4978.

(67) Finefield, J. M.; Williams, R. M. Synthesis of Notoamide J: A Potentially Pivotal Intermediate in the Biosynthesis of Several Prenylated Indole Alkaloids. *J. Org. Chem.* **2010**, *75* (9), 2785–2789.

(68) Jeffrey M. Schkeryantz; Jonathan C. G. Woo; Phieng Siliphaivanh; Kristopher M. Depew, A.; Danishefsky*, S. J. Total Synthesis of Gypsetin, Deoxybrevianamide E, Brevianamide E, and Tryprostatin B: Novel Constructions of 2,3-Disubstituted Indoles. **1999**, *121* (51), 11964–11975.

(69) Grubbs, A. W.; Artman, G. D.; Williams, R. M. Concise Syntheses of the 1,7-Dihydropyrano[2,3-g]Indole Ring System of the Stephacidins, Aspergamides and Norgeamides. *Tetrahedron Lett.* **2005**, *46* (52), 9013–9016.

(70) Miller, K. A.; Tsukamoto, S.; Williams, R. M. Asymmetric Total Syntheses of (+)- and (-)-Versicolamide B and Biosynthetic Implications. *Nat. Chem.* **2009**, *1* (1), 63–68.

(71) Luis R. Domingo, *; Ramón J. Zaragozá, and; Williams§, R. M. Studies on the Biosynthesis of Paraherquamide A and VM99955. A Theoretical Study of Intramolecular Diels−Alder Cycloaddition. *J. Org. Chem.* **2003**, *68* (7), 2895–2902.

(72) Xiong, J.; Onal, M.; Jilka, R. L.; Weinstein, R. S.; Manolagas, S. C.; O'Brien, C. A. Matrix-Embedded Cells Control Osteoclast Formation. *Nat. Med. 2011 1710* **2011**, *17* (10), 1235–1241.

(73) Nakashima, T.; Hayashi, M.; Fukunaga, T.; Kurata, K.; Oh-hora, M.; Feng, J. Q.; Bonewald, L. F.; Kodama, T.; Wutz, A.; Wagner, E. F.; et al. Evidence for Osteocyte Regulation of Bone Homeostasis through RANKL Expression. *Nat. Med. 2011 1710* **2011**, *17* (10), 1231–1234.

(74) Xiong, J.; Piemontese, M.; Onal, M.; Campbell, J.; Goellner, J. J.; Dusevich, V.; Bonewald, L.; Manolagas, S. C.; O'Brien, C. A. Osteocytes, Not Osteoblasts or Lining Cells, Are the Main Source of the RANKL Required for Osteoclast Formation in Remodeling Bone. *PLoS One* **2015**, *10* (9), e0138189.

(75) McClung, M. Role of RANKL Inhibition in Osteoporosis. *Arthritis Res. Ther.* **2007**, *9* (Suppl 1), S3.

(76) Landor, S. R.; Patel, A. N.; Whiter, P. F.; Greaves, P. M. Allenes. Part XI. The Preparation of 3-Alkyl- and 3,3-Dialkyl-1-Bromoallenes. *J. Chem. Soc. C Org.* **1966**, No. 0, 1223.

(77) Somei, M.; Yoshio, K.; Keneko, C. Selective Mono-Alkylation of Carbon Nucleophiles with Gramine. *Heterocycles* **1981**, *16* (6), 941–948.

(78) Kametani, T.; Kanaya, N.; Ihara, M. Studies on the Syntheses of Heterocyclic Compounds. Part 876. The Chiral Total Synthesis of Brevianamide E and Deoxybrevianamide E. *J. Chem. Soc. Perkin Trans. 1* **1981**, *0* (0), 959.

(79) Indoles from 2-Mehtylnitrobenenes by Condensation with Formamide Acetals Followed by Reduction: 4-Benzyloxyindole. *Org. Synth.* **1985**, *63*, 214.

(80) Sissouma, D.; Collet, S. C.; Guingant, A. Y. A Synthesis of Calothrixin B. *Synlett* **2004**, No. 14, 2612–2614.

(81) Gautam, D.; Gautam, P.; P. Chaudhary, R. Expedient and Green Synthesis of Some Novel 4-Thiazolidinones and New 2,4-Disubstituted Thiazoles with Tetrahydro Carbazole Pendant. *Lett. Org. Chem.* **2012**, *9* (9), 660–663.

(82) Dilek, Ö.; Patir, S.; Ertürk, E. Enantioselective Synthesis of 1- and 4-Hydroxytetrahydrocarbazoles through Asymmetric Transfer Hydrogenation. *Synlett* **2019**, *30* (01), 69–72.

(83) Stocking, E. M.; Sanz-Cervera, J. F.; Williams, R. M. Studies on the Biosynthesis of Paraherquamide: Synthesis and Incorporation of a Hexacyclic Indole Derivative as an Advanced Metabolite. *Angew. Chemie Int. Ed.* **2001**, *40* (7), 1296–1298.

(84) Finefield, J. M.; Kato, H.; Greshock, T. J.; Sherman, D. H.; Tsukamoto, S.; Williams, R. M. Biosynthetic Studies of the Notoamides: Isotopic Synthesis of Stephacidin A and Incorporation into Notoamide B and Sclerotiamide. *Org. Lett.* **2011**, *13*, 3.

(85) and, T. J. G.; Robert M. Williams*, †,‡. Improved Biomimetic Total Synthesis of d,l-Stephacidin A. *Org. Lett.* **2007**, *9* (21), 4255–4258.

(86) Cushing, T. D.; Sanz-Cervera, J. F.; Williams, R. M. Stereocontrolled Total Synthesis of (+)-Paraherquamide B. *J. Am. Chem. Soc.* **1993**, *115* (20), 9323–9324.

(87) Harkness, D. R.; Roth, S.; Peterson, C. M.; Tsairis, P.; Ohnishi, A.; Lu, Y. S.; Grady, R.; Cerami, A.; Dyck, P. J.; Klotz, I. M.; et al. *O-Carbamoylsalicylates: Agents for Modification of Hemoglobins*; 1987; Vol. 30.

(88) Singh, R.; Nagesh, K.; Parameshwar, M. Rhodium(II)-Catalyzed Undirected and Selective C(Sp^2)–H Amination En Route to Benzoxazolones. *ACS Catal.* **2016**, *6* (10), 6520–6524.

(89) and, J. P. D.; Corey*, E. J. First Enantiospecific Total Synthesis of the Antitubercular Marine Natural Product Pseudopteroxazole. Revision of Assigned Stereochemistry. *J. Am. Chem. Soc.* **2003**, *125* (44), 13486–13489.

(90) Fábio Cesar Gozzo; Sergio Antonio Fernandes; Denise Cristina Rodrigues; Marcos Nogueira Eberlin, * and; Marsaioli*, A. J. Regioselectivity in Aromatic Claisen Rearrangements. *J. Org. Chem.* **2003**, *68* (14), 5493–5499.

(91) Williams, R. M.; Glinka, T.; Kwast, E. Synthetic Studies on Paraherquamide: Regioselectivity of Indole Oxidation. *Tetrahedron Lett.* **1989**, *30* (41), 5575–5578.

(92) FujimoriKunihide; YamaneKameji. Synthesis of 6-Hydroxy-12-Methyl-7,12-Dihydrobenzo[6,7]Cyclohept[1,2-b]Indol-7-One. *Bull. Chem. Soc. Jpn.* **2006**, *51* (12), 3579–3581.

(93) Stahl, R.; Galli, R.; Güller, R.; Borschberg, H.-J. Synthesis of Aristotelia-Type Alkaloids. Part XIII. Total Syntheses of (+)-Makonine, (+)-Aristotelinone, and (+)-11,12-Didehydroaristoteline. *Helv. Chim. Acta* **1994**, *77* (8), 2125–2132.

(94) Pimenta, E. F.; Vita-Marques, A. M.; Tininis, A.; Seleghim, M. H. R.; Sette, L. D.; Veloso, K.; Ferreira, A. G.; Williams, D. E.; Patrick, B. O.; Dalisay, D. S.; et al. Use of Experimental Design for the Optimization of the Production of New Secondary Metabolites by Two Penicillium Species. *J. Nat. Prod.* **2010**, *73* (11), 1821–1832.

(95) Takao Mugishima, †; Masashi Tsuda, †; Yuu Kasai, †; Haruaki Ishiyama, †; Eri Fukushi, ‡; Jun Kawabata, ‡; Masayuki Watanabe, §; Kenichi Akao, § and; Jun'ichi Kobayashi*, †. Absolute Stereochemistry of Citrinadins A and B from Marine-Derived Fungus. *J. Org. Chem.* **2005**, *70* (23), 9430–9435.

(96) Masashi Tsuda, †; Yuu Kasai, †; Kazusei Komatsu, †; Teruo Sone, ‡; Michiko Tanaka, ‡; Yuzuru Mikami, § and; Jun'ichi Kobayashi*, †. Citrinadin A, a Novel Pentacyclic Alkaloid from Marine-Derived Fungus Penicillium Citrinum. **2004**.

(97) Bian, Z.; Marvin, C. C.; Martin, S. F. Enantioselective Total Synthesis of (−)-Citrinadin A and Revision of Its Stereochemical Structure. *J. Am. Chem. Soc.* **2013**, *135* (30), 10886–10889.

(98) Kong, K.; Enquist, J. A.; McCallum, M. E.; Smith, G. M.; Matsumaru, T.; Menhaji-Klotz, E.; Wood, J. L. An Enantioselective Total Synthesis and Stereochemical Revision of (+)-Citrinadin B. *J. Am. Chem. Soc.* **2013**, *135* (30), 10890–10893.

(99) Mundal, D. A.; Sarpong, R. Synthetic Studies toward the Citrinadin A and B Core Architecture. *Org. Lett.* **2013**, *15* (19), 4952–4955.

(100) Kushida, N.; Watanabe, N.; Okuda, T.; Yokoyama, F.; Gyobu, Y.; Yaguchi, T. PF1270A, B and C, Novel Histamine H3 Receptor Ligands Produced by Penicillium Waksmanii PF1270. *J. Antibiot. (Tokyo).* **2007**, *60* (11), 667–673.

(101) Mercado-Marin, E. V.; Garcia-Reynaga, P.; Romminger, S.; Pimenta, E. F.; Romney, D. K.; Lodewyk, M. W.; Williams, D. E.; Andersen, R. J.; Miller, S. J.; Tantillo, D. J.; et al. Total Synthesis and Isolation of Citrinalin and Cyclopiamine Congeners. *Nature* **2014**, *509* (7500), 318–324.

(102) F. Bond, R.; A. Boeyens, J. C.; W. Holzapfel, C.; S. Steyn, P. Cyclopiamines A and B, Novel Oxindole Metabolites of Penicillium Cyclopium Westling. *J. Chem. Soc. Perkin Trans. 1* **1979**, *0* (0), 1751–1761.

(103) Steyn, P. S.; Vleggaar, R.; Rabie, C. J. Alkaloids from Aspergillus Caespitosus. *Phytochemistry* **1981**, *20* (3), 538–539.

(104) Li, C.-W.; Wu, C.-J.; Cui, C.-B.; Xu, L.-L.; Cao, F.; Zhu, H.-J. Penicimutamides A–C: Rare Carbamate-Containing Alkaloids from a Mutant of the Marine-Derived Penicillium Purpurogenum G59. *RSC Adv.* **2016**, *6* (77), 73383–73387.

(105) Wu, C.-J.; Li, C.-W.; Gao, H.; Huang, X.-J.; Cui, C.-B. Penicimutamides D–E: Two New Prenylated Indole Alkaloids from a Mutant of the Marine-Derived Penicillium Purpurogenum G59. *RSC Adv.* **2017**, *7* (40), 24718–24722.

(106) Greshock, T. J.; Grubbs, A. W.; Williams, R. M. Concise, Biomimetic Total Synthesis of d,l-Marcfortine C. *Tetrahedron* **2007**, *63* (27), 6124–6130.

(107) Baran, P. S.; Guerrero, C. A.; Ambhaikar, N. B.; Hafensteiner, B. D. Short, Enantioselective Total Synthesis of Stephacidin A. *Angew. Chemie Int. Ed.* **2005**, *44* (4), 606–609.

(108) Luis R. Domingo, *; Juan F. Sanz-Cervera; Robert M. Williams, †; M. Teresa Picher, and; Marco, J. A. Biosynthesis of the Brevianamides. An Ab Initio Study of the Biosynthetic Intramolecular Diels−Alder Cycloaddition. **1997**.

Appendix I: Contributions to Work

Chapter 2, Section II: Former graduate student Poramate Songthammawat performed some of the reactions listed in **Tables 2.1-2.3** (Chapter 2, section II-*ii*).

Chapter 2, Section III: John Manganaro of the Williams/Crans groups assisted in the DDQ oxidation (**85** to **89**) and performed the debenzylation reaction (**89** to **90**).

Appendix II: Supporting Information

I. Experimental

i. General Procedures

Flash column chromatography was performed with silica gel grade 60 (230-400 mesh) from Sorbent Technologies. Preparative TLC was performed with glassed backed precoated silica gel 60 F254 20 x 20 cm plates. Unless otherwise noted, materials were obtained from commercially available sources. Dichloromethane (CH_2Cl_2), tetrahydrofuran (THF), N, N-dimethylformamide (DMF), acetonitrile (MeCN), triethylamine (NEt_3), toluene, and methanol (MeOH) were all degassed with argon and passed through a solvent purification system containing alumina or molecular sieves in most cases.

All spectra were obtained from spectra were obtained on instruments in the Colorado State University Analytical Resource Core Materials and Molecular Analysis Center. All ^{1}H and ^{13}C spectra were obtained using 400 MHz spectrometers. The chemical shifts are given in parts per million (ppm) relative to $CDCl_3$ δ 7.26 ppm, CD_3OD δ 3.31 ppm, $(CD_3)_2CO$ δ 2.05 ppm or $(CD_3)_2SO$ δ 2.50 ppm for proton spectra and relative to $CDCl_3$ at δ 77.23 ppm, CD_3OD δ 49.00 ppm, $(CD_3)_2CO$ δ 29.84 ppm or $(CD_3)_2SO$ δ 39.52 ppm for carbon spectra. Splitting patterns are described using the following abbreviations: s = singlet, br. s = broad singlet, d = doublet, t = triplet, q = quartet, quin = quintet, sext = sextet, sept = septet, m = multiplet. Mass spectra were obtained using Agilent 6230 TOF LC-MS.

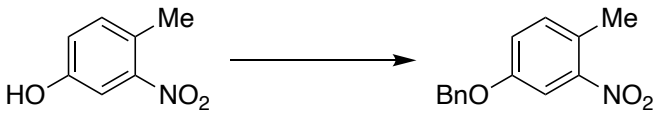

15 **16**

BnCl (42 mL, 0.362 mol) and K_2CO_3 (45.2 g, 0.326 mol) were added to a solution of phenol **15** (50.0 g, 0.326 mol) in DMF (320 mL) and heated to 90 °C, refluxing for 18 hours. The solution was cooled to room temperature, then partitioned between 170 mL of both EtOAc and H_2O. The aqueous was extracted with EtOAc (2 x 80 mL). Then, the combined organics were washed with 1M NaOH (2 x 160 mL), brine (2 x 160 mL), dried with $MgSO_4$, filtered, and concentrated under reduced pressure, affording 79.3 g of nitrophenol **16** as a yellow solid (quant.). The product was carried forward without further purification. **16**: ^{1}H NMR (300 MHz, $CDCl_3$) δ 7.60 (d, J = 2.7 Hz, 1H), 7.45 – 7.34 (m, 5H), 7.23 (d, J = 8.5 Hz, 1H), 7.12 (dd, J = 8.5, 2.7 Hz, 1H), 5.10 (s, 2H), 2.53 (s, 3H).

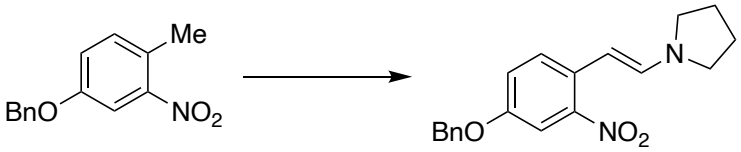

16 **17**

Dimethylformamide (137 mL, 1.03 mol), pyrrolidine (71.48 g, 1.005 mol), and **16** (79.56 g, 0.329 mol) were combined and heated to 90 °C, refluxing for 18 hours. Solution was cooled to room temperature and EtOH was added until crystals crashed out of solution. The crystals were isolated by filtration and washed with cold EtOH, yielding 105.7 g of dark purple crystals (99% yield). **17**: ^{1}H NMR (400 MHz, $CDCl_3$) δ 7.50 (d, *J* = 2.8 Hz, 1H), 7.44 – 7.33 (m, 6H), 7.10 (d, *J* = 13.6 Hz, 1H), 7.05 (dd, *J* = 9.0, 2.8 Hz, 1H), 5.85 (d, *J* = 13.6 Hz, 1H), 5.06 (s, 2H), 3.37 –

3.24 (m, 4H), 1.96 – 1.89 (m, 4H). ^{13}C NMR (101 MHz, $CDCl_3$) δ 154.20, 139.65, 136.47, 130.13, 128.80, 128.33, 127.76, 125.86, 122.35, 109.64, 91.67, 70.66, 49.28, 47.97, 25.42, 25.35.

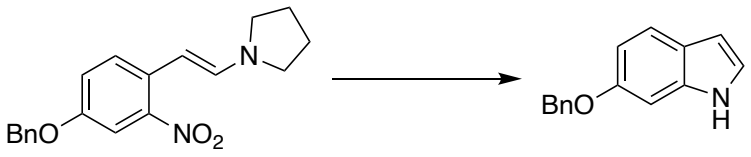

17 **77**

To a stirred solution of 50 g (154.2 mol) of enamine **17**, in methanol (308 mL) and THF (308 mL) at 30 ºC, Raney nickel slurry (3.1 mL) was added, followed by 55% hydrazine hydrate (20.5 mL, 231.3 mmol). The reaction temperature rose to 40 ºC as vigorous gas evolution was observed and the reaction was then heated to 45 ºC with an oil bath. An additional 20.5 mL of hydrazine hydrate was added after 30 minutes and again 1 hour later. The reaction temperature was maintained at 45 ºC until 2 hours after the last addition. The mixture was cooled to room temperature and the Raney nickel was filtered off over Celite. The Celite was washed several times with DCM and the resulting filtrate was concentrated under reduced pressure. The residue was purified using 10-20% EtOAc/Hexanes, affording 32.02 g of pale-yellow solid (93% yield). **77**: ^{1}H NMR (400 MHz, $CDCl_3$) δ 7.98 (s, 1H), 7.56 – 7.34 (m, 6H), 7.07 (s, 1H), 6.92 (d, J = 7.0 Hz, 2H), 6.50 (s, 1H), 5.11 (s, 2H). ^{13}C NMR (101 MHz, MeOD) δ 185.45, 176.07, 172.07, 157.88, 145.64, 143.85, 127.58, 125.12, 115.65, 114.12, 104.61, 80.96, 70.38, 67.73, 63.44, 57.45, 46.68, 44.94, 34.55, 31.15, 30.42, 27.48, 27.45, 25.75, 23.69, 20.40.

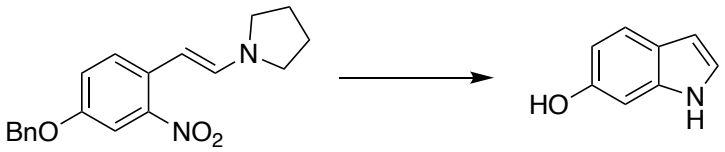

17 **14**

10 % Pd/C was added to a solution of enamine **17** (5 g, 15.42 mmol) and ammonium formate (4.86 g, 77.01 mmol) in MeOH (50 mL). Solution was purged with argon for 10 minutes, then stirred at room temperature for 3 hours. Catalyst was removed by filtering over Celite and rinsing with MeOH. Solution was concentrated under reduced pressure and taken up in acetone until salts precipitated. The salts were removed by Celite filtration, and the resulting solution was concentrated. The residue was purified with flash column chromatography, eluting with ether. This afforded a light-yellow solid, which is carried forward immediately for protection. **14**: ^{1}H NMR (400 MHz, DMSO) δ 10.64 (s, 1H), 8.84 (s, 1H), 7.28 (d, J = 8.4 Hz, 1H), 7.08 (t, J = 2.8 Hz, 1H), 6.74 (d, J = 2.1 Hz, 1H), 6.51 (dd, J = 8.4, 2.2 Hz, 1H), 6.25 (s, 1H). ^{13}C NMR (101 MHz, DMSO) δ 152.85, 136.96, 123.10, 120.97, 120.25, 109.44, 100.82, 96.42.

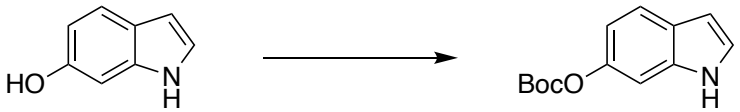

14 **18**

Boc anhydride (3.70 g, 16.96 mmol) and DMAP (19 mg, 0.154 mmol) were added to a solution of hydroxyindole **14** (2.55 g, 15.42 mmol) in MeCN (30 mL) at 0 ºC. The reaction was then allowed to warm to room temperature and stirred for 15 minutes. The reaction was partitioned between ether (125 mL) and 1M HCl (65 mL). The organics were then washed with 1M NaOH (125 mL) then brine (2 x 125 mL). The organics were then dried over $MgSO_4$, filtered, and concentrated under reduced pressure. The residue was purified with flash chromatography eluting with 5-20%

EtOAc/Hexanes. This yielded 1.98 g of white solid (55% yield). **18**: ^{1}H NMR (400 MHz, $CDCl_3$) δ 8.16 (s, 1H), 7.59 (d, J = 8.5 Hz, 1H), 7.23 (d, J = 1.9 Hz, 1H), 7.22 – 7.20 (m, 1H), 6.94 (dd, J = 8.6, 2.1 Hz, 1H), 6.55 – 6.52 (m, 1H), 1.57 (s, 9H).

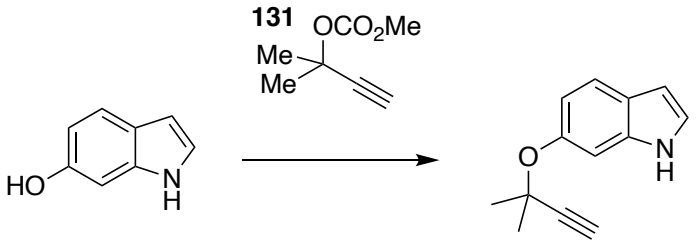

14 **132**

Phenol **14** (1.93 g, 14.5 mmol) was dissolved in MeCN (29 mL) and cooled to 0 ºC. $CuCl_2$•H_2O (74.1 mg, 0.435 mmol) was added, followed by carbonate **131** (8.01 g, 43.5 mmol). The reaction was stirred for 15 minutes, then DBU (6.55 mL, 43.5 mmol) was added slowly. The solution was stirred for 3 hours at 0 ºC at which point consumption of starting material was seen on TLC (40% EtOAc/hexane). MeCN was removed under reduced pressure and the resulting oil was taken up with EtOAc (110 mL). This was washed with 1M HCl (38 mL), H_2O (38 mL), and brine (38 mL). The organics were dried over Na_2SO_4, filtered, and concentrated under reduced pressure. The residue was purified by flash chromatography, eluting with 20% EtOAc/hexane which gave 1.50 g of **132** as a light-yellow oil (52% yield). ^{1}H NMR (400 MHz, $CDCl_3$) δ 8.06 (s, 1H), 7.51 (d, J = 8.5 Hz, 1H), 7.30 (s, 1H), 7.15 (s, 1H), 7.00 (dt, J = 8.4, 1.7 Hz, 1H), 6.51 (s, 1H), 2.55 (s, 1H), 1.65 (s, 6H). ^{1}H NMR (400 MHz, $CDCl_3$) δ 3.88, 3.86, 3.85, 3.84, 3.32, 3.30, 3.28, 3.27, 3.04, 3.01, 3.00, 2.98.

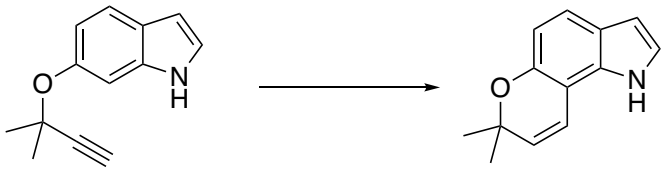

132 **133**

132 (1.50 g, 7.53 mmol) was taken up in MeCN (17 mL) and heated in a chemical microwave for 1 hour at 180 °C (power = 150W). MeCN was removed under reduced pressure which gave 1.50 g of **133** in quantitative yield. ^{1}H NMR (400 MHz, $CDCl_3$) δ 8.07 (s, 1H), 7.50 (d, J = 8.5 Hz, 1H), 7.31 – 7.29 (m, 1H), 7.16 (dd, J = 3.2, 2.4 Hz, 1H), 6.99 (dd, J = 8.5, 2.1 Hz, 1H), 6.50 (ddd, J = 3.1, 2.0, 1.0 Hz, 1H), 1.65 (s, 6H).

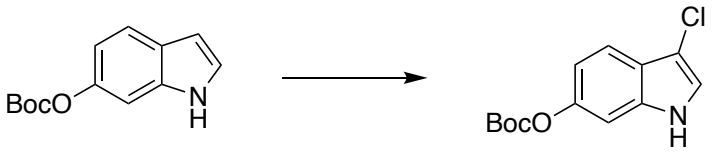

18 **19**

N-Chlorosuccinimide (2.98 g, 22.31 mmol) was added to **18** (5 g, 21.45 mmol) in DMF (105 mL). The solution was allowed to stir at room temperature for 3 hours while being kept from light. The solution was then taken up in EtOAc (200 mL) and H_2O (200 mL) and the organics were washed with two more portions of H_2O (2 x 150 mL) followed by brine (100 mL). The organics were dried with Na_2SO_4, filtered, and concentrated under reduced pressure. The crude product was purified by silica plug (20% EtOAc/Hexane) and recrystallized in EtOAc/Hexane giving 5.06 g of white crystal (85% yield). **17**: ^{1}H NMR (400 MHz, $CDCl_3$) δ 8.08 (s, 1H), 7.59 (d, J = 8.6 Hz, 1H), 7.19 (dd, J = 15.3, 2.2 Hz, 2H), 7.01 (dd, J = 8.6, 2.0 Hz, 1H), 1.57 (s, 9H).

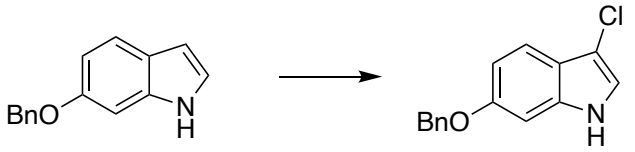

77 **78**

N-Chlorosuccinimide (13.02 g, 97.53 mmol) was added to **77** (20.94 g, 93.78 mmol) in DMF (434 mL). The solution was allowed to stir at room temperature for 3 hours while being kept from light. The solution was then taken up in EtOAc (250 mL) and H_2O (500 mL) and the aqueous was washed EtOAc (3 x 250 mL). The organics were washed with H_2O (500 mL) followed by brine (500 mL). The organics were dried with Na_2SO_4, filtered, and concentrated under reduced pressure. The crude product was purified by silica plug (20% EtOAc/Hexane) and recrystallized in EtOAc/Hexane giving 21.35 g of white crystal (85% yield). **78**: ^{1}H NMR (400 MHz, $CDCl_3$) δ 7.89 (s, 1H), 7.51 (d, J = 8.7 Hz, 1H), 7.46 (d, J = 7.3 Hz, 2H), 7.39 (t, J = 7.4 Hz, 2H), 7.33 (d, J = 7.2 Hz, 1H), 7.06 (d, J = 2.1 Hz, 1H), 6.95 (dd, J = 8.7, 2.1 Hz, 1H), 6.89 (d, J = 1.9 Hz, 1H), 5.11 (s, 2H). (ESI-B-TOFMS) *m/z* 258.0672 [$C_{15}H_{12}N_1O_1Cl_1$ (M+H) requires 258.0680]

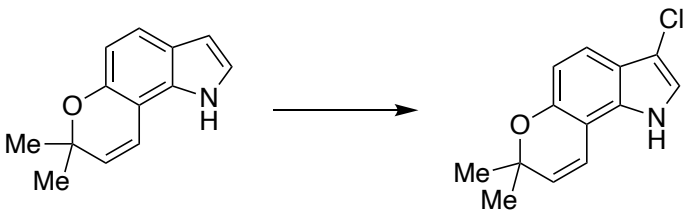

133 **134**

N-Chlorosuccinimide (3.37 g, 25.2 mmol) was added to **133** (4.83 g, 24.2 mmol) in DMF (121 mL). The solution was allowed to stir at room temperature for 3 hours while being kept from light. The solution was then taken up in EtOAc (60 mL) and H_2O (120 mL) and the aqueous was washed EtOAc (3 x 60 mL). The organics were washed with H_2O (120 mL) followed by brine

(120 mL). The organics were dried with Na_2SO_4, filtered, and concentrated under reduced pressure. The crude product was purified by silica plug (20% EtOAc/Hexane) and recrystallized in EtOAc/Hexane giving 5.10 g of **134** as a white crystal (90% yield).

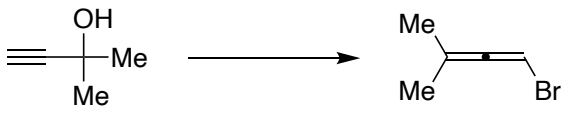

61 **62**

NH_4Br (37.35 g, 381 mmol), CuBr (46.65 g, 325 mmol), Cu (2.37 g, 37.3 mmol) and HBr (180 mL, 3.315 mol) were added to a 1L round bottom flask while a mixture of 2-methyl-3-butyn-2-ol 205 (90 mL, 929 mmol) and pentane (225 mL) was added dropwise over the course of 1.5 hours. After addition, the flask was heated to 30°C and stirred for 3 additional hours. Once the solution was cooled to rt, the mixture was extracted with equal volumes of concentrated HBr (2 x 500 mL) and water (3 x 500 mL), dried overnight over $MgSO_4$ at 0 °C. The dried compound was run through a silica plug, eluting with pentane, and concentrated at 0 °C to yield **62** as a clear yellow liquid (98.7 g, 72%).

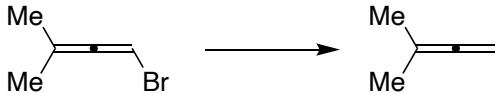

62 **63**

Zn dust (37 g, 571 mmol) and AcOH (238 mL) were added to a multi-neck round bottom flask equipped with an addition funnel and a short-path distillation apparatus with the receiving flask set in a -78 °C bath. The flask was heated to 50 °C, and bromoallene (70g, 476 mmol) was added dropwise, maintaining a distillation temperature below 45 °C. Once the bromoallene was fully incorporated, the flask was heated to 60 °C. Once the distillation was complete, allene was

isolated from any remaining AcOH by freezing off the AcOH to give 20.7 g of allene (89% yield). **63**: ^{1}H NMR (400 MHz, $CDCl_3$) δ 4.44 (hept, J = 3.1 Hz, 2H), 1.62 (t, 6H). ^{13}C NMR (101 MHz, $CDCl_3$) δ 206.70, 93.83, 72.42, 19.98.

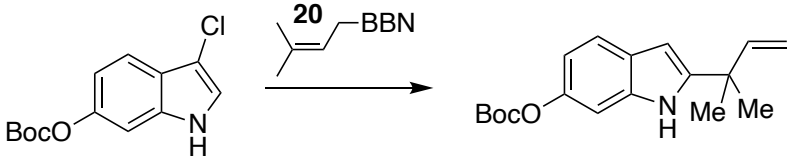

19 **21**

Allene **63** (3.89 mL, 39.65 mmol) was added to a 0.5M solution of 9-BBN in THF (66.08 mL, 33.04 mmol) at 0 °C then warmed to room temperature and stirred for 16 h. Chlorinated indole **19** (3.01 g, 11.23 mmol) was added at room temperature and stirred for 15 min before addition of triethylamine (4.65 mL, 33.37 mmol). The solution stirred for 8 more hours then was washed with 1M HCl (80 mL) and $NaHCO_3$ (80 mL). The organics were cooled to 0 °C with a dry ice/acetone bath and 2M NaOH (73 mL) was added dropwise while keeping the temperature between 0-5 °C. The same was repeated with H_2O_2 (73 mL). The solution was extracted with ether (160 mL) then washed twice with brine (80 mL). The solution was dried with $MgSO_4$, filtered, and concentrated under reduced pressure. The residue was purified with flash chromatography, eluting with 3-6% EtOAc/Hexanes, yielding 1.49 g of yellow oil (48% yield). **21**: ^{1}H NMR (400 MHz, $CDCl_3$) δ 7.96 (s, 1H), 7.47 (d, *J* = 8.5 Hz, 1H), 7.11 (d, *J* = 2.0 Hz, 1H), 6.88 (dd, *J* = 8.5, 2.1 Hz, 1H), 6.27 (d, *J* = 1.3 Hz, 1H), 6.05 – 5.94 (m, 1H), 5.12 – 5.05 (m, 2H), 1.57 (s, 9H), 1.45 (s, 6H). ^{13}C NMR (101 MHz, $CDCl_3$) δ 152.88, 146.73, 146.44, 146.05, 135.73, 126.64, 120.41, 113.69, 112.39, 103.43, 98.00, 83.25, 42.07, 38.32, 27.87, 27.46.

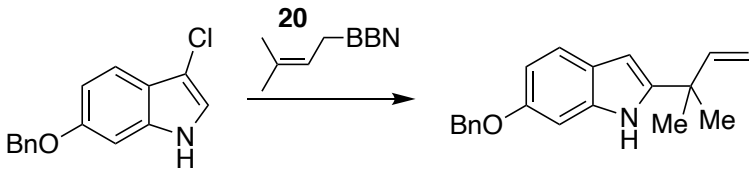

78 **79**

Allene **63** (4.89 mL, 49.8 mmol) was added to a 0.5M solution of 9-BBN in THF (84 mL, 41.9 mmol) at 0 °C then warmed to room temperature and stirred for 16 h. Chlorinated indole **78** (3.67 g, 14.2 mmol) was added at room temperature and stirred for 15 min before triethylamine (5.89 mL, 42.3 mmol) was added. The solution stirred for 8 more hours and was then washed with 1M HCl (90 mL) and $NaHCO_3$ (90 mL). The organics were cooled to 0 °C with a dry ice/acetone bath and 2M NaOH (83 mL) was added dropwise while keeping the temperature between 0-5 °C. The same was repeated with H_2O_2 (83 mL). The solution was extracted with ether (180 mL) then washed twice with brine (90 mL). The solution was dried with $MgSO_4$, filtered, and concentrated under reduced pressure. The residue was purified with flash chromatography, eluting with 3-5% EtOAc/Hexanes, yielding 2.72 g of pale-yellow oil (65% yield). **79**: ^{1}H NMR (400 MHz, $CDCl_3$) δ 7.79 (s, 1H), 7.49 – 7.31 (m, 6H), 6.90 – 6.80 (m, 2H), 6.23 (d, J = 2.2 Hz, 1H), 6.03 (dd, J = 17.7, 10.6 Hz, 1H), 5.13 – 5.05 (m, 4H), 1.46 (s, 6H). ^{13}C NMR (101 MHz, $CDCl_3$) δ 155.20, 146.36, 144.86, 137.77, 136.61, 128.64, 127.86, 127.52, 123.13, 120.73, 112.90, 112.14, 110.18, 97.74, 96.05, 70.82, 42.07, 32.13, 28.20, 27.48. (ESI-B-TOFMS) *m/z* 292.1700 [$C_{20}H_{21}N_1O_1$ (M+H) requires 292.1696]

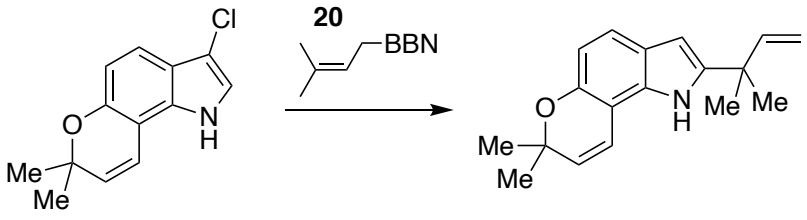

134 **135**

Allene **63** (1.67 mL, 17.0 mmol) was added to a 0.5M solution of 9-BBN in THF (28.5 mL, 14.3 mmol) at 0 °C then warmed to room temperature and stirred for 16 h. Chlorinated indole **134** (1.25 g, 4.85 mmol) was added at room temperature and stirred for 15 min before triethylamine (2.01 mL, 14.4 mmol) was added. The solution stirred for 8 more hours and was then washed with 1M HCl (30 mL) and $NaHCO_3$ (30 mL). The organics were cooled to 0 °C with a dry ice/acetone bath and 2M NaOH (28 mL) was added dropwise while keeping the temperature between 0-5 °C. The same was repeated with H_2O_2 (28 mL). The solution was extracted with ether (60 mL) then washed twice with brine (30 mL). The solution was dried with $MgSO_4$, filtered, and concentrated under reduced pressure. The residue was purified with flash chromatography, eluting with 3-5% EtOAc/Hexanes, yielding 0.98 g of pale-yellow/green oil (69% yield). **135**: ^{1}H NMR (400 MHz, $CDCl_3$) δ 7.65 (s, 1H), 7.29 (s, 1H), 6.65 – 6.52 (m, 2H), 6.21 (d, J = 2.2 Hz, 1H), 6.03 (dd, J = 17.4, 10.5 Hz, 1H), 5.64 (d, J = 9.7 Hz, 1H), 5.18 – 5.07 (m, 2H), 1.46 (s, 6H), 1.45 (s, 6H).

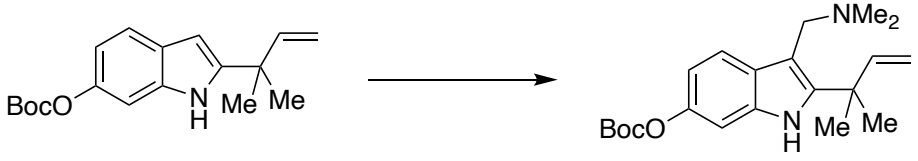

21 **22**

Prenylated indole **21** (1.73 g, 5.74 mmol) was dissolved in glacial acetic acid/MeCN (5.5 mL/0.55 mL) and cooled to 0 °C using an ice bath. Aqueous formaldehyde (37% w/w, 0.5 mL, 6.03 mmol)

and aqueous dimethylamine (40% w/w, 0.8 mL, 6.32 mmol) were added, then the reaction was allowed to warm to room temperature, stirring for 4 hours. The mixture was partitioned between 1 M HCl (50 mL) and ether (100 mL). The aqueous was then basified with 2 M NaOH (150 mL) and washed with ether (2 x 200 mL). The combined organics were washed with $NaHCO_3$ (2 x 50 mL), brine (2 x 200 mL), dried with $MgSO_4$, filtered, and concentrated under reduced pressure. The crude residue was carried forward without further purification.

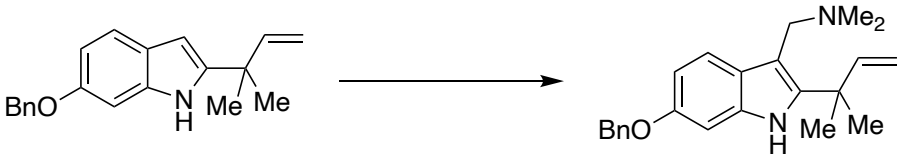

79 **80**

Prenylated indole **79** (3.19 g, 10.95 mmol) was dissolved in glacial acetic acid/MeCN (10 mL/1 mL) and cooled to 0 °C in an ice bath. Aqueous formaldehyde (40% w/w, 0.86 mL, 11.50 mmol) and aqueous dimethylamine (37% w/w, 1.5 mL, 12.05 mmol) were added, then the reaction was allowed to warm to room temperature, stirring for 4 hours. The mixture was partitioned between 1 M HCl (100 mL) and ether (200 mL). The aqueous was then basified with 2M NaOH (300 mL) and washed with ether (2 x 400 mL). The combined organics were washed with $NaHCO_3$ (2 x 100 mL), brine (2 x 400 mL), dried with $MgSO_4$, filtered, and concentrated under reduced pressure. The crude residue was carried forward without further purification. (ESI-B-TOFMS) *m/z* 349.2274 [$C_{23}H_{28}N_2O_1$ (M+H) requires 349.2274]

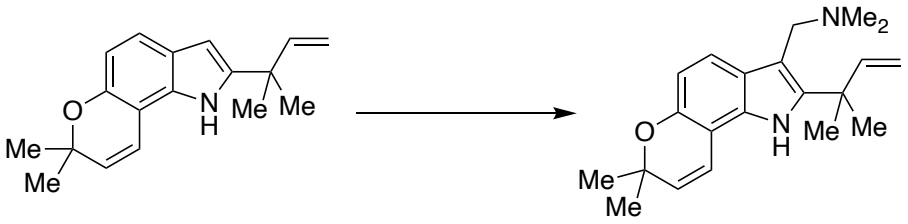

135 **136**

Prenylated indole **135** (2.523 g, 9.436 mmol) was dissolved in glacial acetic acid/MeCN (8.8 mL/0.88 mL) and cooled to 0 ºC in an ice bath. Aqueous formaldehyde (40% w/w, 0.74 mL, 9.91 mmol) and aqueous dimethylamine (37% w/w, 1.3 mL, 10.38 mmol) were added, then the reaction was allowed to warm to room temperature, stirring for 4 hours. The mixture was partitioned between 1 M HCl (80 mL) and ether (160 mL). The aqueous was then basified with 2M NaOH (240 mL) and washed with ether (2 x 320 mL). The combined organics were washed with $NaHCO_3$ (2 x 80 mL), brine (2 x 320 mL), dried with $MgSO_4$, filtered, and concentrated under reduced pressure. The crude residue was carried forward without further purification.

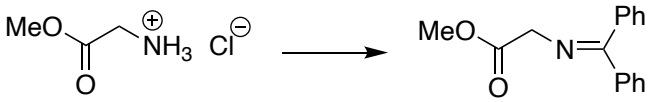

23

To a solution of benzophenone (6.0 g, 33.11 mmol) in DCM (120 mL), glycine HCl (4.12 g, 32.82 mmol) was added. This solution was allowed to stir for 24 hours, then the precipitated salts were filtered off and the filtrate was concentrated under reduced pressure. The residue was taken up in ether (120 mL) and washed with H_2O (2 x 60 mL). The organics were dried over $MgSO_4$, filtered, and concentrated under reduced pressure. This resulted in 5.49 g of **23** as a light-yellow powder (66% yield). All spectral data matched that of previously reported.

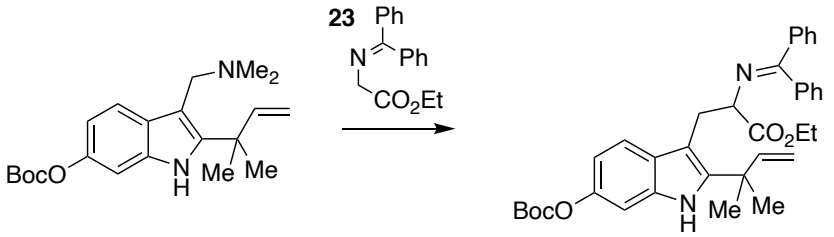

22 **64**

DBU (0.8 mL, 5.255 mmol) was added to a solution of gramine **22** (1.58 g, 4.411 mmol) and glycine derivative **23** (1.18 g, 4.411 mmol) in MeCN (21 mL) at 0 °C. Solution was heated to reflux and stirred for 18 hours. Solution turned from light to dark orange. Solution was cooled to room temperature, then poured into NH_4Cl (50 mL) and extracted with ether (2 x 50 mL). The organics were washed with brine (2 x 100 mL), dried over Na_2SO_4, filtered, and concentrated under reduced pressure. The crude residue was carried forward for hydrolysis.

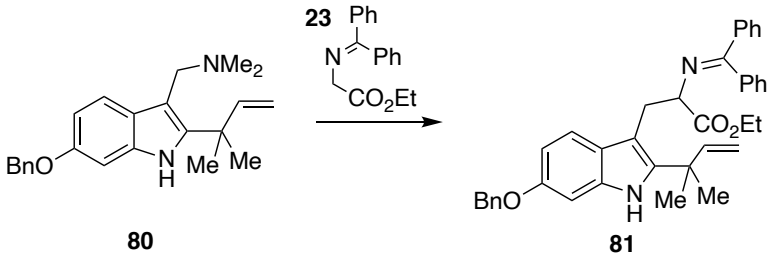

80 **81**

DBU (0.49 mL, 3.2 mmol) was added to a solution of gramine **80** (0.88 g, 2.5 mmol) and **23** (0.68 g, 2.5 mmol) in MeCN (12 mL) at 0 °C. Solution was heated to reflux and stirred for 18 hours. Solution turned from light to dark orange. Solution was cooled to room temperature, then poured into NH_4Cl (70 mL) and extracted with ether (2 x 70 mL). The organics were washed with brine (2 x 140 mL), dried over Na_2SO_4, filtered, and concentrated under reduced pressure. The crude residue was carried forward for hydrolysis.

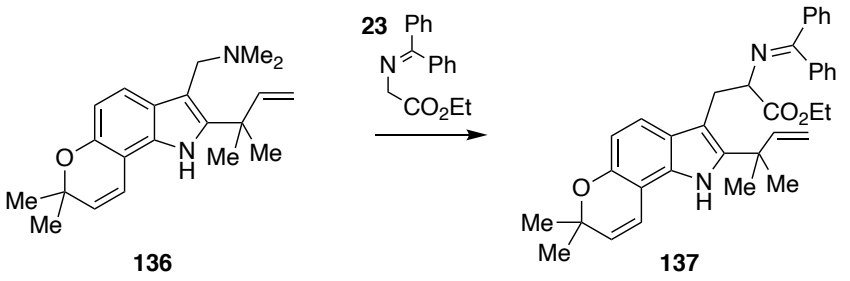

136 137

DBU (1.82 mL, 12.1 mmol) was added to a solution of gramine **136** (3.06 g, 9.43 mmol) and glycine derivative **23** (2.52 g, 9.43 mmol) in MeCN (47 mL) at 0 ºC. Solution was heated to reflux and stirred for 18 hours. Solution turned from light to dark orange. Solution was cooled to room temperature, then poured into NH_4Cl (100 mL) and extracted with ether (2 x 100 mL). The organics were washed with brine (2 x 200 mL), dried over Na_2SO_4, filtered, and concentrated under reduced pressure. The crude residue was carried forward for hydrolysis.

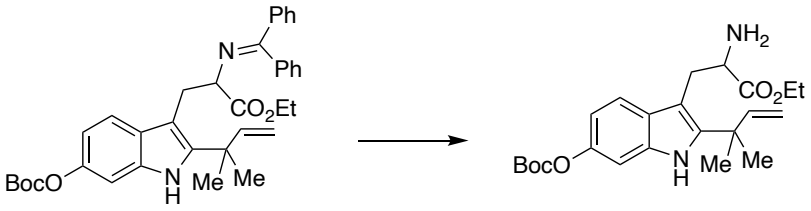

64 24

Crude imine **64** (2.50 g, 4.305 mmol) was taken up in MeCN (26 mL) and cooled to 0 ºC. 1M HCl (12.5 mL) was added at 0 ºC then stirred at room temperature for 4 hours. The solution was basified at 0 ºC with 1 M NaOH (34 mL), extracted with ether (200 mL), washed with brine (2 x 100 mL), dried with $MgSO_4$, filtered, and concentrated under reduced pressure. The residue was purified with flash chromatography, eluting first with DCM, then 3% MeOH/DCM to yield 1.25 g of orange oil (52% yield over 3 steps). **24**: ^{1}H NMR (400 MHz, $CDCl_3$) δ 7.93 (s, 1H), 7.50 (d, *J* = 8.5 Hz, 1H), 7.10 (t, *J* = 1.5 Hz, 1H), 6.89 (dt, *J* = 8.4, 1.6 Hz, 1H), 6.11 (dd, *J* = 17.5, 10.4 Hz, 1H), 5.20 – 5.12 (m, 2H), 3.84 (dd, *J* = 9.4, 5.1 Hz, 1H), 3.67 (d, *J* = 1.1 Hz, 3H), 3.35 –

3.27 (m, 1H), 3.04 (dd, *J* = 14.5, 9.4 Hz, 1H), 1.56 (s, 6H), 1.54 (s, 9H), 1.42 (dd, *J* = 19.9, 8.2 Hz, 2H).

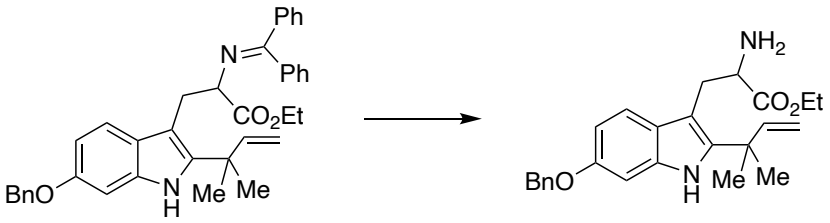

81 **82**

Crude imine **81** (1.40 g, 2.45 mmol) was taken up in MeCN (15 mL) and cooled to 0 °C. 1M HCl (7.1 mL) was added at 0 °C then stirred at room temperature for 4 hours. The solution was basified at 0 °C with 1 M NaOH (14 mL), extracted with ether (80 mL), washed with brine (2 x 40 mL), dried with $MgSO_4$, filtered, and concentrated under reduced pressure. The residue was purified with flash chromatography, eluting first with DCM, then 3% MeOH/DCM to yield 0.55 g of dark orange oil (55% yield over 3 steps). **82**: ^{1}H NMR (400 MHz, $CDCl_3$) δ 7.83 (s, 1H), 7.48 – 7.28 (m, 7H), 6.84 (d, *J* = 7.5 Hz, 2H), 6.12 (dd, *J* = 17.4, 10.6 Hz, 1H), 5.19 – 5.13 (m, 2H), 5.10 (s, 2H), 3.86 (s, 1H), 3.68 (s, 3H), 3.30 (d, *J* = 13.3 Hz, 1H), 3.03 (dd, *J* = 14.5, 9.4 Hz, 1H), 1.89 (s, 2H), 1.54 (s, 6H). ^{13}C NMR (101 MHz, $CDCl_3$) δ 155.44, 146.29, 139.40, 137.67, 134.89, 128.66, 127.90, 127.50, 124.46, 119.35, 112.09, 110.05, 106.83, 95.83, 70.79, 52.11, 39.29, 28.04, 27.97. (ESI-B-TOFMS) *m/z* 407.2334 [$C_{25}H_{30}N_2O_3$ (M+H) requires 407.2329]

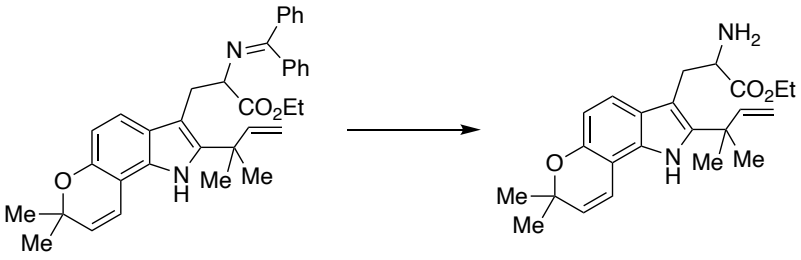

137 **138**

Crude imine **137** (5.48 g, 10.0 mmol) was taken up in MeCN (60 mL) and cooled to 0 °C. 1M HCl (29.1 mL) was added at 0 °C then stirred at room temperature for 4 hours. The solution was basified at 0 °C with 1 M NaOH (55 mL), extracted with ether (320 mL), washed with brine (2 x 640 mL), dried with $MgSO_4$, filtered, and concentrated under reduced pressure. The residue was purified with flash chromatography, eluting first with DCM, then 3% MeOH/DCM to yield 2.71 g of dark orange oil (65% yield over 3 steps). **138**: ^{1}H NMR (400 MHz, $CDCl_3$) δ 7.68 (s, 1H), 7.28 (d, J = 8.7 Hz, 1H), 6.59 (dd, J = 24.2, 9.1 Hz, 2H), 6.13 (dd, J = 17.5, 10.6 Hz, 1H), 5.65 (d, J = 9.9 Hz, 1H), 5.22 – 5.12 (m, 2H), 4.19 – 4.04 (m, 2H), 3.80 (dd, J = 9.5, 5.1 Hz, 1H), 3.26 (dd, J = 14.4, 5.1 Hz, 1H), 2.99 (dd, J = 14.4, 9.6 Hz, 1H), 1.56 (s, 6H), 1.44 (s, 6H), 1.18 (td, J = 7.1, 0.9 Hz, 3H).

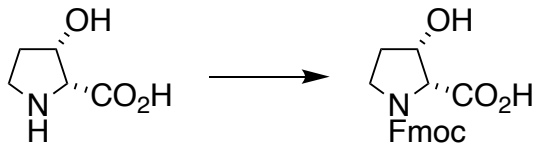

65

Aqueous 1M K_2CO_3 (191 mL, 191 mmol) followed by FmocOSu (14.5 g, 43.1 mmol) were added to a solution of L-proline (5.0 g, 38.1 mmol) in dioxane (219 mL) and the reaction was stirred at room temperature for 18 h. The solution was diluted with H_2O (290 mL) and extracted with ether (725 mL x 2). The layers were separated, and the aqueous phase was acidified with 2M HCl (250 mL), then extracted with EtOAc (725 mL x 1, 360 mL x 2). The organic phase was washed with

saturated aqueous NaCl (725 mL x 2), then dried ($MgSO_4$), filtered and concentrated under reduced pressure to yield 10.5 g protected hydroxyproline **65** as a yellow solid (78% yield). ^1H NMR (400 MHz, DMSO) δ 7.93 – 7.86 (m, 2H), 7.66 (d, J = 7.4 Hz, 2H), 7.42 (t, J = 7.3 Hz, 2H), 7.34 (td, J = 7.5, 4.0 Hz, 2H), 4.27 (s, 1H), 4.17 (m, 2H), 3.47 (m, 1H), 3.40 (m, 2H), 2.05 – 1.92 (m, 1H), 1.89 –1.80 (m, 1H). 13C NMR (101 MHz, DMSO) δ 171.76, 171.23, 154.41, 144.31, 144.25, 144.22, 144.12, 141.21, 141.10, 135.85, 133.71, 129.96, 128.19, 128.15, 127.63, 125.82, 125.78, 125.63, 125.58, 124.41, 121.68, 120.62, 120.59, 120.56, 71.55, 70.59, 67.47, 67.01, 64.03, 63.68, 47.16, 47.10, 44.85, 44.39, 32.92, 32.05.

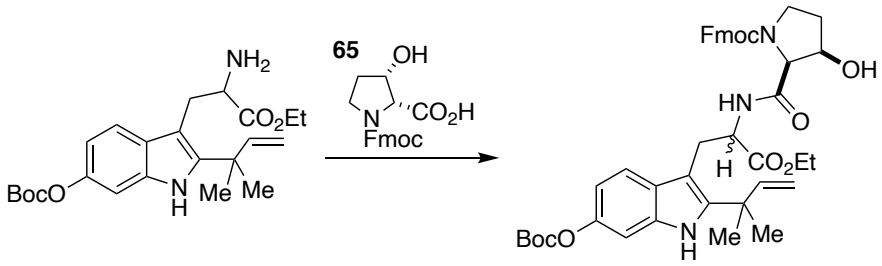

24 **66**

HATU (1.55 g, 4.084 mmol) and *i*-Pr_2NEt (2.1 mL, 12.012 mmol) were added to a solution of hydroxyproline **65** (1.41 g, 3.99 mmol) and tryptophan **66** (1.25 g, 3.00 mmol) in MeCN (22 mL) at room temperature and was stirred for 4 hours. The reaction was concentrated under reduced pressure and the residue was dissolved in ethyl acetate, then partitioned between ether (340 mL) and 1M HCl (192 mL). The organics were washed with brine (192 mL), dried over $MgSO_4$, filtered, and concentrated under reduced pressure. The crude material was purified by flash chromatography with 60-80% EtOAc/Hexanes, yielding 1.67 g of yellow-orange foam (74% yield). All spectral data matched that of previously reported.

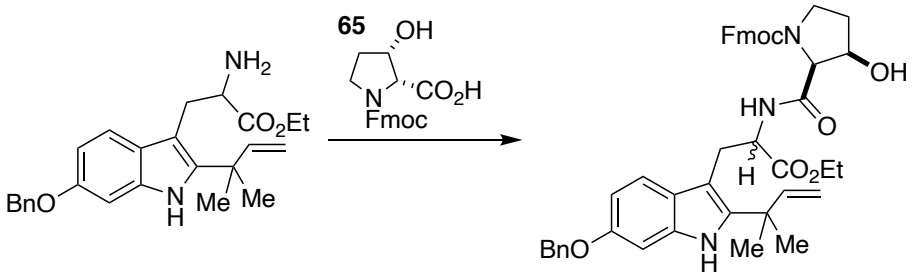

82 **83**

HATU (1.69 g, 4.44 mmol) and *i*-Pr_2NEt (2.3 mL, 13.1 mmol) were added to a solution of hydroxyproline **65** (1.53 g, 4.34 mmol) and tryptophan **82** (1.36 g, 3.27 mmol) in MeCN (30 mL) at room temperature and was stirred for 4 hours. The reaction was concentrated under reduced pressure and the residue was partitioned between DCM (400 mL) and 1M HCl (220 mL). The organics were washed with brine (220 mL), dried over $MgSO_4$, filtered, and concentrated under reduced pressure. The crude material was purified by flash chromatography with 60-80% EtOAc/Hexanes, yielding 1.85 g (75% yield) of pale-orange foam. **83**: ^{13}C NMR (101 MHz, $CDCl_3$) δ 171.25, 166.67, 165.89, 155.29, 150.00, 145.87, 141.29, 139.67, 137.50, 135.52, 134.71, 129.84, 129.61, 128.51, 128.49, 127.76, 127.36, 127.14, 125.12, 120.31, 120.18, 112.28, 99.38, 95.90, 80.71, 60.44, 53.84, 52.55, 39.04, 38.63, 31.94, 29.72, 29.38, 27.75, 27.62, 22.71, 21.06, 20.61, 17.43, 14.21, 14.14. (ESI-B-TOFMS) *m/z* 728.3333 [$C_{44}H_{45}N_3O_7$ (M+H) requires 728.3330]

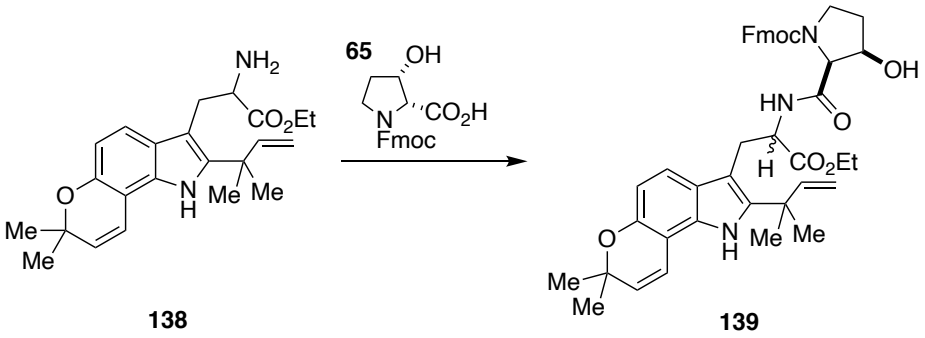

138 **139**

HATU (1.14 g, 2.99 mmol) and *i*-Pr_2NEt (1.53 mL, 8.78 mmol) were added to a solution of hydroxyproline **65** (1.03 g, 2.92 mmol) and tryptophan **138** (0.840 g, 2.20 mmol) in MeCN (18 mL) at room temperature and was stirred for 4 hours. The reaction was concentrated under reduced pressure and the residue was partitioned between DCM (250 mL) and 1M HCl (132 mL). The organics were washed with brine (132 mL), dried over $MgSO_4$, filtered, and concentrated under reduced pressure. The crude material was purified by flash chromatography with 60-80% EtOAc/Hexanes, yielding 1.29 g (78% yield) of orange foam.

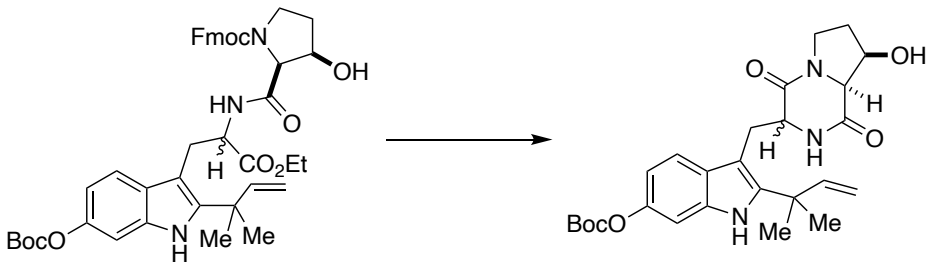

66 **67**

Triethylamine (2.45 mL, 17.568 mmol) and 2-hydroxypyridine (37 mg, 0.387 mmol) were added to dipeptide **66** (1.32 g, 1.757 mmol) in MeCN (34 mL) at room temperature. The solution was heated to reflux and stirred for 22 hours. Solution was then allowed to cool to room temperature and partitioned between DCM (84 mL) and 1 M HCl (42 mL). The aqueous was washed with DCM (2 x 21 mL) and the combined organics were washed with brine (84 mL), dried over $MgSO_4$, filtered, and concentrated under reduced pressure. The resulting residue was purified by

flash chromatography with 3-5% MeOH/DCM resulting in *cis* and *trans* isomers of **67**, totaling 424 mg of orange oil (50% yield). **67a**: ^{1}H NMR (400 MHz, $CDCl_3$) δ 8.14 (s, 1H), 7.43 (d, *J* = 8.6 Hz, 1H), 7.15 (s, 1H), 6.92 (d, *J* = 8.6 Hz, 1H), 6.09 (dd, *J* = 17.3, 10.6 Hz, 1H), 5.80 (s, 1H), 5.16 (s, 2H), 4.68 (s, 1H), 4.39 (d, *J* = 9.2 Hz, 1H), 4.10 (s, 1H), 3.93 – 3.82 (m, 1H), 3.72 (s, 2H), 3.16 (dd, *J* = 15.3, 11.7 Hz, 1H), 3.04 (s, 1H), 2.17 (dd, *J* = 14.0, 7.5 Hz, 1H), 2.04 (s, 1H), 1.52 (s, 6H). ^{13}C NMR (101 MHz, $CDCl_3$) δ 167.63, 165.79, 152.70, 147.14, 145.53, 142.58, 134.26, 127.08, 118.40, 114.34, 113.15, 104.69, 103.97, 83.56, 70.97, 64.65, 54.91, 44.17, 39.19, 30.33, 28.04, 27.94, 27.87, 26.36. **67b**: ^{1}H NMR (400 MHz, $CDCl_3$) δ 8.08 (s, 1H), 7.39 (d, *J* = 8.6 Hz, 1H), 7.01 (s, 1H), 6.81 (d, *J* = 8.7 Hz, 1H), 6.16 (d, *J* = 4.0 Hz, 1H), 5.99 (dd, *J* = 17.4, 10.5 Hz, 1H), 5.11 – 5.01 (m, 2H), 4.46 (s, 1H), 4.17 – 4.09 (m, 1H), 3.78 – 3.66 (m, 1H), 3.50 – 3.30 (m, 3H), 3.17 (dd, *J* = 14.7, 8.9 Hz, 1H), 3.03 (s, 1H), 1.94 (dd, *J* = 13.8, 7.5 Hz, 1H), 1.78 – 1.61 (m, 1H), 1.50 (s, 9H), 1.39 (d, *J* = 3.6 Hz, 6H). ^{13}C NMR (101 MHz, $CDCl_3$) δ 167.23, 166.09, 152.71, 146.68, 145.85, 142.34, 133.99, 126.87, 118.91, 113.72, 112.01, 104.92, 103.50, 83.44, 70.87, 63.75, 58.29, 44.14, 39.14, 29.85, 29.56, 27.83, 27.74, 27.69.

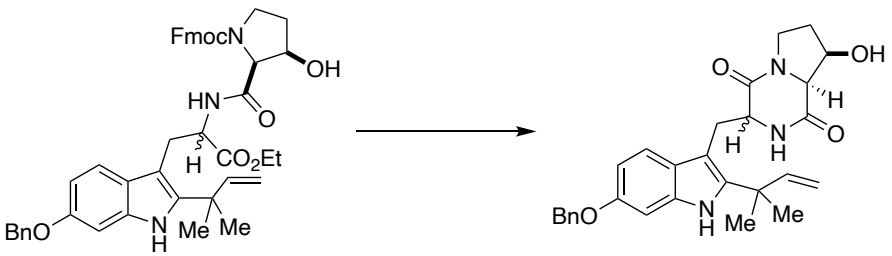

83 **84**

Triethylamine (0.81 mL, 5.83 mmol) and 2-hydroxypyridine (12 mg, 0.128 mmol) were added to dipeptide **83** (438 mg, 0.583 mmol) in MeCN (11 mL) at room temperature. The solution was heated to reflux and stirred for 22 hours. Solution was then allowed to cool to room temperature and partitioned between DCM (28 mL) and 1 M HCl (14 mL). The aqueous was washed with

DCM (2 x 7 mL) and the combined organics were washed with brine (28 mL), dried over $MgSO_4$, filtered, and concentrated under reduced pressure. The resulting residue was purified by flash chromatography with 3-5% MeOH/DCM resulting in *cis* and *trans* isomers of **84**, totaling 198 mg of red-orange oil (70% yield). **84a**: ^{1}H NMR (400 MHz, $CDCl_3$) δ 7.85 (s, 1H), 7.45 (d, J = 6.8 Hz, 2H), 7.41 – 7.36 (m, 3H), 7.33 (d, J = 7.3 Hz, 1H), 6.88 – 6.83 (m, 2H), 6.10 (dd, J = 17.5, 10.5 Hz, 1H), 5.79 (d, J = 3.7 Hz, 1H), 5.21 – 5.13 (m, 2H), 5.10 (s, 2H), 4.28– 4.15 (m, 2H), 3.66 – 3.55 (m, 1H), 3.50 – 3.41 (m, 2H), 3.36 (d, J = 8.5 Hz, 1H), 3.29 – 3.18 (m, 2H), 2.26 (m, 1H), 1.76 (m, 1H), 1.50 (d, J = 3.2 Hz, 6H). **84b**: ^{1}H NMR (400 MHz, $CDCl_3$) δ 8.09 (s, 1H), 8.01 (s, 1H), 7.44 (d, J = 7.3 Hz, 2H), 7.41 – 7.30 (m, 4H), 6.89 – 6.81 (m, 2H), 6.10 (dd, J = 17.5, 10.4 Hz, 1H), 5.86 (s, 1H), 5.18 – 5.12 (m, 2H), 5.09 (s, 2H), 4.67 (s, 1H), 4.38 (d, J = 9.3 Hz, 1H), 4.10 (s, 1H), 3.88 (td, J = 11.0, 7.5 Hz, 1H), 3.75 – 3.64 (m, 2H), 3.14 (dd, J = 15.2, 11.7 Hz, 1H), 3.08 (s, 1H), 2.95 (s, 3H), 2.87 (s, 3H), 2.16 (m, 1H), 2.09 – 1.95 (m, 1H). (ESI-B-TOFMS) m/z 474.2410 [$C_{28}H_{31}N_3O_4$ (M+H) requires 474.2393]

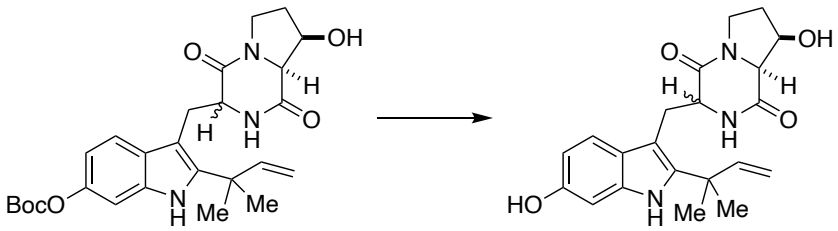

67 **68**

TFA (1.13 mL, 14.7 mmol) was added to a solution of diketopiperazine **67** (354 mg, 0.732 mmol) and DCM (4.1 mL) at 0 °C and stirred for 2 hours. The solution was then allowed to warm to room temperature and stirred for 3 hours. The reaction mixture was diluted with EtOAc (38 mL), and sodium bicarbonate (38 mL) was slowly added. The aqueous was washed with EtOAc (2 x 19 mL) then the combined organics were washed with brine (38 mL), dried with

$MgSO_4$, and concentrated under reduced pressure. The resulting residue was purified by flash column chromatography with 3-6% MeOH/DCM to yield 202 mg of white powder (72% yield). **68**: ^{1}H NMR (400 MHz, MeOD) δ 7.28 (d, *J* = 8.6 Hz, 1H), 6.80 (d, *J* = 2.2 Hz, 1H), 6.59 (dd, *J* = 8.5, 2.2 Hz, 1H), 6.17 (dd, *J* = 17.4, 10.5 Hz, 1H), 5.15 – 5.03 (m, 2H), 4.56 (t, *J* = 3.3 Hz, 1H), 4.44 (ddd, *J* = 11.6, 3.8, 2.2 Hz, 1H), 4.15 (t, *J* = 2.6 Hz, 1H), 3.89 (dt, *J* = 11.9, 8.9 Hz, 1H), 3.62 (dd, *J* = 14.8, 3.9 Hz, 1H), 3.51 (ddd, *J* = 12.2, 10.0, 2.3 Hz, 1H), 3.08 (dd, *J* = 14.8, 11.6 Hz, 1H), 2.15 – 1.95 (m, 2H), 1.53 (s, 3H), 1.51 (s, 3H). ^{13}C NMR (101 MHz, MeOD) δ 167.97, 167.87, 154.16, 147.79, 141.56, 137.73, 128.64, 127.00, 124.12, 119.23, 111.97, 110.38, 104.74, 97.63, 71.72, 66.00, 56.52, 44.57, 40.20, 32.02, 29.11, 28.61, 28.56.

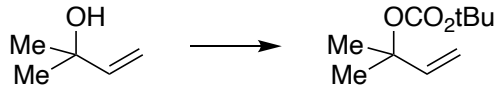

69

1.6 M n-BuLi in hexanes (31 mL, 50.0 mmol) was added to 2-methyl-3-buten-2-ol (5.2 mL, 50.0 mmol) in THF (90 mL) at 0 ºC over 10 minutes. The solution was allowed to stir at 0 ºC for 20 minutes then Boc anhydride was added, and the reaction stirred at room temperature for 4 hours. Sodium bicarbonate (200 mL) was added, then the organics were washed with H_2O (30 mL) and brine (150 mL), dried with $MgSO_4$, filtered, and concentrated under reduced pressure to yield 8.01 g of **69** as a yellow liquid (86% yield). All spectral data matched that of previously reported.

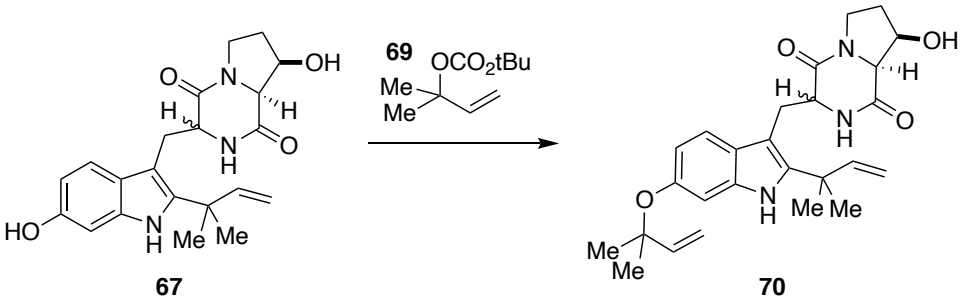

67 **70**

Phenol **67** (218 mg, 0.593 mmol) and carbonate **69** (292 mg, 1.57 mmol) were taken up in THF (5 mL). The solution was degassed (freeze pump thaw, 3 cycles), then $Pd(PPh_3)_4$ (11.6 mg, 0.010 mmol) was added and the mixture was stirred at room temperature for 24 hours. The mixture was then filtered through a silica plug (5 g), washing with THF and DCM, then concentrated and purified by flash column chromatography, eluting with 3-6% MeOH/DCM. This yielded 222 mg of **70** as a mixture of diastereomers as tan solids (83% yield). All spectral data matched that of previously reported.

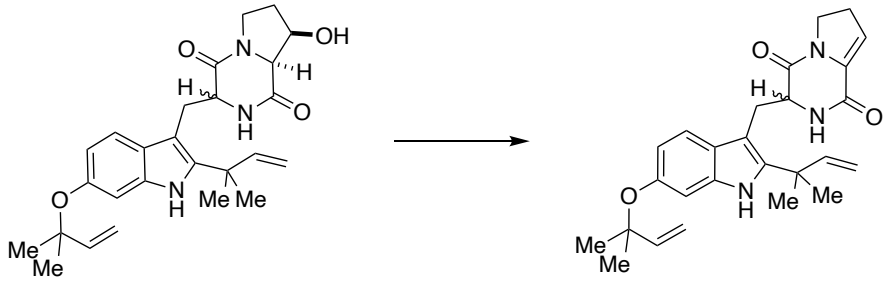

70 **71**

DEAD (0.20 mL, 0.399 mmol) was added at room temperature to **70** (30.0 mg, 0.067 mmol) in MeCN (7 mL). The solution stirred at room temperature for 10 minutes and then PBu_3 (0.10 mL, 0.399 mmol) was added after cooling to 0 °C. The reaction was then stirred for 4 hours at room temperature, then was concentrated under reduced pressure. The residue was purified by flash column chromatography with 60-100% EtOAc/hexane to give 18.5 mg of **71** as a mixture of diastereomers as an off-white solid (64% yield). **71:** ^{1}H NMR (400 MHz, MeOD) δ 8.63 (s, 1H), 8.53 (s, 1H), 7.30 (d, J = 8.6 Hz, 1H), 7.17 – 7.10 (m, 2H), 6.96 (d, J = 2.0 Hz, 1H), 6.69 (dd, J =

8.6, 2.1 Hz, 1H), 6.62 (dd, J = 13.6, 8.5 Hz, 2H), 6.24 – 6.12 (m, 4H), 5.30 (dddd, J = 12.9, 8.6, 6.5, 3.6 Hz, 2H), 5.19 – 5.06 (m, 8H), 4.57 (s, 2H), 4.45 (d, J = 9.0 Hz, 1H), 4.39 – 4.34 (m, 2H), 4.18 (t, J = 4.6 Hz, 2H), 3.94 – 3.86 (m, 1H), 3.72 – 3.64 (m, 3H), 3.60 (dd, J = 10.7, 5.6 Hz, 2H), 3.55 (d, J = 7.4 Hz, 2H), 3.53 – 3.44 (m, 2H), 3.41 (dd, J = 13.5, 4.8 Hz, 2H), 3.21 (d, J = 2.7 Hz, 1H), 3.11 – 3.04 (m, 1H), 1.87 (s, 3H), 1.84 (s, 3H), 1.73 (s, 3H), 1.71 (s, 3H), 1.54 (s, 3H), 1.53 (s, 3H), 1.52 (s, 3H), 1.51 (s, 3H). ^{13}C NMR (101 MHz, MeOD) δ 168.98, 167.88, 151.14, 148.24, 148.01, 147.79, 145.99, 132.68, 124.52, 118.95, 117.36, 116.82, 113.68, 112.25, 111.77, 111.71, 111.07, 110.49, 105.91, 105.48, 104.84, 80.73, 71.75, 71.63, 66.04, 65.16, 59.27, 56.63, 44.75, 44.59, 40.57, 40.28, 32.06, 31.31, 29.27, 28.70, 28.48, 28.38, 27.36, 27.28, 25.97, 24.61, 24.56, 18.04.

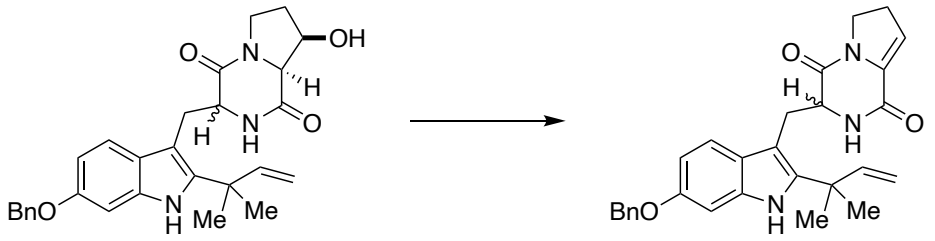

84 **143**

DEAD (0.62 mL, 3.90 mmol) was added at room temperature to **84** (1.23 g, 2.59 mmol) in DCM (46 mL). The solution stirred at room temperature for 10 minutes and then PBu_3 (0.96 mL, 3.90 mmol) was added after cooling to 0 ºC. The reaction was then stirred for 4 hours at room temperature, then was concentrated under reduced pressure. The residue was purified by flash column chromatography with 60-100% EtOAc/hexane to give 1.06 g of beige solid (90% yield). **143**: ^{1}H NMR (400 MHz, $CDCl_3$) δ 7.91 (s, 1H), 7.45 (d, *J* = 7.1 Hz, 2H), 7.42 – 7.29 (m, 4H), 6.89 – 6.83 (m, 2H), 6.15 – 6.04 (m, 2H), 5.69 (s, 1H), 5.19 – 5.12 (m, 2H), 5.10 (s, 2H), 4.48 (d, *J* = 10.2 Hz, 1H), 4.21 (q, *J* = 7.1 Hz, 1H), 4.06 (s, 2H), 3.68 (dd, *J* = 14.6, 3.6 Hz, 1H), 3.18 (dd,

J = 14.6, 11.2 Hz, 1H), 2.77 (s, 2H), 1.52 (d, J = 1.6 Hz, 6H). ^{13}C NMR (101 MHz, $CDCl_3$) δ 162.67, 156.61, 155.78, 145.96, 140.59, 137.56, 135.11, 133.24, 128.72, 127.98, 127.51, 123.45, 119.01, 118.97, 112.38, 110.70, 104.47, 96.16, 70.80, 62.44, 57.61, 45.70, 39.15, 30.91, 28.09, 28.02, 27.95, 14.57.

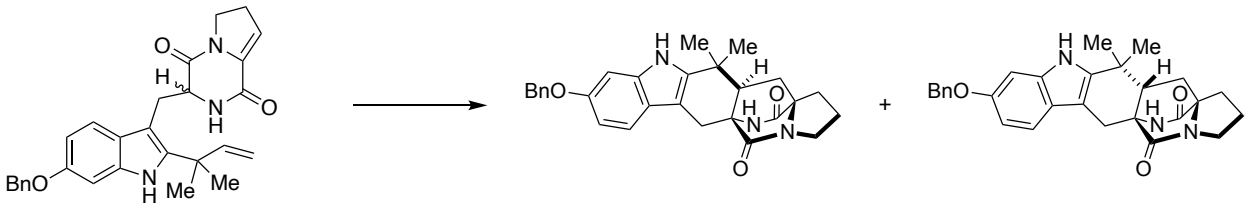

143 **85** **86**

Diketopiperazine **143** (400 mg, 0.88 mmol) was dissolved in MeOH (19 mL) and THF (38 mL) at 0 °C and 20% KOH (11.5 mL) was added. The reaction was stirred at room temperature for 18 hours. The solution was partitioned between DCM (60 mL) and 1M HCl saturated with NaCl (20 mL). The aqueous phase was extracted with DCM (3 x 20 mL) and the combined organics were dried with $MgSO_4$, filtered, and concentrated under reduced pressure. The residue was purified with PTLC using 6% MeOH/DCM to give separate bands of **85** (117 mg) and **86** (107 mg) as white solids (56% yield, 1.1:1 d.r.). **86**: ^{1}H NMR (400 MHz, MeOD) δ 7.45 (d, J = 7.4 Hz, 2H), 7.39 – 7.24 (m, 4H), 6.91 (d, J = 2.2 Hz, 1H), 6.75 (dd, J = 8.5, 2.3 Hz, 1H), 5.09 (s, 2H), 3.72 (d, J = 17.5 Hz, 1H), 3.59 – 3.44 (m, 2H), 2.91 (d, J = 17.6 Hz, 1H), 2.74 – 2.65 (m, 1H), 2.27 – 2.15 (m, 2H), 2.11 – 1.88 (m, 4H), 1.32 (s, 3H), 1.25 (s, 3H). ^{13}C NMR (101 MHz, MeOD) δ 174.08, 170.53, 155.03, 139.11, 137.93, 137.67, 128.04, 127.30, 127.19, 122.00, 117.78, 108.68, 102.17, 96.00, 70.34, 67.20, 61.50, 45.99, 43.77, 34.41, 31.92, 28.52, 27.51, 23.95, 23.44, 22.66. (ESI-B-TOFMS) m/z 456.2273 [$C_{28}H_{29}N_3O_3$ (M+H) requires 456.2282] **85**: ^{1}H NMR (400 MHz, Acetone) δ 7.47 (d, J = 7.1 Hz, 2H), 7.41 – 7.28 (m, 4H), 6.88 (d, J = 2.1 Hz, 1H), 6.77 (dd, J = 8.5, 2.2 Hz, 1H), 5.62 (s, 1H), 5.11 (s, 2H), 3.68 (d, J = 15.1 Hz, 1H), 3.48 – 3.39 (m, 1H), 3.37

– 3.28 (m, 1H), 2.76 (d, 1H), 2.68 (dd, *J* = 11.8, 6.3 Hz, 1H), 2.60 (dd, *J* = 10.1, 5.0 Hz, 1H), 2.25 – 2.13 (m, 2H), 2.12 – 2.09 (m, 1H), 1.90 (d, *J* = 12.6 Hz, 2H), 1.36 (s, 3H), 1.12 (s, 3H). ^{13}C NMR (101 MHz, DMSO) δ 182.57, 178.01, 163.67, 149.08, 147.24, 146.45, 137.88, 137.06, 136.88, 130.65, 127.57, 118.05, 112.66, 105.55, 79.08, 75.47, 69.19, 58.61, 53.04, 43.98, 39.59, 38.18, 37.48, 33.51, 33.33, 31.13. (ESI-B-TOFMS) *m/z* 456.2287 [$C_{28}H_{29}N_3O_3$ (M+H) requires 456.2282]

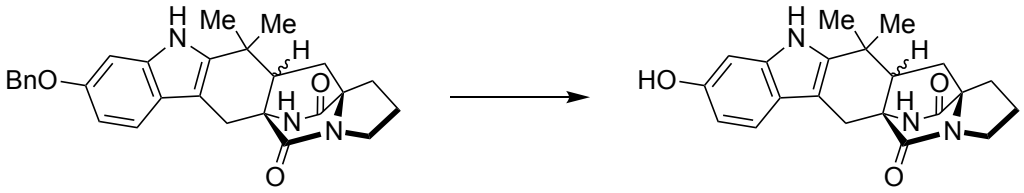

87 **88**

10 % Pd/C (88 mg, 0.827 mmol) was added to a solution of cycloadduct **87** (0.942 g, 2.068 mmol) in MeOH (6.7 mL) and THF (7 mL). Solution was sparged with hydrogen gas for 10 minutes, then stirred at room temperature under hydrogen atmosphere for 3 hours. Catalyst was removed by filtering over Celite and rinsing with 1:1 MeOH/THF. Solution was concentrated under reduced pressure which gave pure product **88** in quantitative yield (75 mg). **88**: ^{1}H NMR (400 MHz, MeOD) δ 7.24 (d, J = 8.4 Hz, 1H), 6.73 (d, J = 2.2 Hz, 1H), 6.57 (dd, J = 8.4, 2.2 Hz, 1H), 3.70 (d, J = 17.6 Hz, 1H), 3.60 – 3.45 (m, 3H), 3.35 (s, 1H), 2.89 (d, J = 17.6 Hz, 1H), 2.71 (dt, J = 13.0, 6.5 Hz, 1H), 2.30 – 2.19 (m, 2H), 2.10 (dd, J = 12.5, 6.6 Hz, 1H), 2.06 – 2.00 (m, 1H), 1.99 – 1.88 (m, 2H), 1.33 (s, 3H), 1.26 (s, 3H). (ESI-B-TOFMS) *m/z* 366.1803 [$C_{21}H_{23}N_3O_3$ (M+H) requires 366.1812]

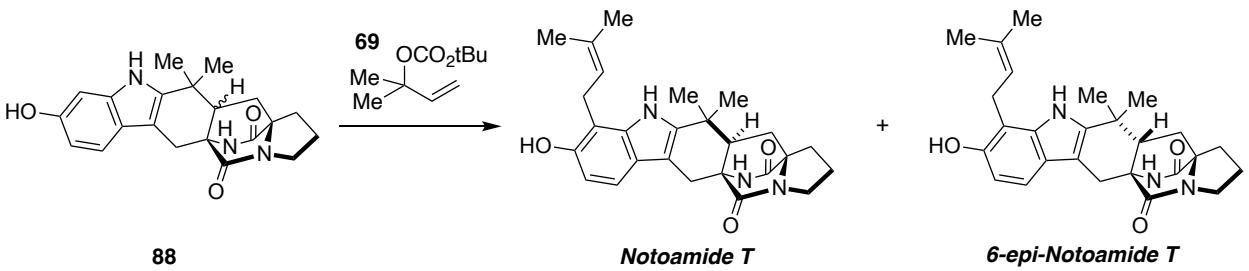

Phenol **88** (21.0 mg, 0.058 mmol) and carbonate **69** (28.0 mg, 0.152 mmol) were taken up in THF (2 mL). The solution was degassed (freeze pump thaw, 3 cycles), then $Pd(PPh_3)_4$ (1.13 mg, 0.977 μmol) was added and the mixture was stirred at room temperature for 24 hours. The mixture was then filtered through a silica plug (2 g), washing with THF and DCM. It was concentrated and purified by PTLC, eluting with 8% MeOH/DCM. This yielded 19.7 mg Notoamide T and 6-*epi*-Notoamide T as a white solid (79% yield). **Notoamide T**: ^{1}H NMR (400 MHz, MeOD) δ 7.32 (d, *J* = 8.5 Hz, 1H), 7.06 (d, *J* = 8.5 Hz, 1H), 5.27 – 5.23 (t, *J* = 6.8 Hz, 1H), 4.57 (s, 1H), 3.69 (d, *J* = 6.9 Hz, 1H), 3.62 (d, *J* = 15.5 Hz, 1H), 3.49 (m, 1H), 3.44 – 3.36 (m, 1H), 3.19 (s, 2H), 2.78 (d, *J* = 15.6 Hz, 1H), 2.75 – 2.66 (m, 1H), 2.68 – 2.55 (m, 1H), 2.31 – 2.03 (m, 3H), 2.04 – 1.89 (m, 2H), 1.82 (s, 3H), 1.68 (s, 3H), 1.40 (s, 3H), 1.14 (s, 3H). ^{13}C NMR (101 MHz, MeOD) δ 175.92, 171.43, 144.14, 143.34, 137.43, 133.17, 127.11, 123.24, 118.92, 116.84, 114.18, 105.67, 68.31, 61.65, 51.11, 45.15, 37.77, 36.37, 31.75, 30.12, 28.56, 25.83, 25.45, 25.13, 22.18, 18.20. **6-*epi*-Notoamide T**: ^{1}H NMR (400 MHz, $CDCl_3$) δ 8.03 (s, 1H), 7.37 (d, J = 8.5 Hz, 1H), 7.06 (d, J = 8.5 Hz, 1H), 5.79 (s, 1H), 5.37 (t, J = 7.2 Hz, 1H), 3.91 (d, J = 18.0 Hz, 1H), 3.71 (d, J = 7.2 Hz, 2H), 3.55 (t, J = 6.8 Hz, 2H), 2.87 (d, J = 18.1 Hz, 1H), 2.83 – 2.78 (m, 1H), 2.37 – 2.30 (m, 2H), 2.17 (dd, J = 13.5, 10.1 Hz, 2H), 2.11 – 2.03 (m, 3H), 1.92 (s, 3H), 1.79 (s, 3H), 1.29 (s, 3H), 1.28 (s, 3H).

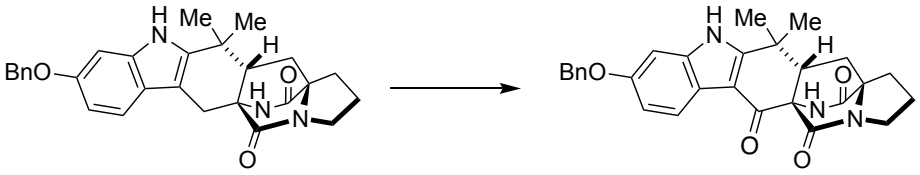

86 **120**

Cycloadduct **86** (49.0 mg, 0.108 mmol) was dissolved in THF (1.5 mL) and water (0.19 mL). The solution was cooled to 0 °C and DDQ (73.2 mg, 0.323 mmol) was slowly added. The resulting mixture was stirred at 0 °C for 20 min, after which time TLC (8% MeOH/DCM) indicated complete consumption of **86**. The reaction was quenched with saturated aqueous $NaHCO_3$. The resulting mixture was extracted with EtOAc three times. The combined organic extracts were washed with saturated aqueous $NaHCO_3$, water, and brine, dried over Na_2SO_4, filtered, and concentrated under reduced pressure. The resulting residue was purified by PTLC, eluting with 7% MeOH/DCM. This yielded 35.5 mg of white solid (70% yield). **120**: ^{1}H NMR (400 MHz, MeOD) δ 7.92 (d, J = 8.6 Hz, 1H), 7.39 – 7.17 (m, 6H), 6.92 (d, J = 2.2 Hz, 1H), 6.87 (dd, J = 8.6, 2.2 Hz, 1H), 5.04 (s, 2H), 3.50 – 3.42 (m, 1H), 3.38 – 3.31 (m, 1H), 2.70 (dd, J = 10.1, 6.2 Hz, 1H), 2.59 (dt, J = 13.6, 7.0 Hz, 1H), 2.26 (dd, J = 13.3, 10.1 Hz, 1H), 2.06 – 1.95 (m, 2H), 1.94 – 1.90 (m, 1H), 1.88 – 1.82 (m, 1H), 1.39 (s, 3H), 1.25 (s, 3H). ^{13}C NMR (101 MHz, MeOD) δ 171.87, 155.23, 142.14, 137.84, 128.03, 127.20, 118.19, 109.44, 105.30, 96.00, 70.28, 67.28, 63.27, 62.99, 43.63, 40.90, 34.94, 31.80, 29.27, 28.73, 28.40, 28.08, 24.02, 23.97. (ESI-B-TOFMS) *m/z* 470.2261 [$C_{28}H_{27}N_3O_4$ (M+H) requires 470.2074]

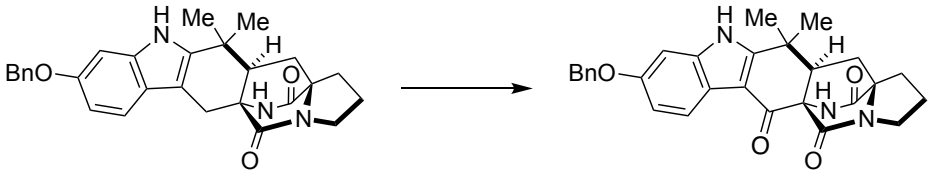

85 **89**

Cycloadduct **85** (15.0 mg, 0.033 mmol) was dissolved in THF (0.45 mL) and water (0.06 mL). The solution was cooled to 0 °C and DDQ (22 mg, 0.99 mmol) was slowly added. The resulting mixture was stirred at 0 °C for 20 min, after which time TLC (8% MeOH/DCM) indicated complete consumption of **85**. The reaction was quenched with saturated aqueous $NaHCO_3$. The resulting mixture was extracted with EtOAc three times. The combined organic extracts were washed with saturated aqueous $NaHCO_3$, water, and brine, dried over Na_2SO_4, filtered, and concentrated under reduced pressure. The resulting residue was purified by PTLC, eluting with 7% MeOH/DCM. This yielded 9.1 mg of white solid (59% yield). **89**: ^{1}H NMR (400 MHz, $CDCl_3$) δ 7.54 (d, *J* = 8.6 Hz, 1H), 7.45 (d, *J* = 7.1 Hz, 2H), 7.36 (t, *J* = 7.4 Hz, 2H), 7.29 (t, *J* = 7.2 Hz, 1H), 6.91 (d, *J* = 2.3 Hz, 1H), 6.81 (dd, *J* = 8.6, 2.3 Hz, 1H), 5.32 (s, 1H), 5.10 (s, 2H), 3.51 – 3.44 (m, 1H), 3.38 (m, 1H), 2.79 (dd, *J* = 8.8, 6.1 Hz, 1H), 2.71 (dd, *J* = 10.3, 4.7 Hz, 1H), 2.17 – 2.12 (m, 2H), 2.11 – 2.04 (m, 1H), 2.02 – 1.93 (m, 2H), 1.37 (s, 3H), 1.09 (s, 3H). ^{13}C NMR (101 MHz, $CDCl_3$) δ 173.40, 171.95, 168.74, 155.38, 137.58, 128.59, 128.57, 127.90, 127.63, 127.61, 119.14, 109.74, 96.66, 70.88, 67.27, 62.84, 60.71, 60.12, 45.60, 45.16, 44.09, 34.84, 30.68, 29.13, 28.12, 24.51, 22.16, 20.96, 14.08.

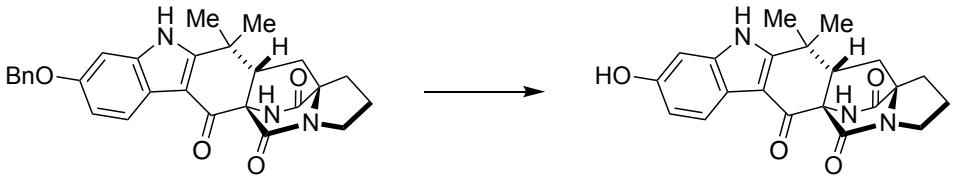

120 **121**

10 % Pd/C (4.5 mg, 0.042 mmol) was added to a solution of cycloadduct **120** (49.6 mg, 0.106 mmol) in MeOH (0.5 mL) and THF (0.5 mL). Solution was sparged with hydrogen gas for 10 minutes, then stirred at room temperature under hydrogen atmosphere for 3 hours. Catalyst was removed by filtering over Celite and rinsing with 1:1 MeOH/THF. Solution was concentrated under reduced pressure which gave 39.5 mg pure product **121** in near quantitative yield. **121:** ^{1}H NMR (400 MHz, MeOD) δ 7.93 (d, *J* = 8.5 Hz, 1H), 6.85 (d, *J* = 2.1 Hz, 1H), 6.76 (dd, *J* = 8.5, 2.2 Hz, 1H), 3.56 (dt, *J* = 11.2, 6.7 Hz, 1H), 3.44 (dt, *J* = 11.2, 7.6 Hz, 1H), 2.76 (dd, *J* = 10.1, 6.2 Hz, 1H), 2.68 (dd, *J* = 12.7, 7.3 Hz, 1H), 2.34 (dd, *J* = 13.5, 10.2 Hz, 1H), 2.15 – 1.93 (m, 4H), 1.48 (s, 3H), 1.35 (s, 3H). ^{13}C NMR (101 MHz, MeOD) δ 182.26, 173.79, 168.50, 160.12, 154.78, 138.36, 121.65, 118.00, 111.80, 111.03, 97.28, 67.19, 66.74, 43.81, 34.67, 30.97, 28.45, 26.76, 26.11, 24.35, 23.87, 23.27, 12.50. (ESI-B-TOFMS) *m/z* 380.1603 [$C_{21}H_{21}N_3O_4$ (M+H) requires 380.1605]

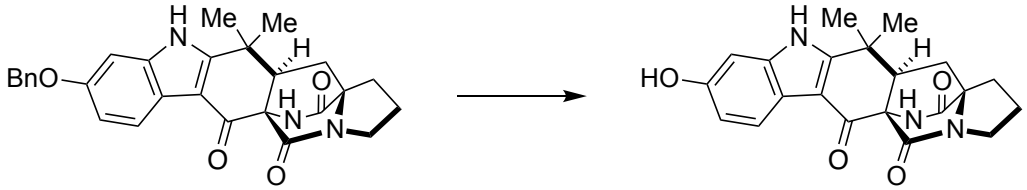

89 **90**

10 % Pd/C (1.0 mg, 0.007 mmol) was added to a solution of cycloadduct **89** (8.3 mg, 0.018 mmol) in MeOH (0.3 mL) and THF (0.3 mL). Solution was sparged with hydrogen gas for 10 minutes, then stirred at room temperature under hydrogen atmosphere for 3 hours. Catalyst was

removed by filtering over Celite and rinsing with 1:1 MeOH/THF. Solution was concentrated under reduced pressure which gave 6.5 mg pure product **90** in near quantitative yield. ^{1}H NMR (400 MHz, MeOD) δ 7.46 (d, J = 8.5 Hz, 1H), 6.76 (d, J = 2.2 Hz, 1H), 6.63 (dd, J = 8.5, 2.2 Hz, 1H), 5.02 (s, 1H), 3.94 – 3.87 (m, 1H), 3.48 – 3.41 (m, 2H), 2.86 (t, J = 7.4 Hz, 1H), 2.74 – 2.67 (m, 1H), 2.10 – 2.04 (m, 2H), 2.02 – 1.92 (m, 4H), 1.37 (d, J = 2.9 Hz, 6H).

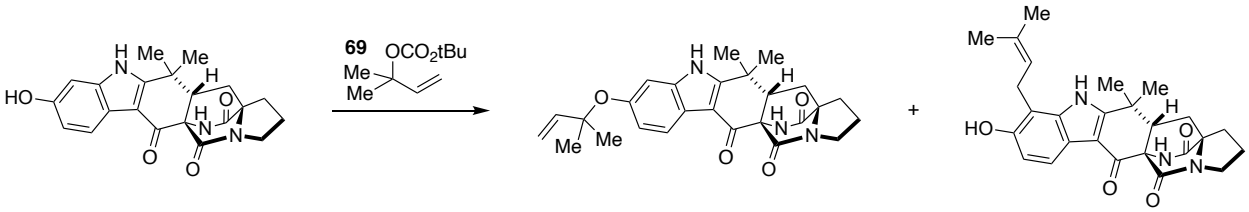

Phenol **121** (30.2 mg, 0.079 mmol) and carbonate **69** (39 mg, 0.21 mmol) were taken up in THF (0.5 mL). The solution was degassed (freeze pump thaw, 3 cycles), then $Pd(PPh_3)_4$ (1.6 mg, 0.0013 mmol) was added, and the mixture was stirred at room temperature for 24 hours. The mixture was then filtered through a silica plug (2 g), washing with THF and DCM, then concentrated and purified by PTLC, eluting with 8% MeOH/DCM. This yielded 8.6 mg of **122** and 2.3 mg of 6-*epi*-Notoamide T10 (combined 31% yield). **6-*epi*-Notoamide T10:** ^{1}H NMR (400 MHz, MeOD) δ 7.80 (d, *J* = 8.4 Hz, 1H), 6.77 (d, *J* = 8.4 Hz, 1H), 5.26 (t, *J* = 6.7 Hz, 1H), 3.64 – 3.58 (m, 2H), 3.58 – 3.52 (m, 1H), 3.46 – 3.40 (m, 1H), 2.82 – 2.75 (m, 1H), 2.73 – 2.65 (m, 1H), 2.57 (s, 1H), 2.36 (dd, *J* = 13.5, 10.2 Hz, 1H), 2.09 – 1.94 (m, 4H), 1.82 (s, 3H), 1.68 (d, *J* = 1.5 Hz, 3H), 1.55 (s, 3H), 1.38 (s, 3H). (ESI-B-TOFMS) *m/z* 448.2208 [$C_{26}H_{29}N_3O_4$ (M+H) requires 448.2231] **122:** ^{1}H NMR (400 MHz, MeOD) δ 7.97 (d, *J* = 8.5 Hz, 1H), 7.08 (d, *J* = 2.0 Hz, 1H), 6.92 (dd, *J* = 8.5, 2.1 Hz, 1H), 6.19 (dd, *J* = 17.6, 10.9 Hz, 1H), 5.24 – 5.12 (m, 2H), 3.59 – 3.52 (m, 1H), 3.44 (dt, *J* = 11.3, 6.6 Hz, 1H), 2.79 (dd, *J* = 10.1, 6.2 Hz, 1H), 2.73 – 2.64 (m, 1H), 2.36 (dd, *J* = 13.5, 10.2 Hz, 1H), 2.14 – 1.90 (m, 5H), 1.49 (s, 3H), 1.45 (s, 6H),

1.35 (s, 3H). ^{13}C NMR (101 MHz, MeOD) δ 182.37, 173.76, 168.41, 160.66, 152.94, 144.39, 137.35, 120.87, 120.42, 118.50, 112.64, 110.86, 104.96, 79.61, 67.20, 66.76, 43.80, 34.72, 30.97, 28.44, 25.93, 24.27, 23.87, 23.26.

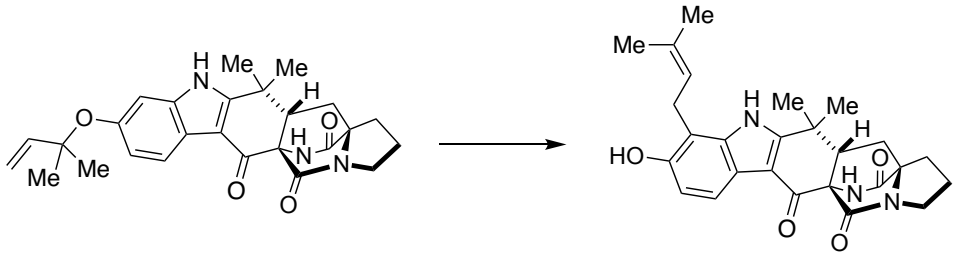

122 ***6-epi-Notoamide T10***

Ether **122** (8.6 mg, 0.019 mmol) was dissolved in MeOH (0.54 mL) at 0 ºC and 20% KOH (0.18 mL) was added. The reaction was stirred at room temperature for 4 hours. The solution was partitioned between DCM (20 mL) and 1M HCl saturated with NaCl (5 mL). The aqueous phase was extracted with DCM (3 x 10 mL) and the combined organics were dried with $MgSO_4$, filtered, and concentrated under reduced pressure. The residue was purified with PTLC using 8% MeOH/DCM to give 3.3 mg of 6-*epi*-Notoamide T10 (38% yield). **6-*epi*-Notoamide T10:** ^{1}H NMR (400 MHz, MeOD) δ 7.80 (d, *J* = 8.4 Hz, 1H), 6.77 (d, *J* = 8.4 Hz, 1H), 5.26 (t, *J* = 6.7 Hz, 1H), 3.64 – 3.58 (m, 2H), 3.58 – 3.52 (m, 1H), 3.46 – 3.40 (m, 1H), 2.82 – 2.75 (m, 1H), 2.73 – 2.65 (m, 1H), 2.57 (s, 1H), 2.36 (dd, *J* = 13.5, 10.2 Hz, 1H), 2.09 – 1.94 (m, 4H), 1.82 (s, 3H), 1.68 (d, *J* = 1.5 Hz, 3H), 1.55 (s, 3H), 1.38 (s, 3H). (ESI-B-TOFMS) *m/z* 448.2208 [$C_{26}H_{29}N_3O_4$ (M+H) requires 448.2231]

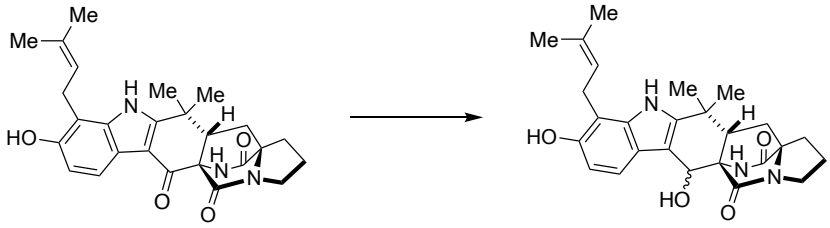

6-epi-Notoamide T10 ***6-epi-Notoamide T11/12* (123)**

6-*epi*-Notoamide T10 (>3 mg, 0.006 mmol) was taken up in THF (0.05 mL) and MeOH (0.03 mL). $NaBH_4$ (0.63 mg, 0.017 mmol) was added, and the reaction stirred for 20 minutes. The solution was then poured into 1M HCl (0.05 mL) and the resulting mixture was concentrated under reduced pressure to remove most of the MeOH and THF. The desired products were extracted with EtOAc (3 x 10 mL) and the organics were dried over Na_2SO_4, filtered, and concentrated under reduced pressure. The residue was purified by PTLC, eluting with 15% MeOH/DCM to yield less than 1 milligram of 6-*epi*-Notoamide T11/12. ^{1}H NMR (400 MHz, DMSO) δ 11.19 (s, 1H), 8.87 (s, 1H), 8.49 (s, 1H), 7.66 (d, J = 8.3 Hz, 1H), 6.87 (s, 1H), 6.75 (d, J = 8.4 Hz, 1H), 6.63 (s, 2H), 6.58 (s, 1H), 5.21 (t, J = 6.2 Hz, 2H), 4.45 – 4.41 (m, 1H), 4.32 (dd, J = 9.6, 4.2 Hz, 2H), 4.08 (d, J = 9.7 Hz, 3H), 2.79 (d, J = 5.7 Hz, 1H), 2.75 (d, J = 5.8 Hz, 1H), 2.68 – 2.65 (m, 2H), 2.61 (dd, J = 10.1, 6.2 Hz, 3H), 2.34 – 2.31 (m, 2H), 2.27 – 2.20 (m, 3H), 2.02 – 1.95 (m, 4H), 1.93 – 1.80 (m, 7H), 1.77 (s, 7H), 1.63 (s, 6H). (ESI-B-TOFMS) *m/z* 472.2210 [$C_{26}H_{31}N_3O_4$ (M+Na) requires 472.2207]

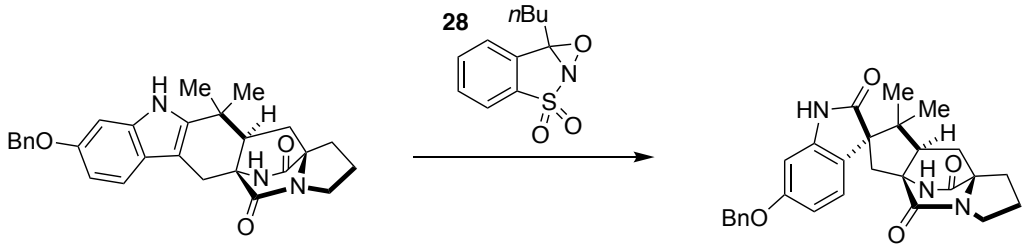

Davis Oxaziridine **28** (15 mg, 0.061 mmol) was added to a solution of bicyclic **85** (9.0 mg, 0.020 mmol) in DCM (1.8 mL) at room temperature. The reaction stirred for 3 hours then was concentrated under reduced pressure. The crude product was purified by PTLC eluted with 6% MeOH/DCM, yielding 4.1 mg of **108** as a white solid (44% yield). ^{1}H NMR (400 MHz, $CDCl_3$) δ 8.70 (s, 1H), 8.00 (s, 1H), 7.41 – 7.29 (m, 6H), 6.61 (dd, *J* = 8.4, 2.4 Hz, 1H), 6.55 (d, *J* = 2.3 Hz, 1H), 5.29 (s, 1H), 5.02 (s, 2H), 3.61 (m, 1H), 3.56 – 3.35 (m, 3H), 3.18 (d, *J* = 14.8 Hz, 1H), 2.25 (d, *J* = 14.8 Hz, 1H), 2.07 – 1.97 (m, 3H), 1.83 – 1.76 (m, 1H), 1.67 (dd, *J* = 12.7, 8.5 Hz, 1H), 0.87 (s, 3H), 0.80 (s, 3H). ^{13}C NMR (101 MHz, $CDCl_3$) δ 184.58, 174.83, 169.83, 159.39, 142.46, 136.86, 128.73, 128.17, 127.63, 122.68, 107.92, 97.87, 70.35, 68.89, 66.79, 62.23, 56.34, 45.97, 44.03, 34.68, 30.80, 29.74, 24.97, 23.38, 20.01. (ESI-B-TOFMS) *m/z* 472.2228 [$C_{28}H_{29}N_3O_4$ (M+H) requires 472.2231]

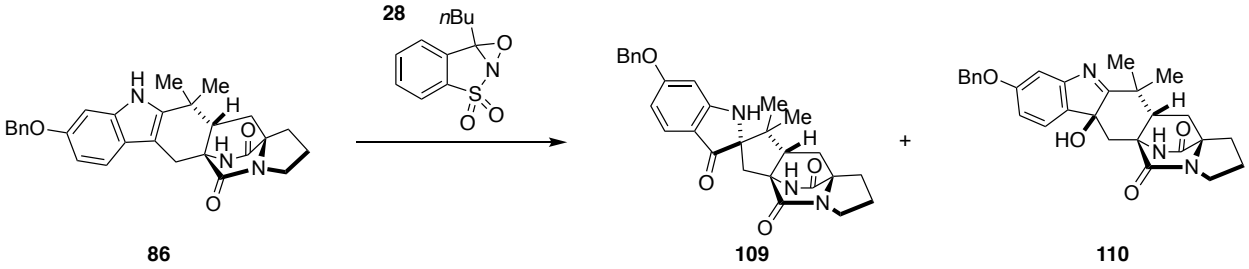

Davis Oxaziridine **28** (36.6 mg, 0.153 mmol) was added to a solution of bicyclic **86** (23.2 mg, 0.051 mmol) in DCM (2.3 mL) at room temperature. The reaction stirred for 3 hours then was concentrated under reduced pressure. The crude product was purified by PTLC eluted with 6%

MeOH/DCM, yielding 2.1 mg of **109** as a white solid (9% yield) and 8.4 mg of **110** as a white solid (35% yield). **109**: ^{1}H NMR (400 MHz, MeOD) δ 7.44 (d, *J* = 7.0 Hz, 2H), 7.37 (t, *J* = 7.7 Hz, 3H), 7.32 – 7.28 (m, 1H), 7.14 (d, *J* = 2.2 Hz, 1H), 6.92 (dd, *J* = 8.2, 2.3 Hz, 1H), 5.15 (s, 2H), 3.44 (m, 3H), 2.80 (d, *J* = 15.5 Hz, 1H), 2.69 (dd, *J* = 12.5, 6.6 Hz, 1H), 2.24 (dd, *J* = 15.0, 11.6 Hz, 1H), 2.11 – 2.02 (m, 3H), 2.02 – 1.86 (m, 4H), 1.81 – 1.71 (m, 3H), 1.58 – 1.50 (m, 3H), 1.47 (s, 3H), 1.32 (s, 3H). ^{13}C NMR (101 MHz, MeOD) δ 192.87, 174.79, 170.56, 161.80, 154.28, 138.52, 135.15, 129.54, 128.92, 128.56, 123.90, 113.95, 108.76, 82.66, 71.31, 68.79, 63.33, 62.68, 54.80, 53.10, 51.83, 45.12, 41.83, 39.34, 33.11, 29.81, 28.15, 27.61, 27.50, 25.26, 25.12, 24.66, 24.62, 20.29, 14.82, 13.90. **110**: ^{1}H NMR (400 MHz, MeOD) δ 7.45 (d, *J* = 6.9 Hz, 2H), 7.37 (t, *J* = 7.8 Hz, 3H), 7.31 (d, *J* = 7.2 Hz, 1H), 7.14 (d, *J* = 2.2 Hz, 1H), 6.92 (dd, *J* = 8.1, 2.3 Hz, 1H), 5.15 (s, 2H), 3.62 – 3.40 (m, 3H), 2.80 (d, *J* = 15.5 Hz, 1H), 2.69 (dd, *J* = 12.4, 6.6 Hz, 1H), 2.24 (dd, *J* = 15.0, 11.6 Hz, 1H), 2.10 – 2.04 (m, 3H), 1.98 – 1.94 (m, 1H), 1.90 (d, *J* = 15.6 Hz, 1H), 1.32 (s, 3H), 1.29 (s, 3H). ^{13}C NMR (101 MHz, MeOD) δ 192.87, 174.80, 170.56, 161.80, 154.28, 138.52, 135.16, 129.54, 128.92, 128.56, 123.90, 113.96, 108.76, 82.66, 73.87, 71.31, 68.80, 64.42, 63.33, 51.84, 45.12, 41.83, 39.35, 33.11, 30.78, 29.81, 27.61, 25.26, 23.74, 20.29. (ESI-B-TOFMS) *m/z* 472.2231 [$C_{28}H_{29}N_3O_4$ (M+H) requires 472.2231]

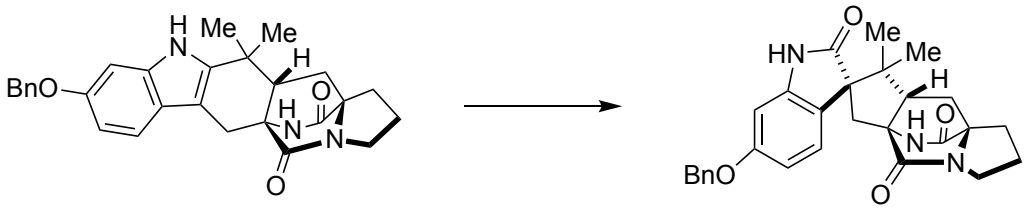

To a solution of Diels-Alder cycloadduct **86** (9.4 mg, 0.021 mmol) in DCM (0.2 mL) at 0 °C, Et_3N (0.06 mL, 0.045 mmol) was added, followed by t-BuOCl (0.05 mL, 0.041 mmol). After 30 minutes, the resulting yellow solution was concentrated to dryness (the flask being kept cold).

The residue was immediately taken up in 1:1 2M HCl (1 mL) and DCM (1 mL) then stirred for 2 days. The solution was extracted with DCM (3 x 10 mL), the combined organics were dried with Na_2SO_4, filtered, and concentrated under reduced pressure. The residue was purified by PTLC with 4% MeOH/DCM, yielding 3.8 mg of white residue (41% yield). **111:** ^{1}H NMR (400 MHz, Acetone) δ 7.47 (d, *J* = 6.7 Hz, 2H), 7.36 (dt, *J* = 26.4, 7.2 Hz, 4H), 7.10 (d, *J* = 8.1 Hz, 1H), 6.63 – 6.58 (m, 2H), 5.10 (s, 2H), 3.49 – 3.36 (m, 2H), 2.76 (s, 1H), 2.72 (dd, *J* = 10.1, 7.2 Hz, 1H), 2.68 – 2.58 (m, 1H), 2.44 (d, *J* = 15.0 Hz, 1H), 1.93 – 1.74 (m, 3H), 1.34 (d, *J* = 3.7 Hz, 1H), 1.14 (s, 3H), 0.59 (s, 3H). ^{13}C NMR (101 MHz, Acetone) δ 206.20, 180.50, 173.09, 170.30, 160.02, 138.32, 129.30, 128.67, 128.46, 127.59, 126.19, 107.66, 98.11, 70.63, 69.84, 69.04, 63.26, 54.86, 48.72, 44.24, 35.27, 25.48, 24.89, 20.76.

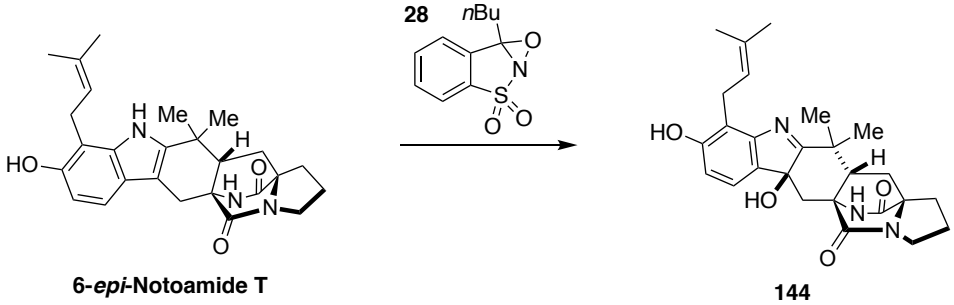

6-*epi*-Notoamide T **144**

Davis Oxaziridine **28** (13 mg, 0.054 mmol) was added to a solution of 6-*epi*-Notoamide T (7.5 mg, 0.017 mmol) in DCM (1.5 mL) at room temperature. The reaction stirred for 3 hours then was concentrated under reduced pressure. The crude product was purified by PTLC eluted with 6% MeOH/DCM, yielding 4.1 mg of **144** as a white solid (54% yield). ^{1}H NMR (400 MHz, MeOD) δ 7.35 (d, *J* = 8.0 Hz, 1H), 7.27 (d, *J* = 8.0 Hz, 1H), 5.30 (t, *J* = 7.2 Hz, 1H), 3.74 (d, *J* = 7.3 Hz, 2H), 3.50 – 3.37 (m, 2H), 2.80 (d, *J* = 15.5 Hz, 1H), 2.70 (dd, *J* = 12.3, 6.6 Hz, 1H), 2.25 (dd, *J* = 14.6, 11.3 Hz, 1H), 2.08 (m, 3H), 2.04 – 1.94 (m, 2H), 1.91 (d, *J* = 15.5 Hz, 1H), 1.81 (s, 3H), 1.66 (s, 3H), 1.36 (s, 3H), 1.29 (s, 3H). ^{13}C NMR (101 MHz, MeOD) δ 191.03, 174.83,

170.60, 153.48, 150.20, 142.07, 133.28, 129.61, 123.02, 121.14, 120.63, 83.13, 68.82, 64.42, 63.38, 51.93, 45.12, 41.83, 39.11, 38.40, 33.14, 29.83, 27.71, 25.90, 25.72, 25.26, 20.22, 18.19.

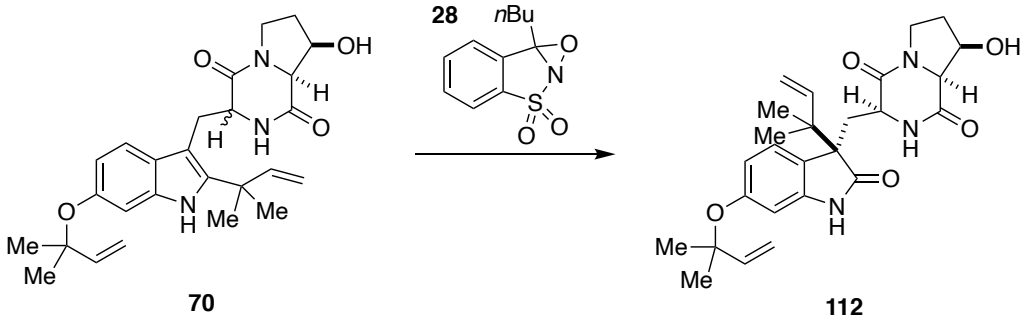

Davis Oxaziridine **28** (27.8 mg, 0.116 mmol) was added to a solution of diketopiperazine **70** (21.0 mg, 0.047 mmol) in DCM (1.1 mL) at room temperature. The reaction stirred for 3 hours then was concentrated under reduced pressure. The crude product was purified by PTLC eluted with 6% MeOH/DCM, yielding 10.8 mg of **112** as a white solid (50% yield). (ESI-B-TOFMS) *m/z* 468.2458 [$C_{26}H_{33}N_3O_5$ (M+H) requires 468.2420]

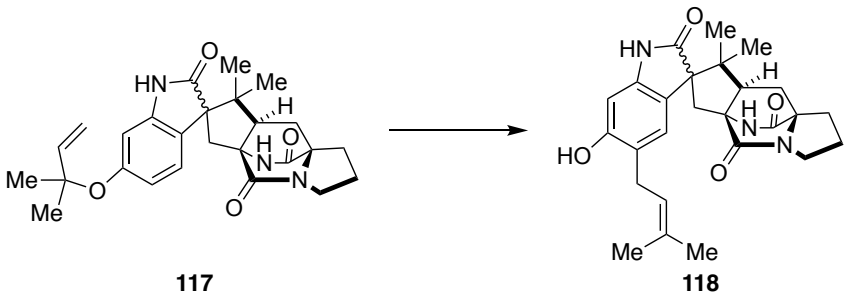

Spiro-oxindole **117** (5 mg, 0.0011 mmol) was dissolved in MeOH (0.24 mL) and THF (0.48 mL) at 0 °C and 20% KOH (0.14 mL) was added. The reaction was stirred at room temperature for 18 hours. The solution was partitioned between DCM (10 mL) and 1M HCl saturated with NaCl (5 mL). The aqueous phase was extracted with DCM (3 x 10 mL) and the combined organics were dried with $MgSO_4$, filtered, and concentrated under reduced pressure. The residue was purified

with PTLC using 6% MeOH/DCM to give 3 mg of **118** as a white solid (60% yield). ^{1}H NMR (400 MHz, MeOD) δ 7.06 (d, *J* = 8.2 Hz, 1H), 6.43 (dd, *J* = 8.2, 2.3 Hz, 1H), 6.38 (d, *J* = 2.3 Hz, 1H), 6.08 (dd, *J* = 17.4, 10.9 Hz, 1H), 5.13 – 4.98 (m, 2H), 4.51 (s, 1H), 4.07 (t, *J* = 2.6 Hz, 1H), 3.73 – 3.63 (m, 1H), 3.44 (m, 1H), 3.10 (d, *J* = 14.8 Hz, 1H), 2.16 (dd, *J* = 14.8, 8.6 Hz, 1H), 2.00 – 1.91 (m, 2H), 1.10 (s, 3H), 1.07 (s, 3H). ^{13}C NMR (101 MHz, MeOD) δ 184.19, 169.05, 167.04, 159.48, 145.04, 144.46, 127.95, 121.06, 114.32, 109.49, 98.92, 71.64, 65.57, 58.99, 53.77, 44.89, 43.25, 33.24, 31.73, 23.00, 22.09.

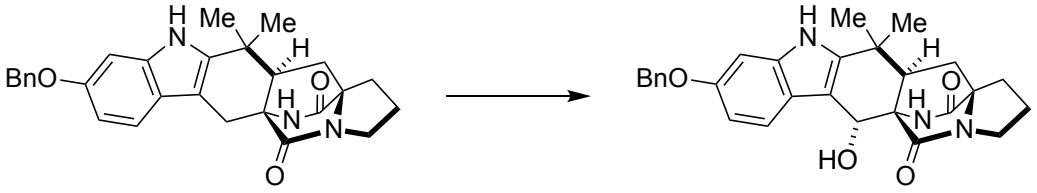

85 **89**

Cycloadduct **85** (50.0 mg, 0.110 mmol) was dissolved in THF (3.0 mL) and water (0.065 mL). The solution was cooled to 0 °C and DDQ (28 mg, 0.121 mmol) was slowly added. The resulting mixture was stirred at 0 °C for 20 min, after which time TLC (8% MeOH/DCM) indicated complete consumption of **85**. The reaction was quenched with saturated aqueous $NaHCO_3$. The resulting mixture was extracted with EtOAc three times. The combined organic extracts were washed with saturated aqueous $NaHCO_3$, water, and brine, dried over Na_2SO_4, filtered, and concentrated under reduced pressure. The resulting residue was purified by PTLC, eluting with 7% MeOH/DCM. This yielded 35.3 mg of white solid (69% yield). **89**: ^{1}H NMR (400 MHz, $CDCl_3$) δ 7.54 (d, J = 8.6 Hz, 1H), 7.45 (d, J = 7.1 Hz, 2H), 7.36 (t, J = 7.4 Hz, 2H), 7.29 (t, J = 7.2 Hz, 1H), 6.91 (d, J = 2.3 Hz, 1H), 6.81 (dd, J = 8.6, 2.3 Hz, 1H), 5.32 (s, 1H), 5.10 (s, 2H), 3.51 – 3.43 (m, 1H), 3.37 (t, J = 6.1 Hz, 1H), 2.79 (dd, J = 8.8, 6.1 Hz, 1H), 2.74 – 2.67 (m, 1H), 2.16 – 2.09 (m, 2H), 2.02 – 1.94 (m, 2H), 1.37 (s, 3H), 1.09 (s, 3H). ^{13}C NMR (101 MHz,

MeOD) δ 173.83, 169.19, 155.22, 140.97, 137.86, 137.78, 128.03, 127.31, 127.19, 121.20, 118.54, 109.28, 107.37, 95.97, 70.29, 67.29, 62.95, 59.92, 53.39, 44.95, 43.66, 34.69, 30.03, 28.56, 27.22, 24.00, 21.31.

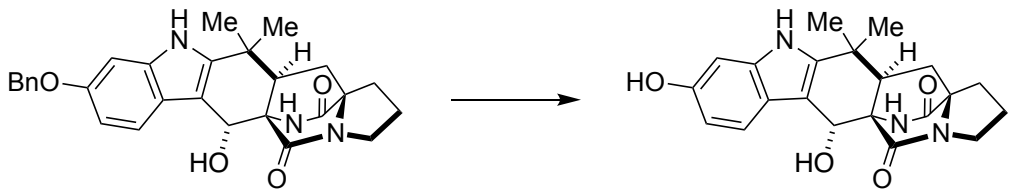

10 % Pd/C (3.19 mg, 0.0299 mmol) was added to a solution of cycloadduct **89** (35.3 mg, 0.0749 mmol) in MeOH (2.0 mL) and THF (2.0 mL). Solution was sparged with hydrogen gas for 10 minutes, then stirred at room temperature under hydrogen atmosphere for 3 hours. Catalyst was removed by filtering over Celite and rinsing with 1:1 MeOH/THF. Solution was concentrated under reduced pressure and carried forward without further purification.

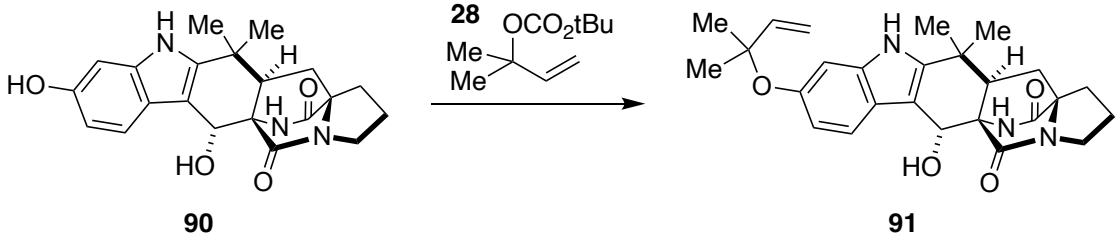

Phenol **90** (39.0 mg, 0.102 mmol) and carbonate **28** (50.3 mg, 0.270 mmol) were taken up in THF (0.64 mL). The solution was degassed (freeze pump thaw, 3 cycles), then $Pd(PPh_3)_4$ (2.1 mg, 0.00174 mmol) was added, and the mixture was stirred at room temperature for 24 hours. The mixture was then filtered through a silica plug (2 g), washing with THF and DCM, then concentrated and purified by PTLC, eluting with 8% MeOH/DCM. This yielded 35.0 mg of **91** as a white amorphous solid (79% yield). **91:** ^{1}H NMR (400 MHz, Acetone) δ 7.35 (d, J = 8.4 Hz,

1H), 6.80 (d, J = 2.0 Hz, 1H), 6.61 (dd, J = 8.5, 2.1 Hz, 1H), 6.06 (dd, J = 17.6, 10.9 Hz, 1H), 5.24 – 5.15 (m, 1H), 5.02 (dd, J = 17.6, 1.3 Hz, 1H), 4.95 (dd, J = 10.9, 1.2 Hz, 1H), 3.33 – 3.27 (m, 1H), 3.21 – 3.14 (m, 1H), 2.72 (d, J = 13.2 Hz, 3H), 2.66 (dd, J = 9.4, 5.7 Hz, 1H), 2.58 – 2.52 (m, 1H), 2.47 – 2.39 (m, 1H), 2.04 – 1.95 (m, 5H), 1.85 – 1.73 (m, 3H), 1.27 (s, 6H), 1.24 (s, 3H), 0.98 (s, 3H). ^{13}C NMR (101 MHz, Acetone) δ 210.05, 173.06, 173.00, 168.86, 152.30, 146.09, 142.64, 137.96, 123.89, 119.07, 116.93, 113.34, 109.42, 105.76, 105.71, 79.82, 69.40, 69.28, 67.79, 63.40, 61.20, 61.10, 54.95, 54.77, 46.03, 44.42, 35.80, 31.41, 28.52, 27.37, 25.15, 22.66.

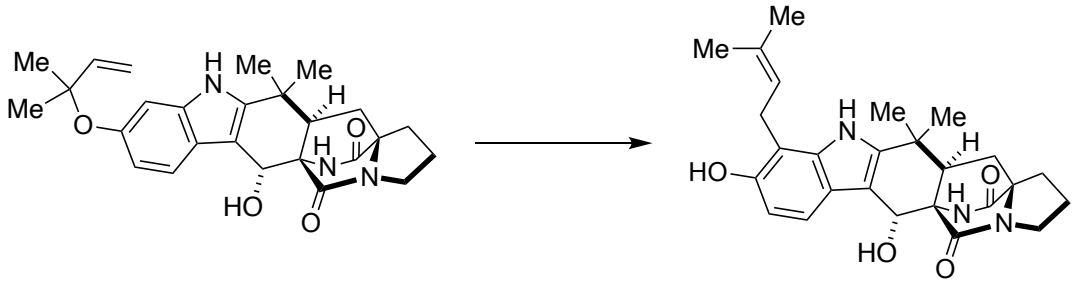

91 ***Notoamide T2***

91 (35.0 mg, 0.0779 mmol) was taken up in toluene (5.0 mL) and heated in a chemical microwave for 2 hours at 180 ºC (power = 150W). Toluene was azeotroped with methanol and both were removed under reduced pressure. The residue was purified by PTLC, eluting with 8% MeOH/DCM. This yielded 25.0 mg of **Notoamide T2** as a white solid (71% yield). ^{1}H NMR (400 MHz, DMSO) δ 10.07 (s, 1H), 8.61 (s, 1H), 7.58 (s, 1H), 7.15 (d, J = 8.3 Hz, 1H), 6.58 (d, J = 8.3 Hz, 1H), 5.25 (t, J = 7.1 Hz, 1H), 5.09 (d, J = 8.8 Hz, 1H), 5.02 (d, J = 7.7 Hz, 1H), 4.52 (s, 1H), 4.47 (s, 1H), 3.48 (d, J = 7.1 Hz, 2H), 3.21 (q, J = 5.9, 4.9 Hz, 2H), 2.64 (t, J = 7.3 Hz, 1H), 2.57 – 2.51 (m, 1H), 2.00 (d, J = 7.5 Hz, 2H), 1.89 – 1.81 (m, 2H), 1.76 (s, 3H), 1.61 (s, 3H), 1.31 (s, 3H), 1.01 (s, 3H). ^{13}C NMR (101 MHz, DMSO) δ 172.30, 168.03, 149.70, 140.15,

136.70, 129.65, 127.14, 123.72, 120.01, 115.61, 109.49, 109.04, 108.46, 66.41, 62.35, 59.56, 44.30, 43.38, 34.64, 29.68, 28.60, 27.87, 25.52, 23.99, 23.52, 21.55, 17.92.

II. NMR Data

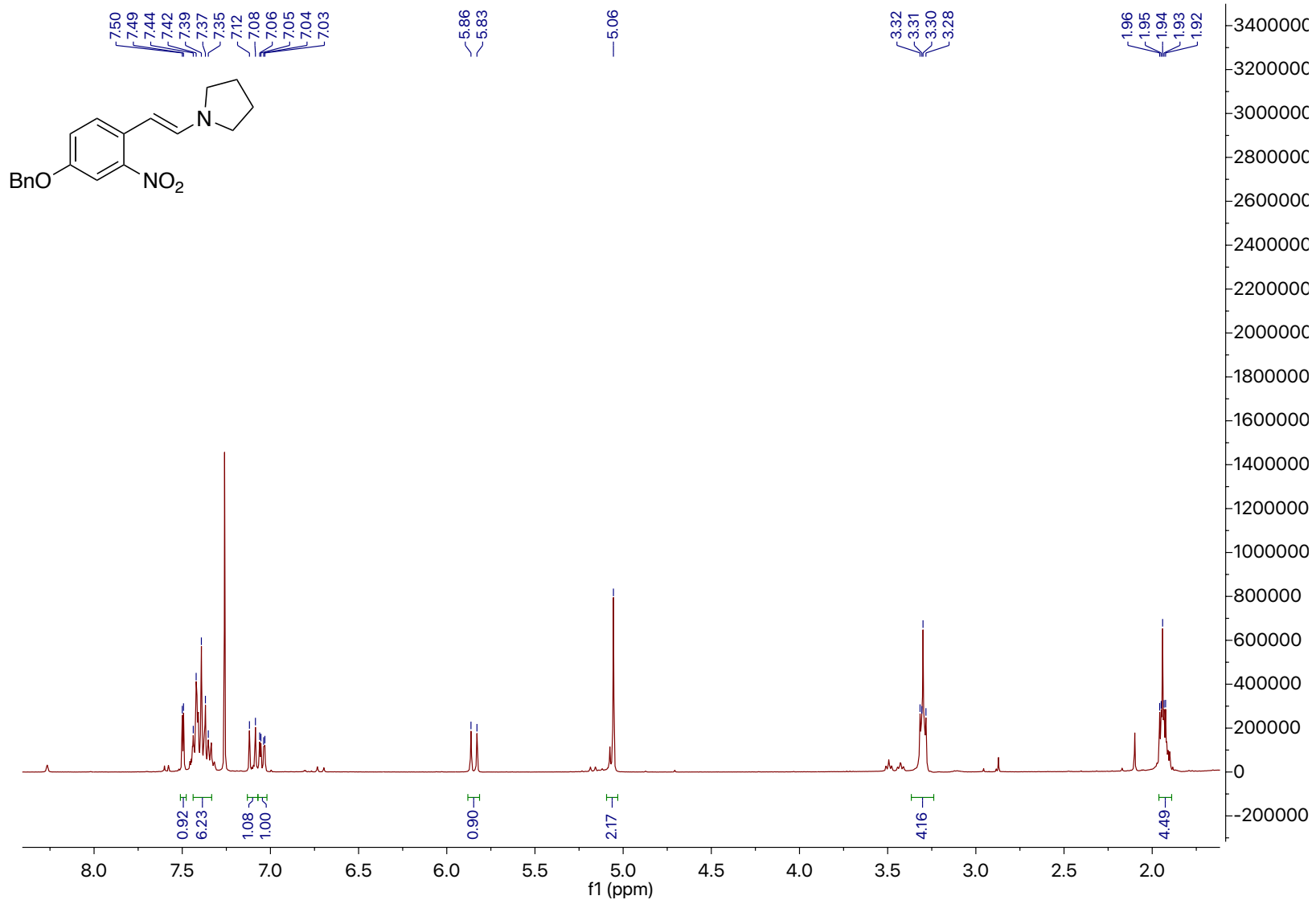

Figure A1. ^{1}H NMR Spectrum of compound **17** ($CDCl_3$).

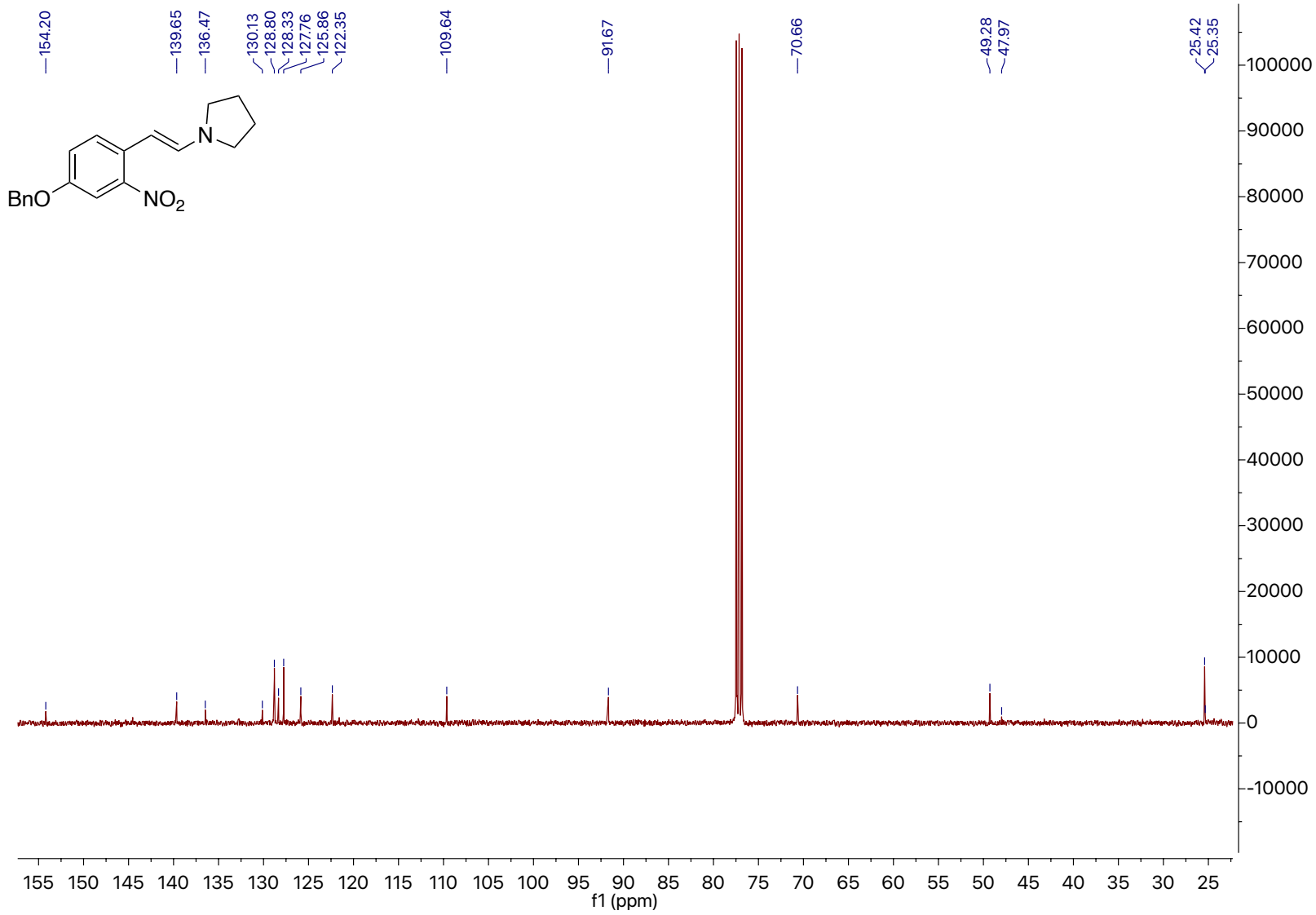

Figure A2. ^{13}C NMR Spectrum of compound **17** ($CDCl_3$).

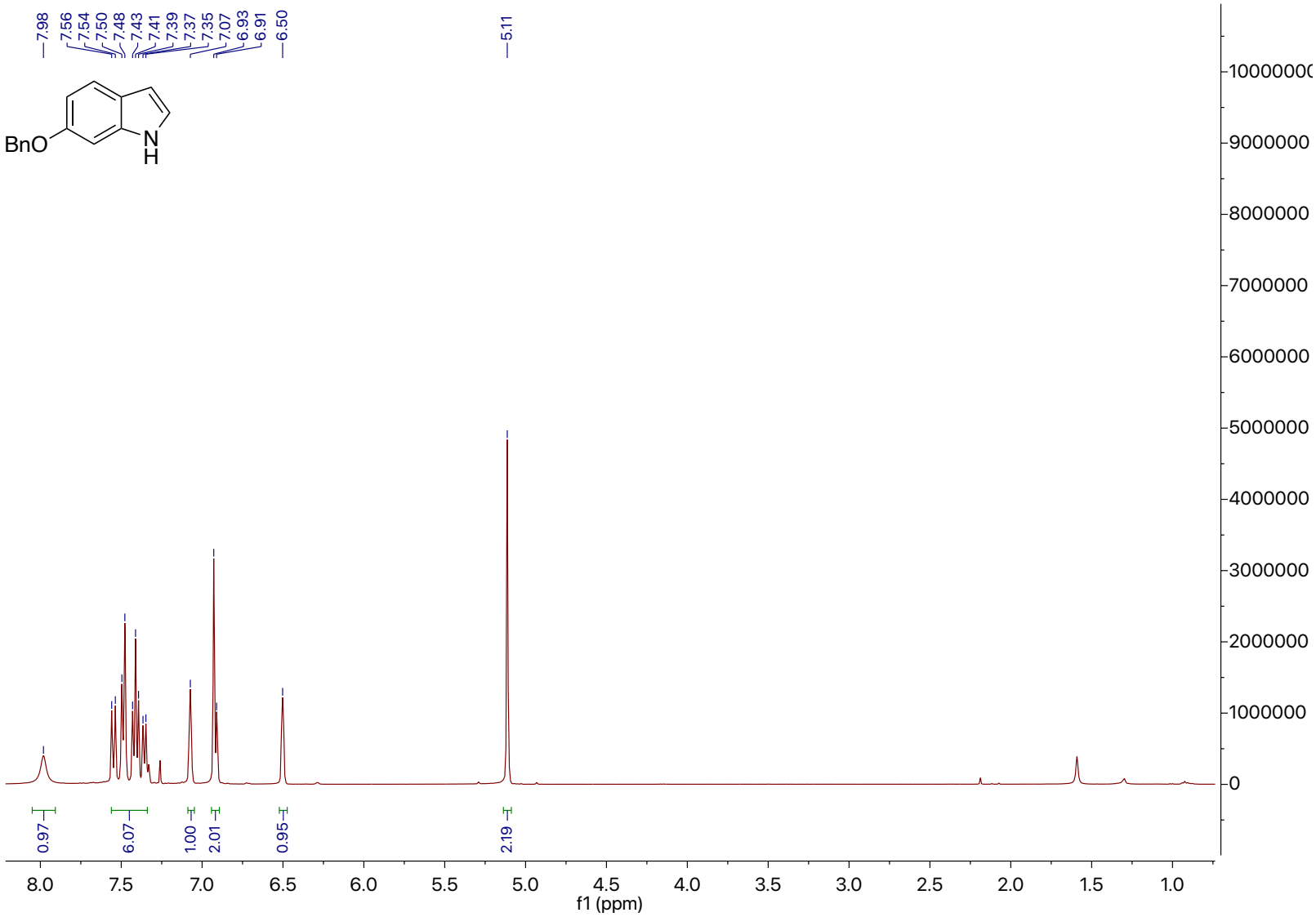

Figure A3. ^{1}H NMR Spectrum of compound **77** ($CDCl_3$).

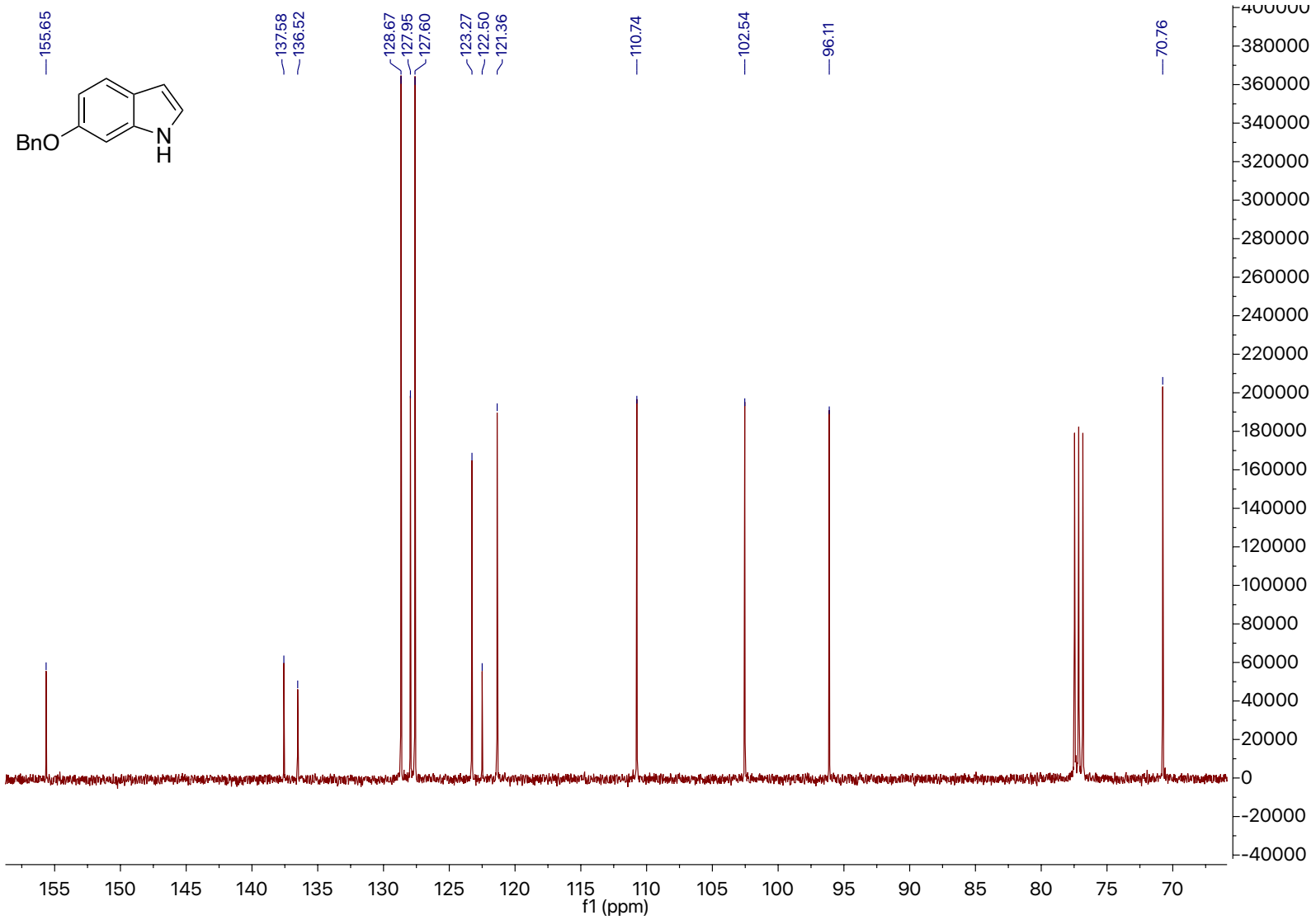

Figure A4. ^{13}C NMR Spectrum of compound **77** ($CDCl_3$).

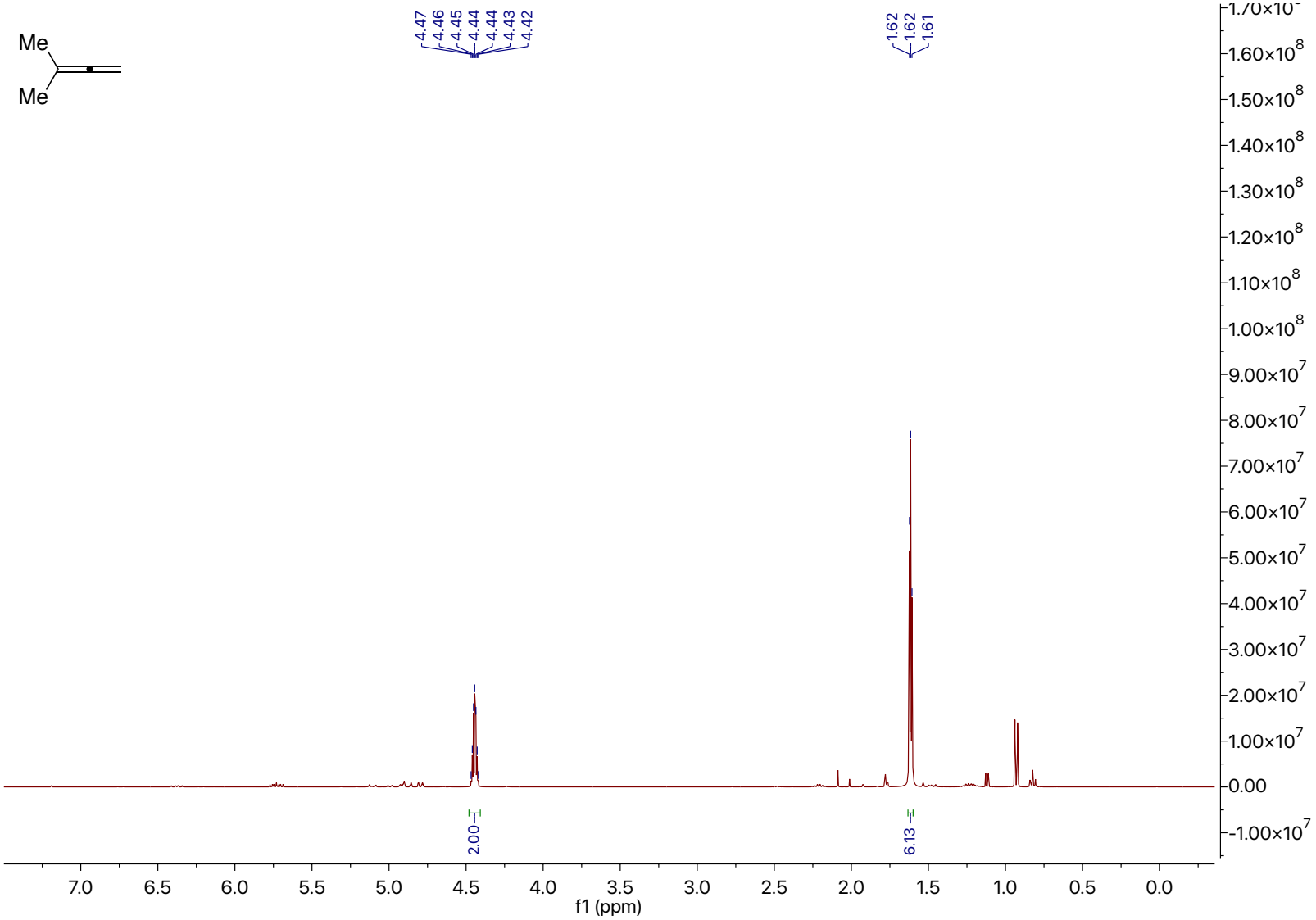

Figure A5. ^{1}H NMR Spectrum of compound **63** ($CDCl_3$).

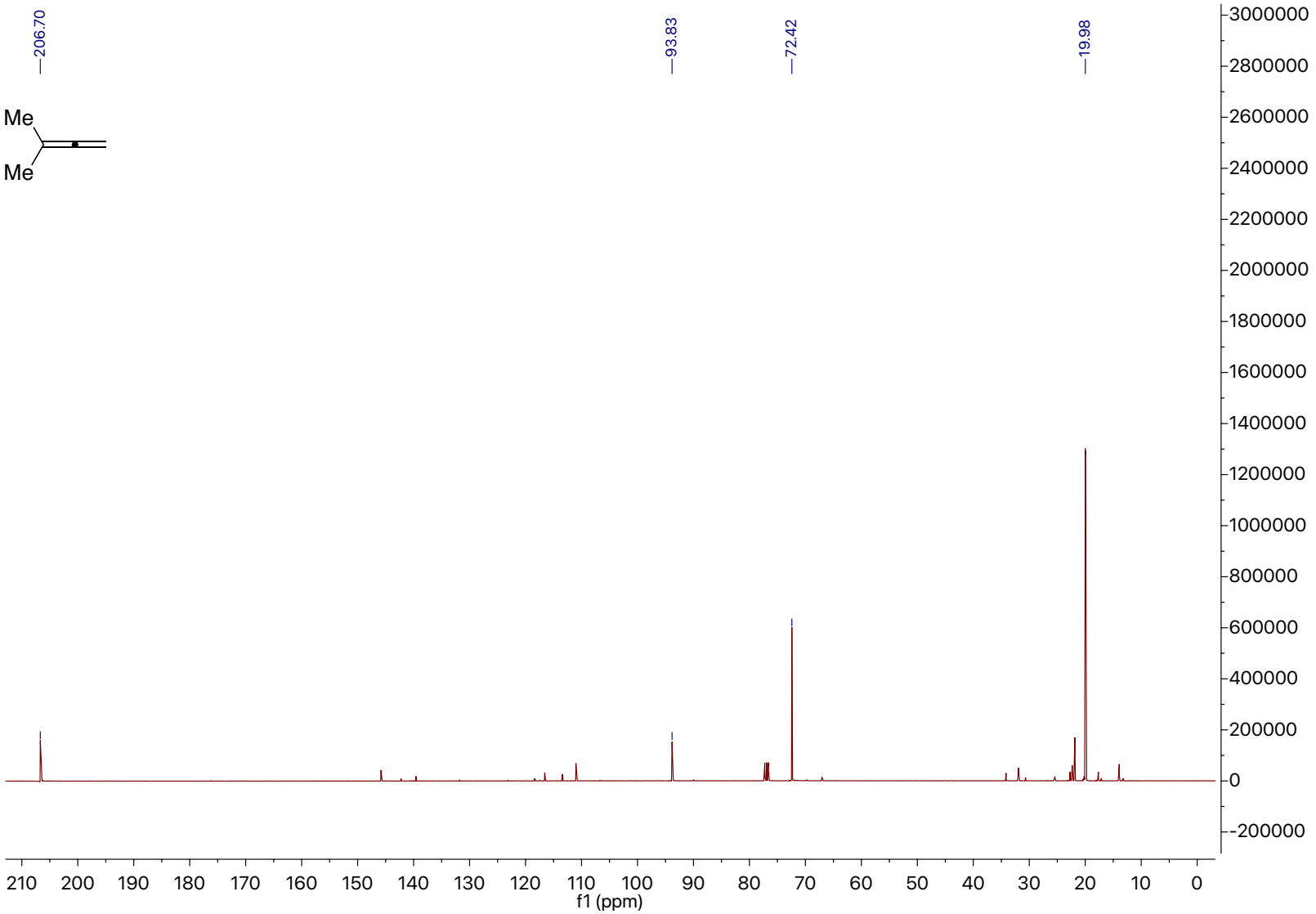

Figure A6. ^{13}C NMR Spectrum of compound **63** ($CDCl_3$).

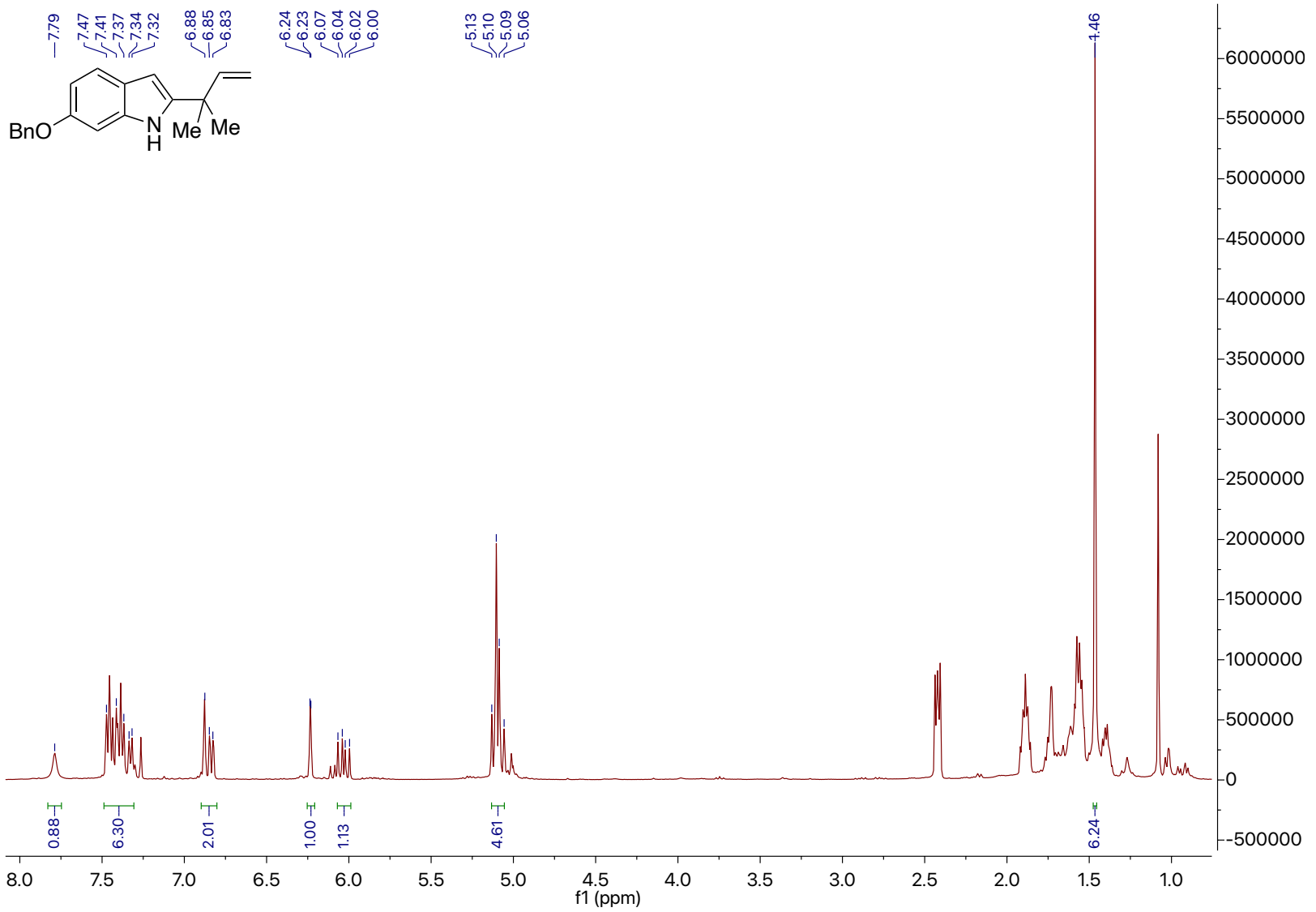

Figure A7. ^{1}H NMR Spectrum of compound **79** ($CDCl_3$).

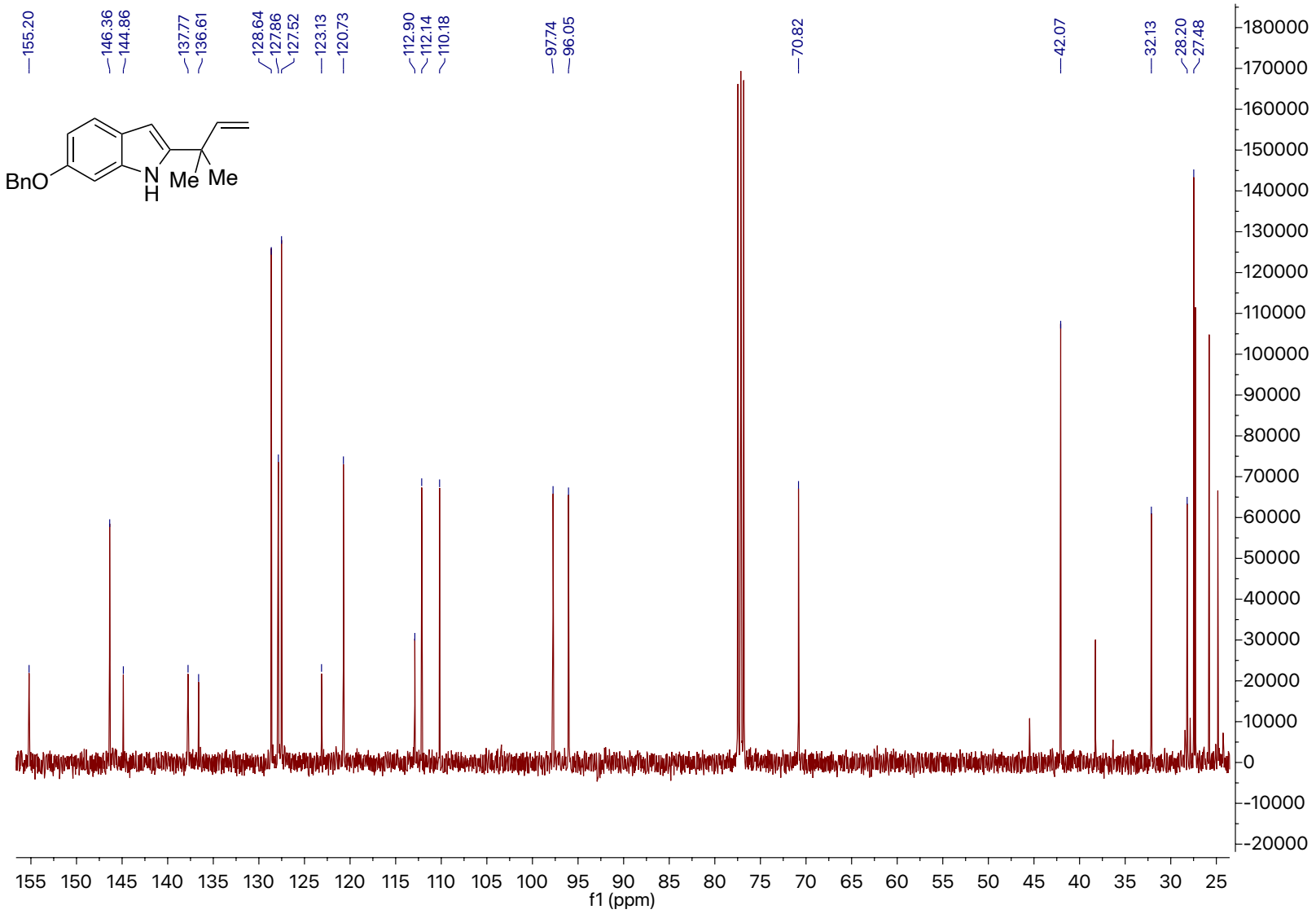

Figure A8. ^{13}C NMR Spectrum of compound **79** ($CDCl_3$).

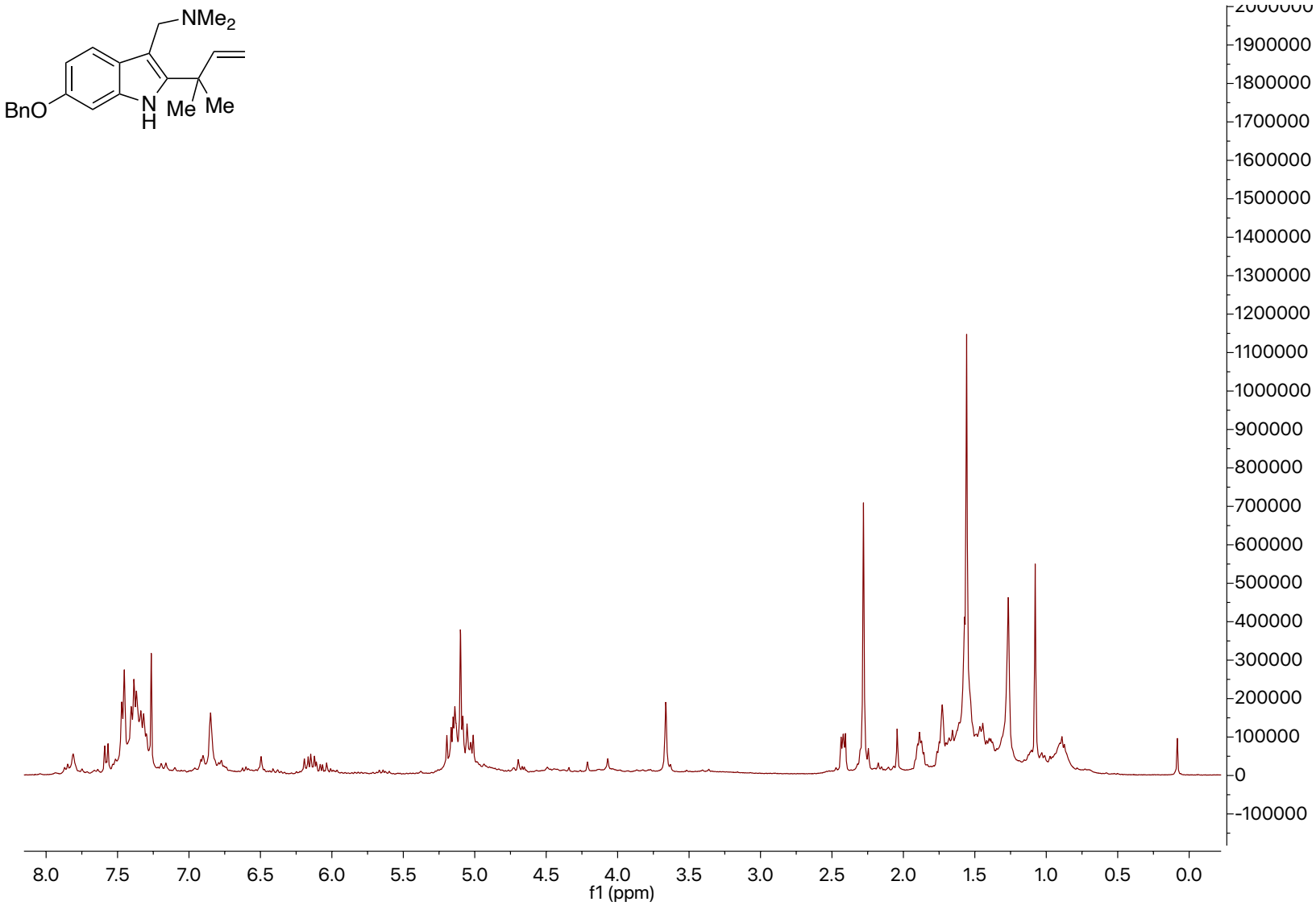

Figure A9. ^{1}H NMR Spectrum of compound **80** ($CDCl_3$).

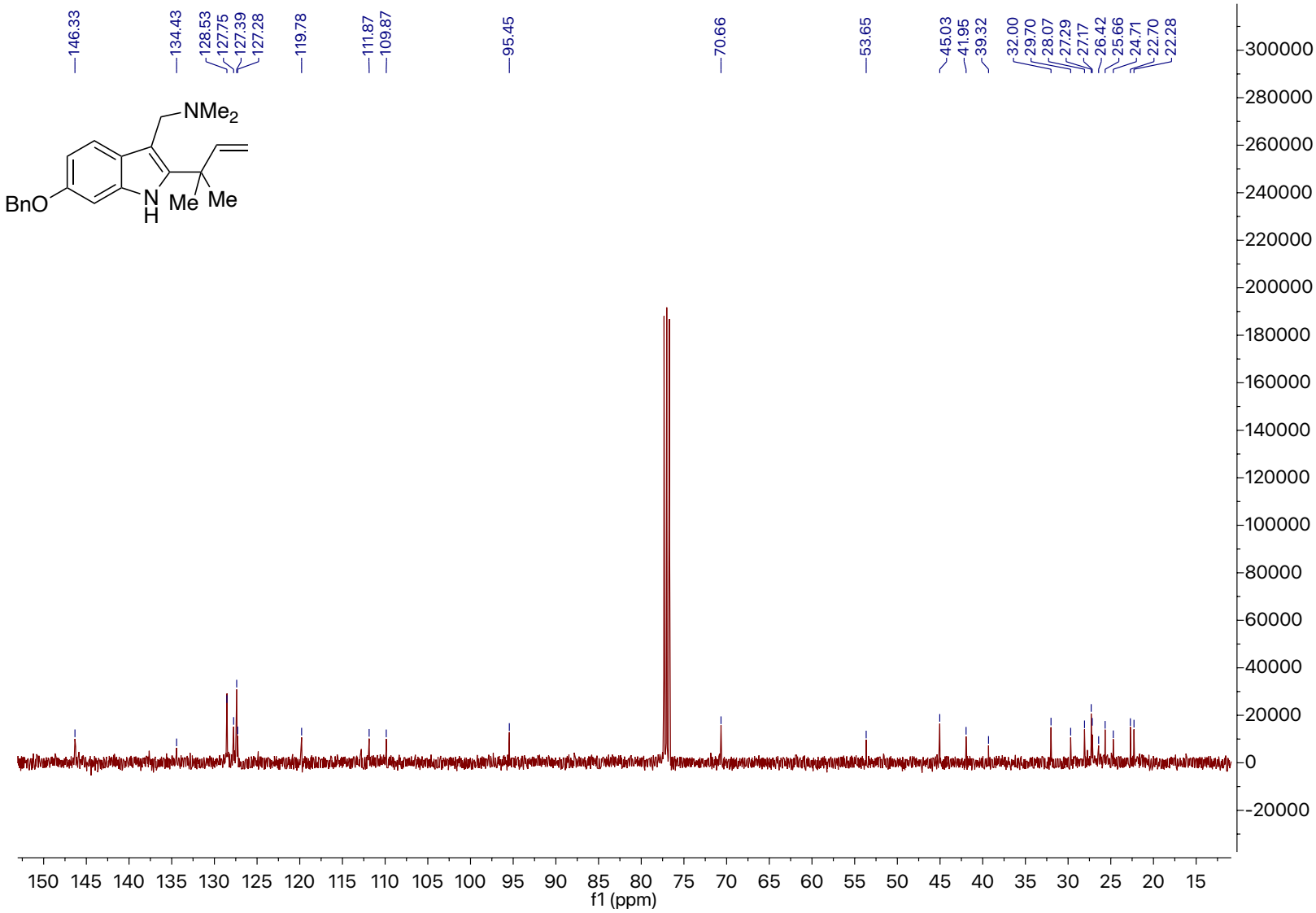

Figure A10. ^{13}C NMR Spectrum of compound **80** ($CDCl_3$).

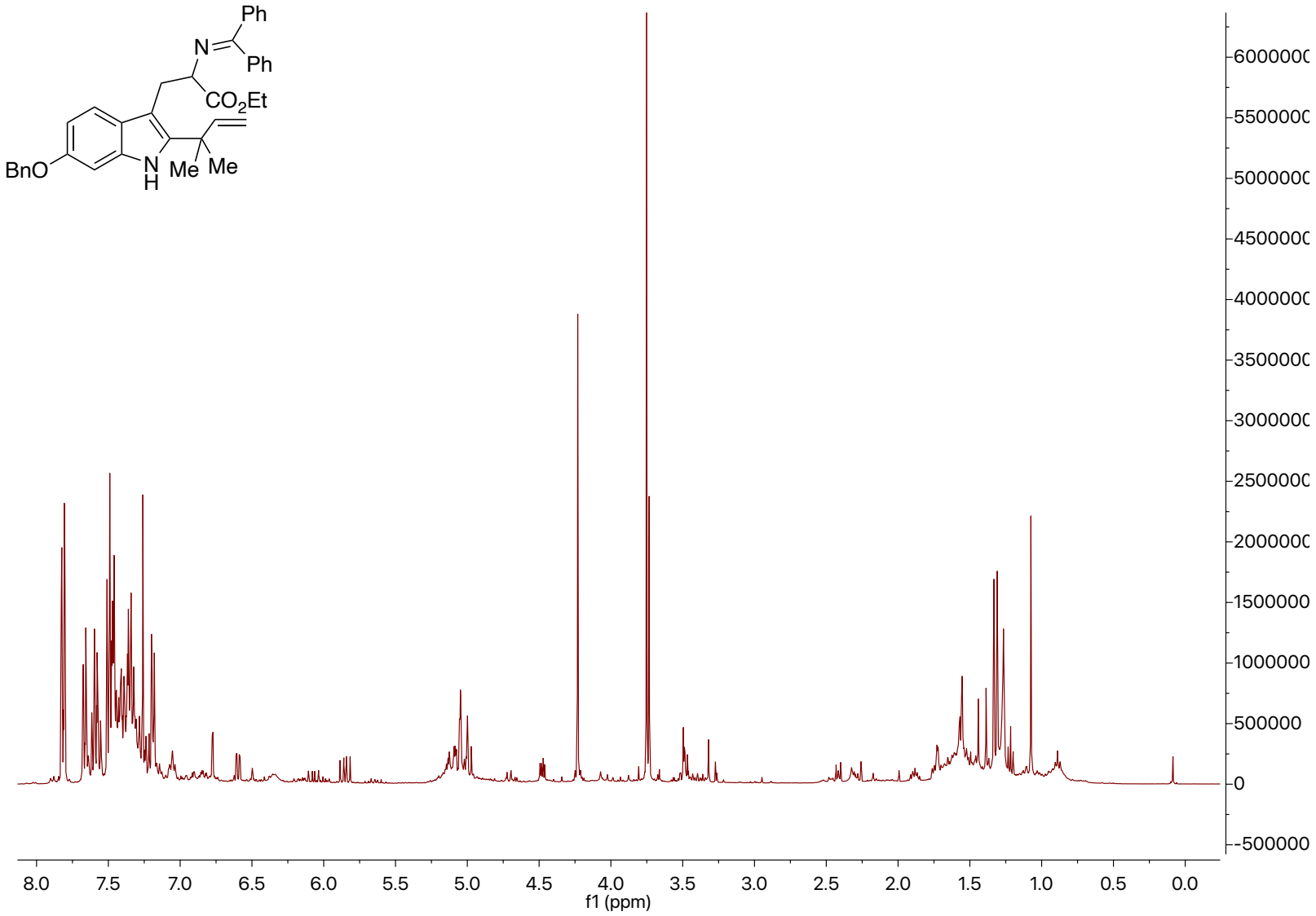

Figure A11. ^{1}H NMR Spectrum of compound **81** ($CDCl_3$).

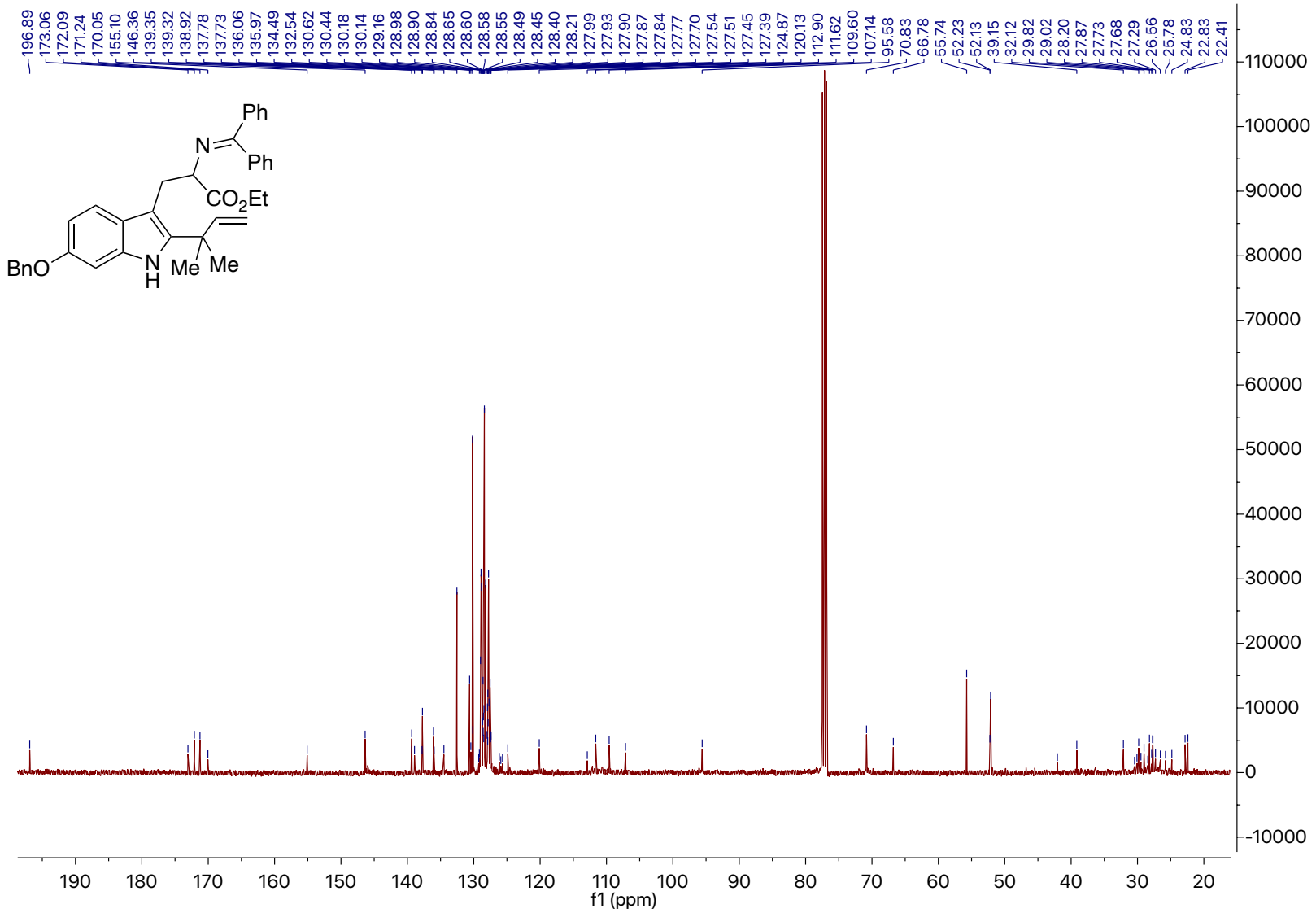

Figure A12. ^{13}C NMR Spectrum of compound **81** ($CDCl_3$).

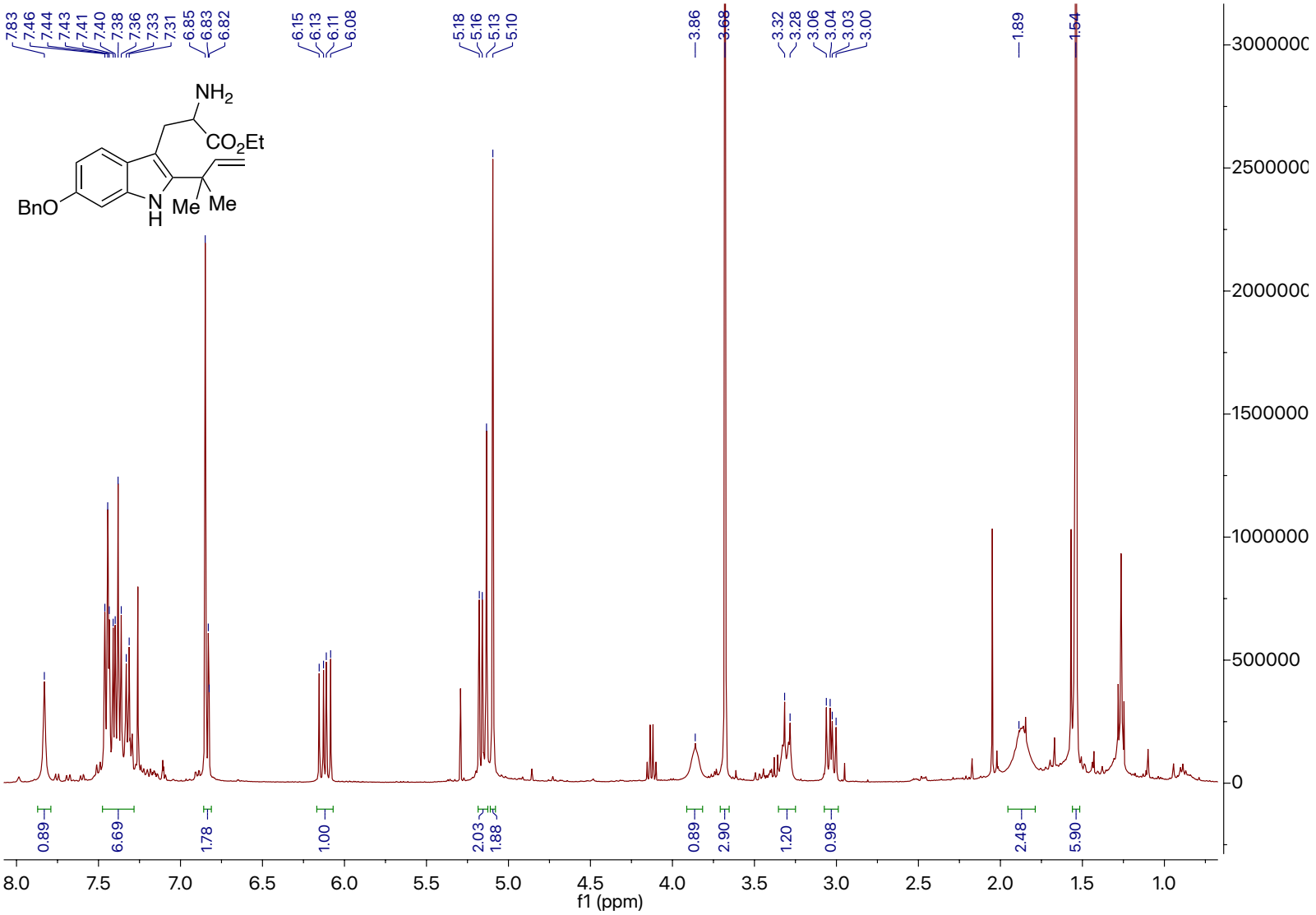

Figure A13. ^{1}H NMR Spectrum of compound **82** ($CDCl_3$).

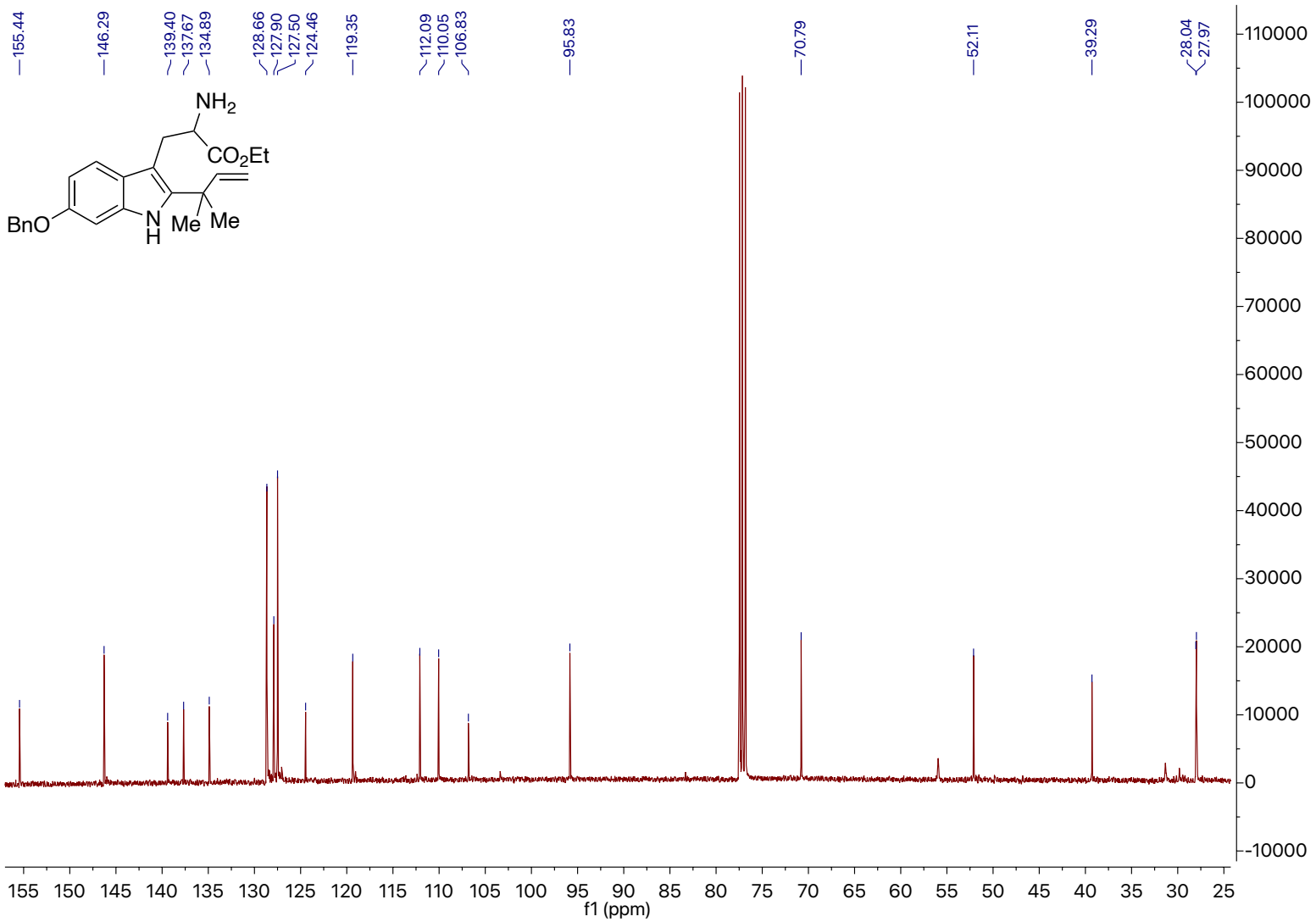

Figure A14. ^{13}C NMR Spectrum of compound **82** ($CDCl_3$).

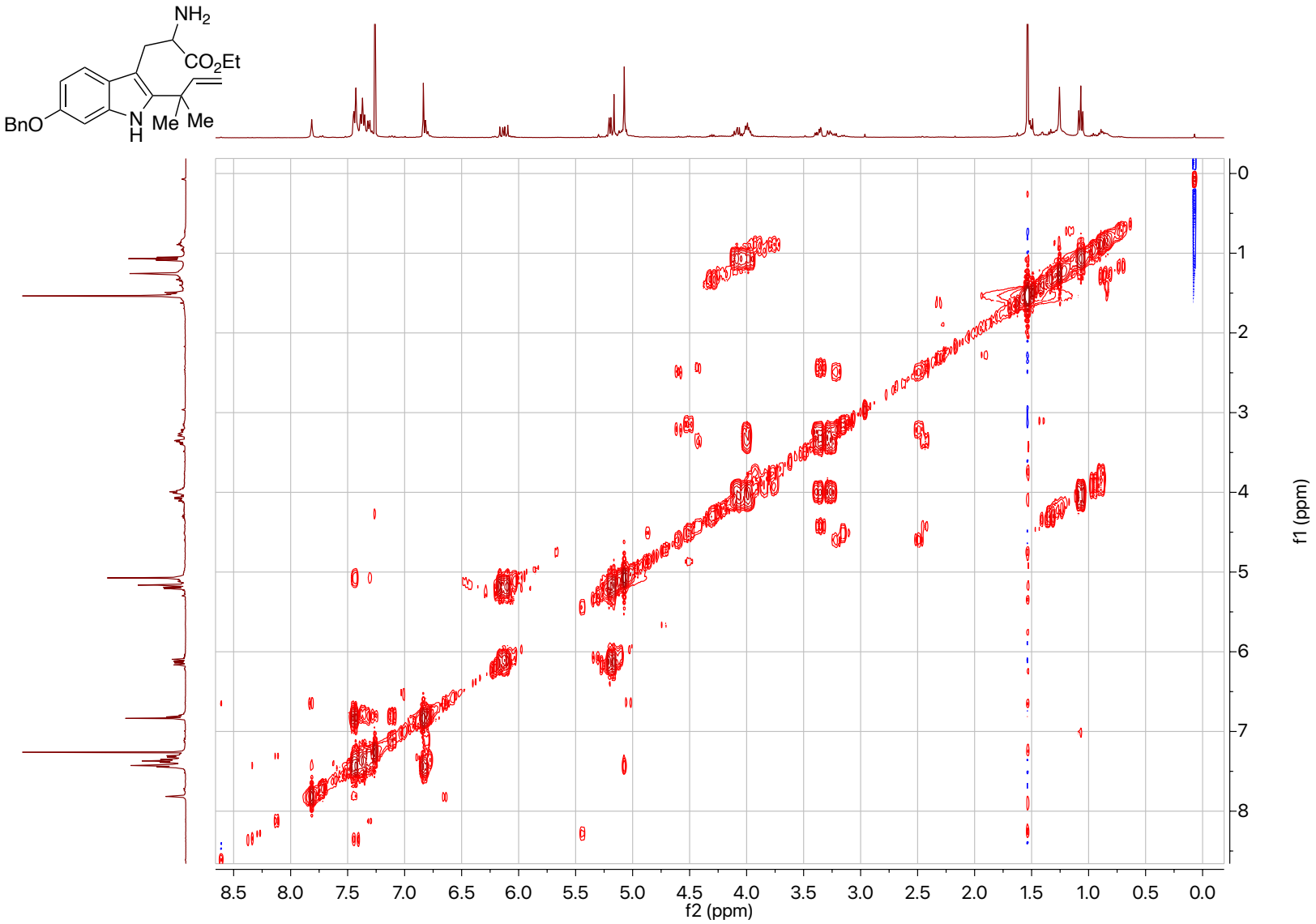

Figure A15. COSY NMR Spectrum of compound **82** ($CDCl_3$).

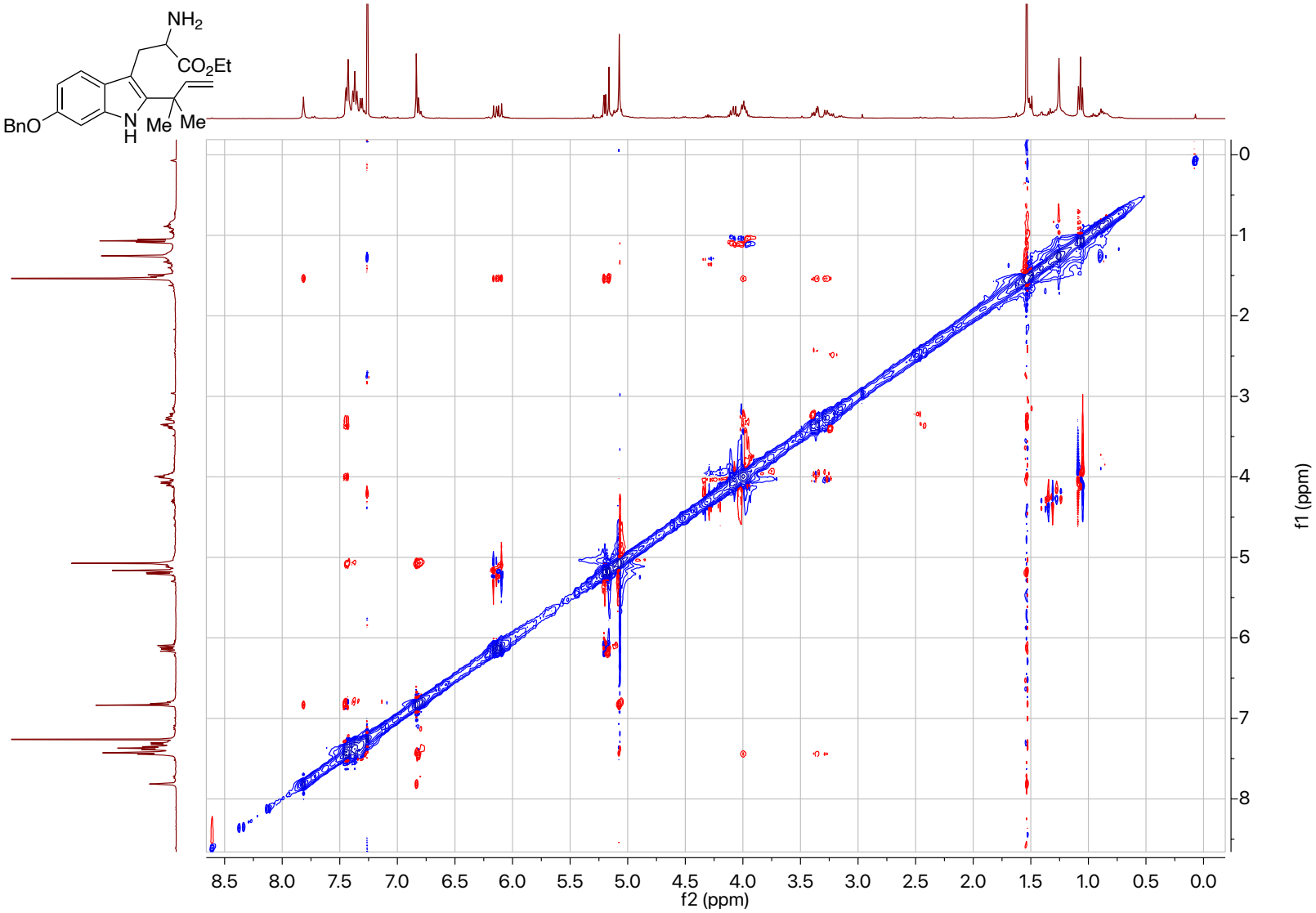

Figure A16. ROESY NMR Spectrum of compound **82** ($CDCl_3$).

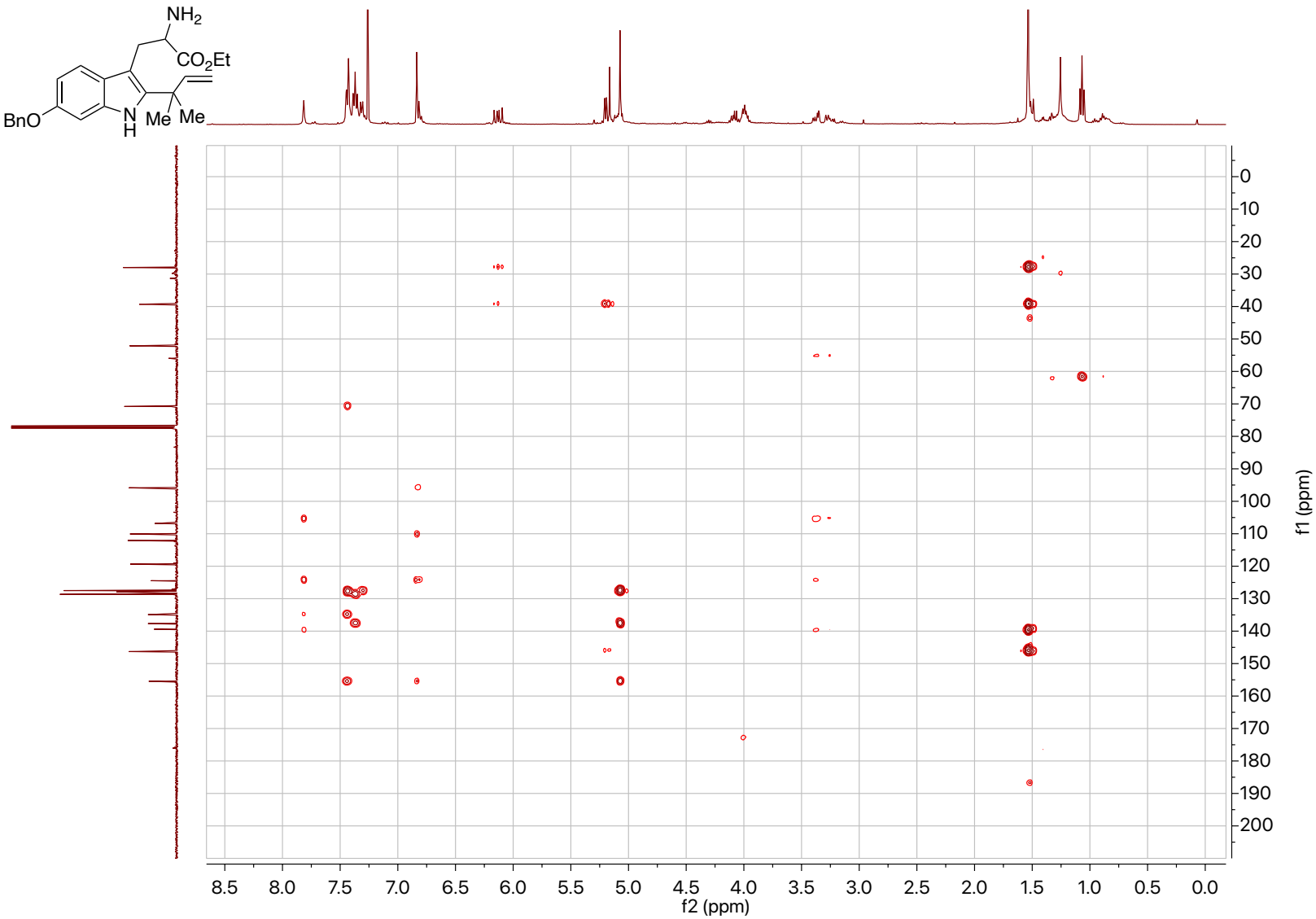

Figure A17. HMBC NMR Spectrum of compound **82** ($CDCl_3$).

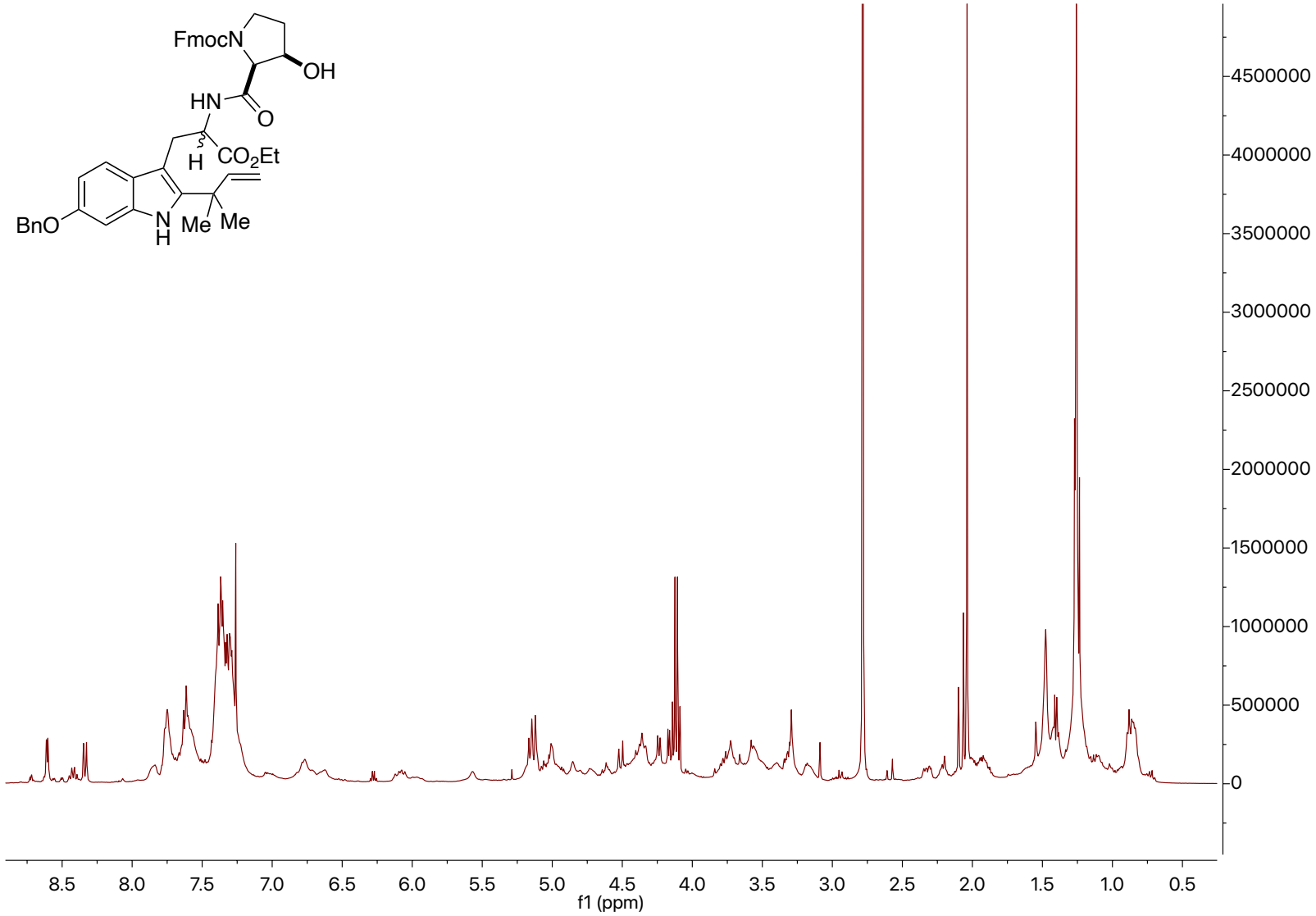

Figure A18. ^{1}H NMR Spectrum of compound **83** (DMSO).

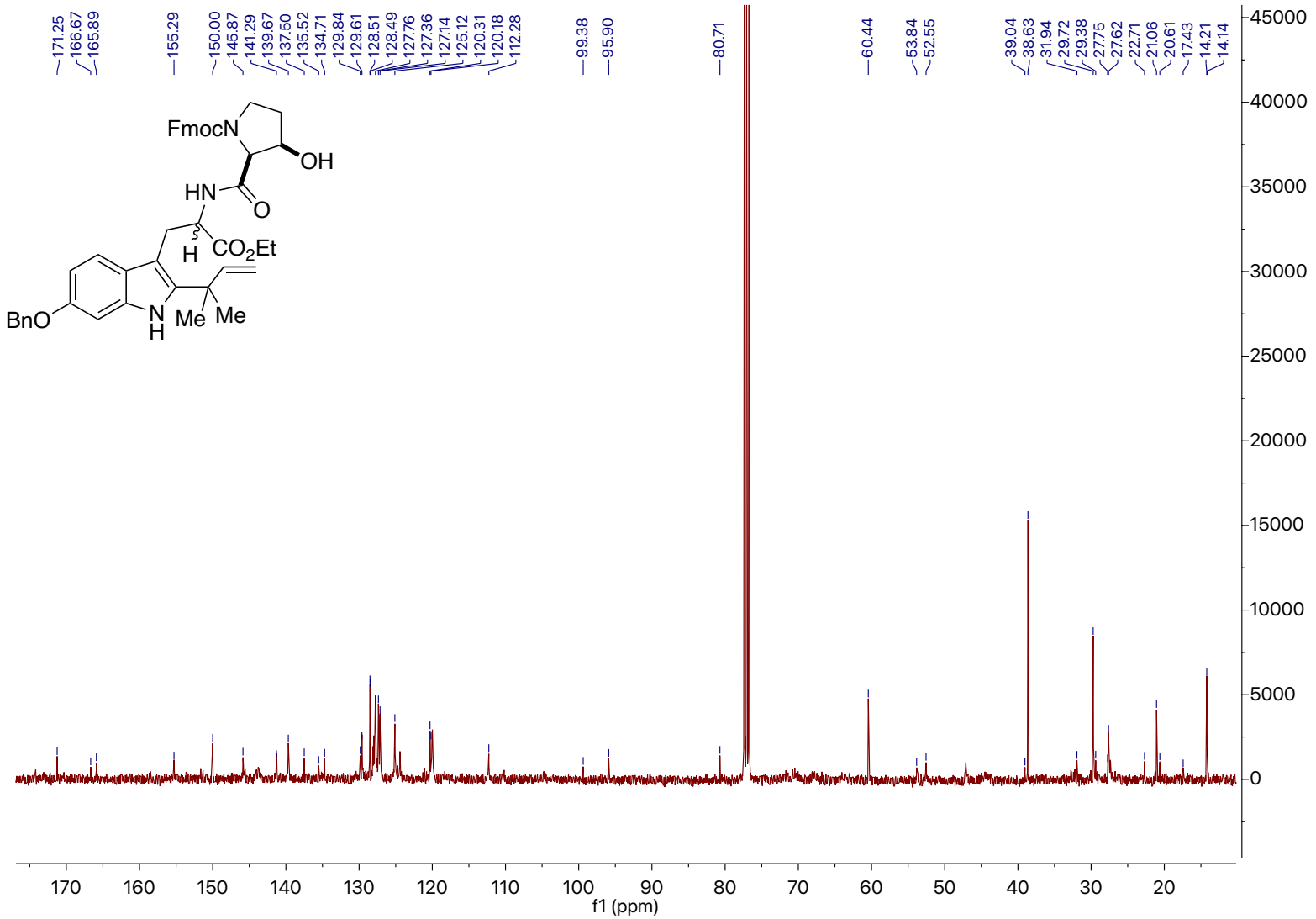

Figure A19. ^{13}C NMR Spectrum of compound **83** ($CDCl_3$).

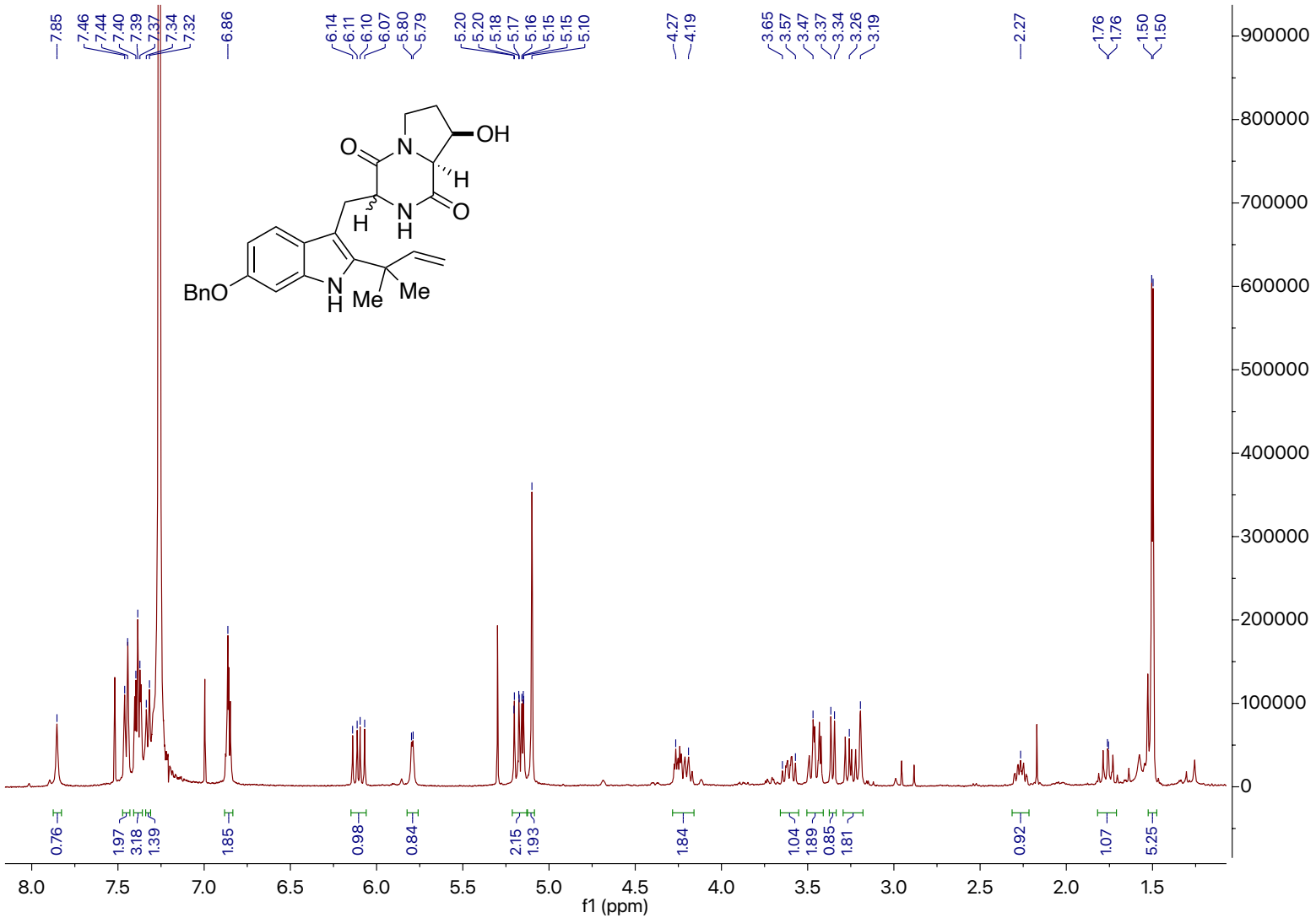

Figure A20. ^{1}H NMR Spectrum of compound **84a** ($CDCl_3$).

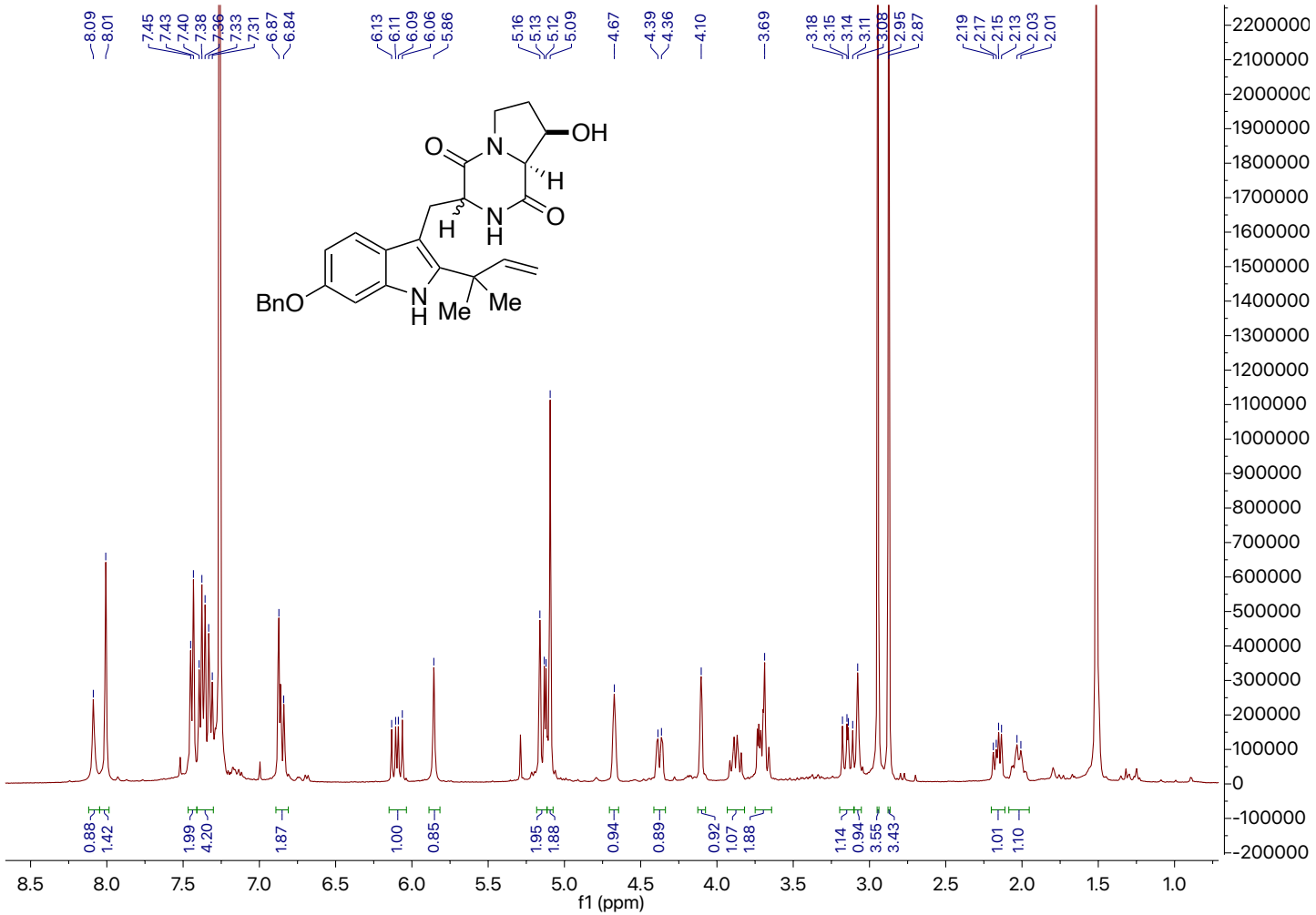

Figure A21. ^{1}H NMR Spectrum of compound **84b** ($CDCl_3$).

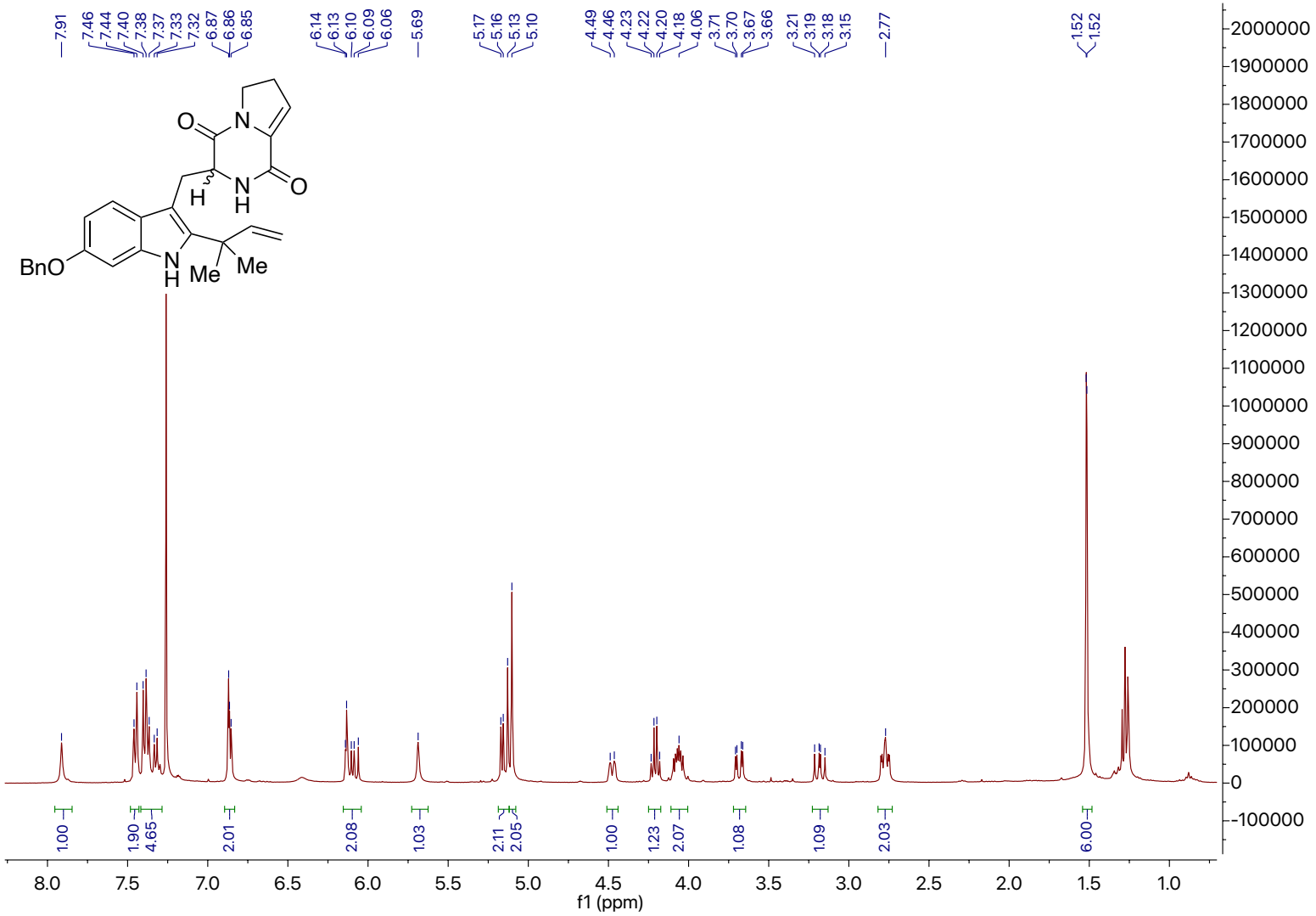

Figure A22. ^{1}H NMR Spectrum of compound **143** ($CDCl_3$).

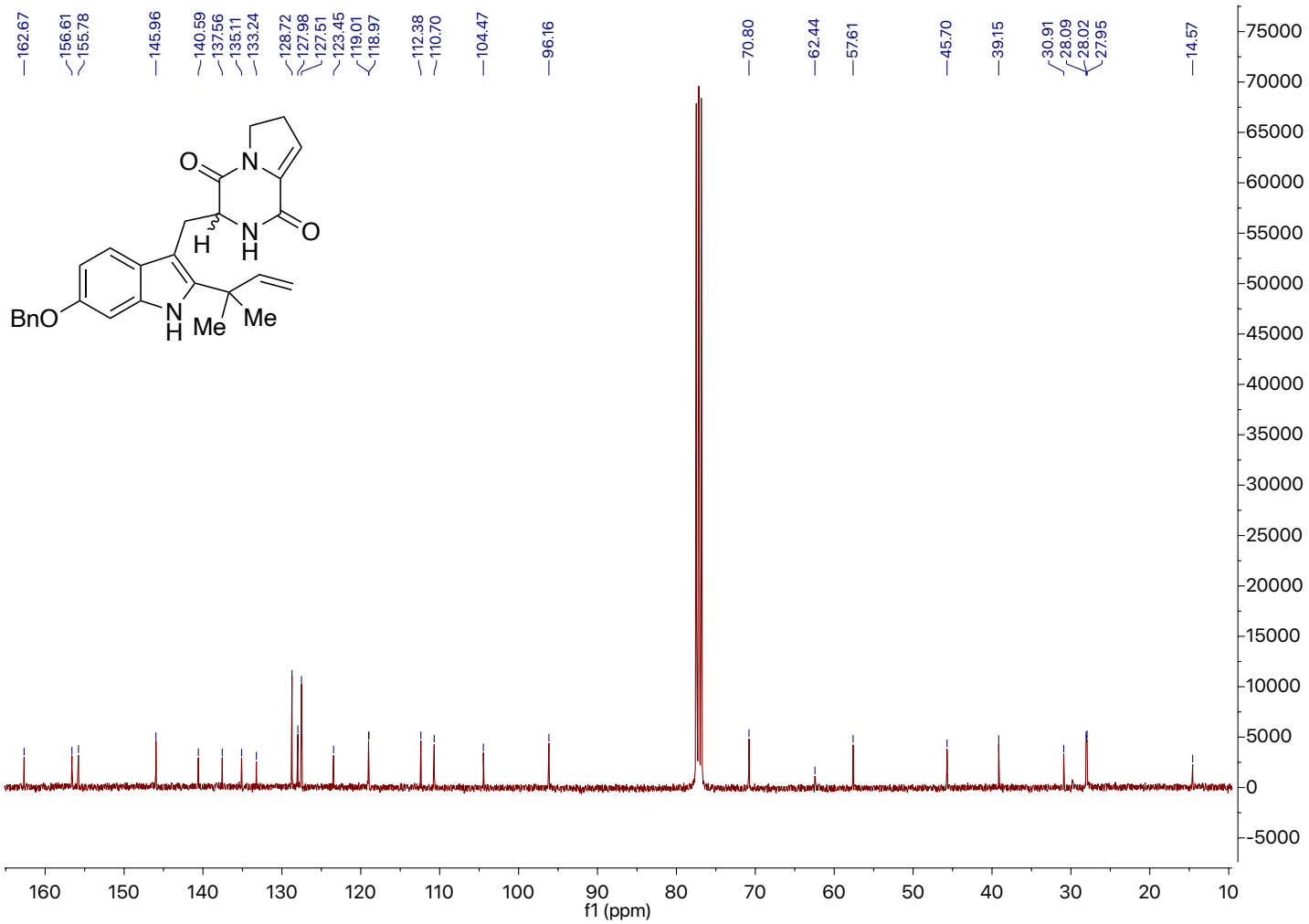

Figure A23. ^{13}C NMR Spectrum of compound **143** ($CDCl_3$).

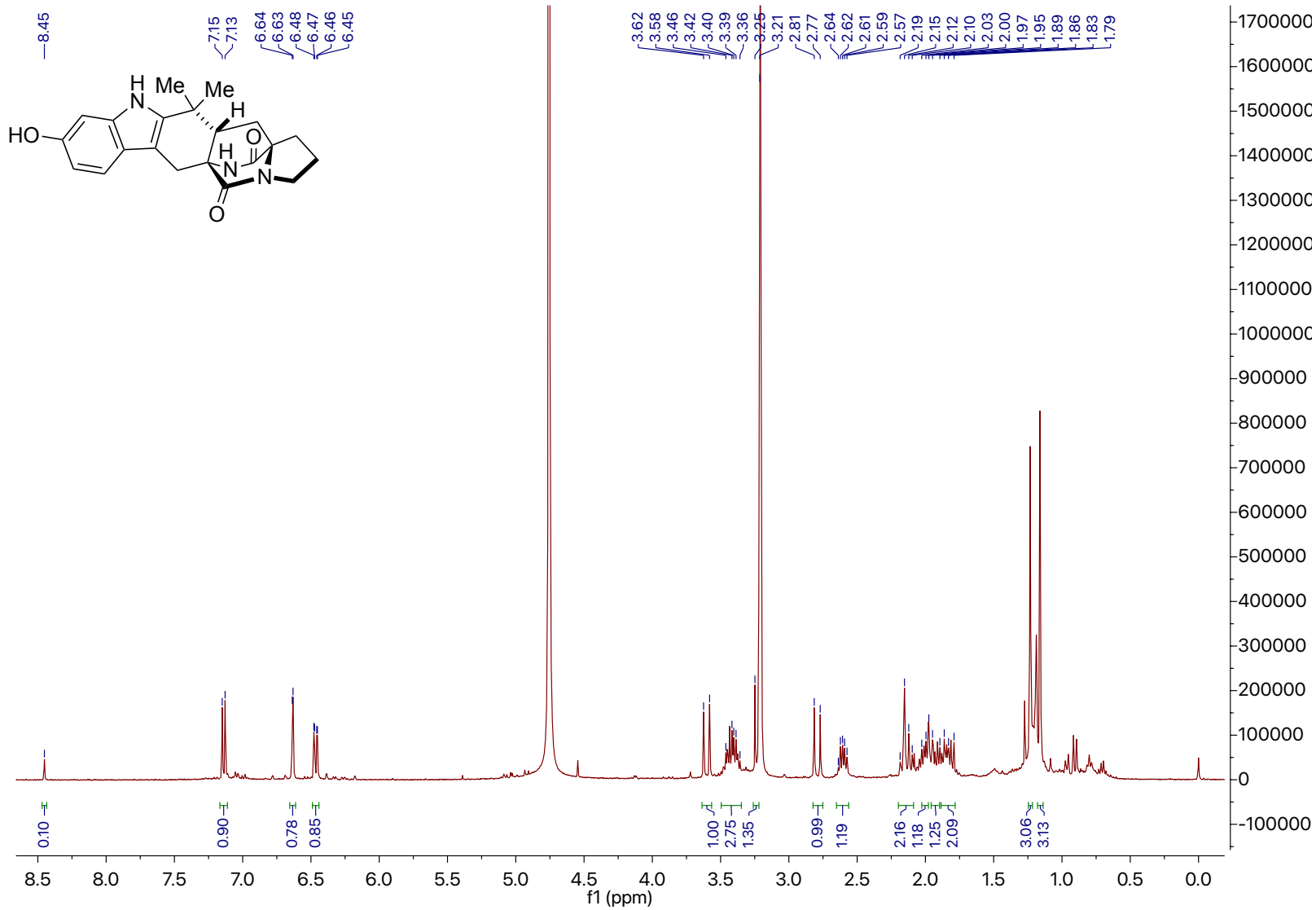

Figure A24. ^{1}H NMR Spectrum of compound **88** (MeOD).

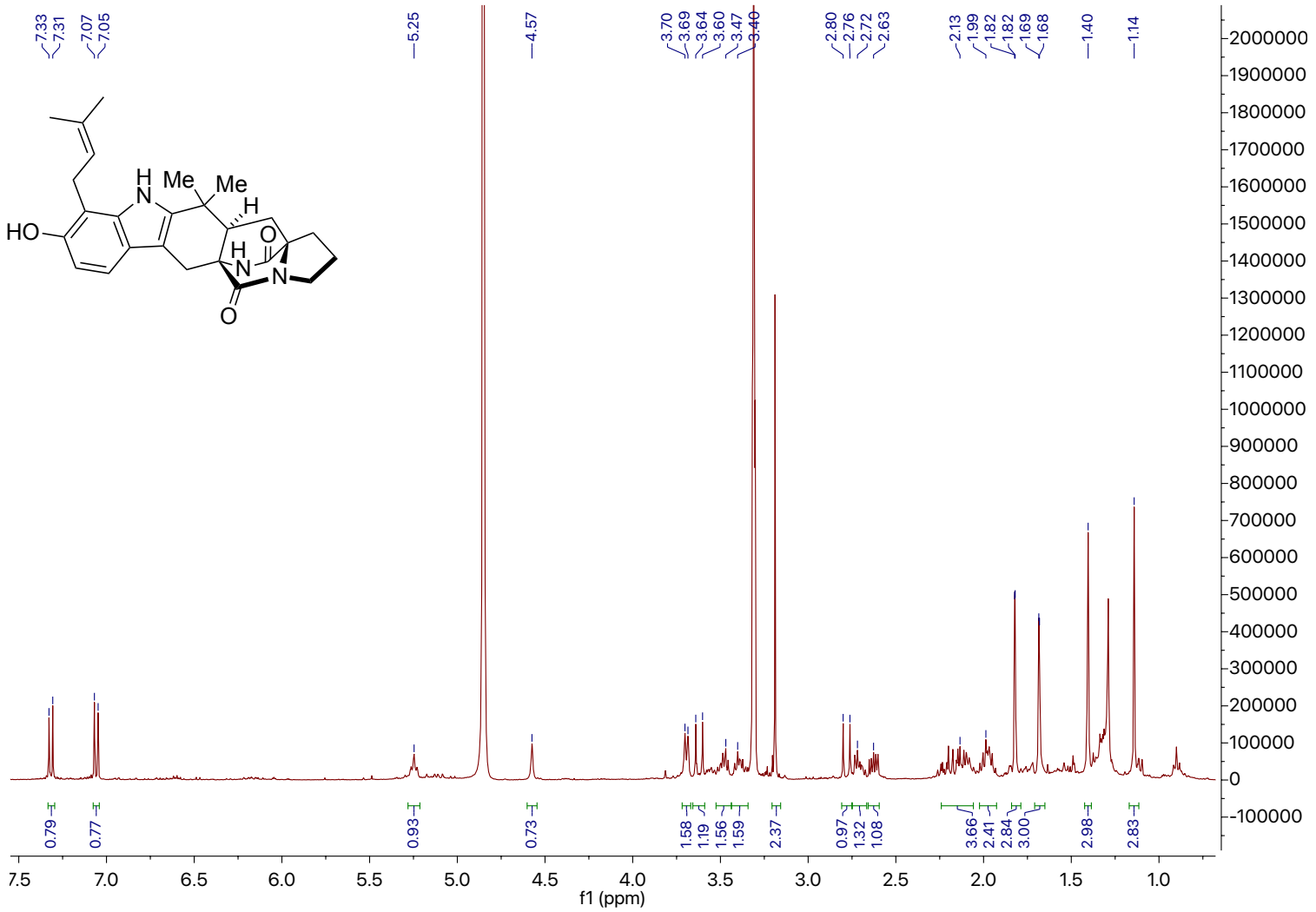

Figure A25. ^{1}H NMR Spectrum of Notoamide T (MeOD).

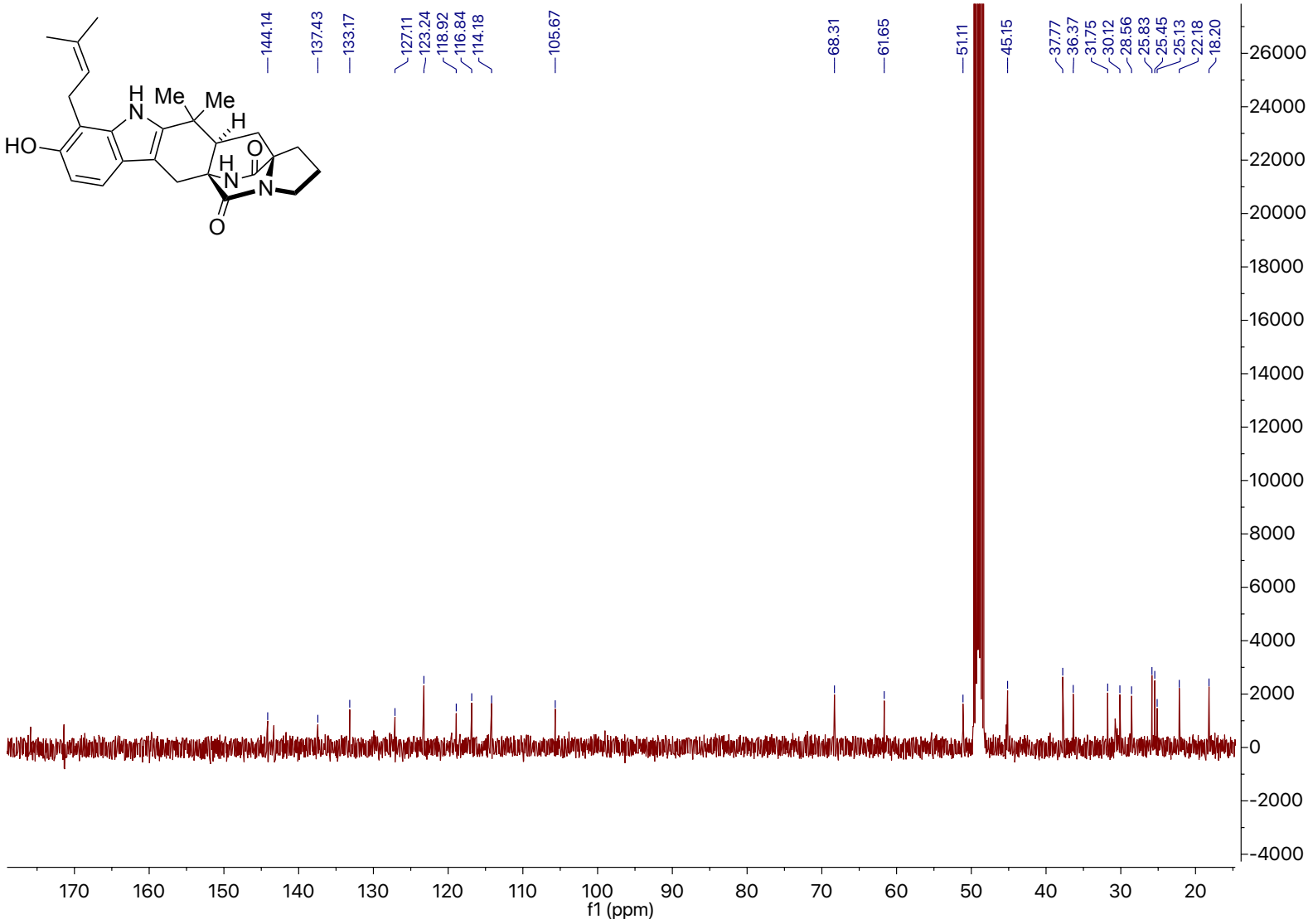

Figure A26. ^{13}C NMR Spectrum of Notoamide T (MeOD).

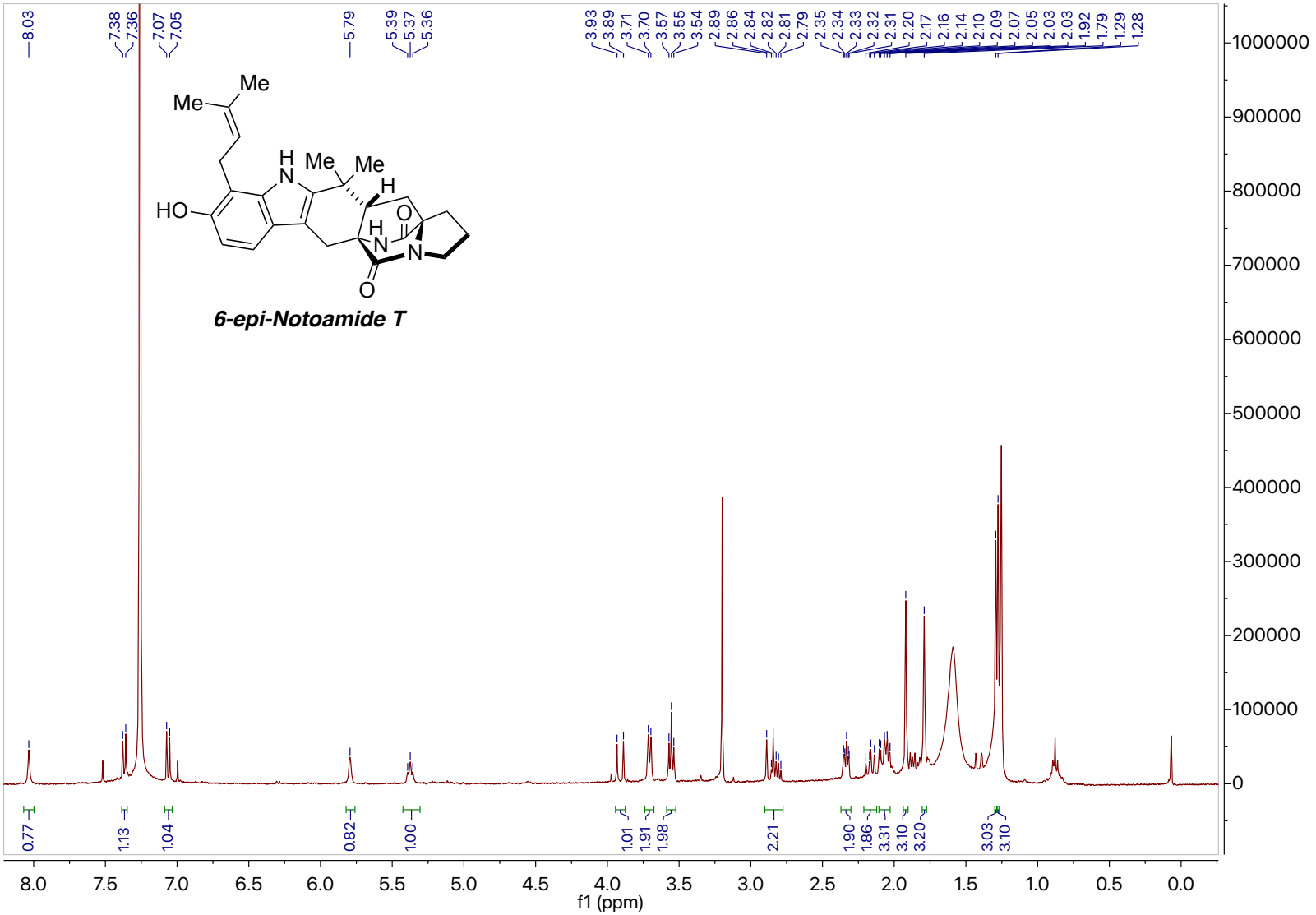

Figure A27. [1]H NMR Spectrum of 6-*epi*-Notoamide T (MeOD).

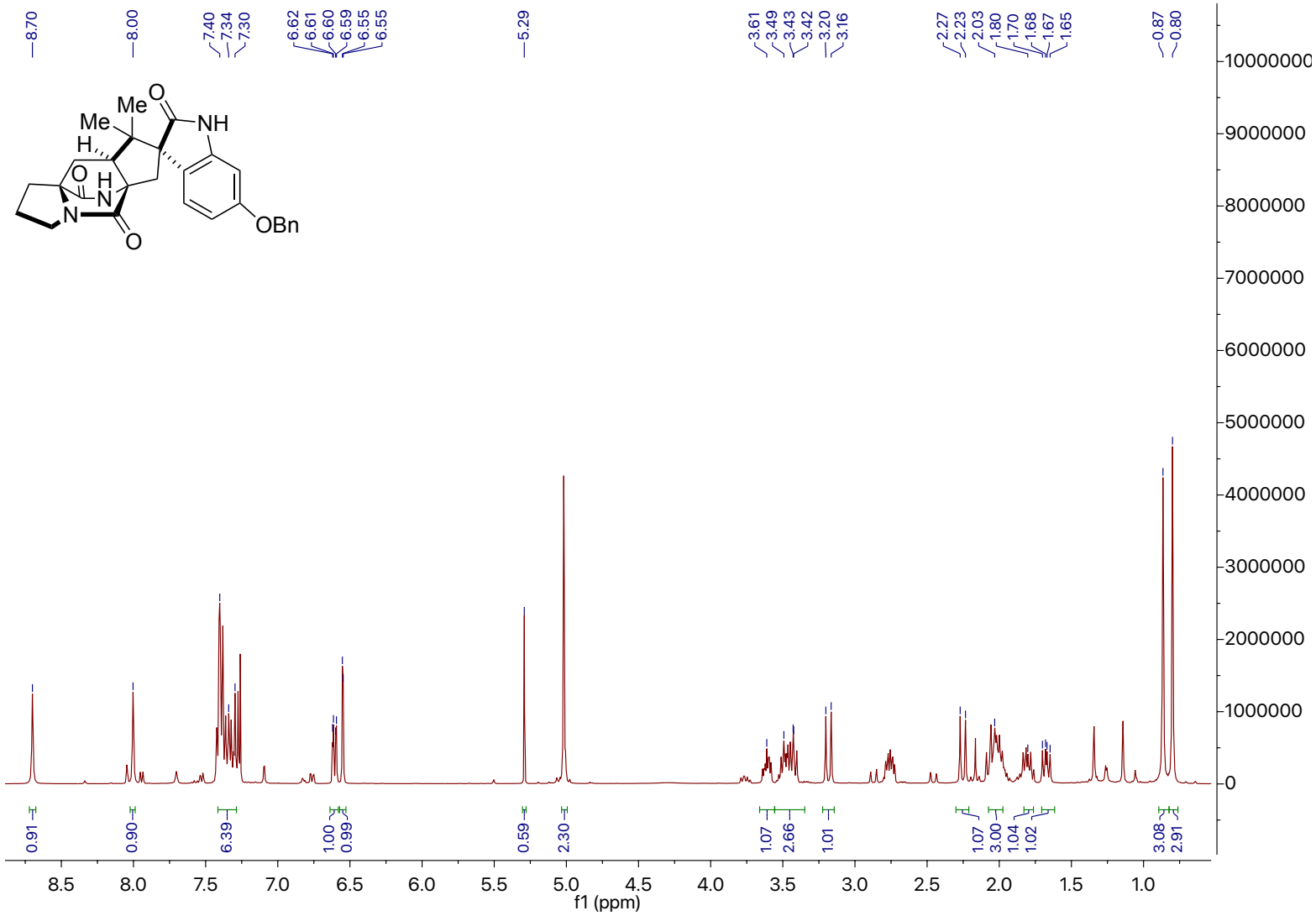

Figure A28. ^{1}H NMR Spectrum of compound **108** (MeOD).

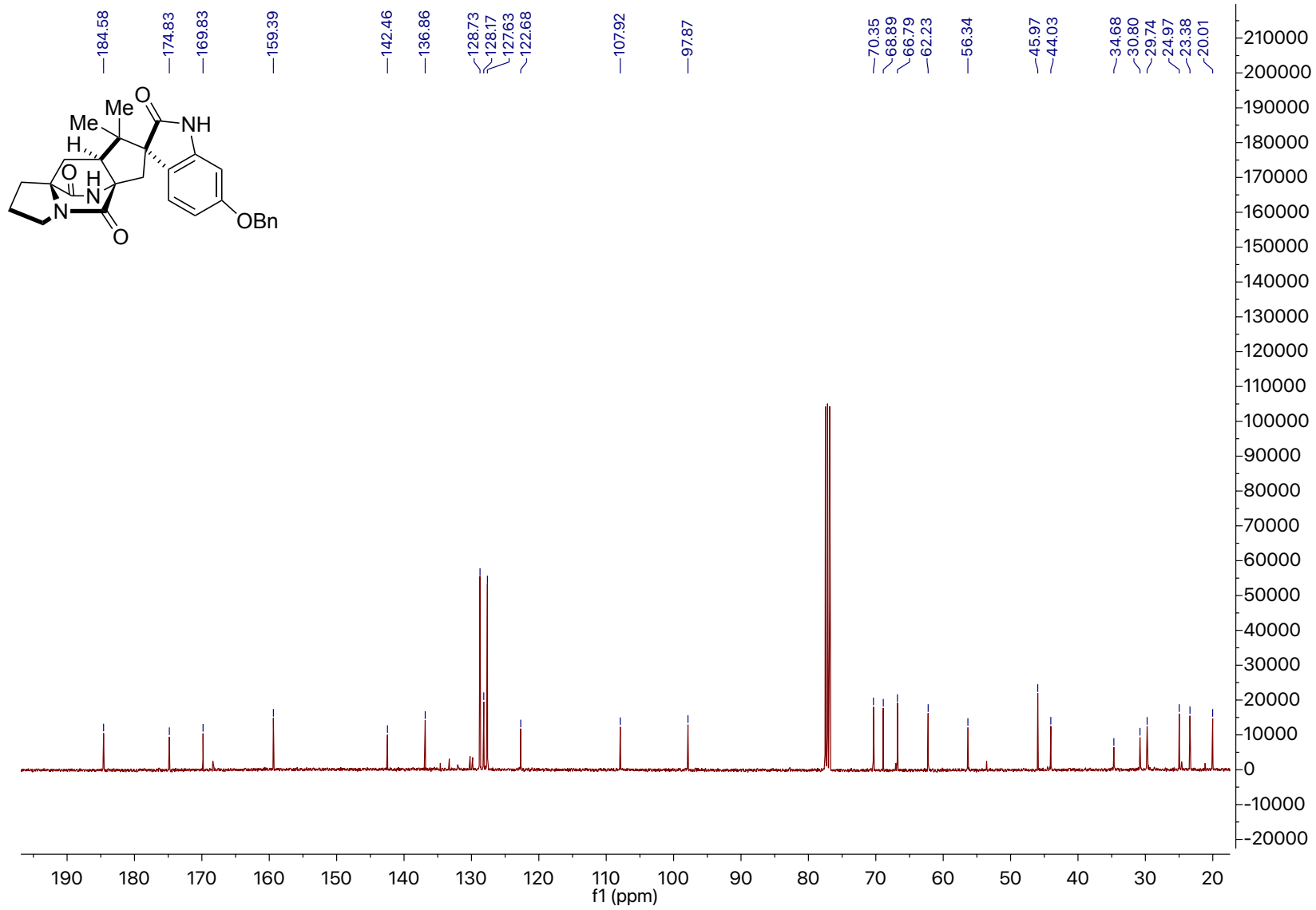

Figure A29. ^{13}C NMR Spectrum of compound **108** (MeOD).

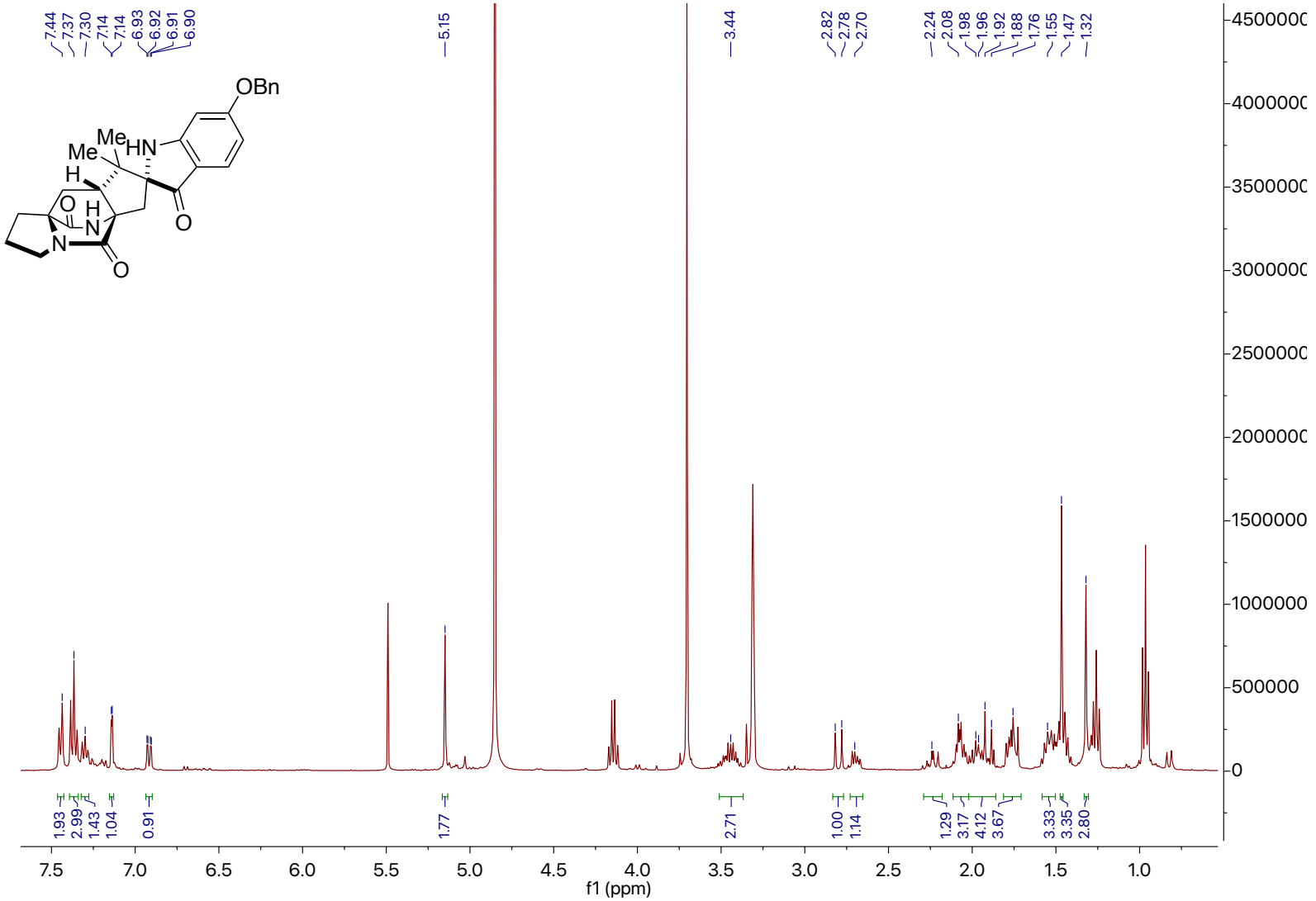

Figure A30. ^{1}H NMR Spectrum of compound **109** (MeOD).

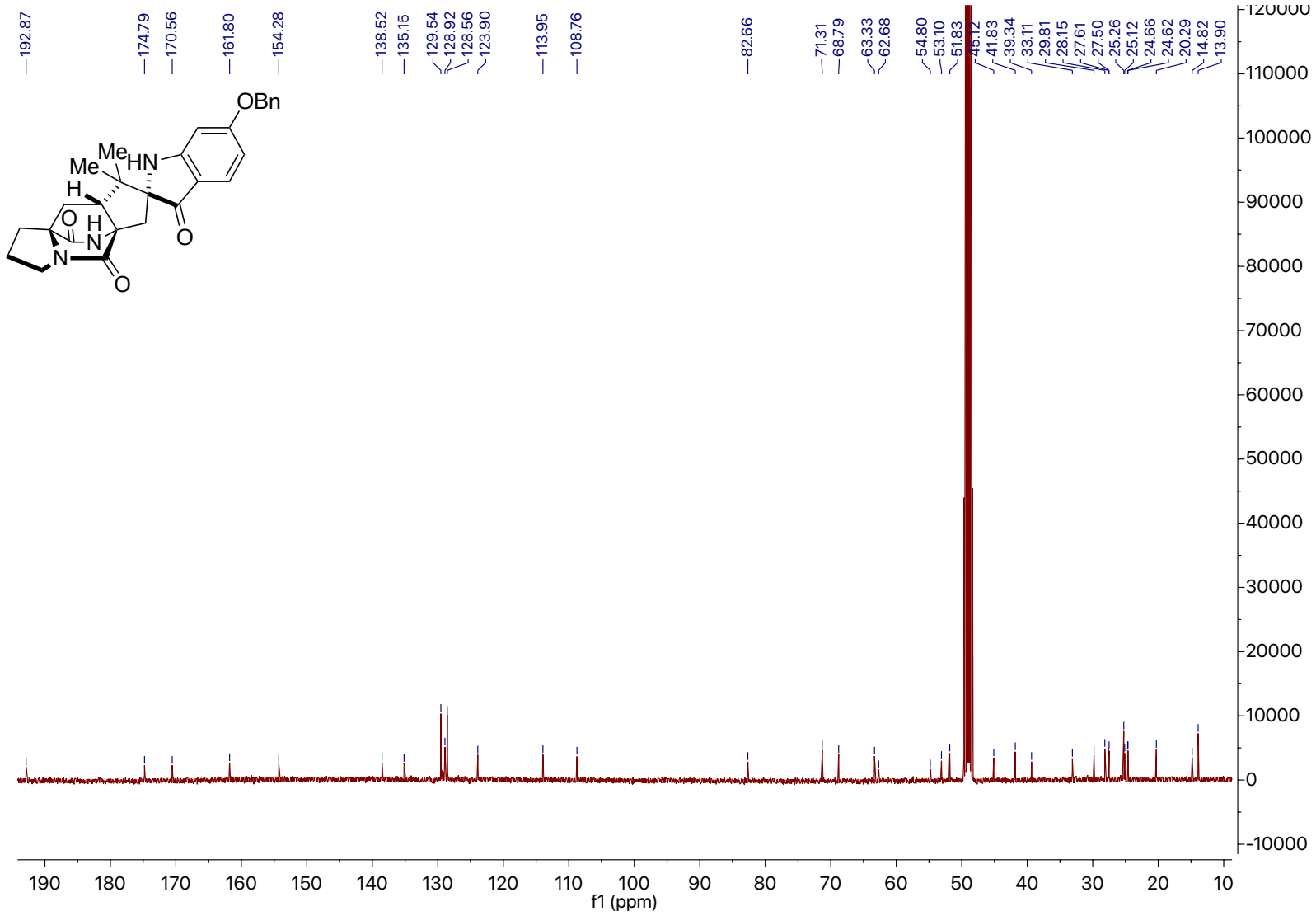

Figure A31. ^{13}C NMR Spectrum of compound **109** (MeOD).

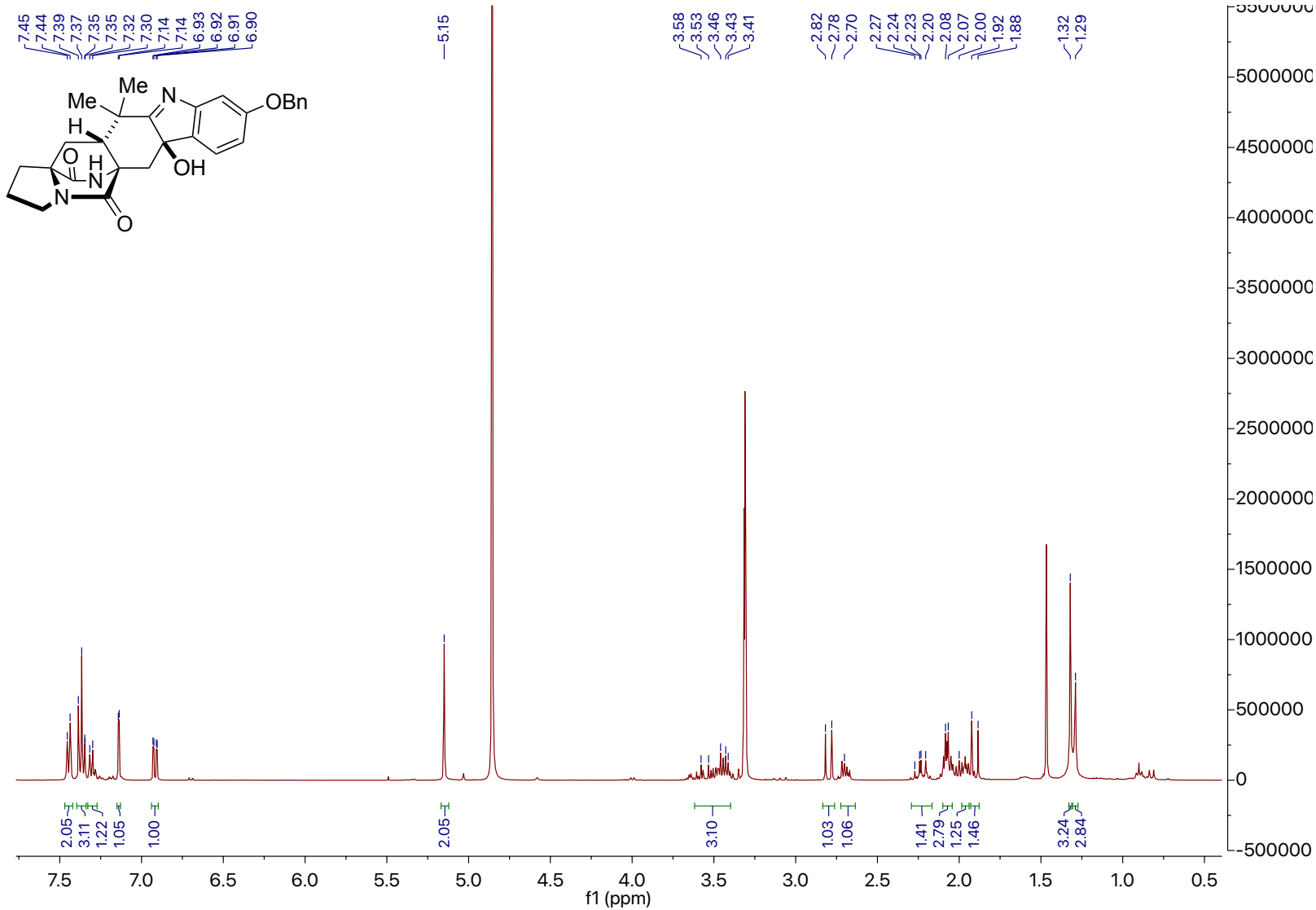

Figure A32. ^{1}H NMR Spectrum of compound **110** (MeOD).

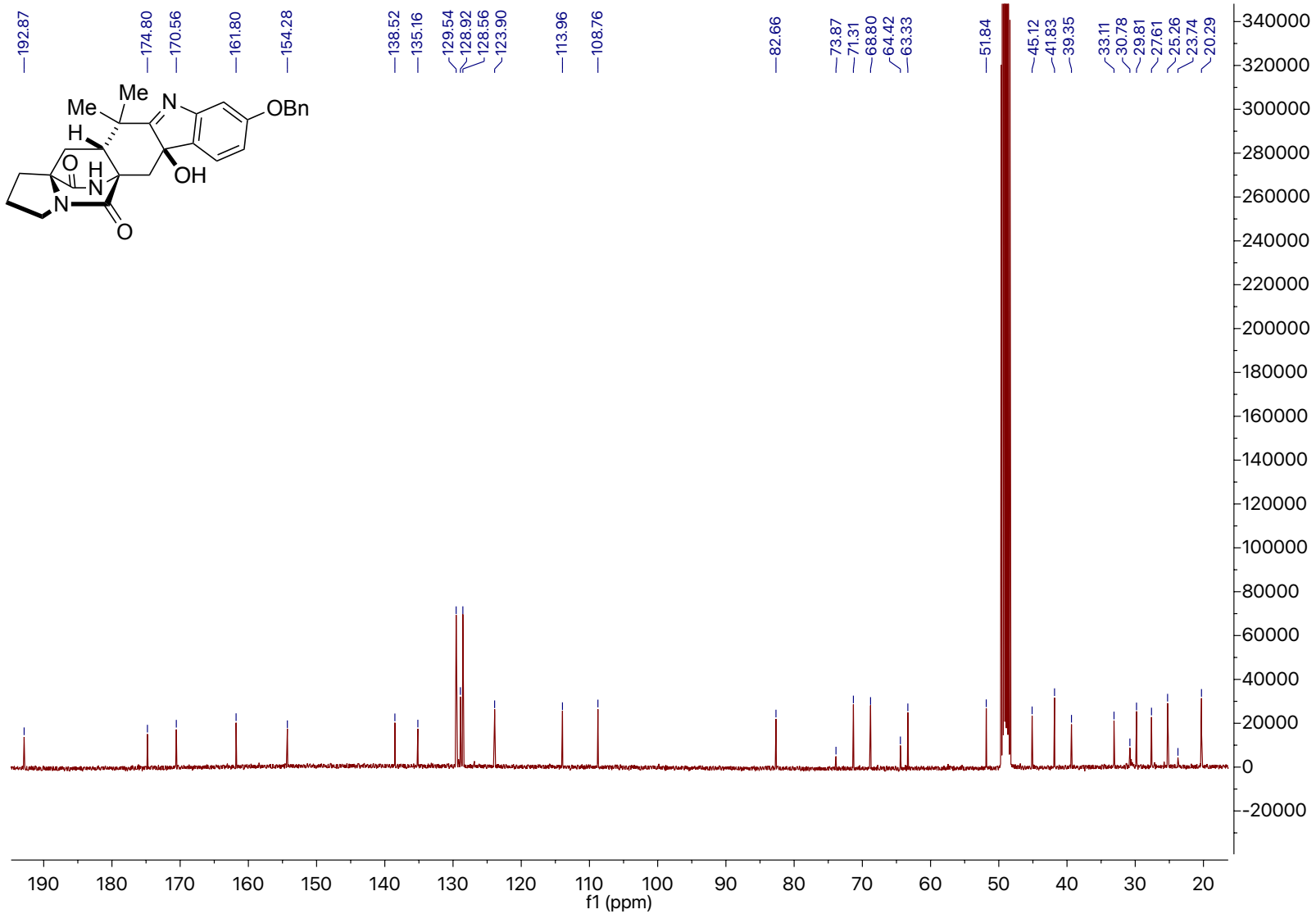

Figure A33. ^{13}C NMR Spectrum of compound **110** (MeOD).

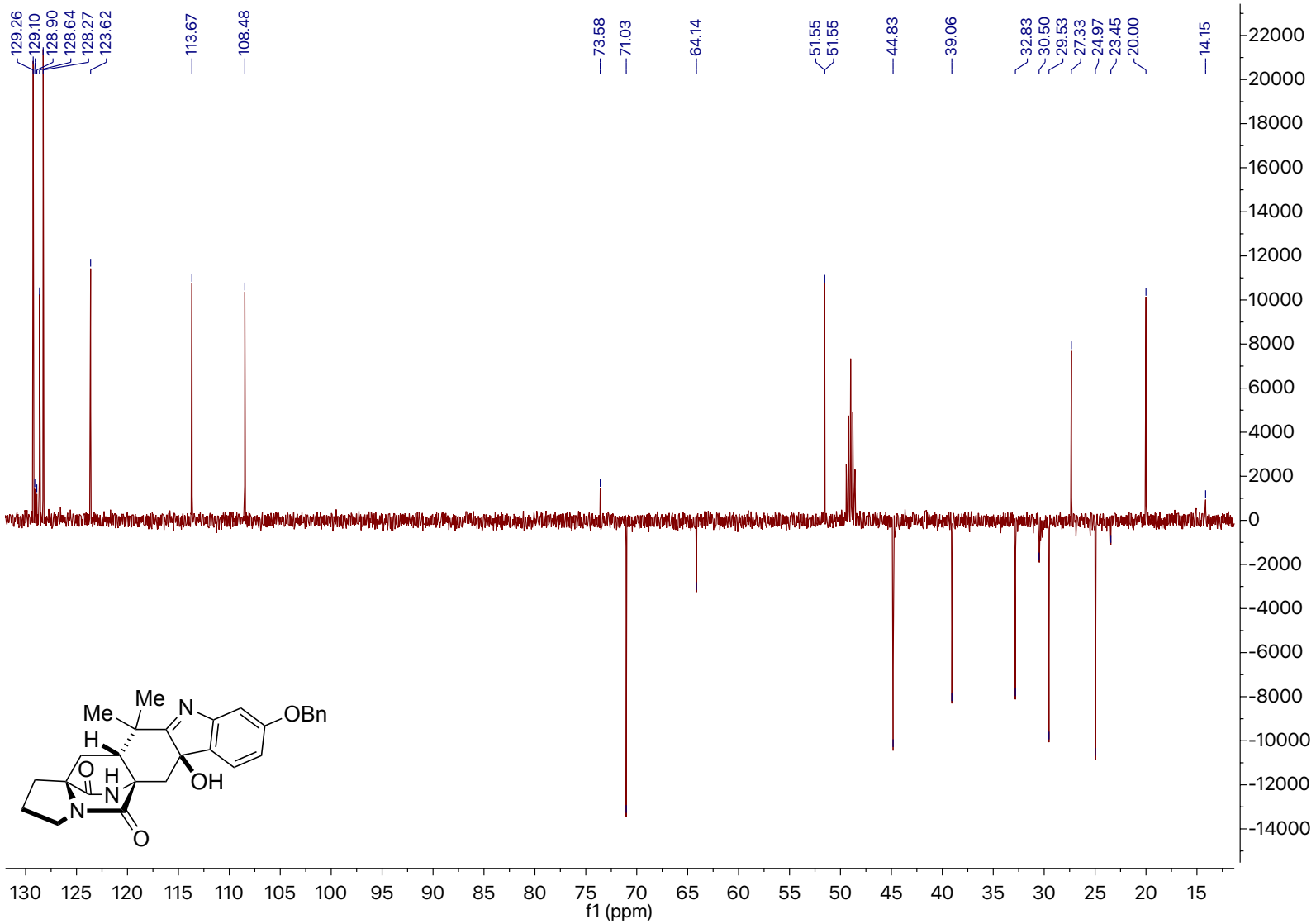

Figure A34. DEPT135 NMR Spectrum of compound **110** (MeOD).

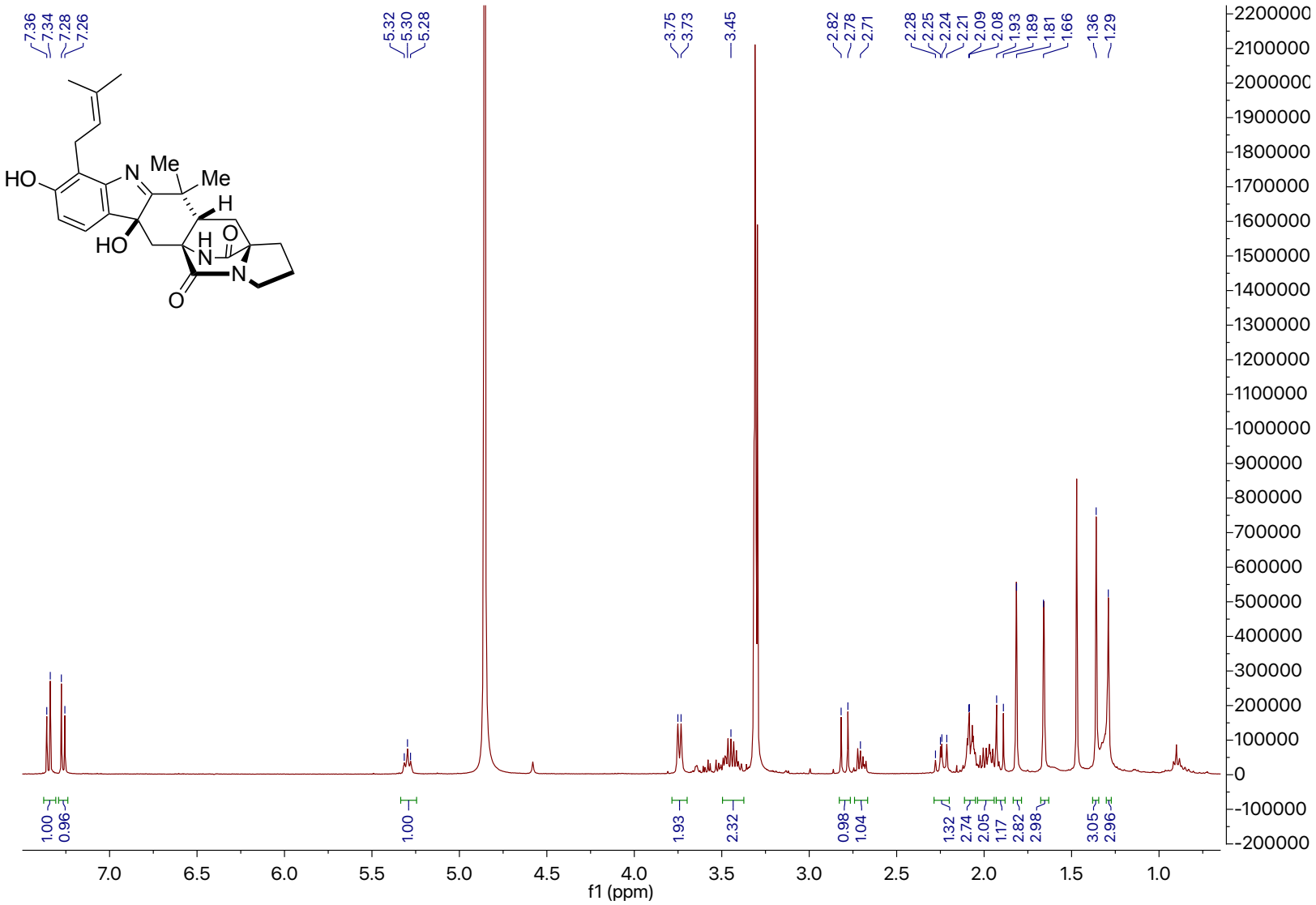

Figure A35. ^{1}H NMR Spectrum of compound **144** (MeOD).

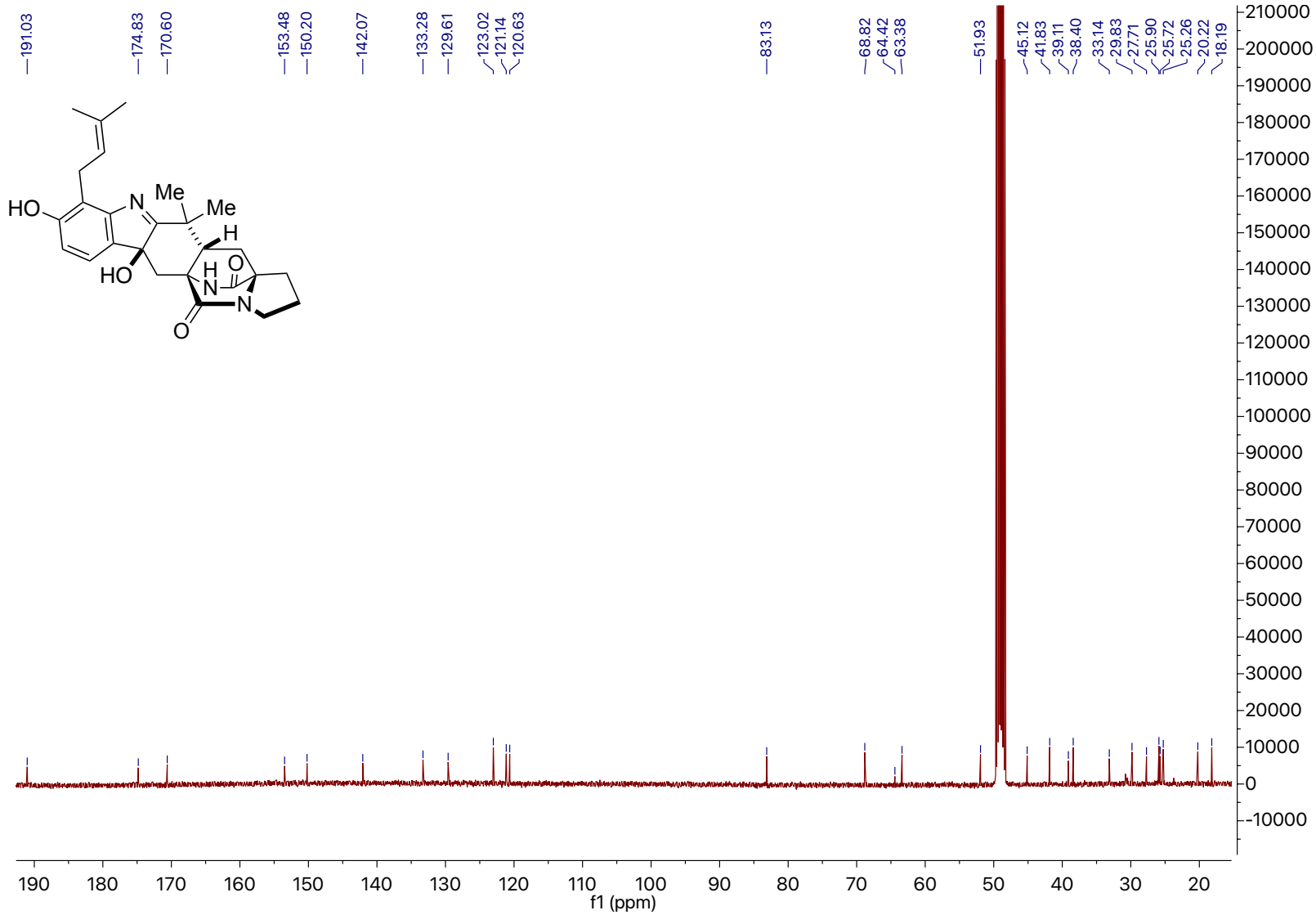

Figure A36. ^{13}C NMR Spectrum of compound **144** (MeOD).

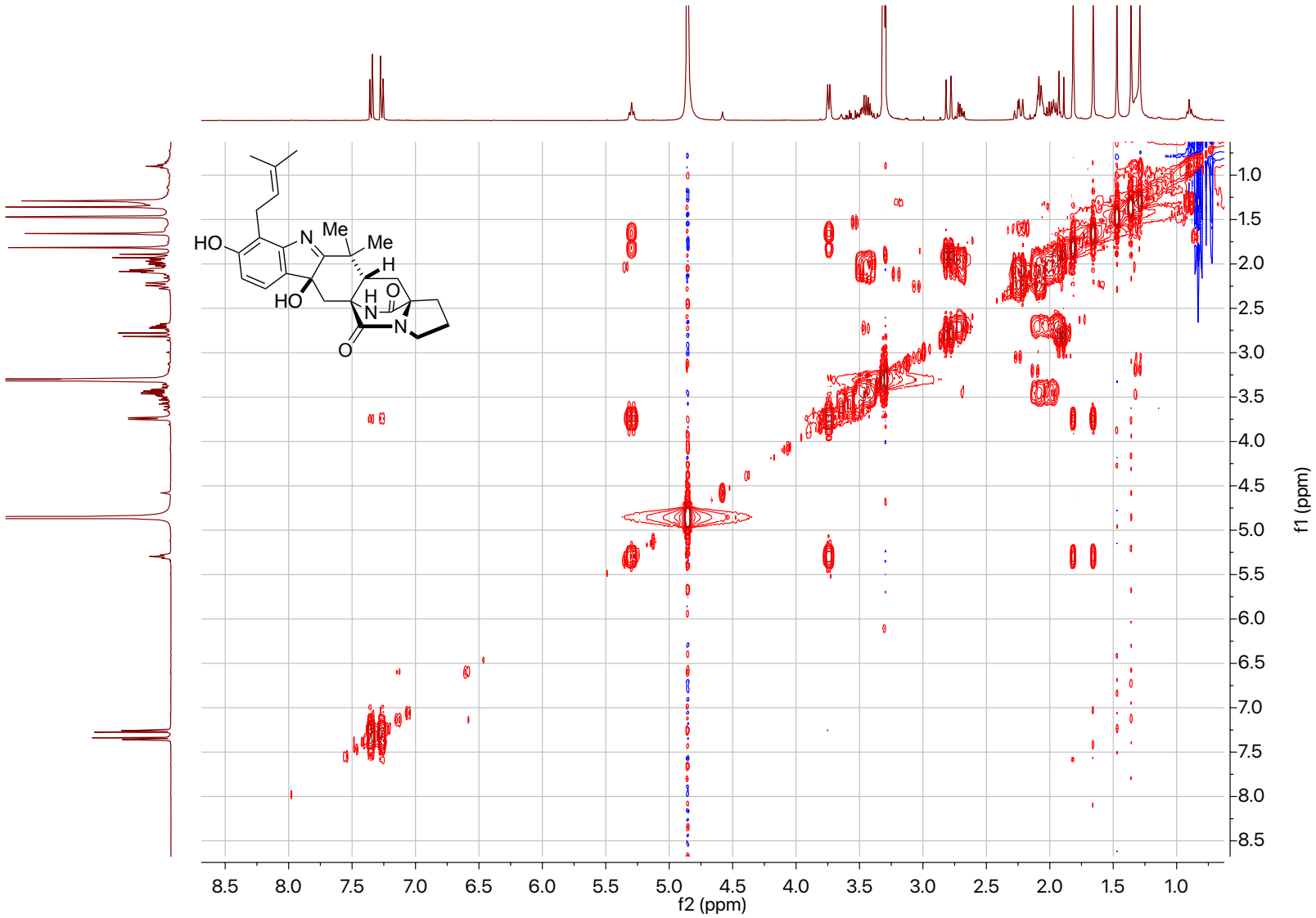

Figure A37. COSY NMR Spectrum of compound **144** (MeOD).

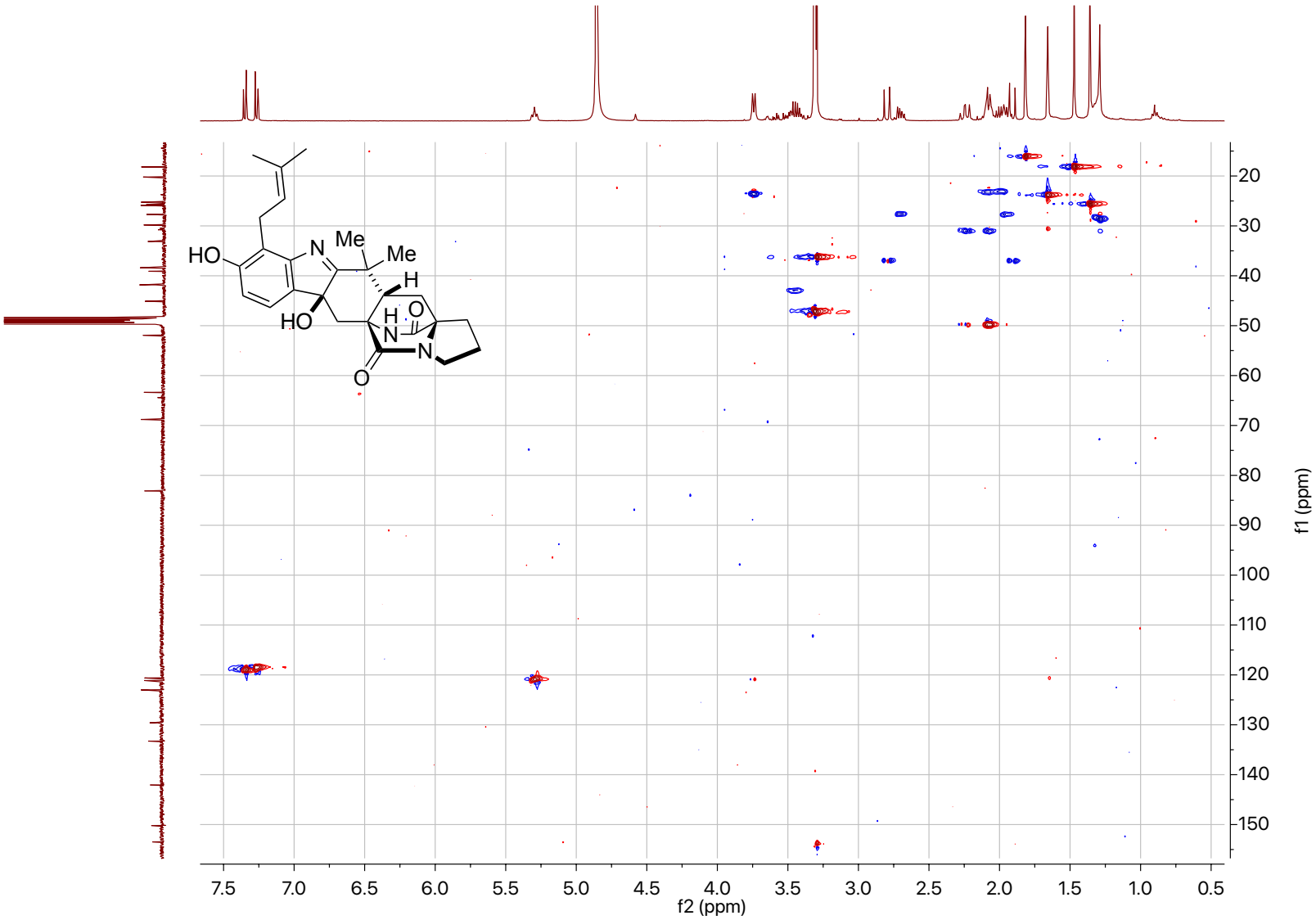

Figure A38. HSQC NMR Spectrum of compound **144** (MeOD).

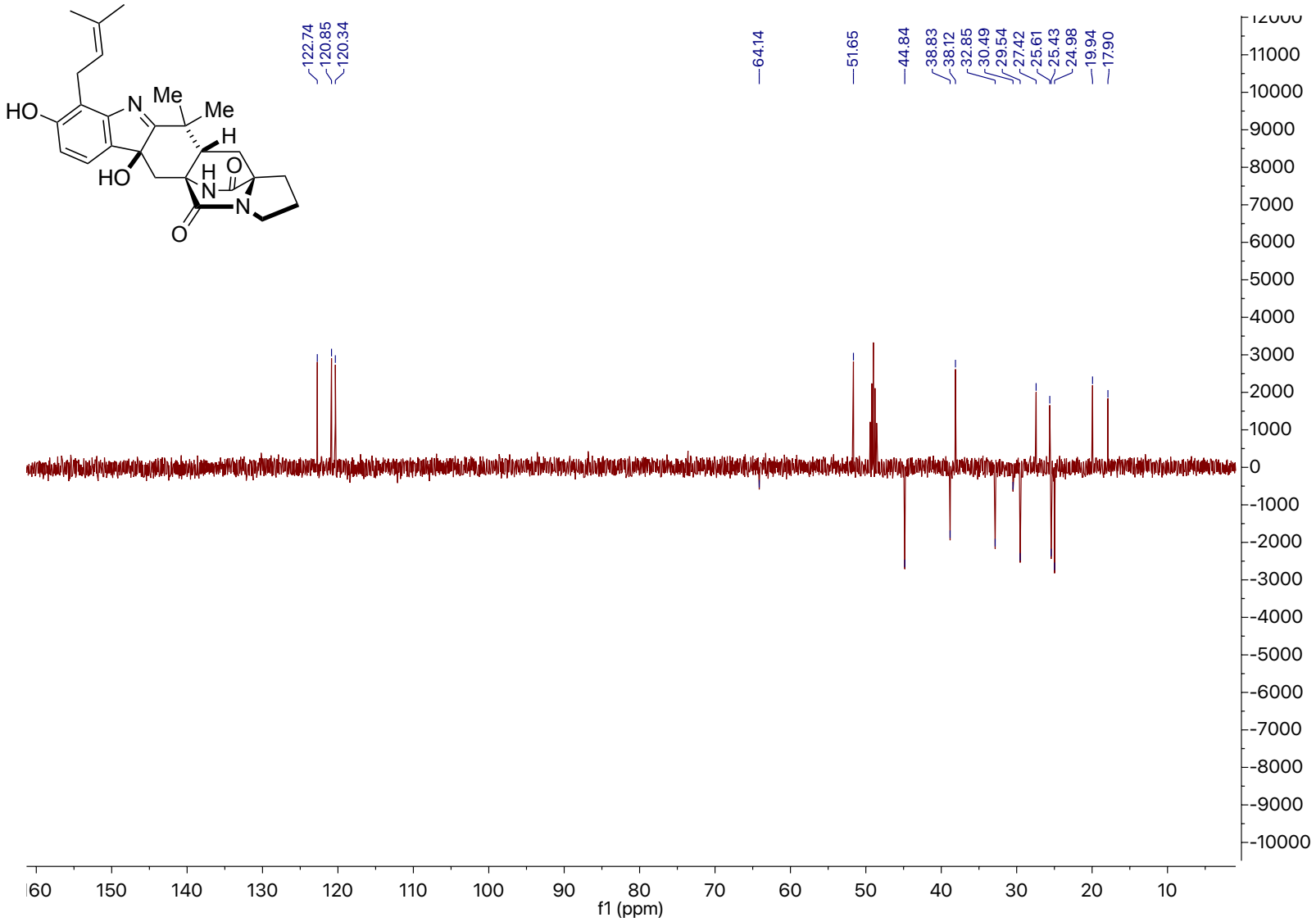

Figure A39. DEPT135 NMR Spectrum of compound **144** (MeOD).

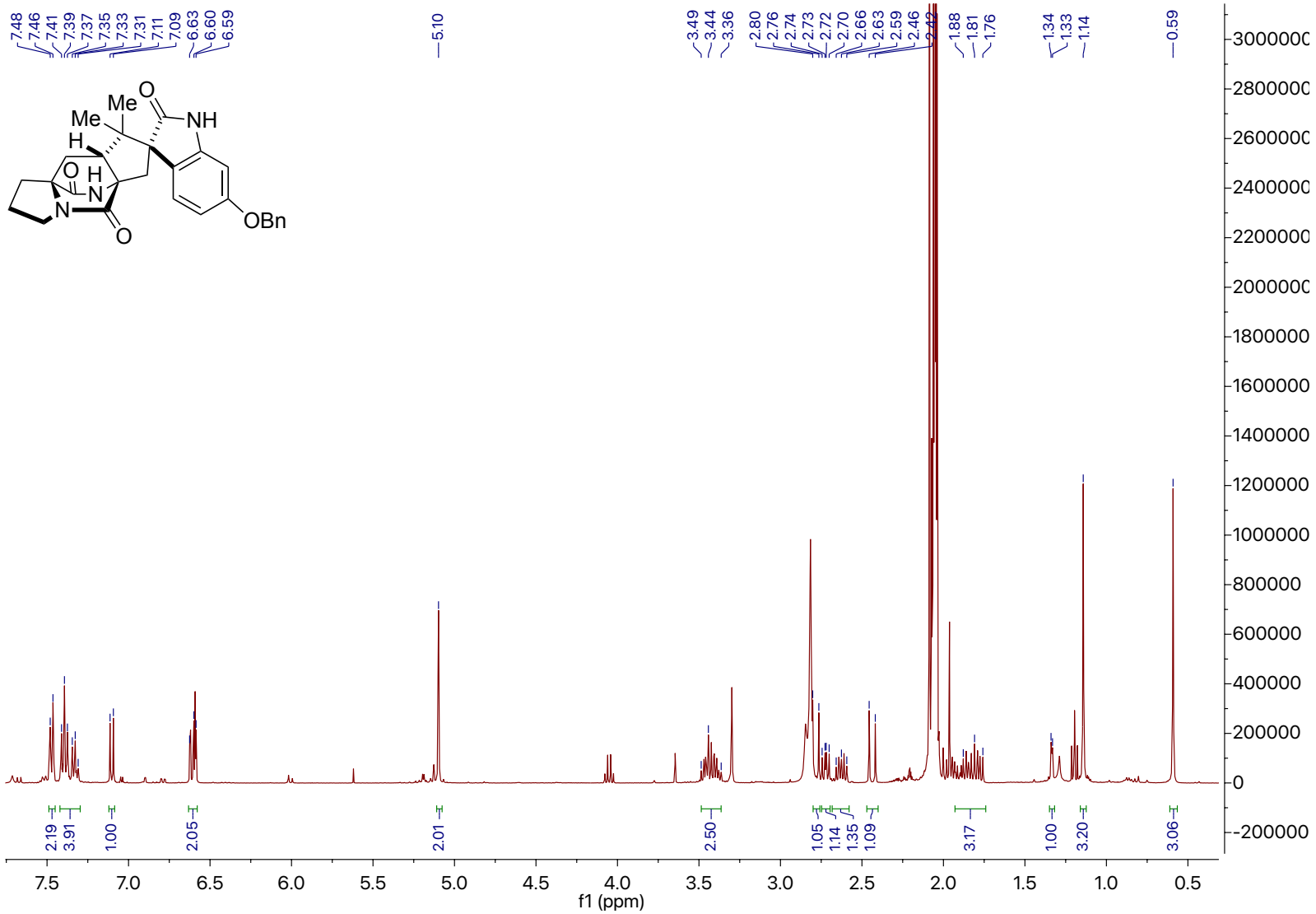

Figure A40. [1]H NMR Spectrum of compound **111** (Acetone).

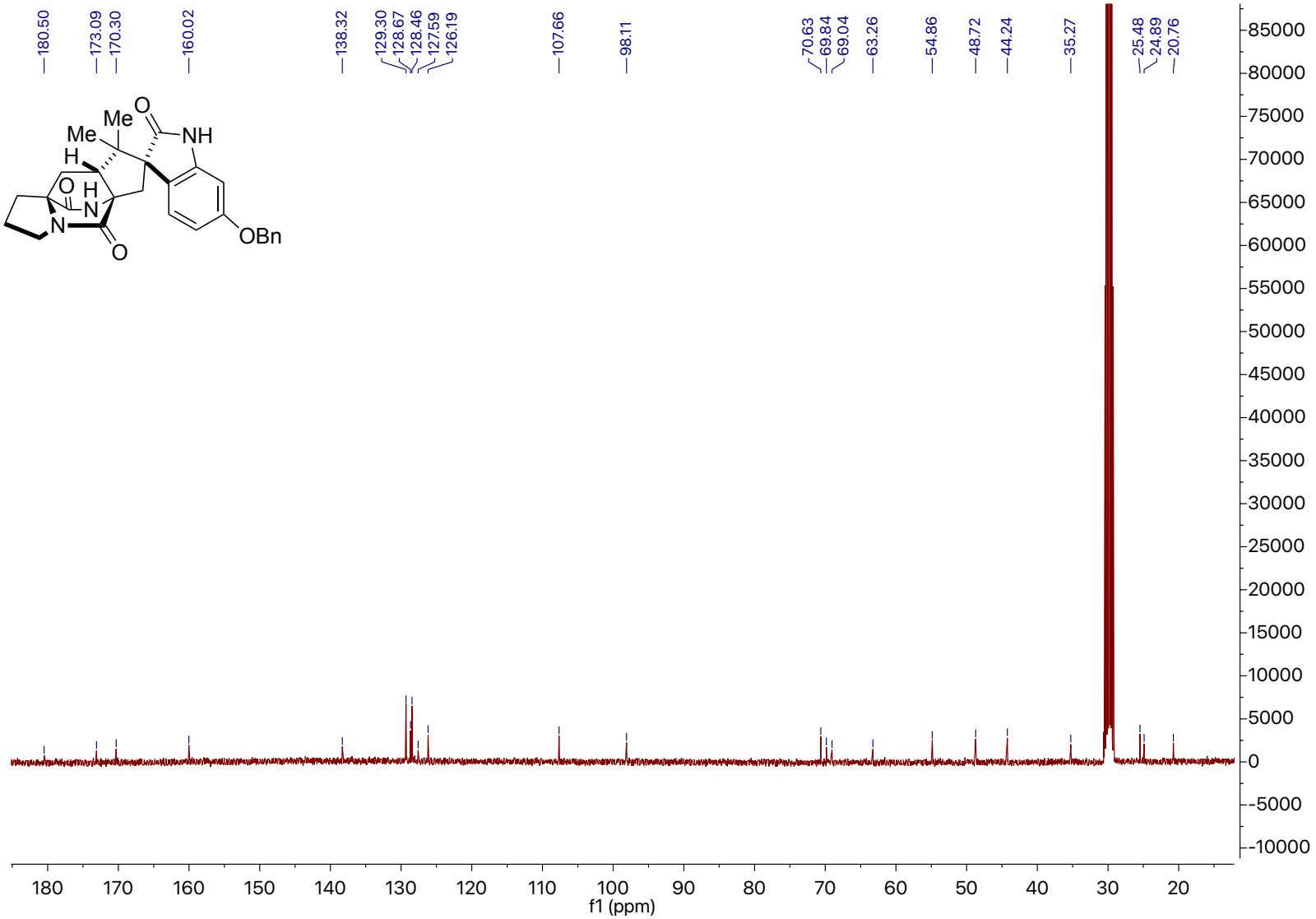

Figure A41. ^{13}C NMR Spectrum of compound **111** (Acetone).

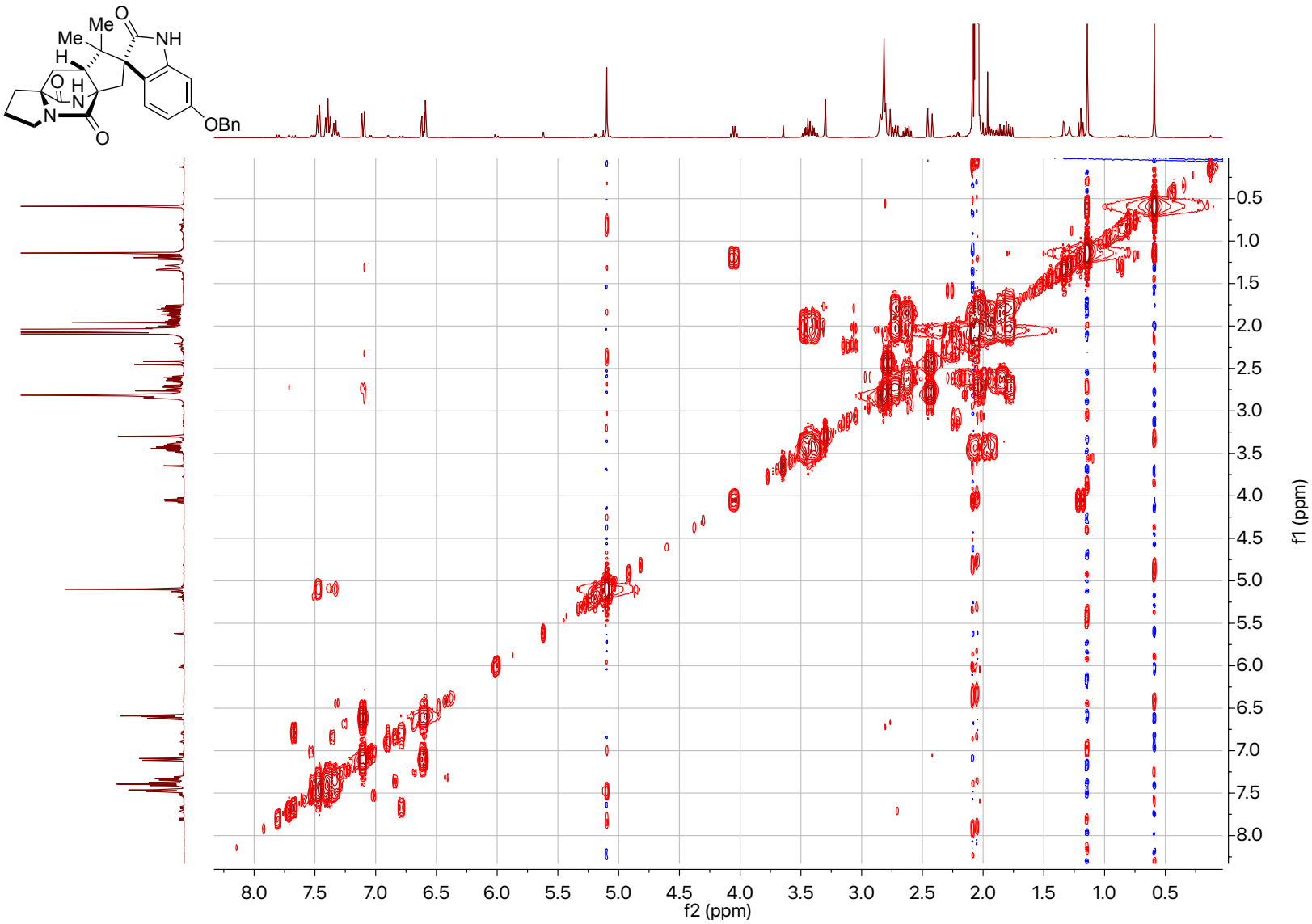

Figure A42. COSY NMR Spectrum of compound **111** (Acetone).

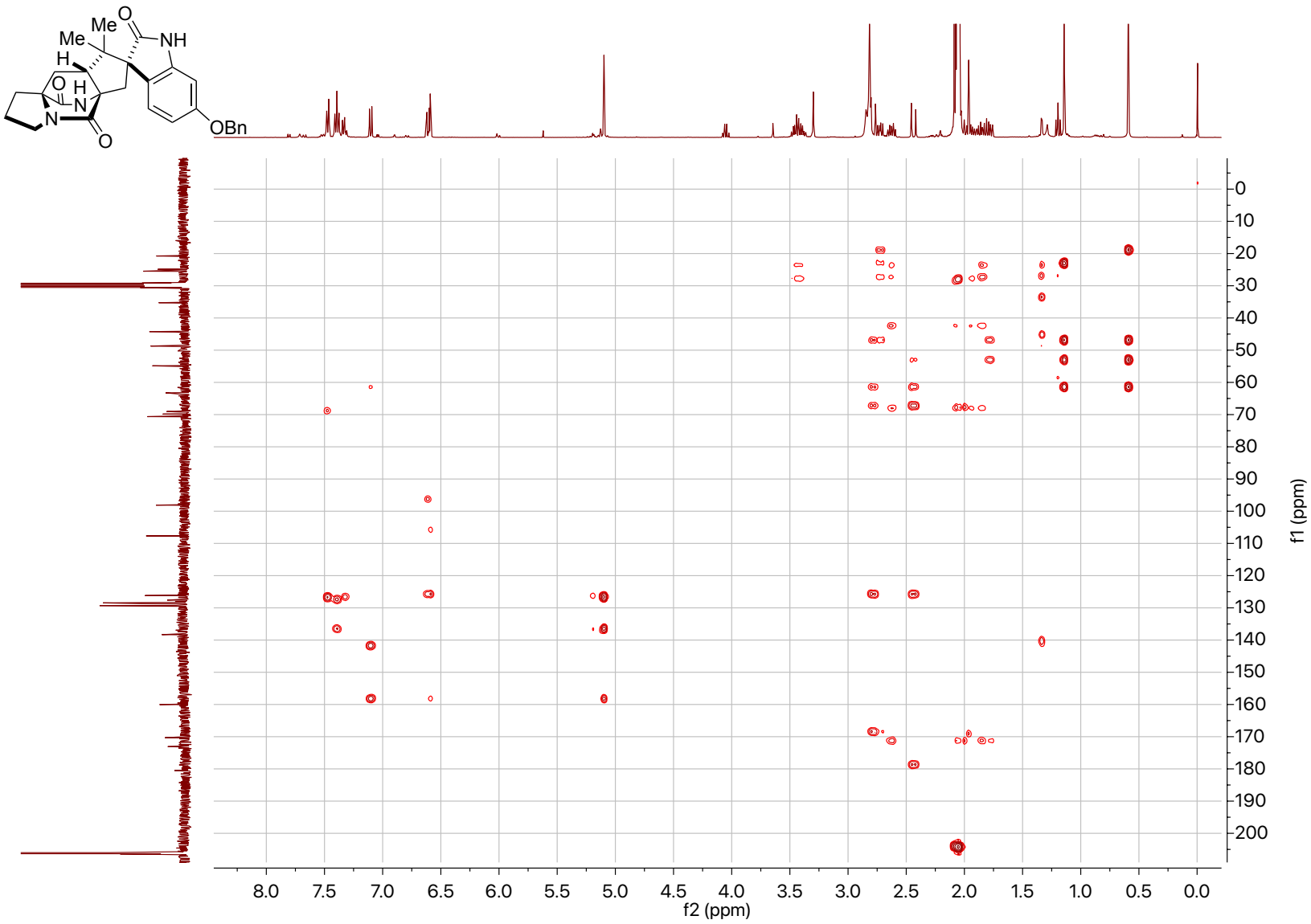

Figure A43. HSQC NMR Spectrum of compound **111** (Acetone).

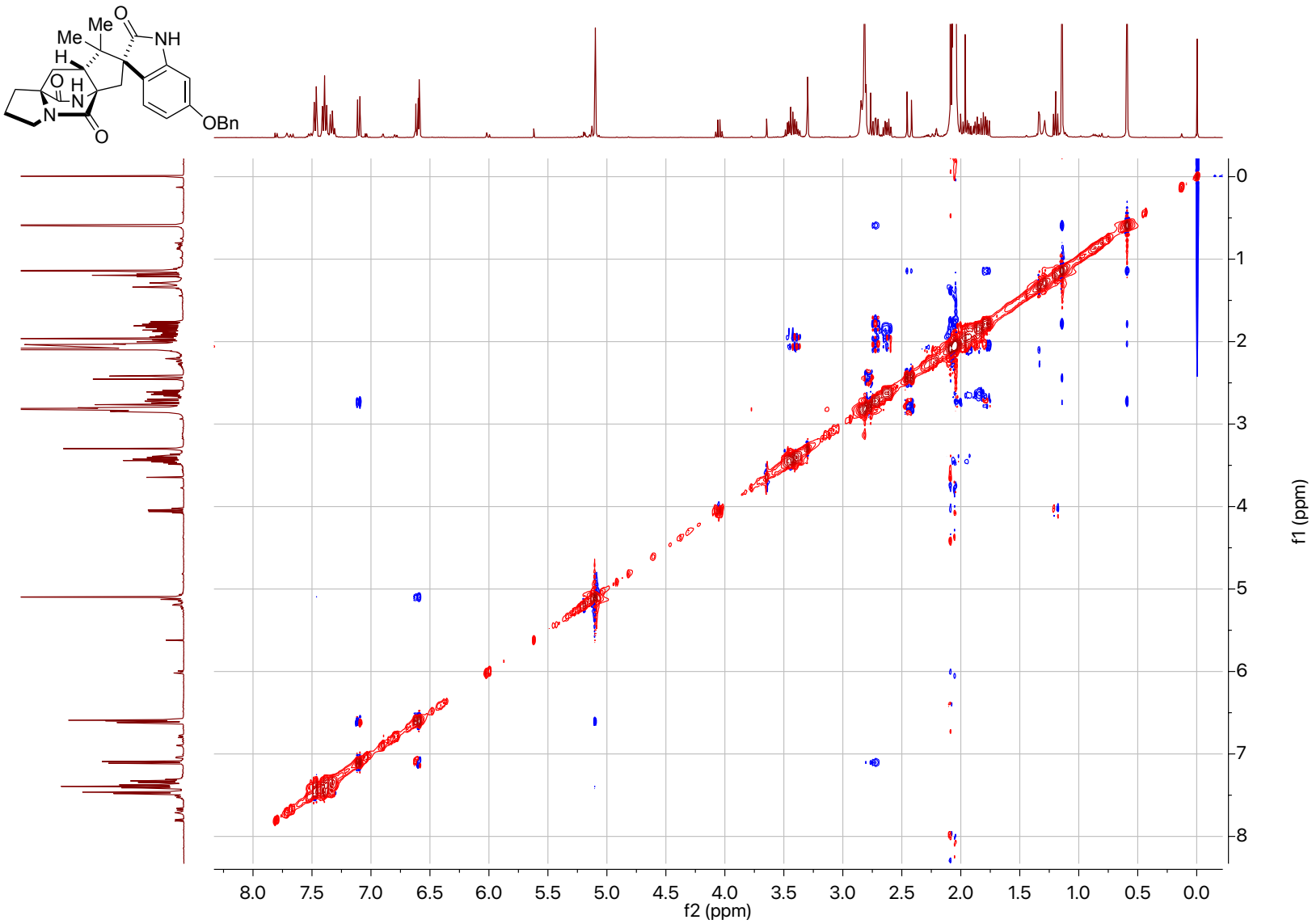

Figure A44. ROESY NMR Spectrum of compound **111** (Acetone).

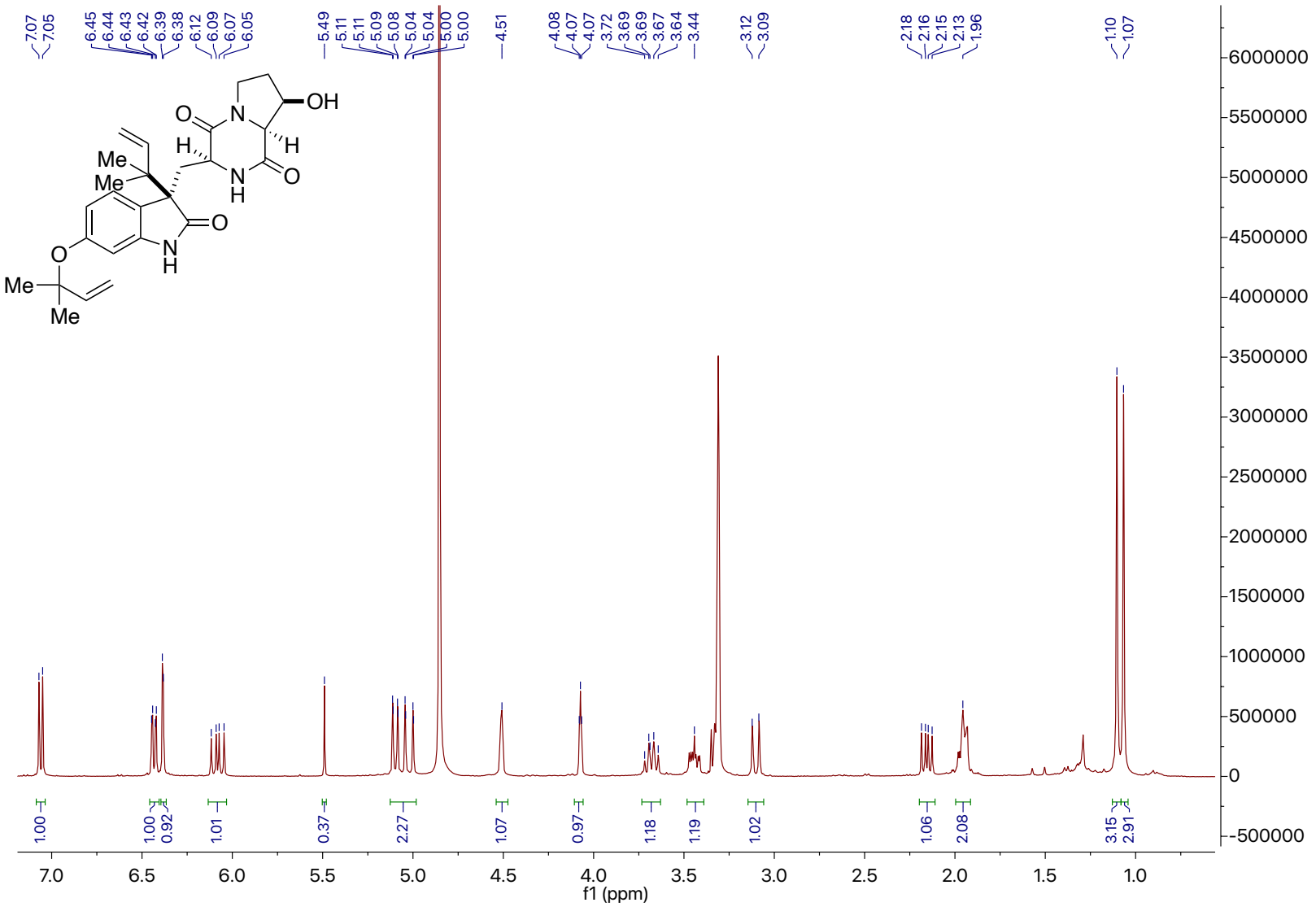

Figure A45. ^{1}H NMR Spectrum of compound **112** (MeOD).

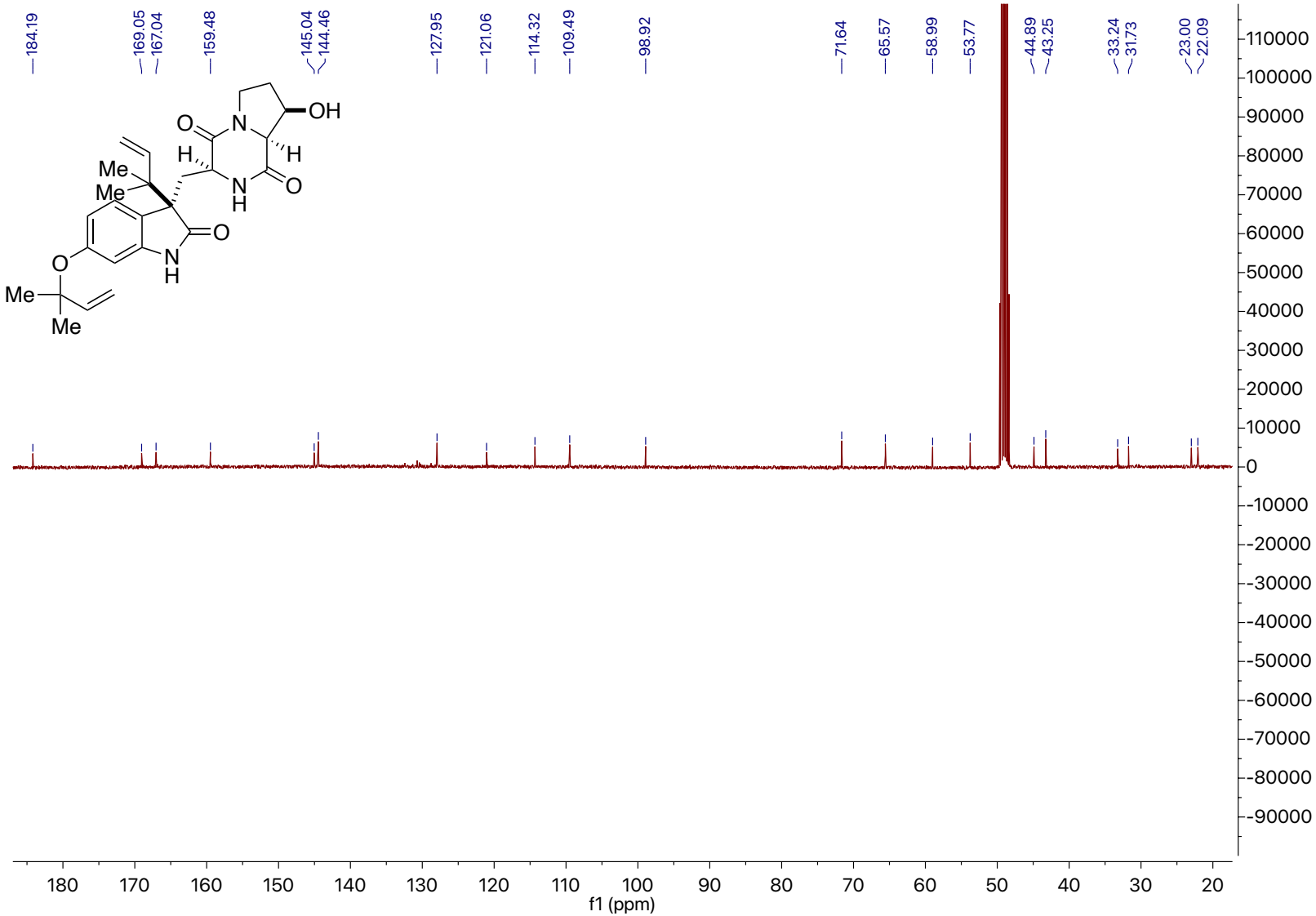

Figure A46. ^{13}C NMR Spectrum of compound **112** (MeOD).

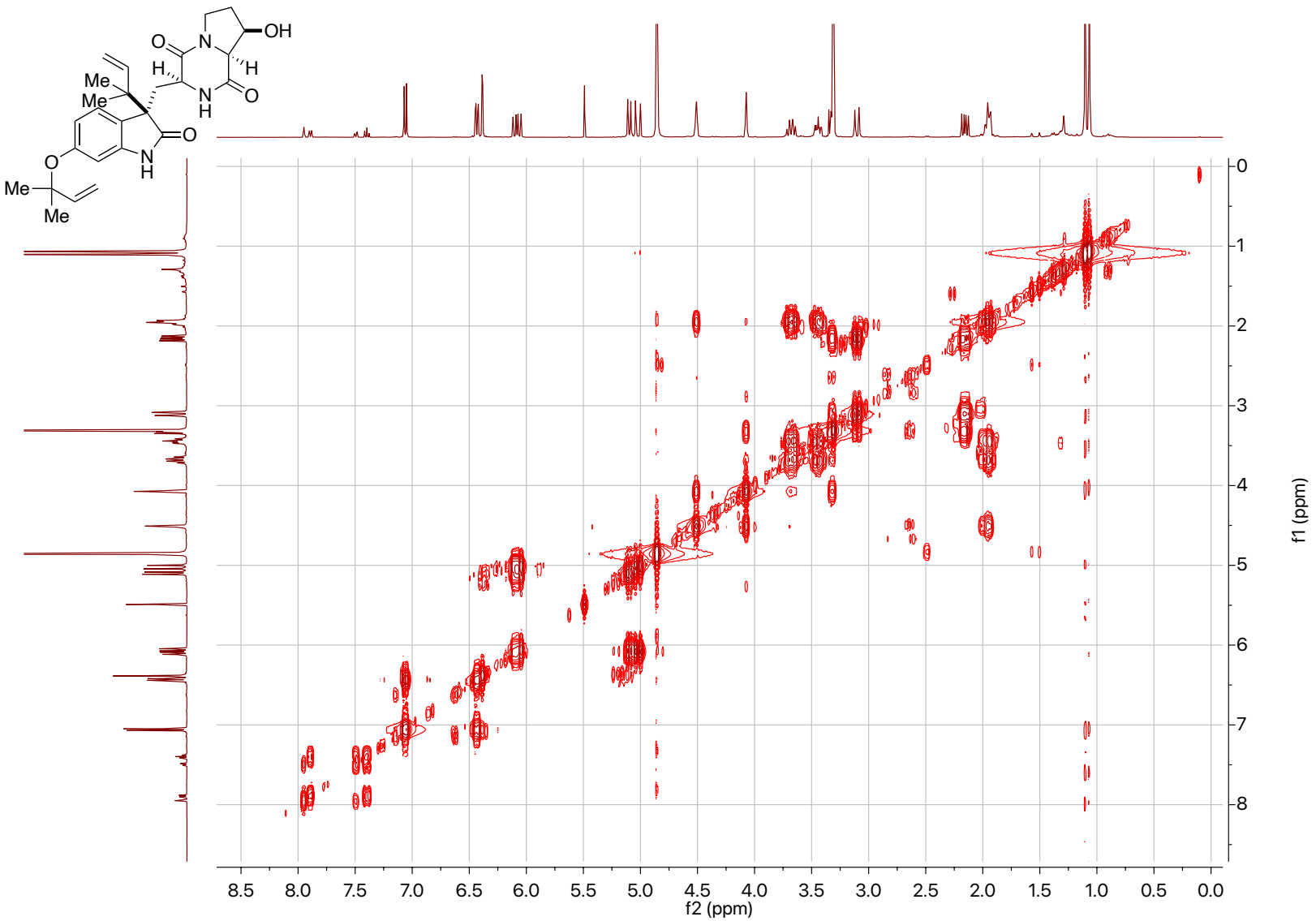

Figure A47. COSY NMR Spectrum of compound **112** (MeOD).

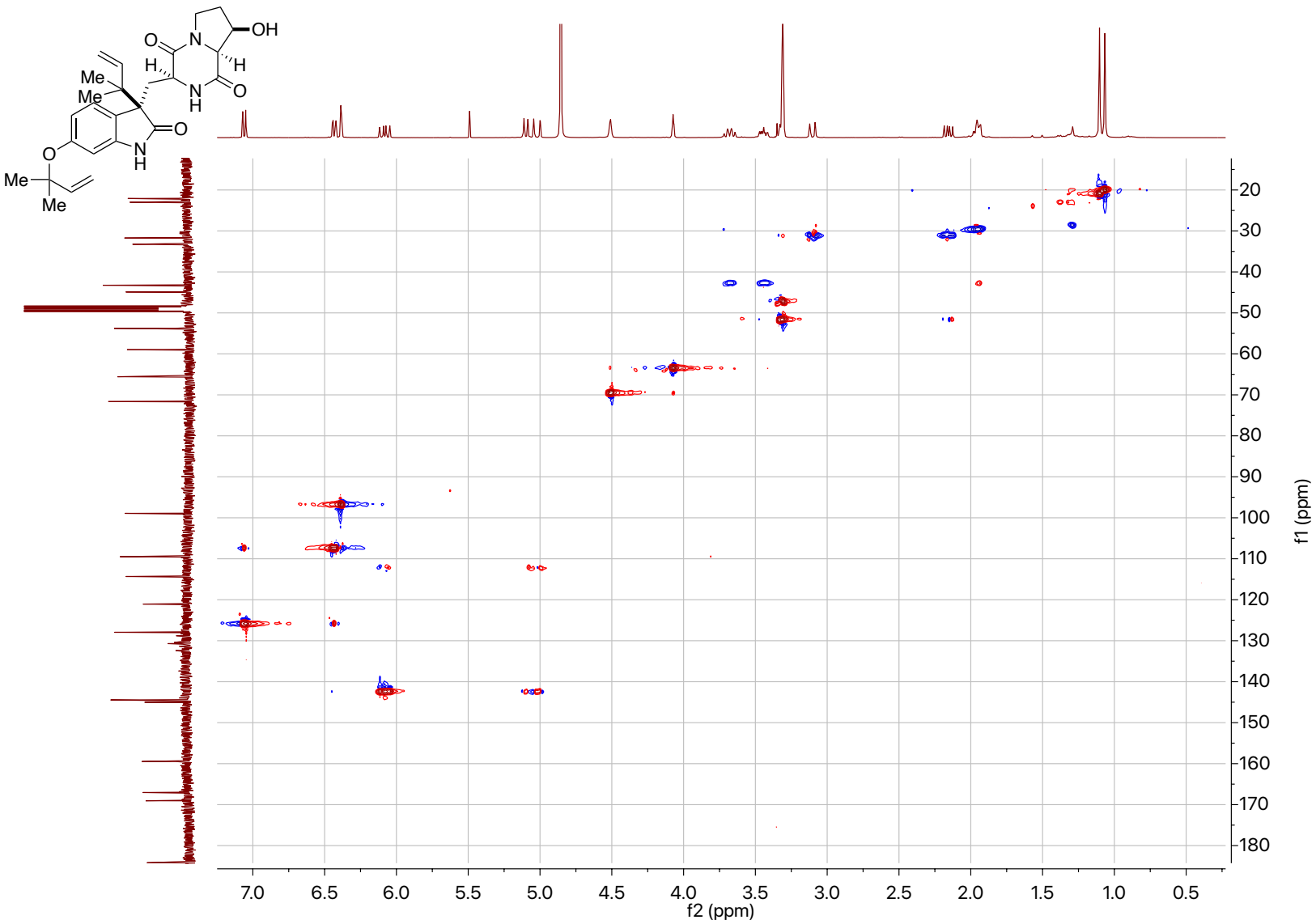

Figure A48. HSQC NMR Spectrum of compound **112** (MeOD).

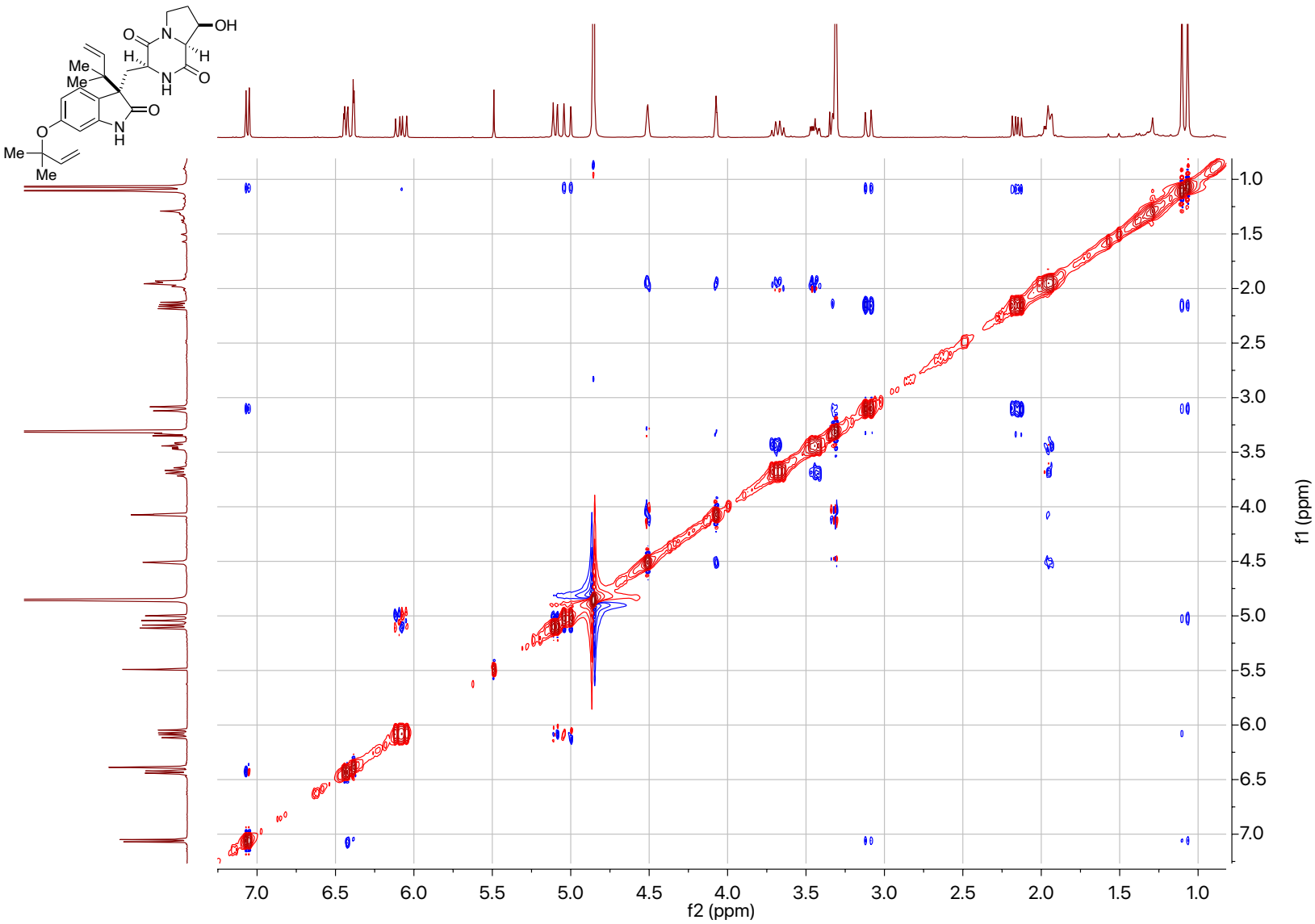

Figure A49. ROESY NMR Spectrum of compound **112** (MeOD).

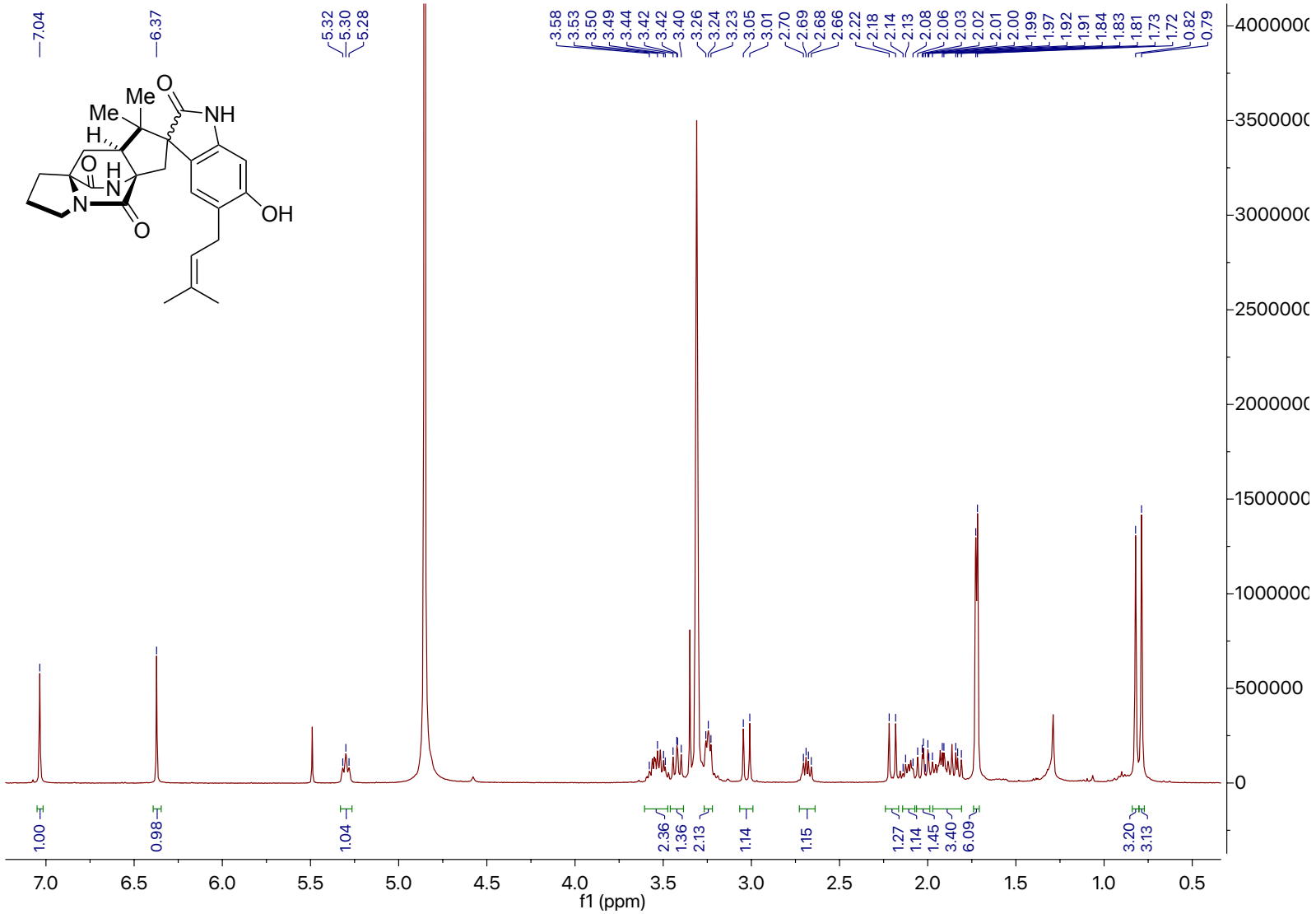

Figure A50. [1]H NMR Spectrum of compound **118** (MeOD).

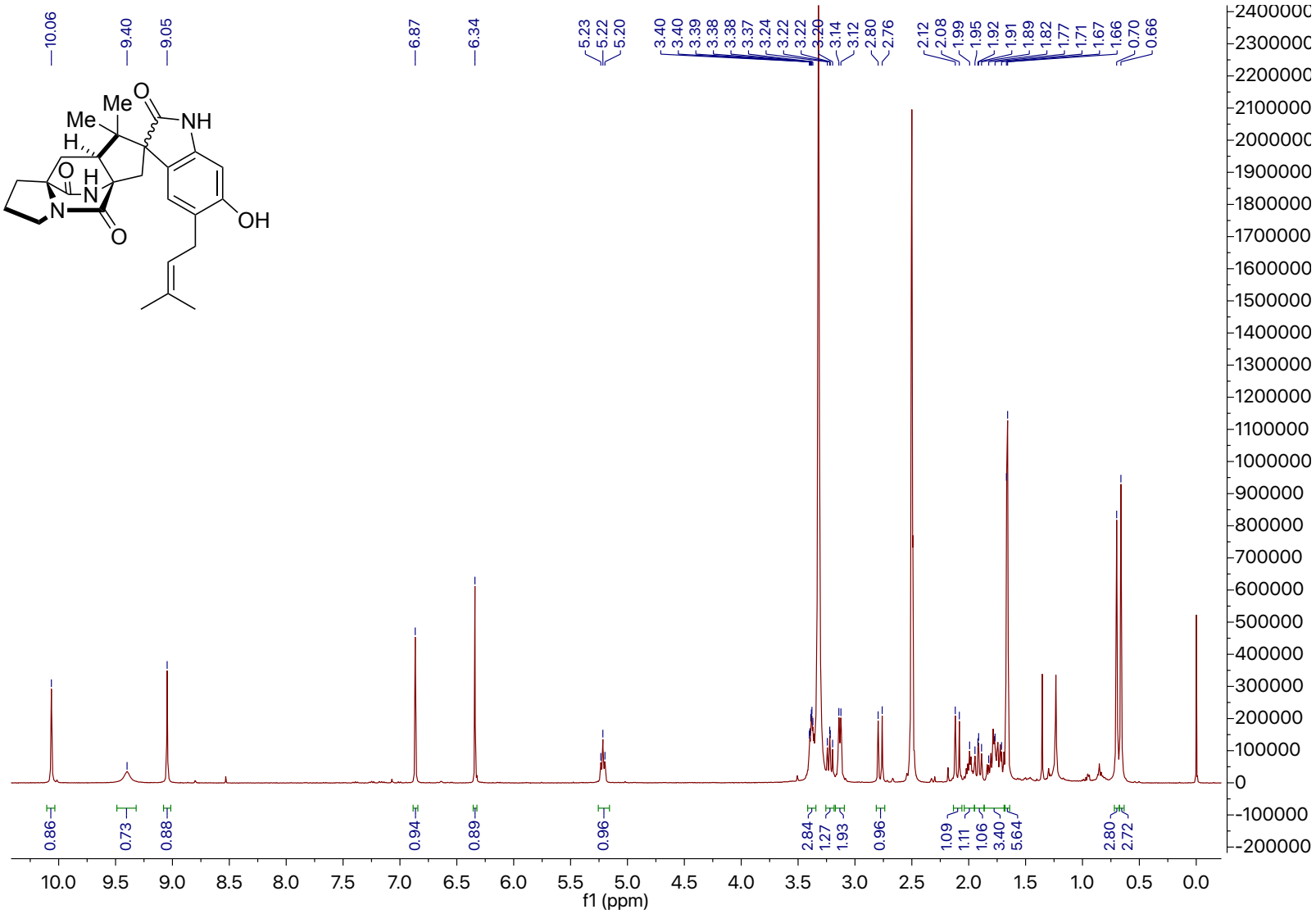

Figure A51. ^{1}H NMR Spectrum of compound **118** (DMSO).

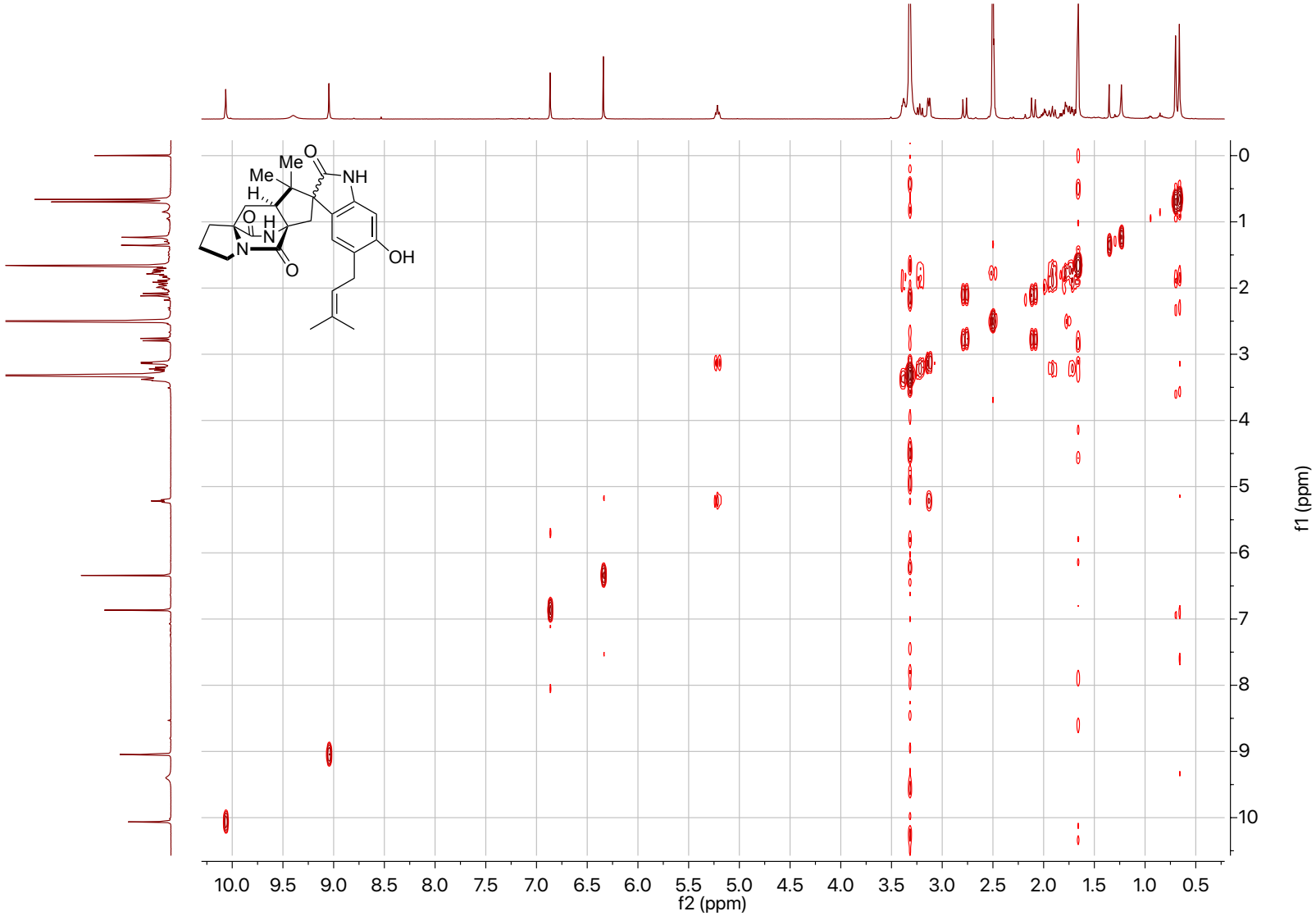

Figure A52. COSY NMR Spectrum of compound **118** (DMSO).

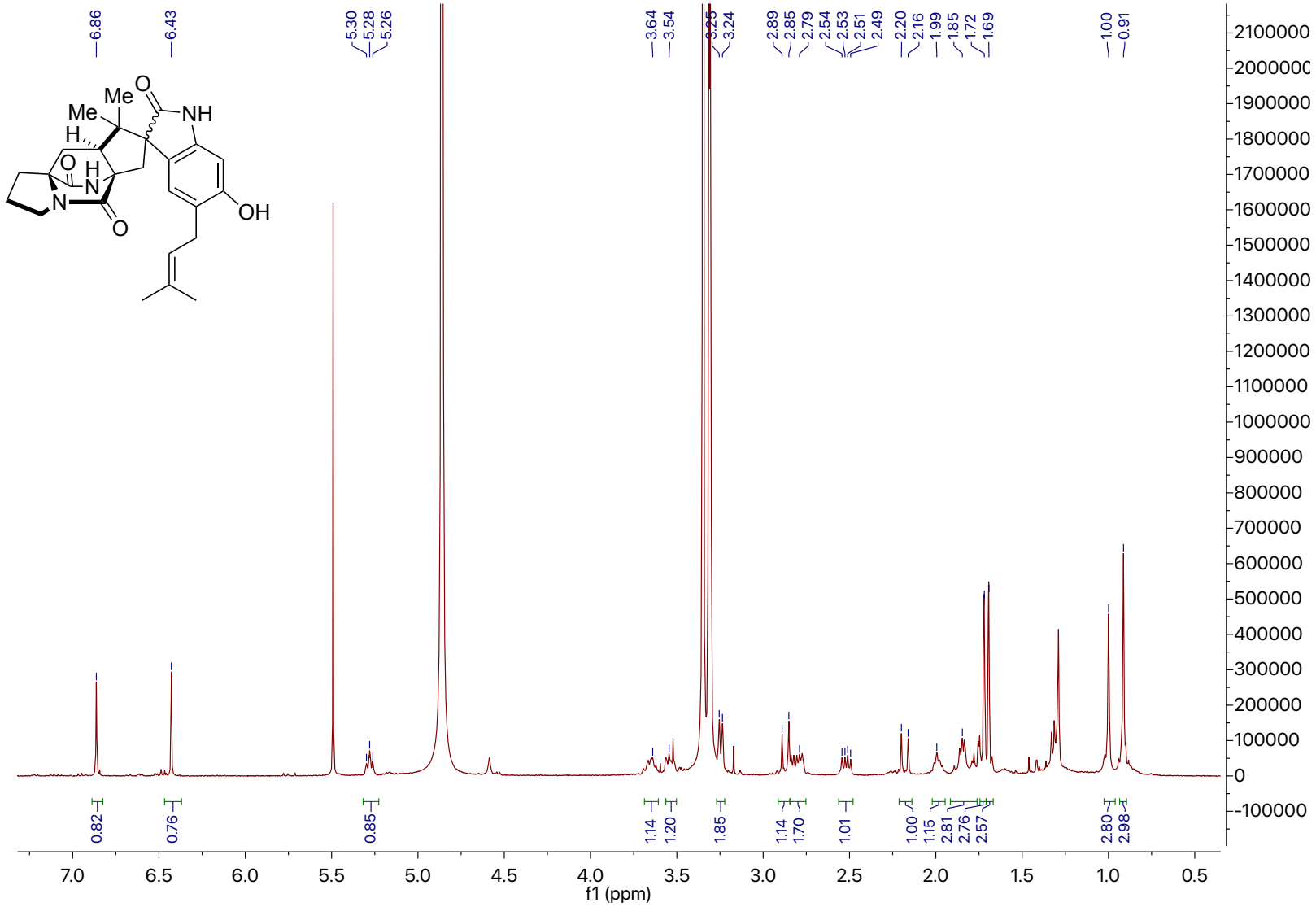

Figure A53. ^{1}H NMR Spectrum of compound **118** (MeOD).

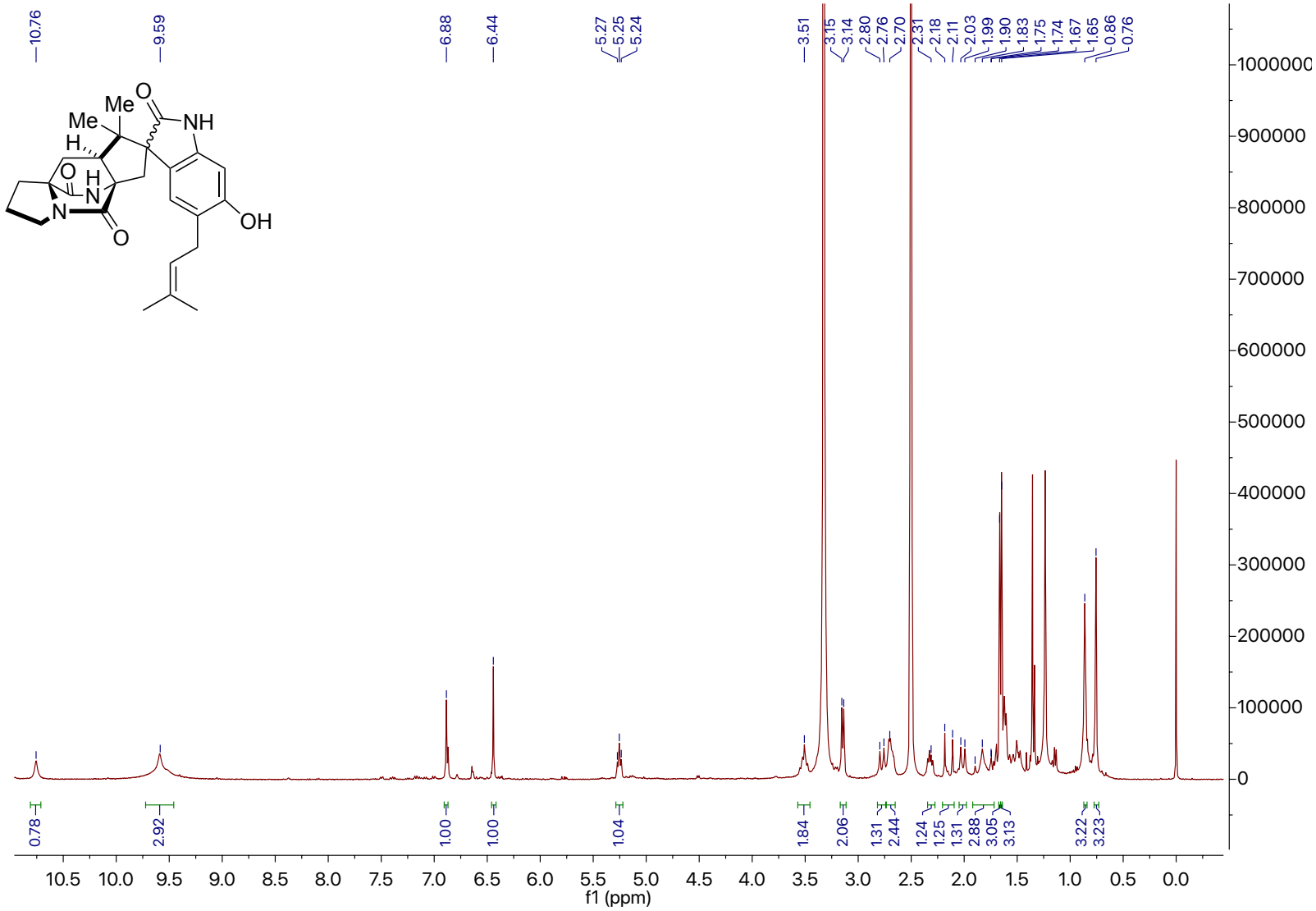

Figure A54. ^{1}H NMR Spectrum of compound **118** (DMSO).

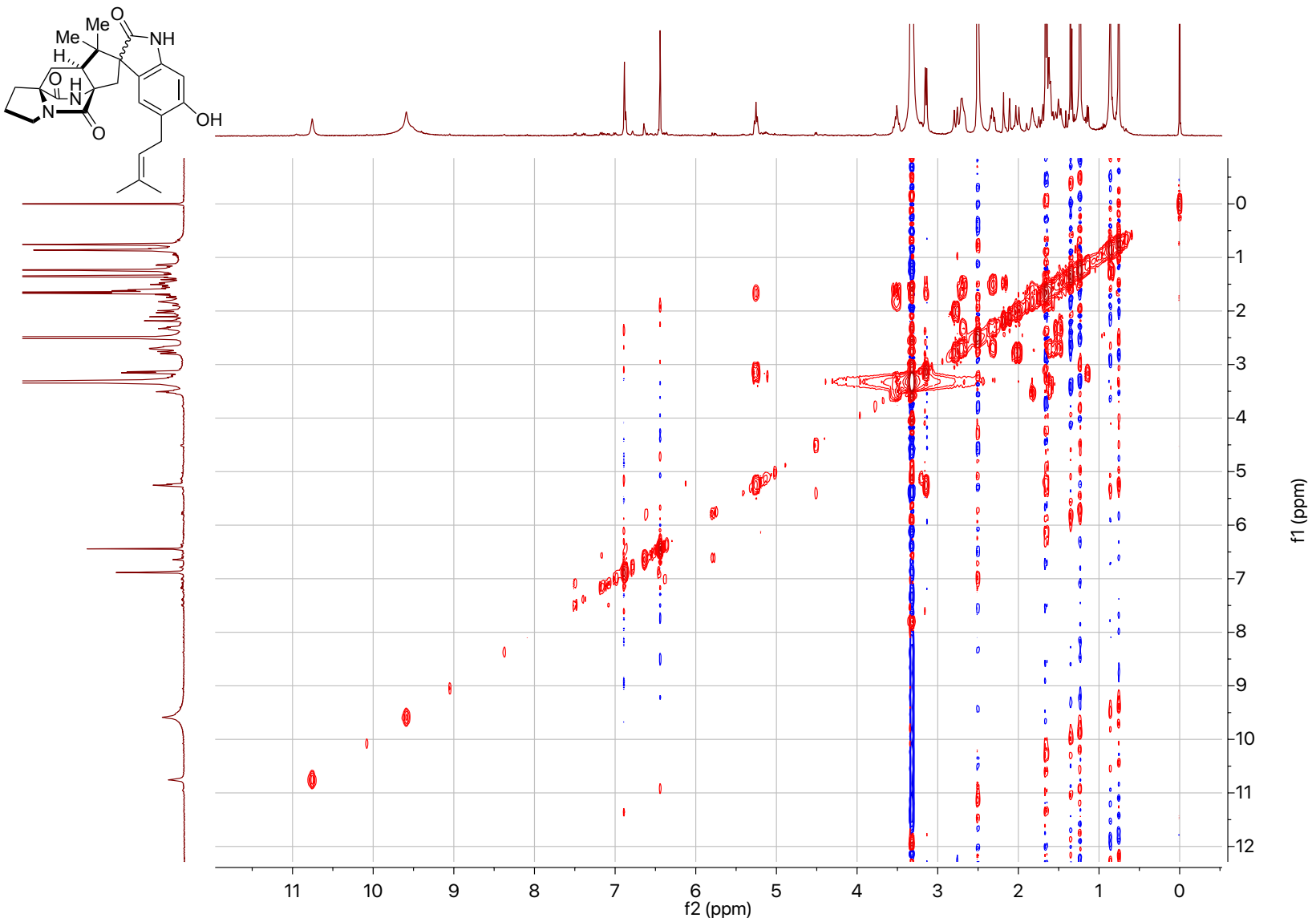

Figure A55. COSY NMR Spectrum of compound **118** (DMSO).

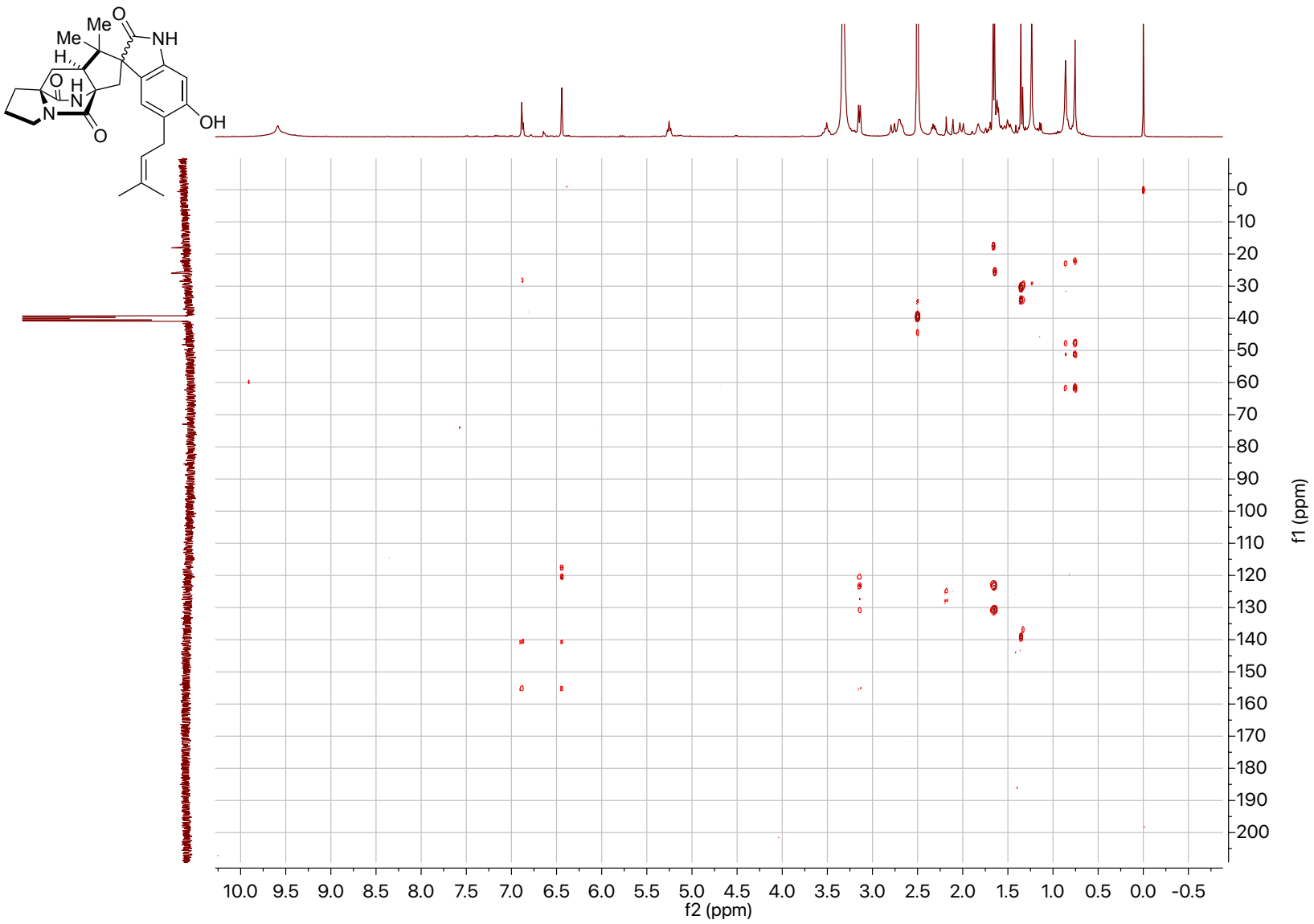

Figure A56. HSQC NMR Spectrum of compound **118** (DMSO).

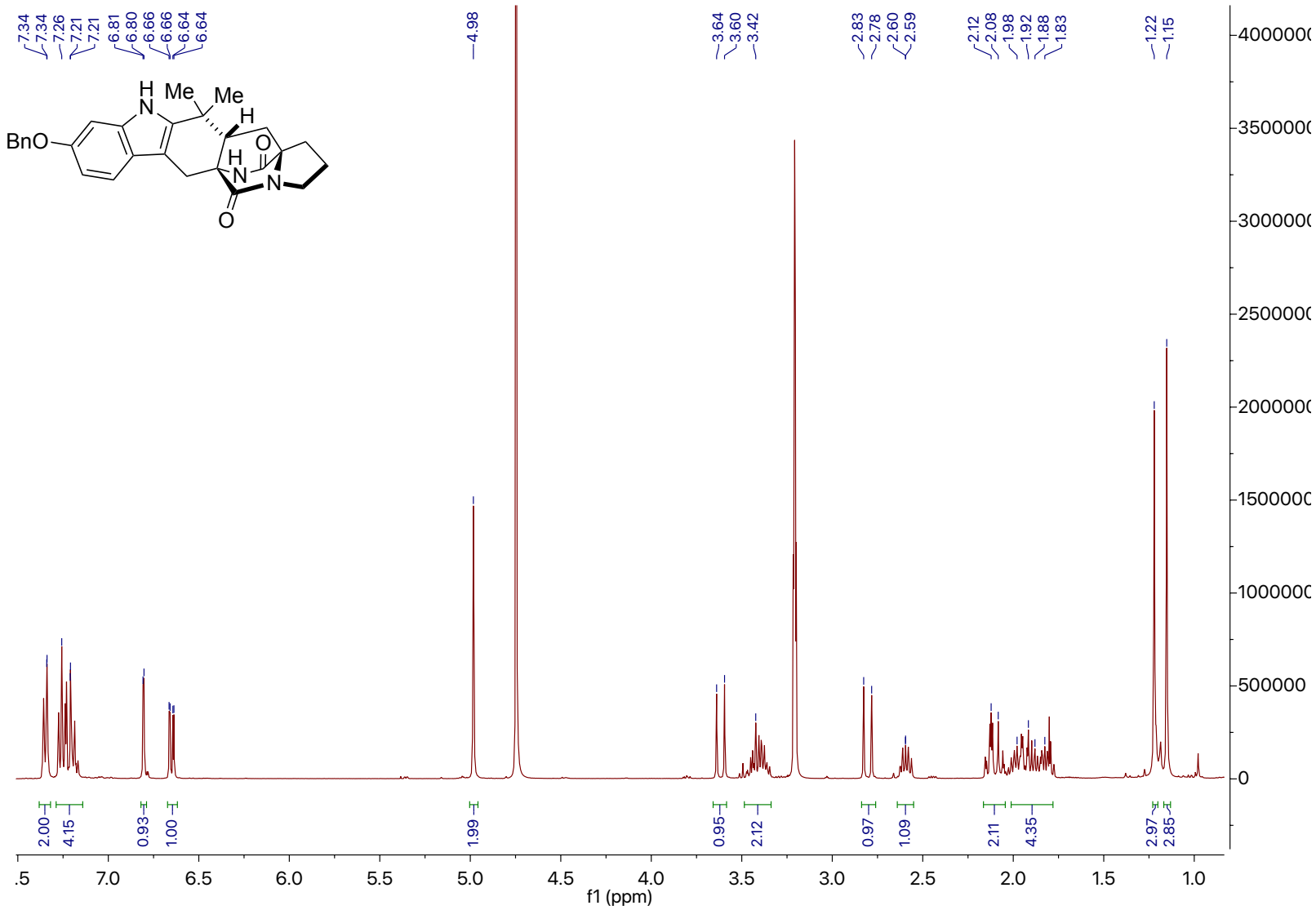

Figure A57. [1]H NMR Spectrum of compound **86** (MeOD).

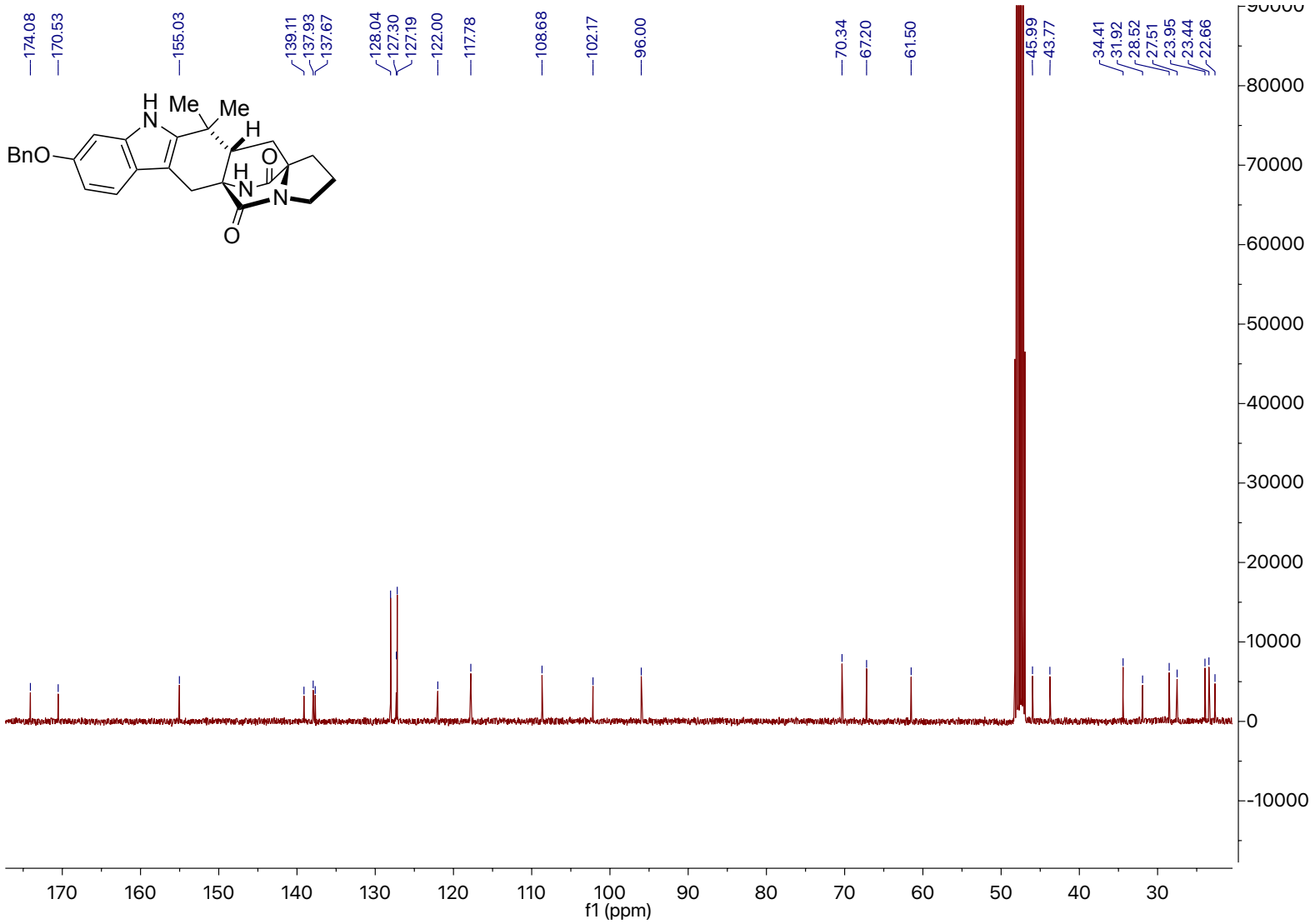

Figure A58. ^{13}C NMR Spectrum of compound **86**.

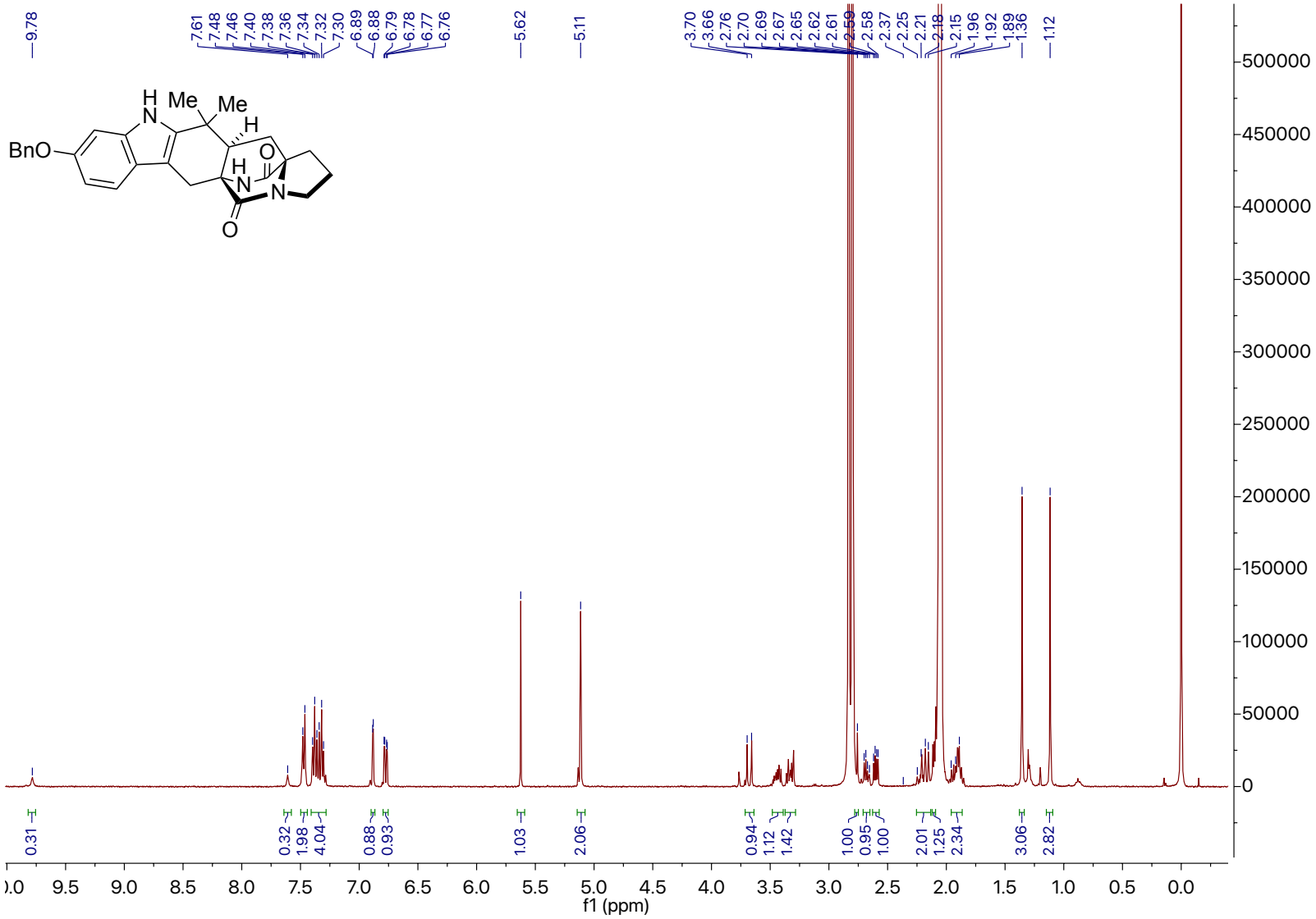

Figure A59. ^{1}H NMR Spectrum of compound **85** (Acetone).

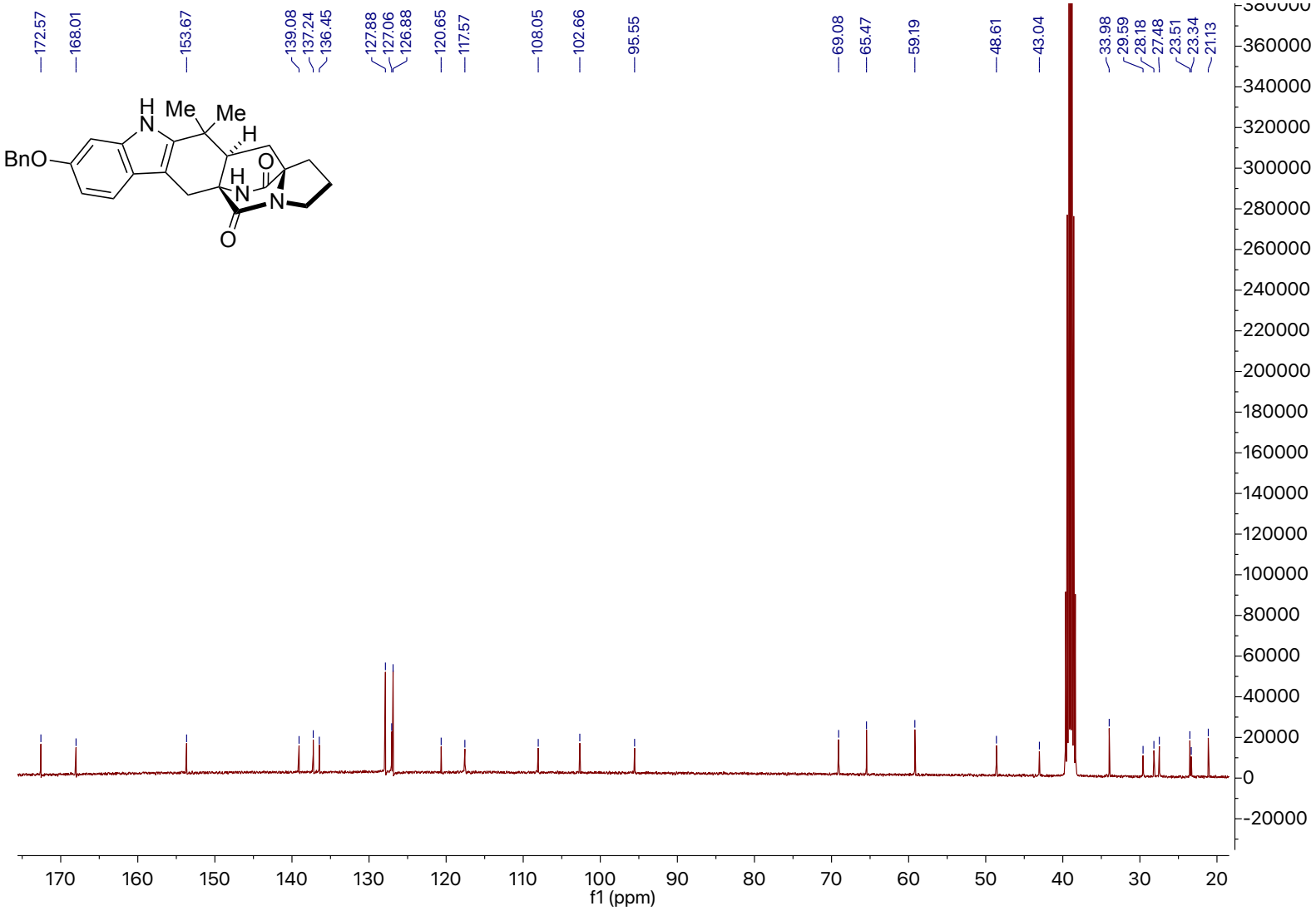

Figure A60. ^{13}C NMR Spectrum of compound **85** (DMSO).

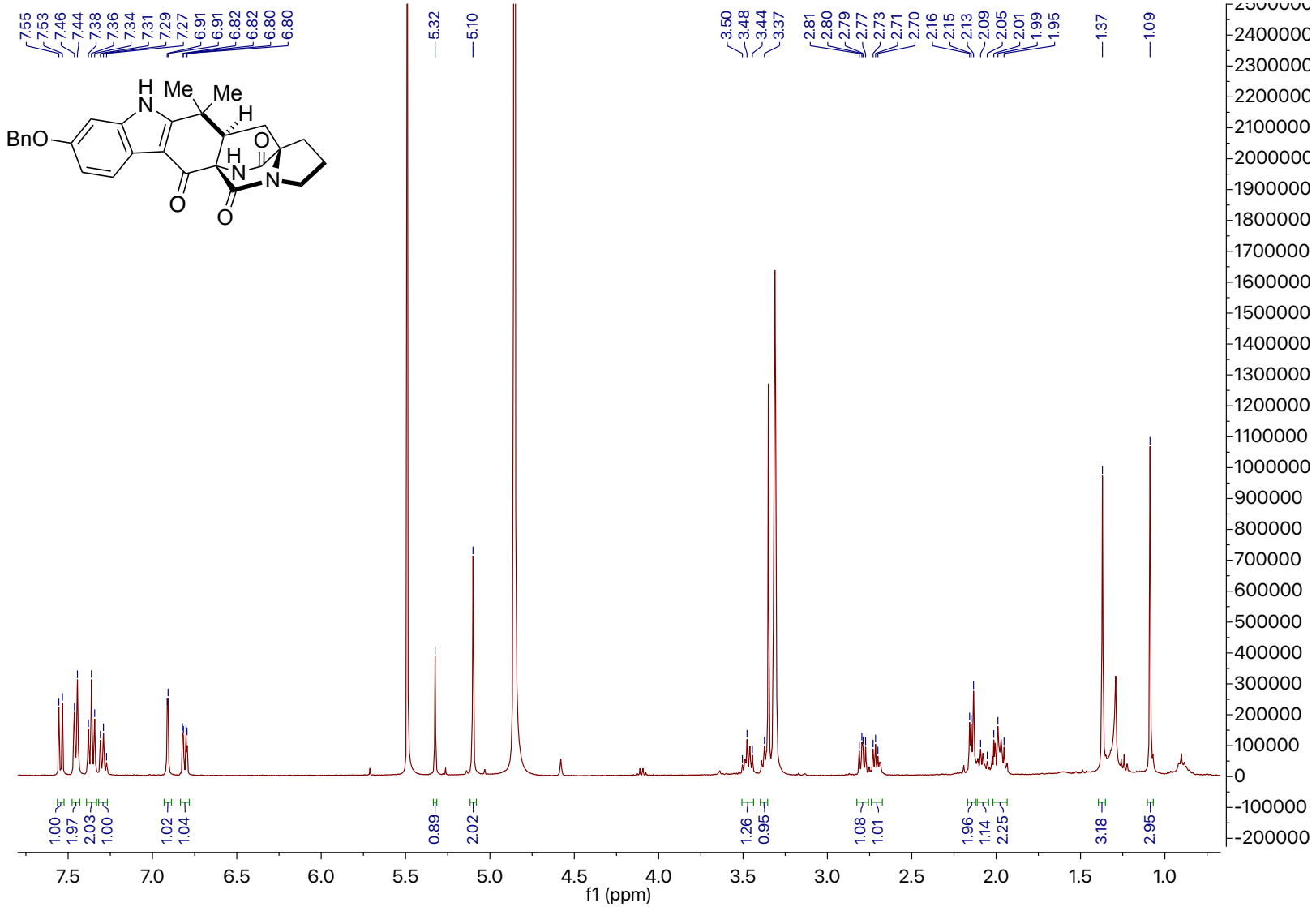

Figure A61. ^{1}H NMR Spectrum of compound **89** ($CDCl_3$).

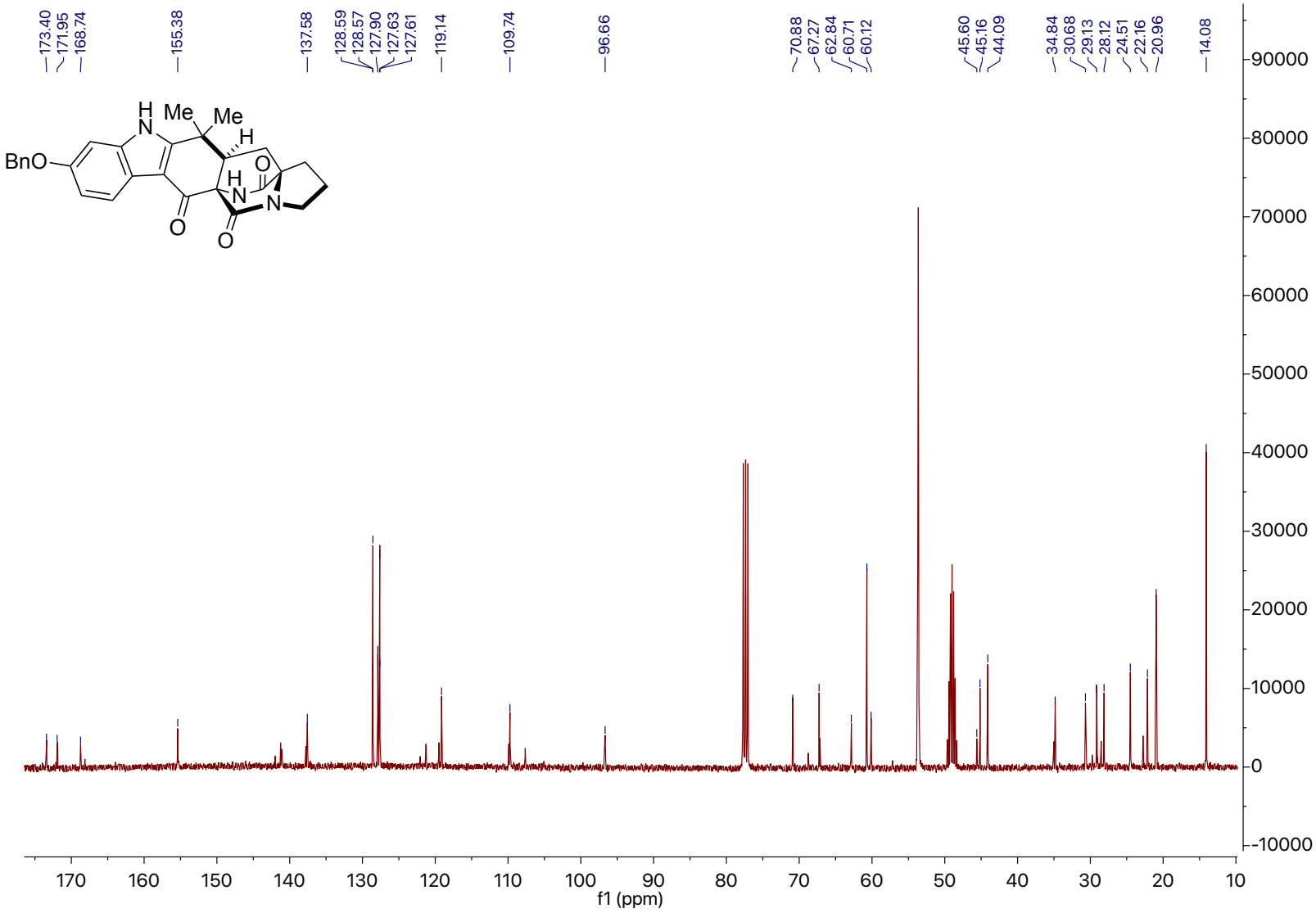

Figure A62. ^{13}C NMR Spectrum of compound **89** ($CDCl_3$).

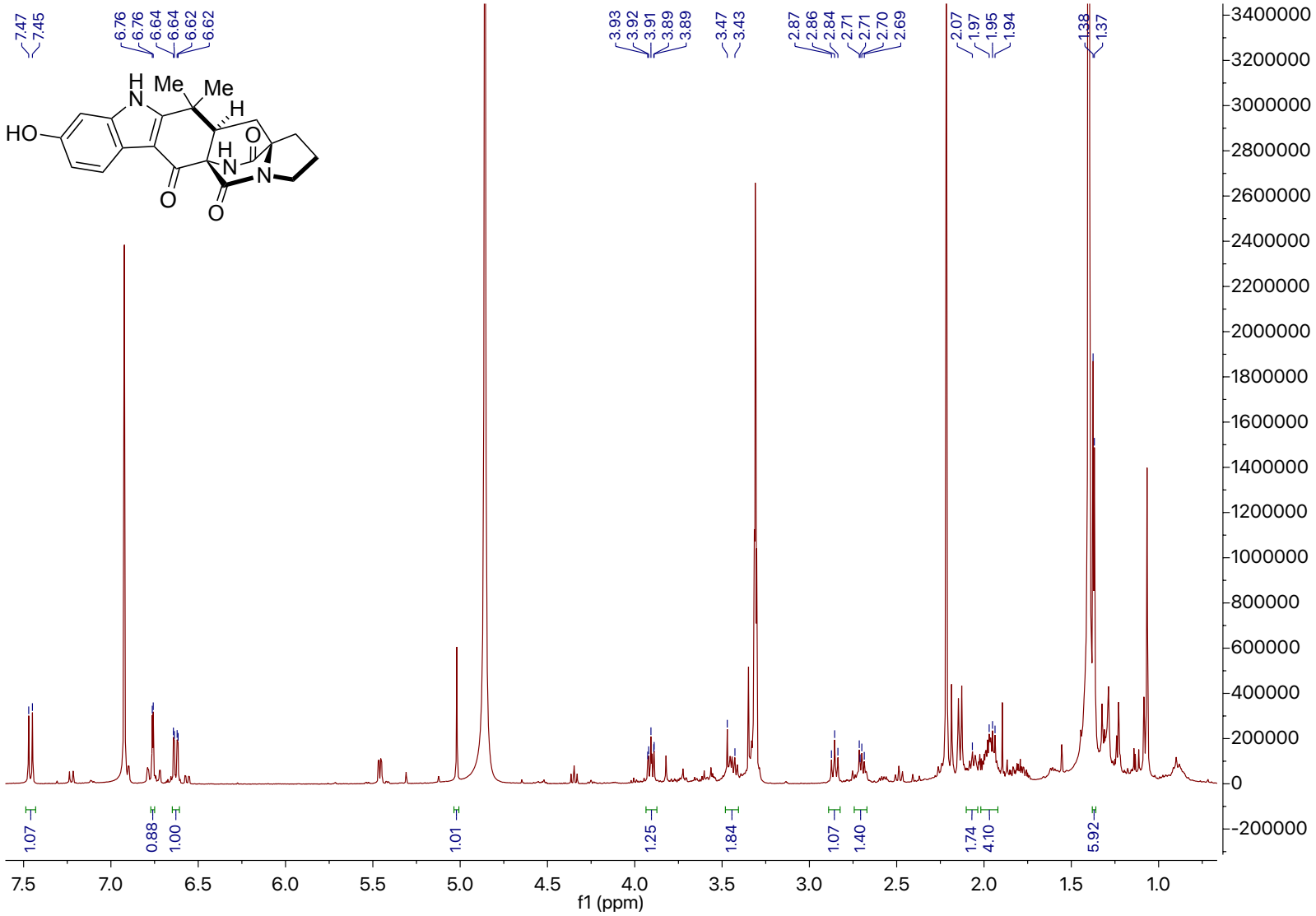

Figure A63. [1]H NMR Spectrum of compound **90** (MeOD).

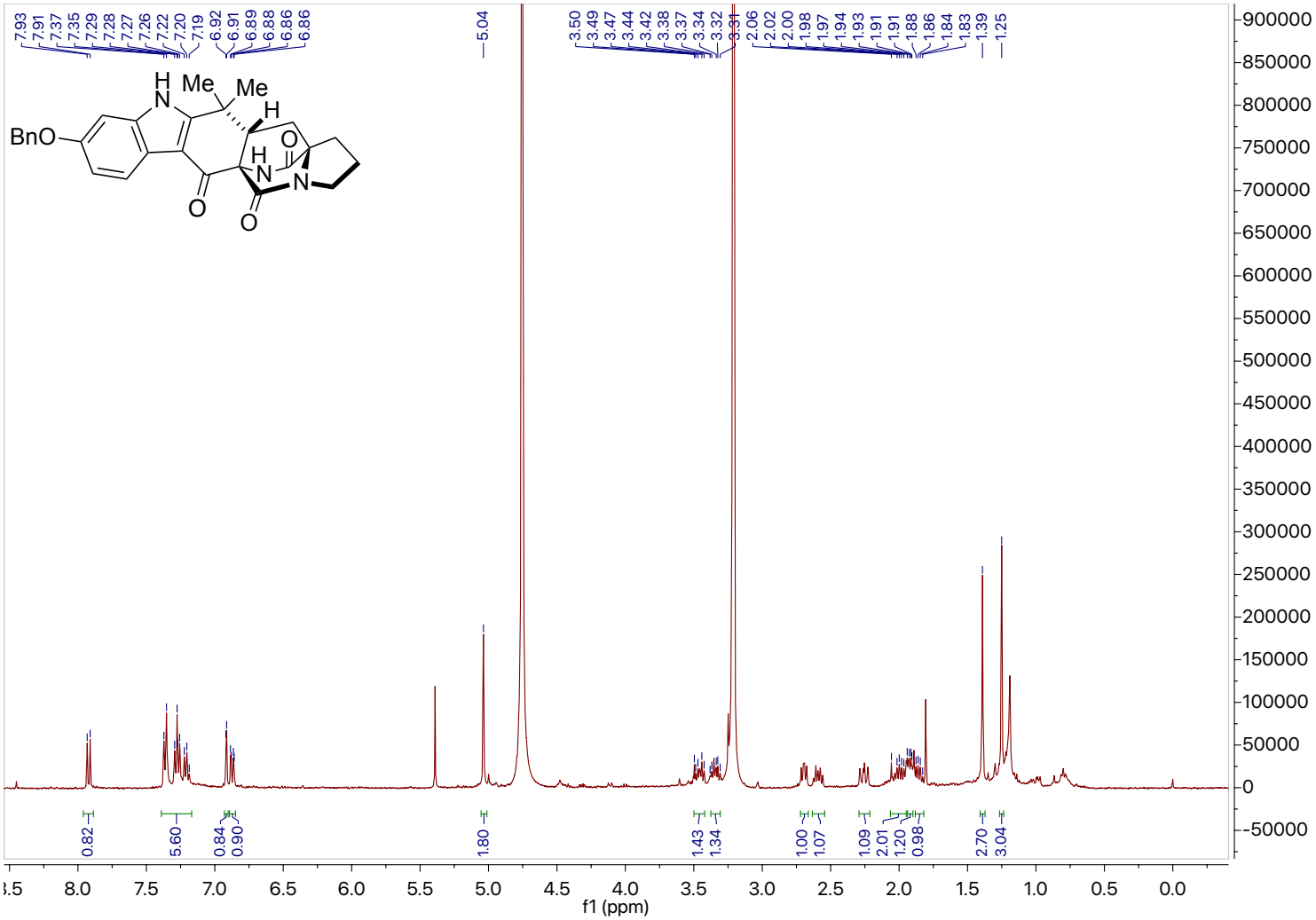

Figure A64. ^{1}H NMR Spectrum of compound **120** (MeOD).

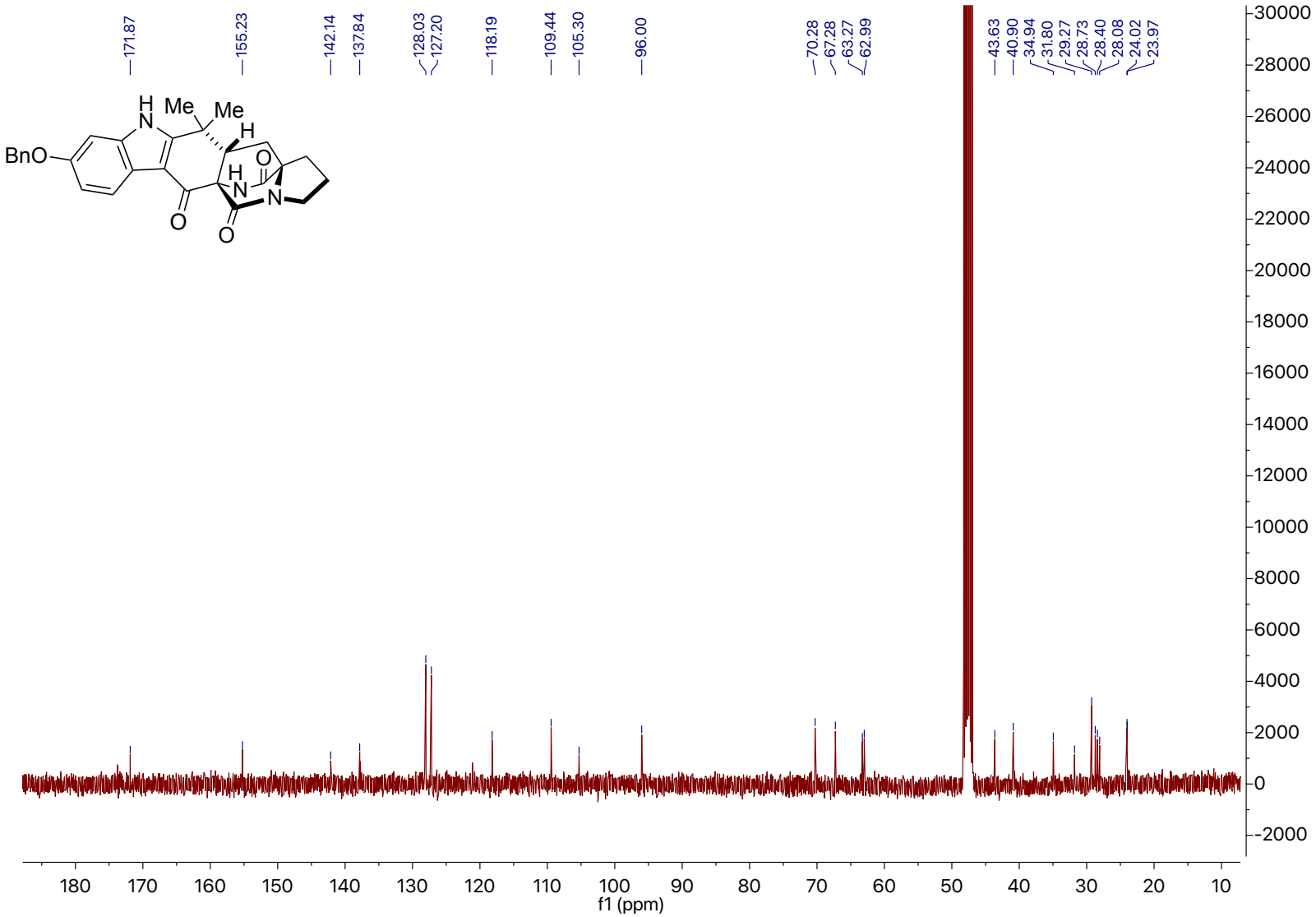

Figure A65. ^{13}C NMR Spectrum of compound **120** (MeOD).

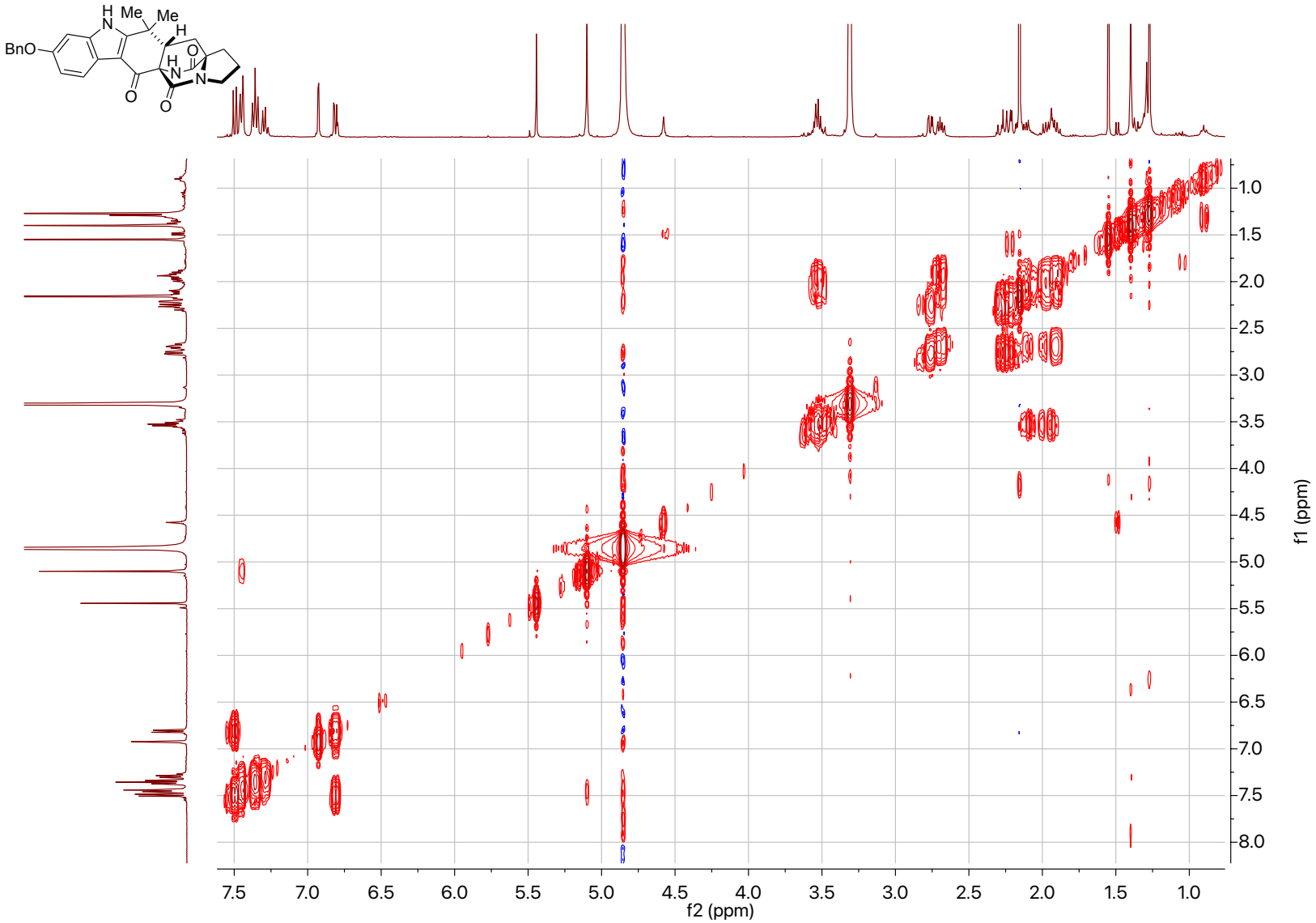

Figure A66. COSY NMR Spectrum of compound **120**.

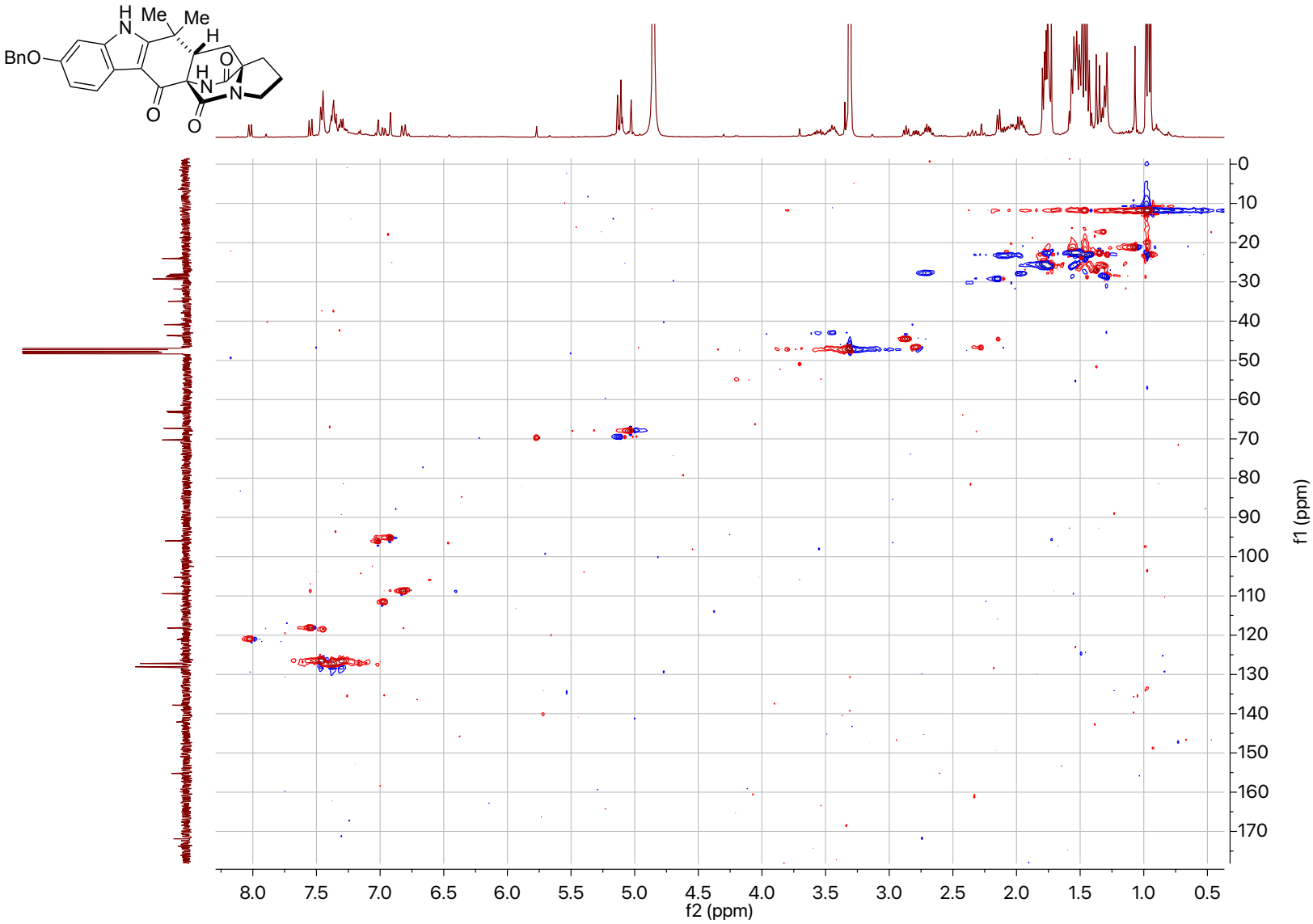

Figure A67. HSQC NMR Spectrum of compound **120**.

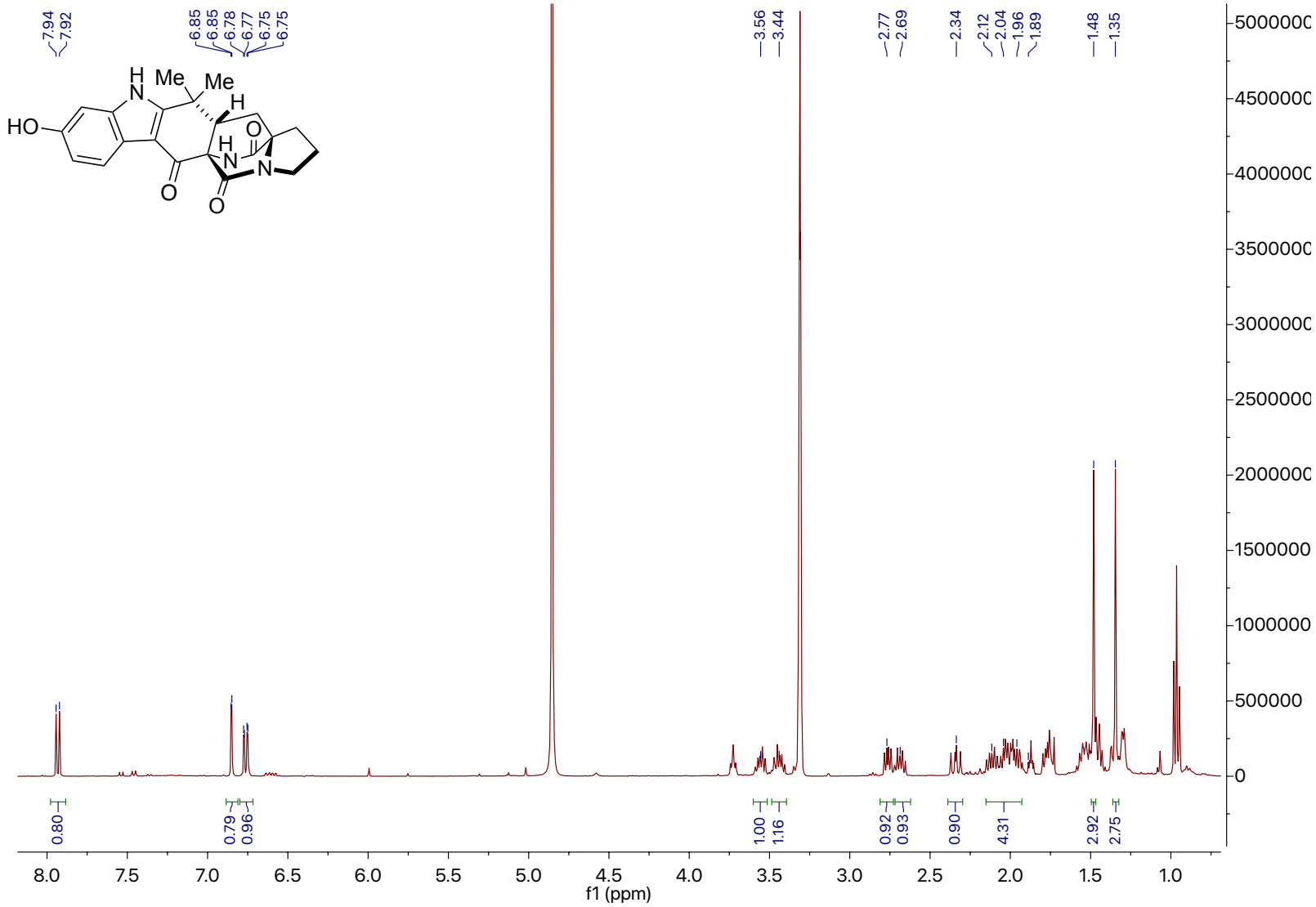

Figure A68. ^{1}H NMR Spectrum of compound **121** (MeOD).

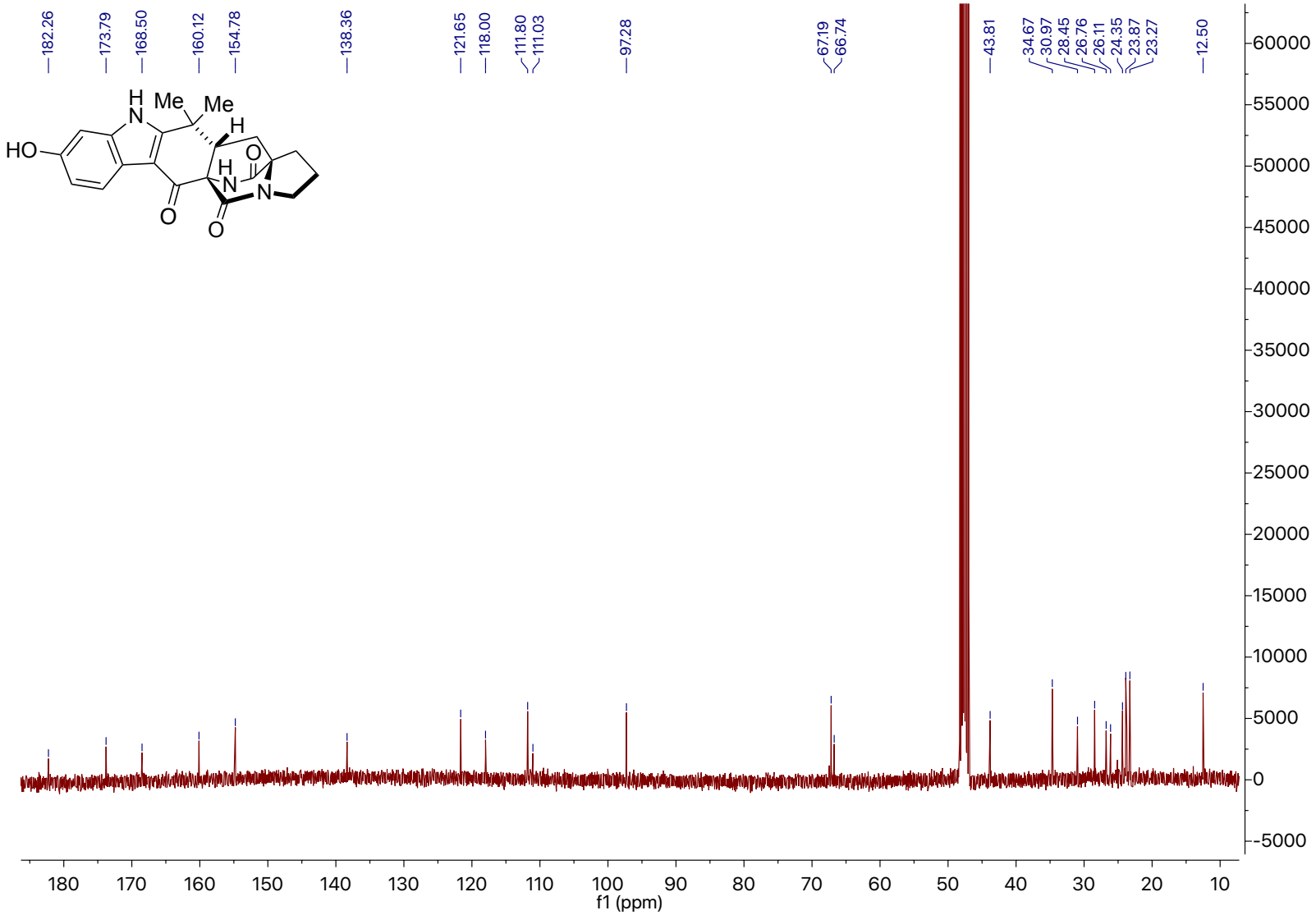

Figure A69. ^{13}C NMR Spectrum of compound **121** (MeOD).

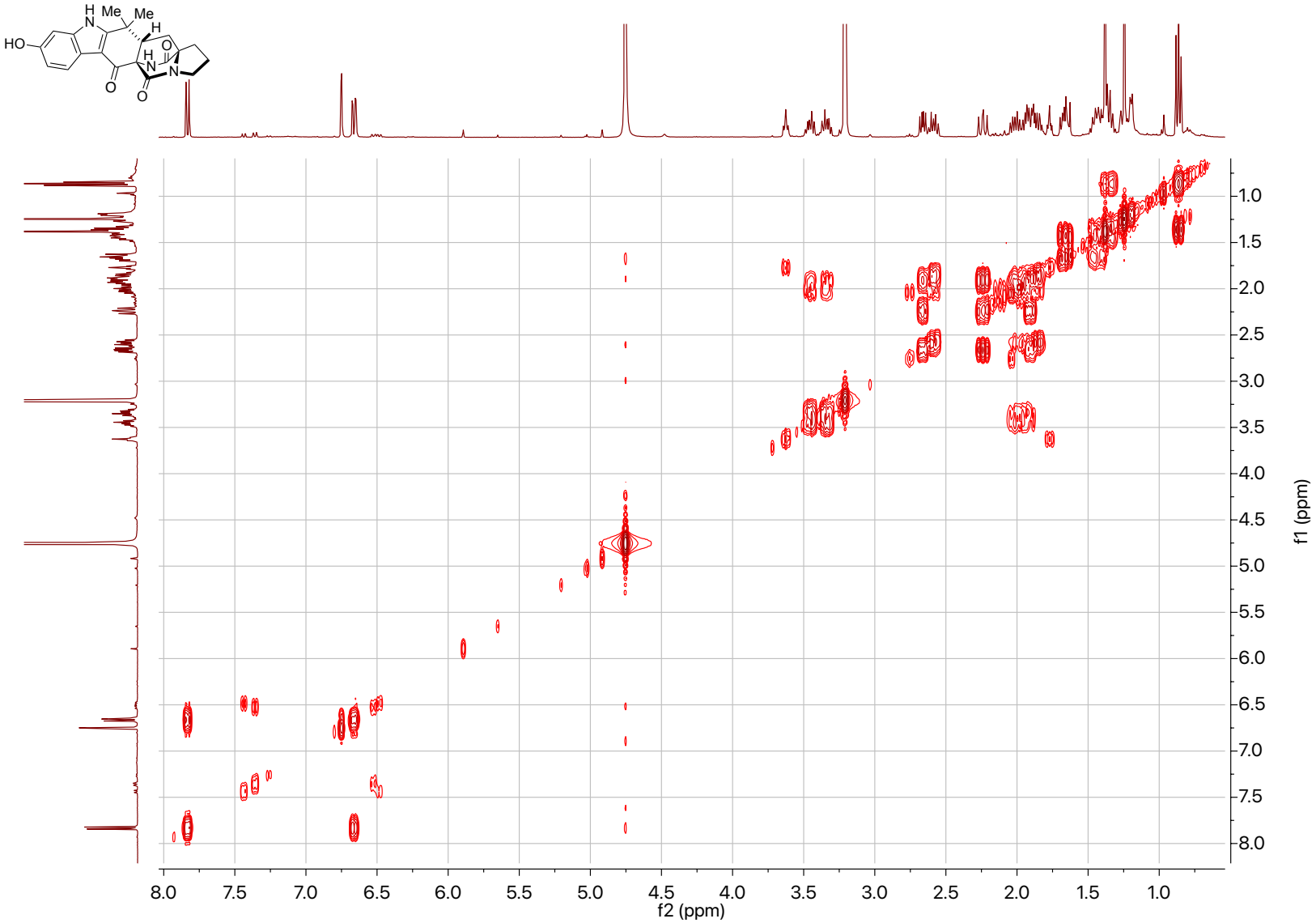

Figure A70. COSY NMR Spectrum of compound **121** (MeOD).

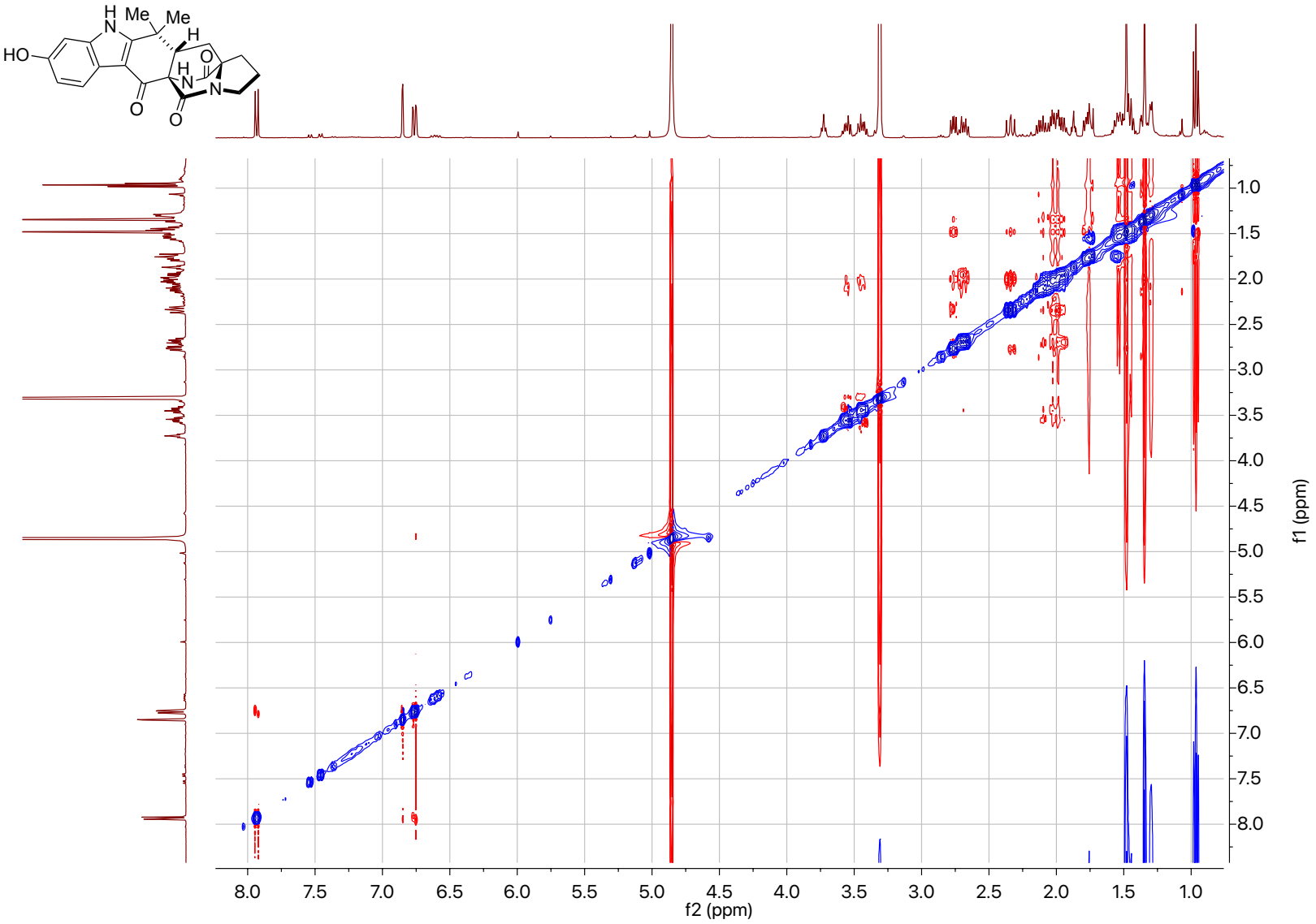

Figure A71. ROESY NMR Spectrum of compound **121** (MeOD).

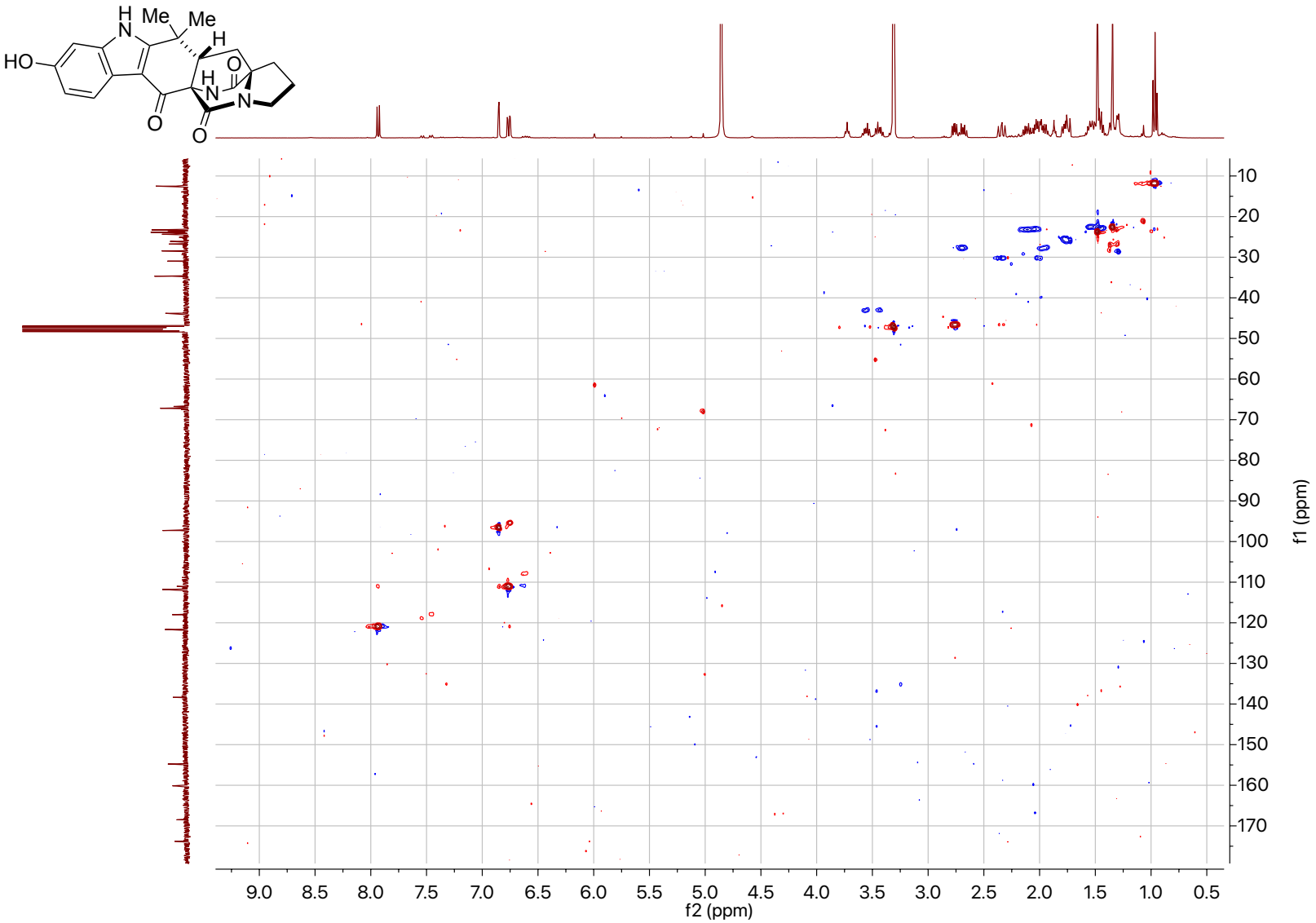

Figure A72. HSQC NMR Spectrum of compound **121** (MeOD).

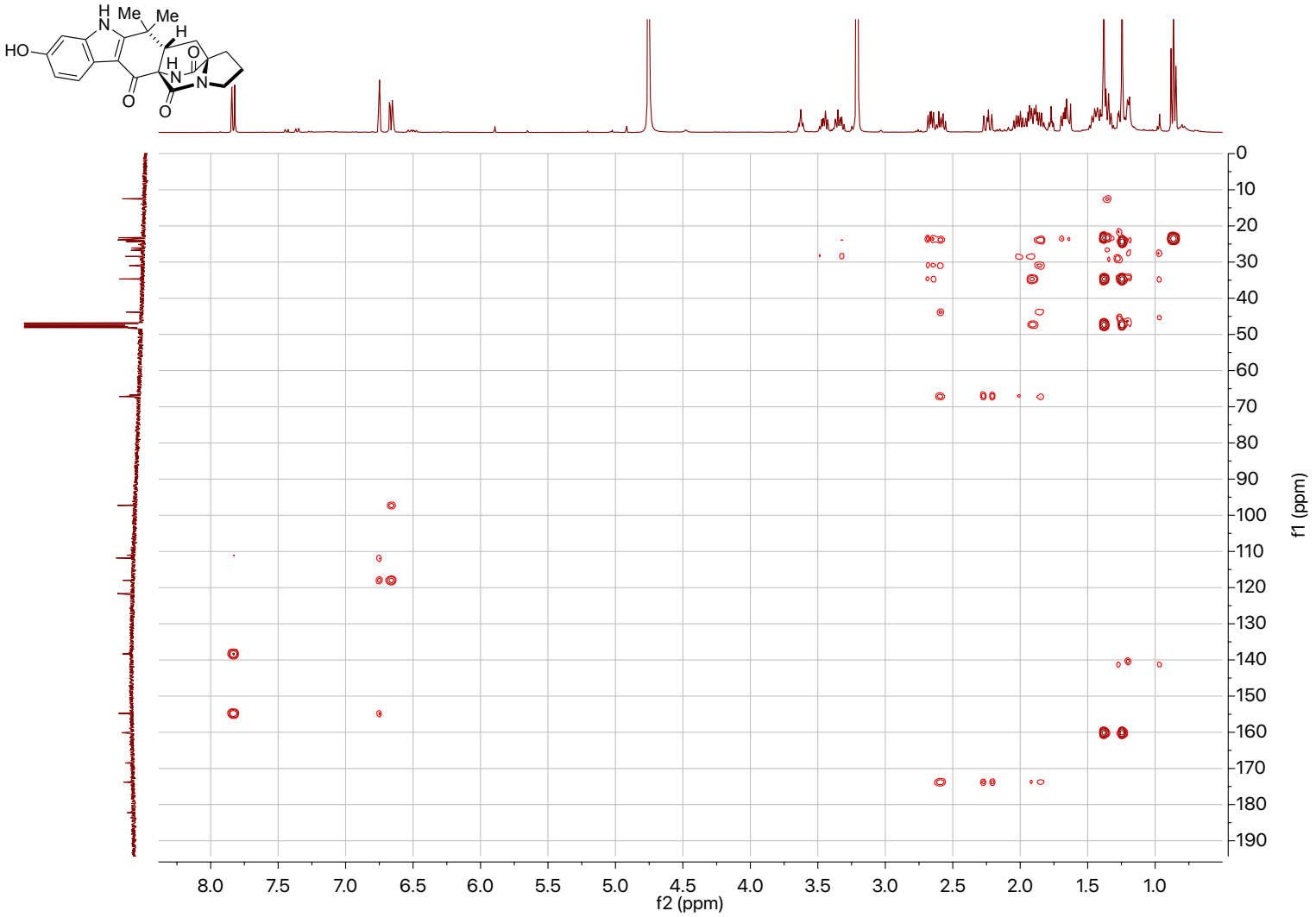

Figure A73. HMBC NMR Spectrum of compound **121** (MeOD).

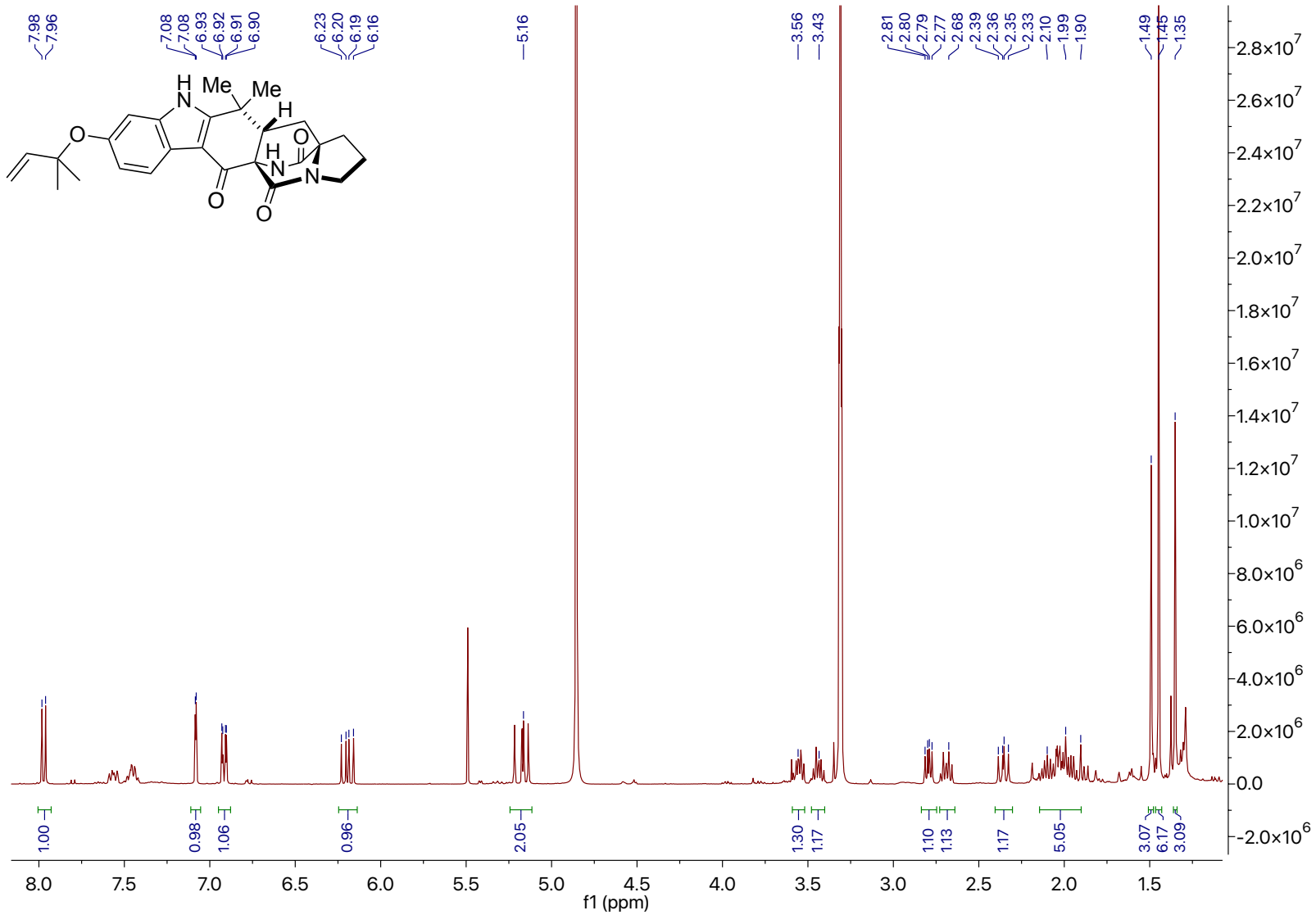

Figure A74. ^{1}H NMR Spectrum of compound **122** (MeOD).

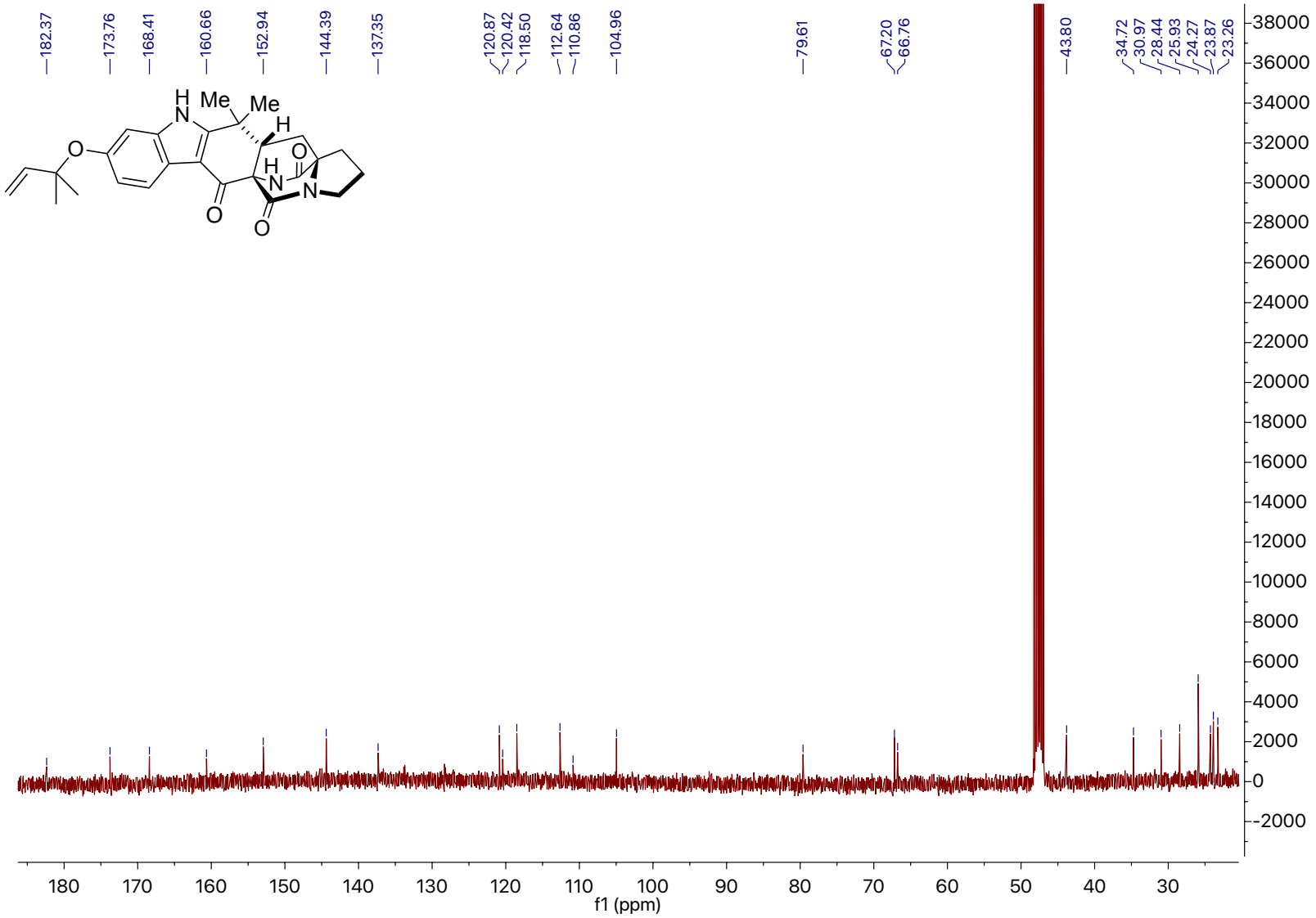

Figure A75. ^{13}C NMR Spectrum of compound **122** (MeOD).

Figure A76. COSY NMR Spectrum of compound **122** (MeOD).

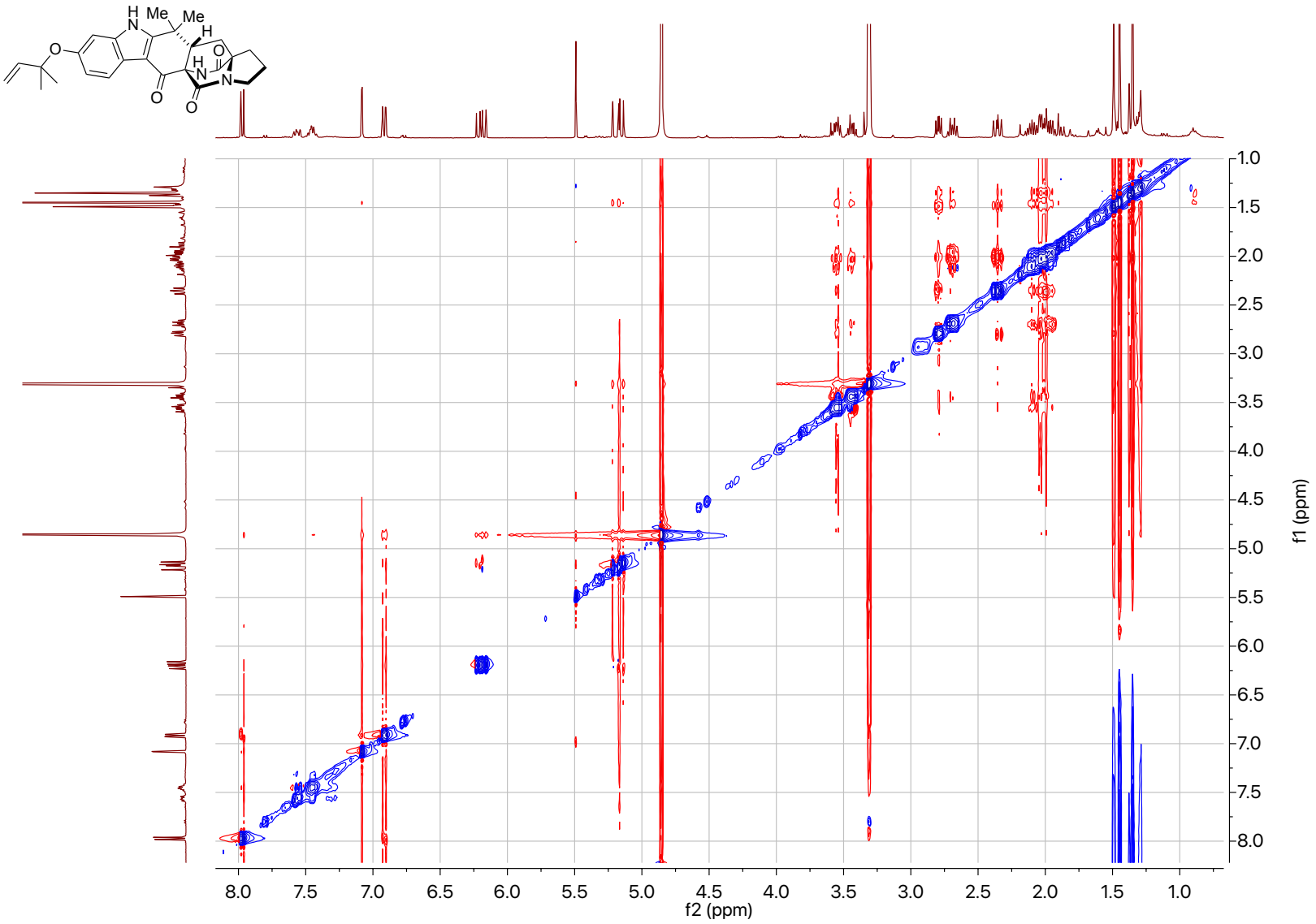

Figure A77. ROESY NMR Spectrum of compound **122** (MeOD).

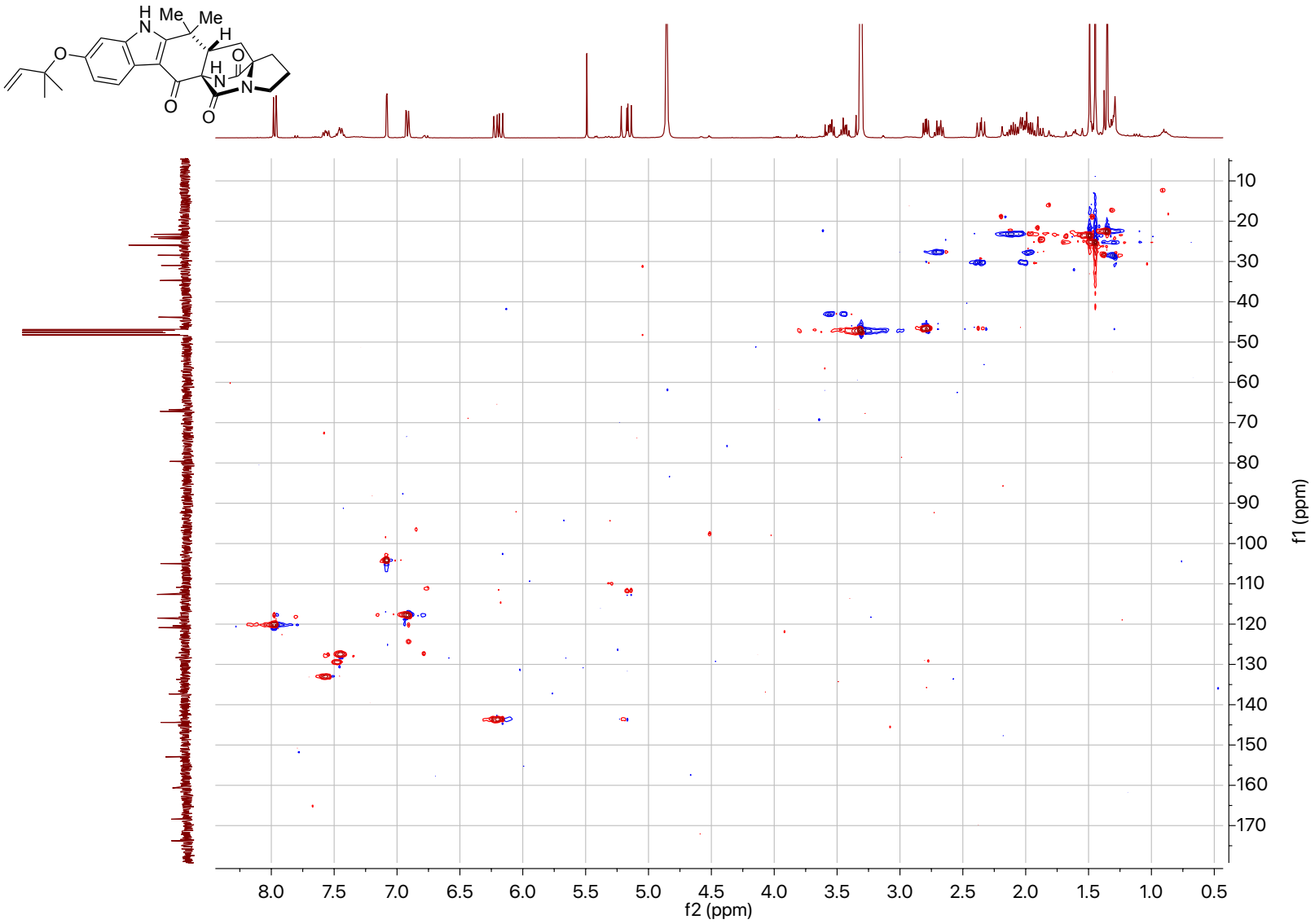

Figure A78. HSQC NMR Spectrum of compound **122** (MeOD).

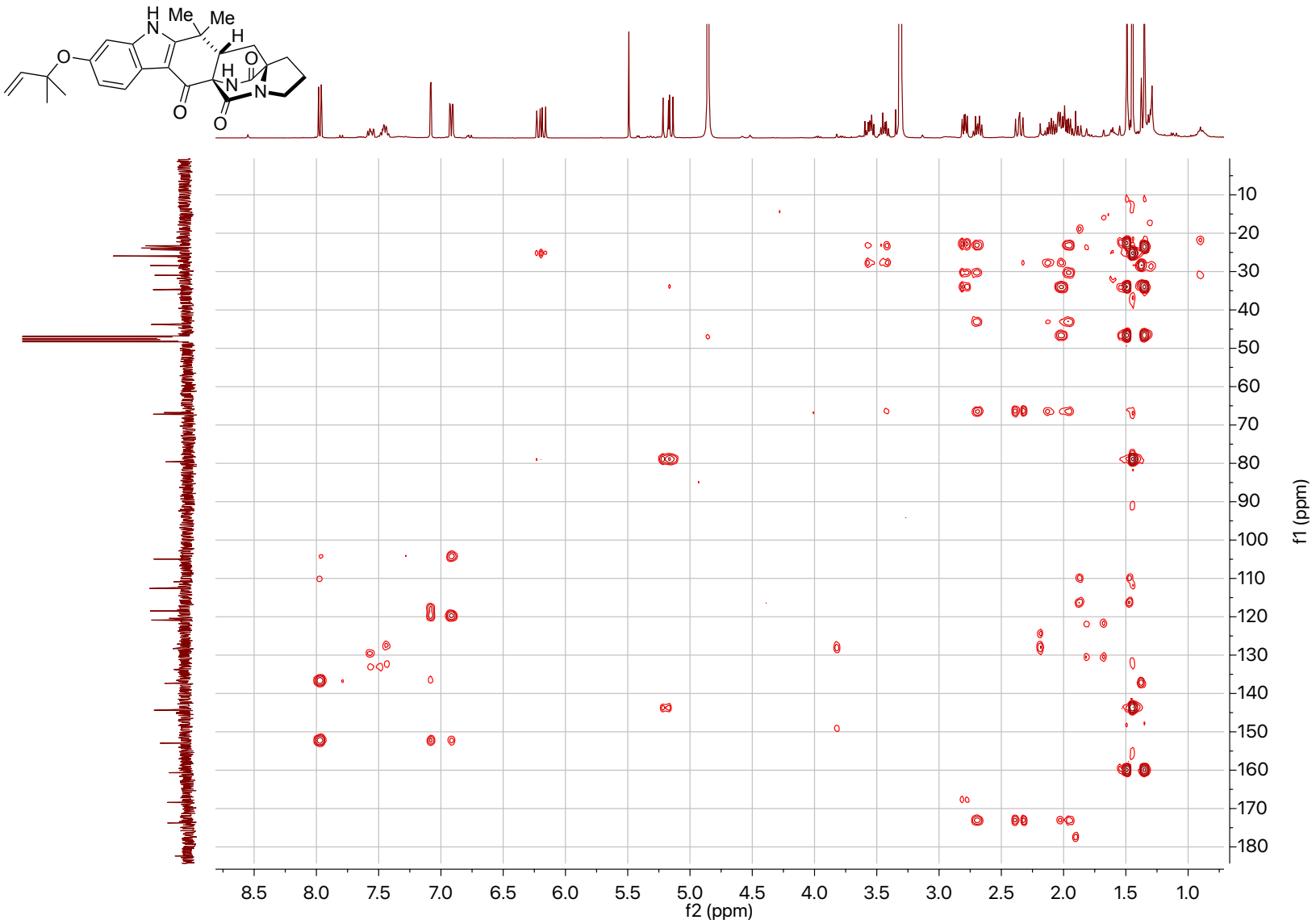

Figure A79. HMBC NMR Spectrum of compound **122** (MeOD).

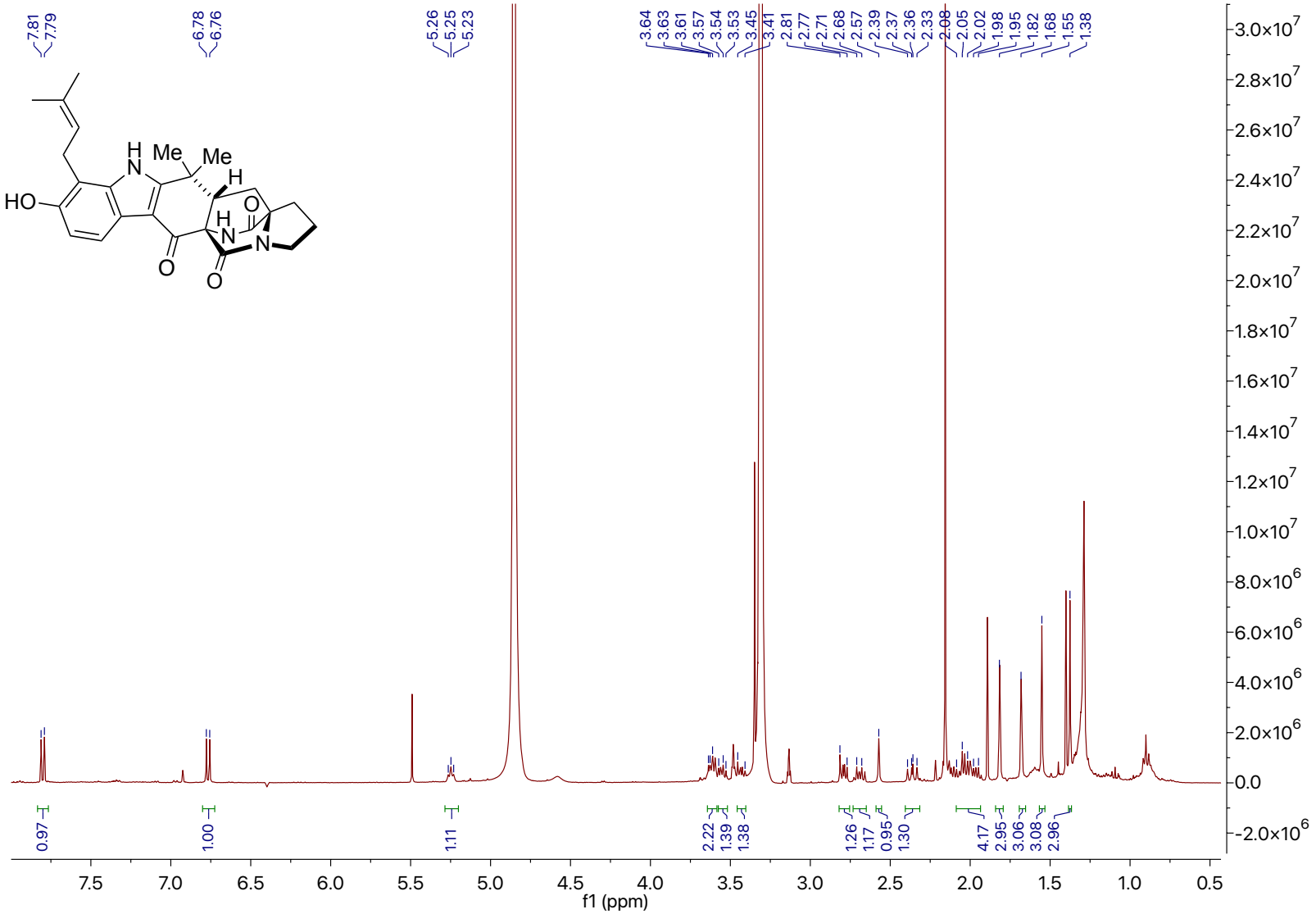

Figure A80. [1]H NMR Spectrum of compound 6-*epi*-Notoamide T10 (MeOD).

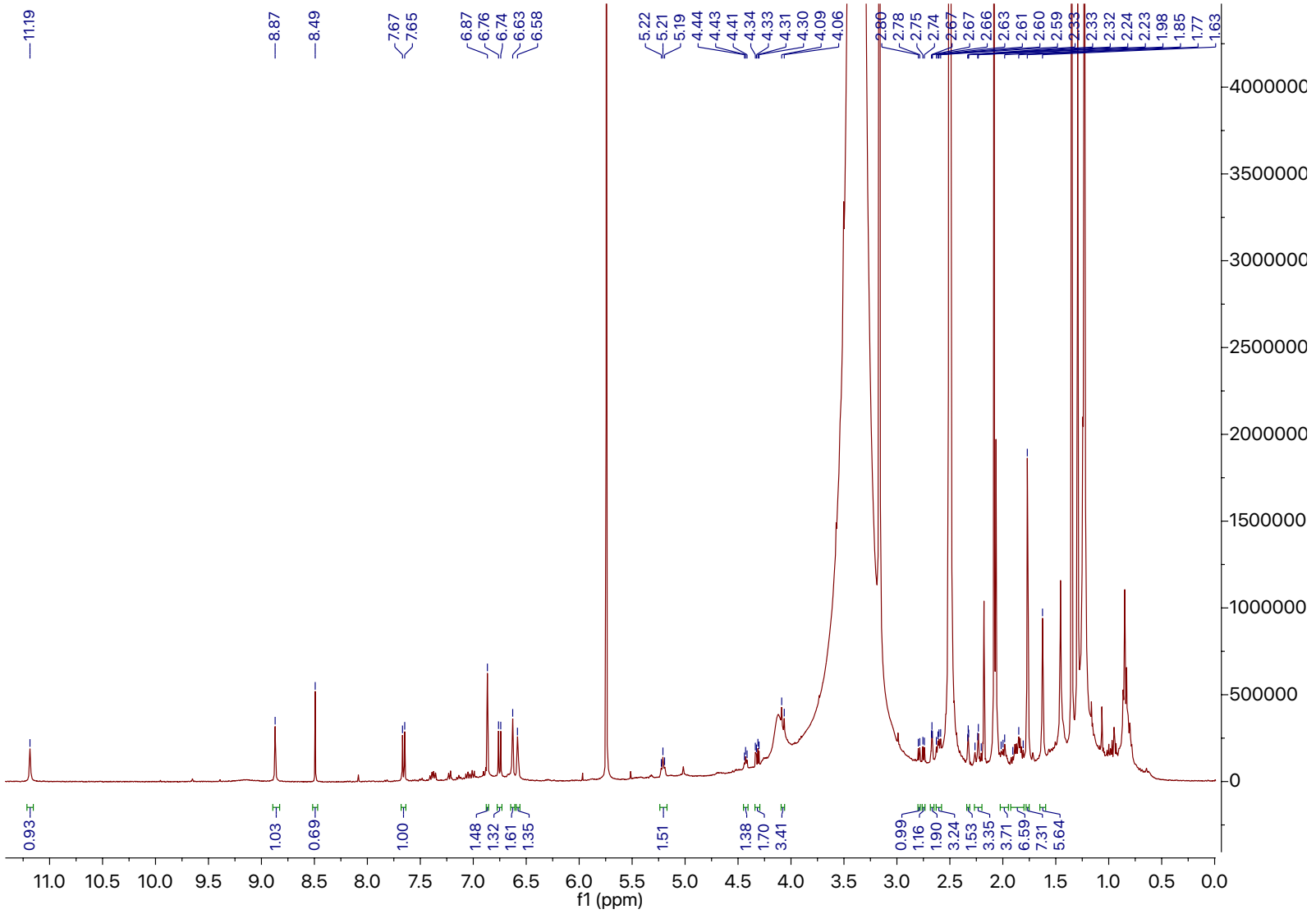

Figure A81. [1]H NMR Spectrum of compound 6-*epi*-Notoamide T11/12 (DMSO).

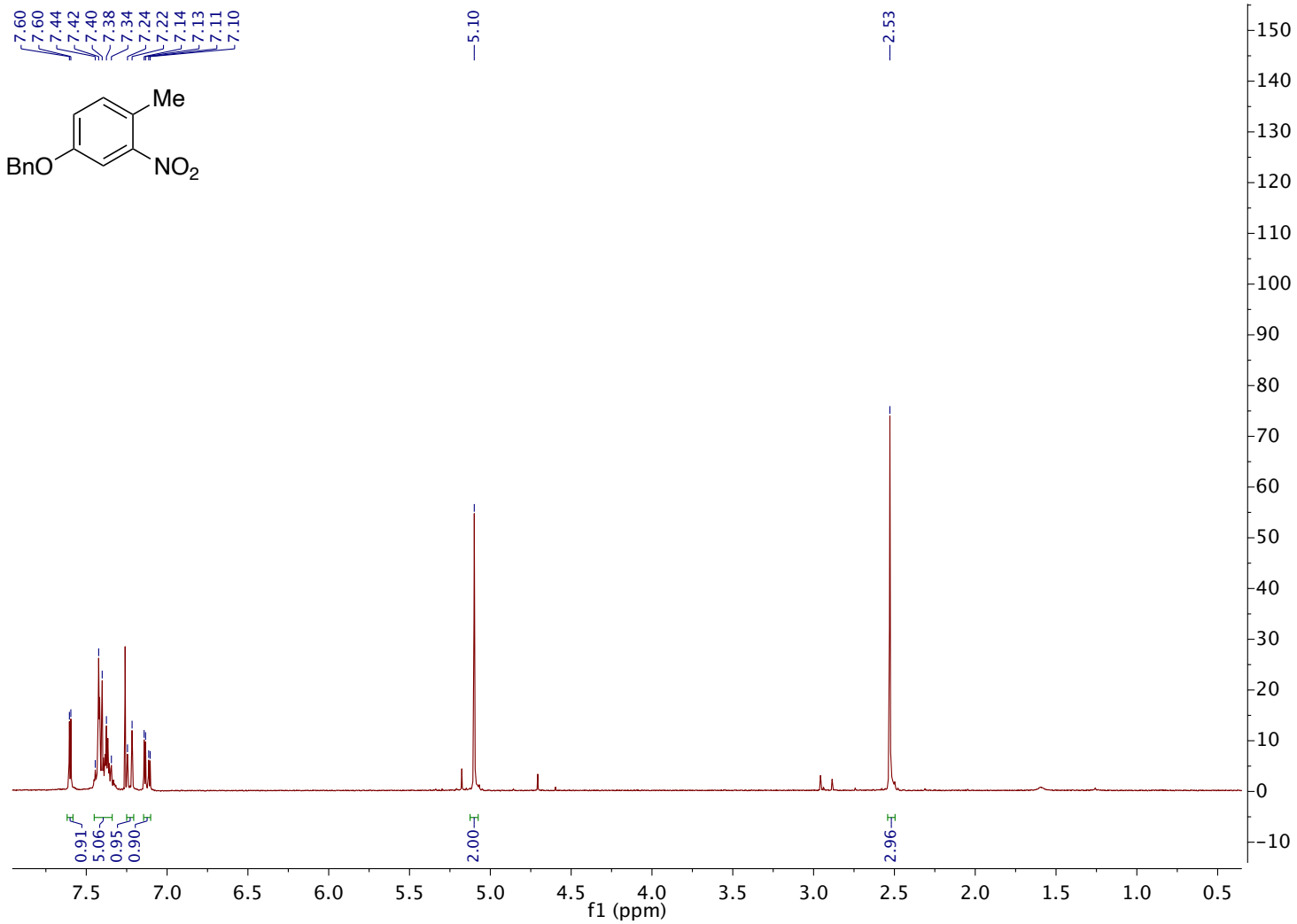

Figure A82. ^{1}H NMR Spectrum of compound **16** ($CDCl_3$).

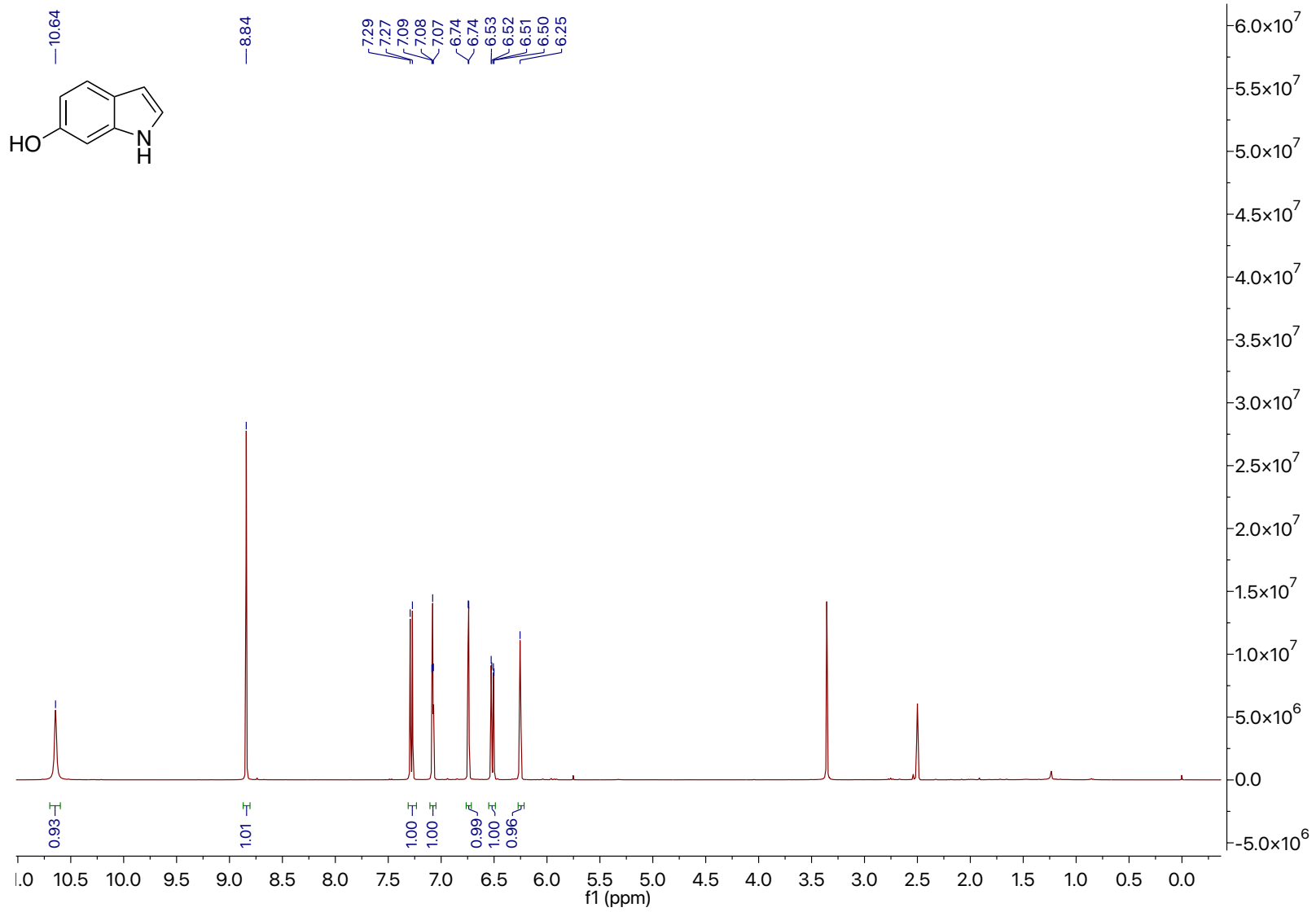

Figure A83. ^{1}H NMR Spectrum of compound **14** (DMSO).

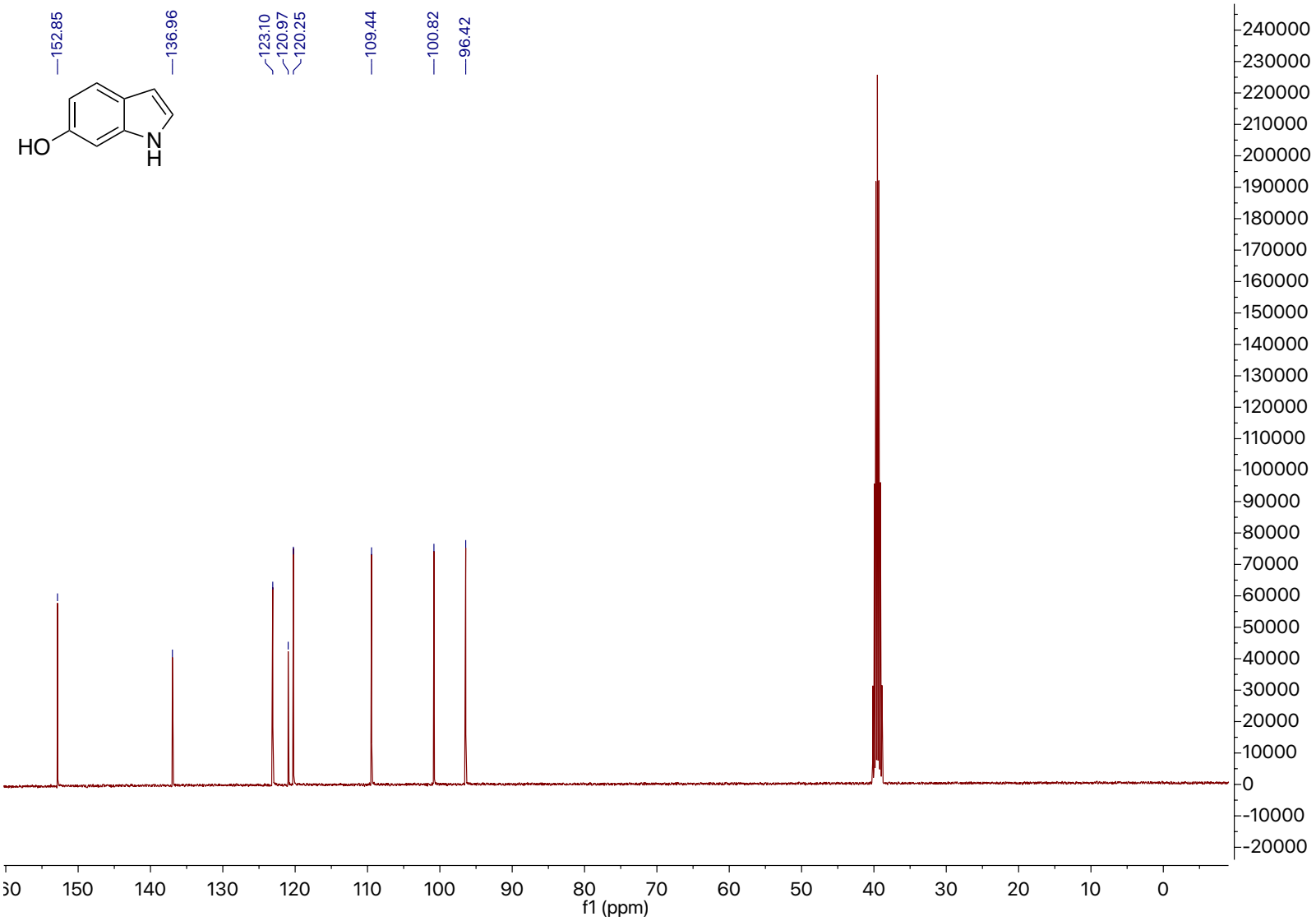

Figure A84. ^{13}C NMR Spectrum of compound **14** (DMSO).

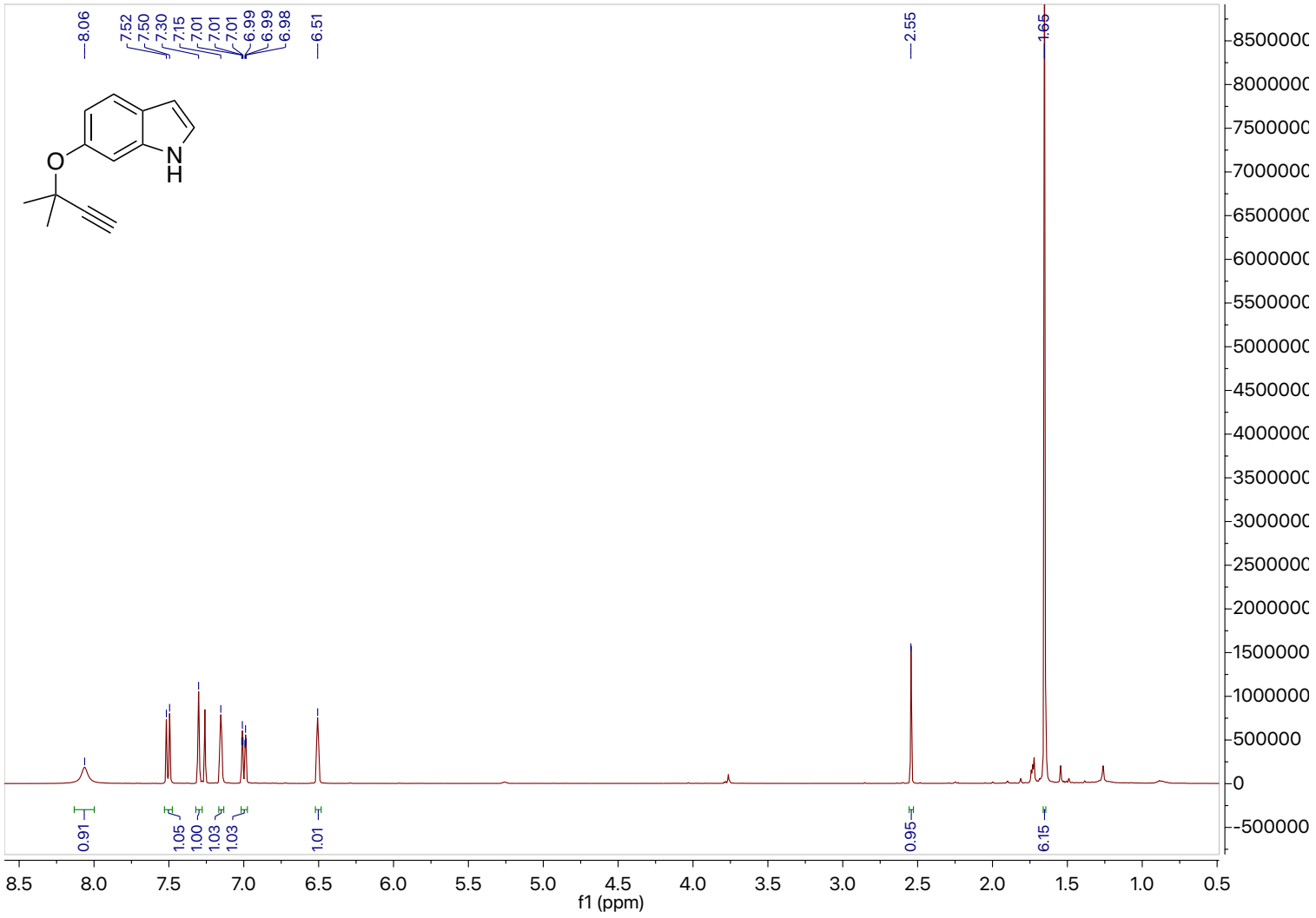

Figure A85. ^{1}H NMR Spectrum of compound **132** ($CDCl_3$).

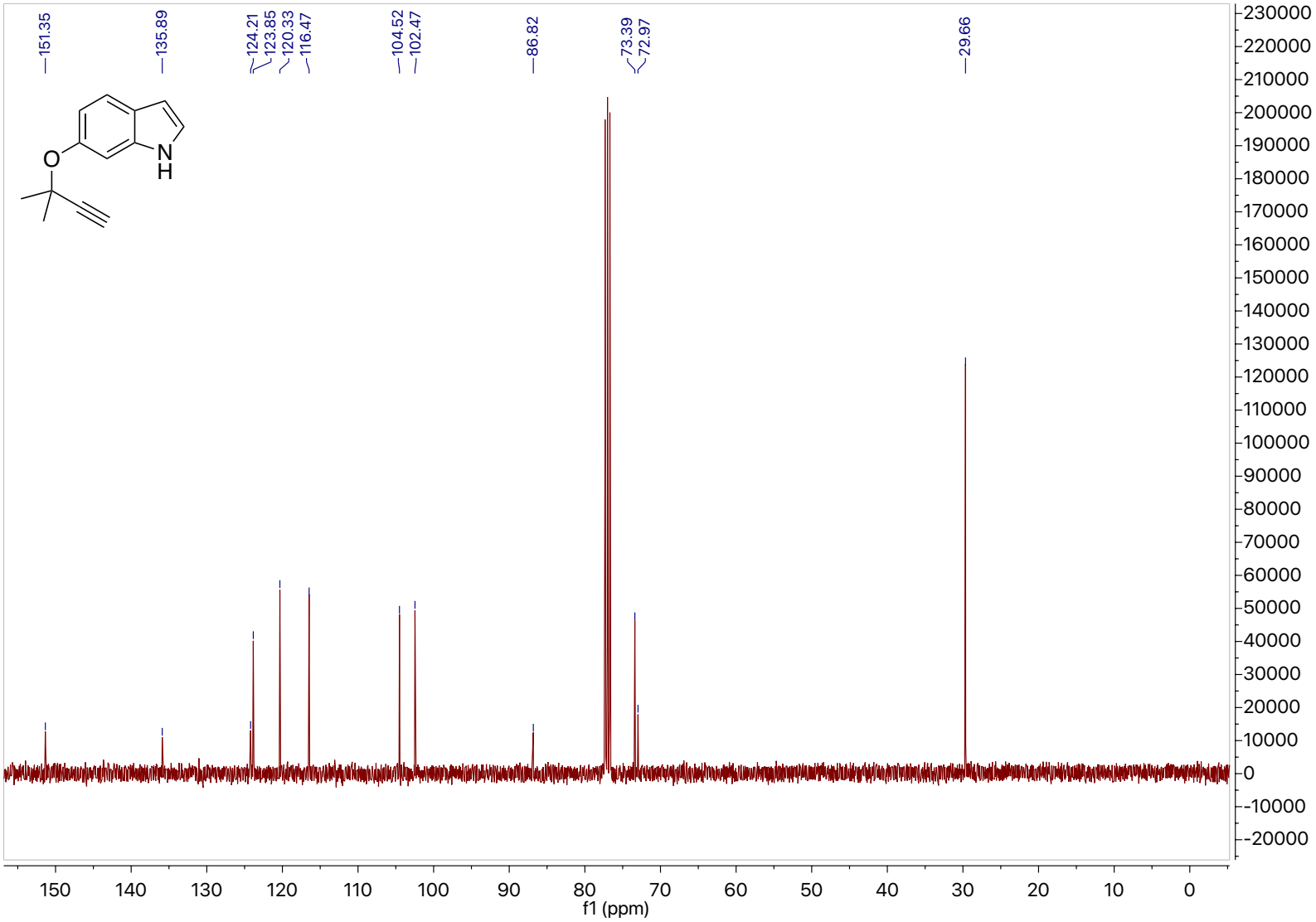

Figure A86. ^{13}C NMR Spectrum of compound **132** ($CDCl_3$).

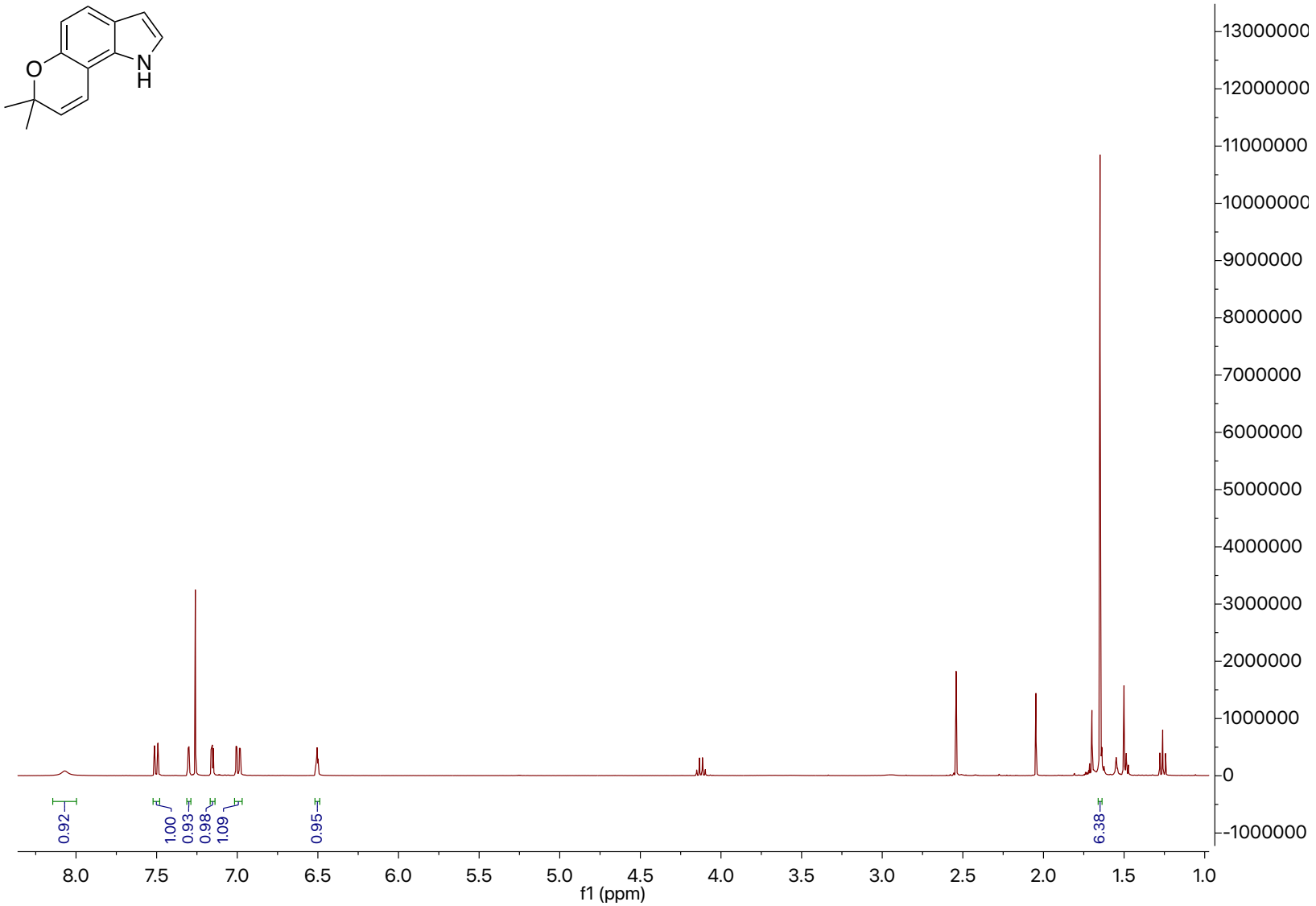

Figure A87. ^{1}H NMR Spectrum of compound **133** ($CDCl_3$).

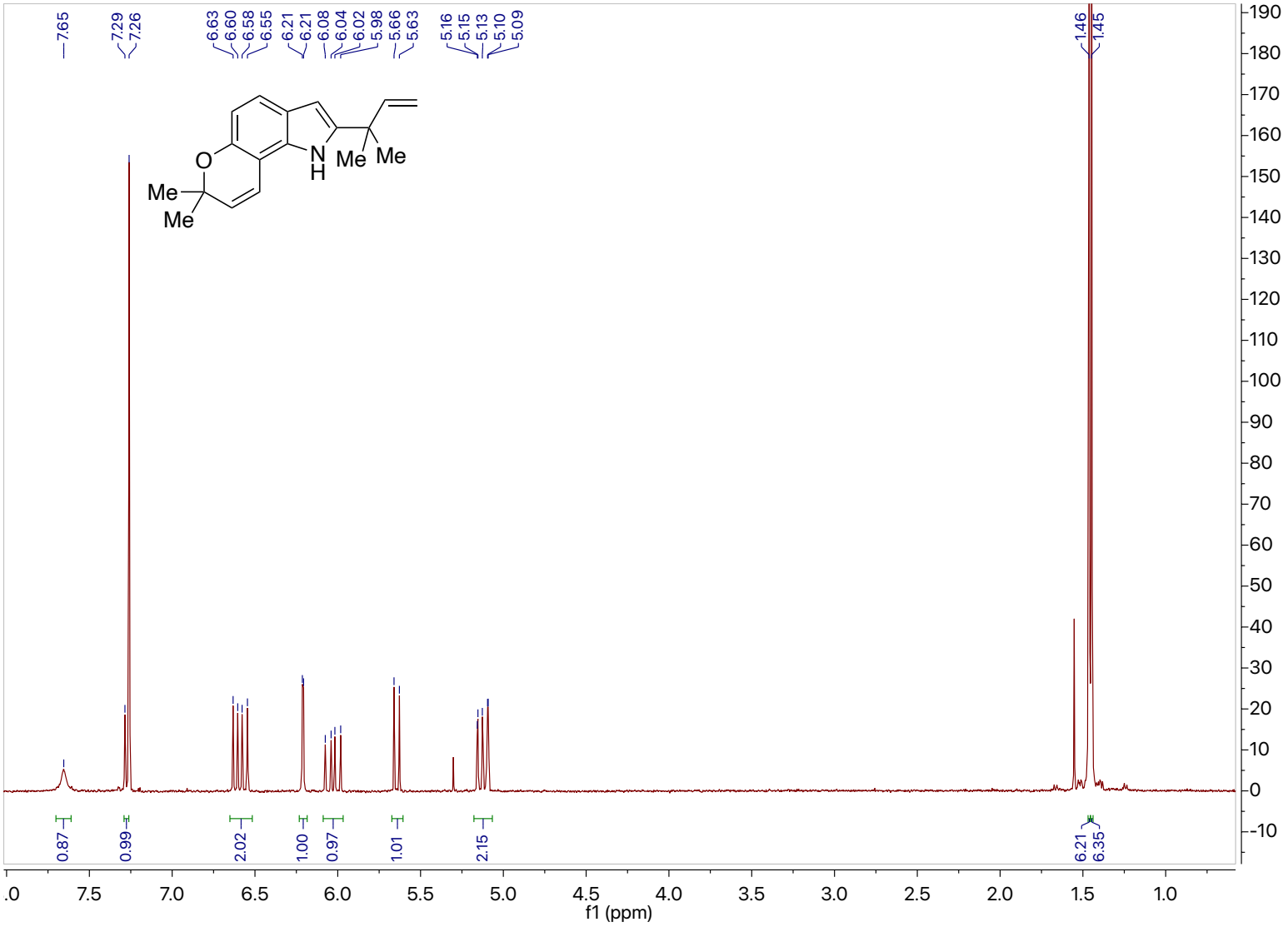

Figure A88. ^{1}H NMR Spectrum of compound **135** ($CDCl_3$).

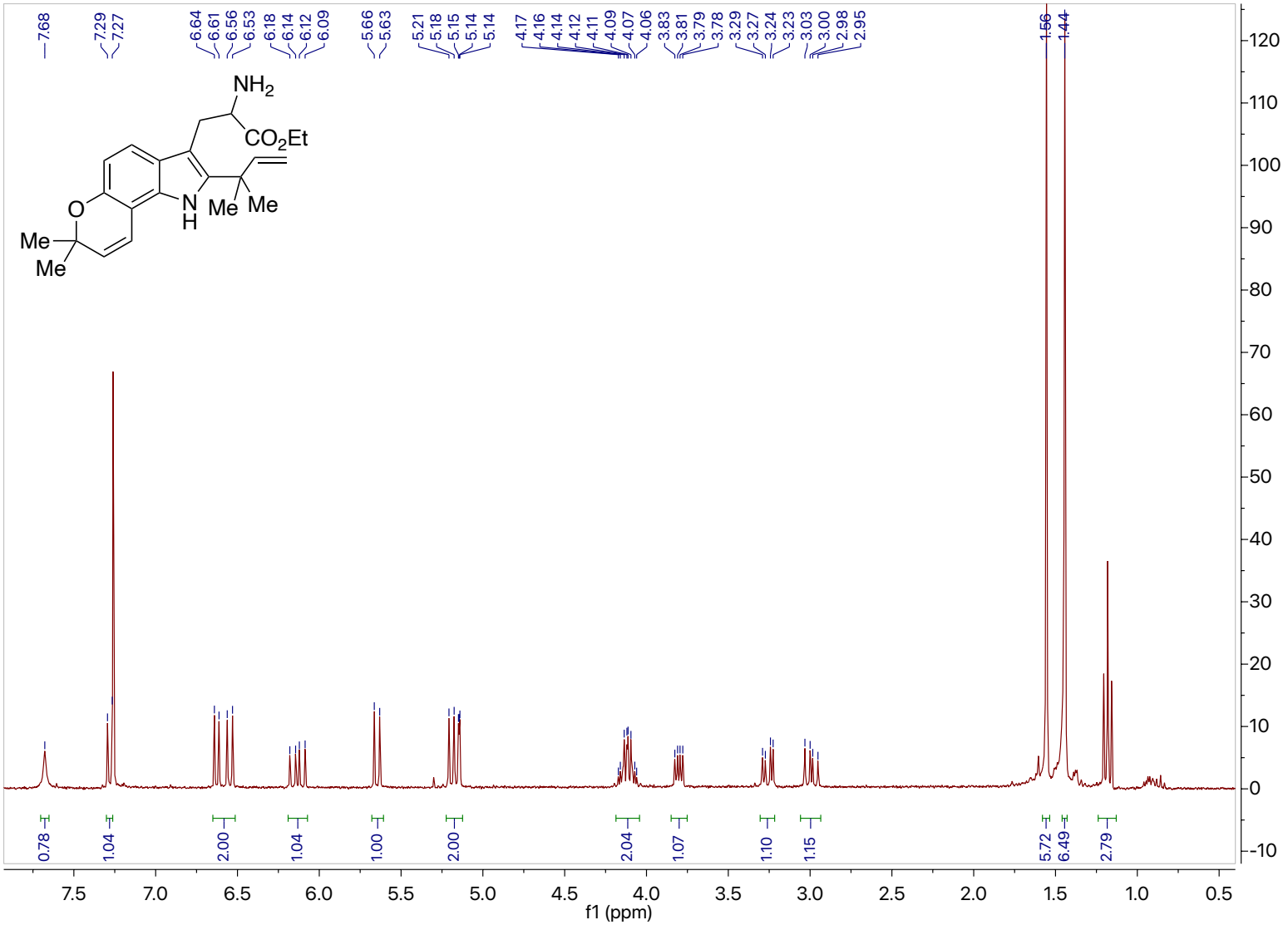

Figure A89. ^{1}H NMR Spectrum of compound **138** ($CDCl_3$).

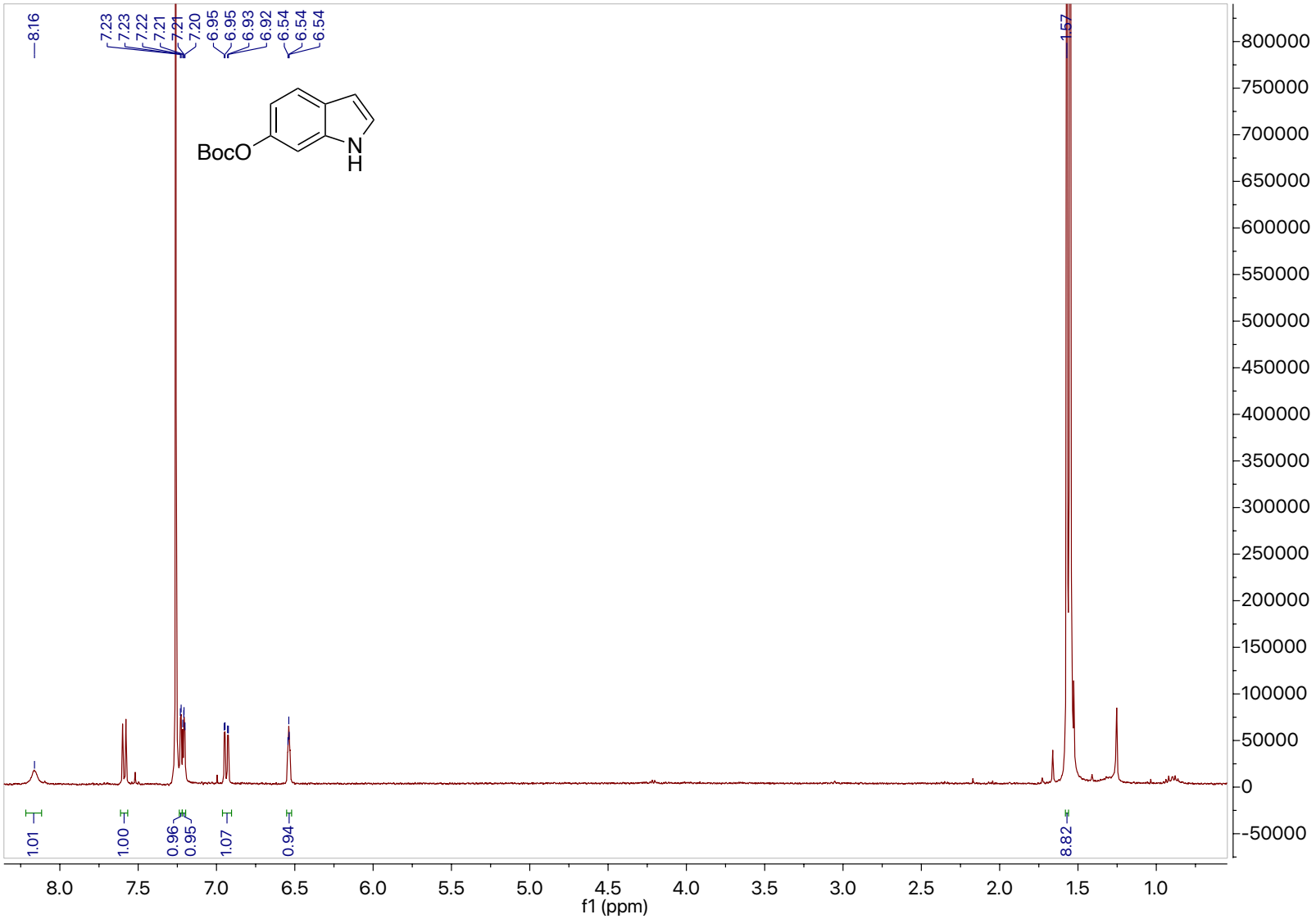

Figure A90. ^{1}H NMR Spectrum of compound **18** ($CDCl_3$).

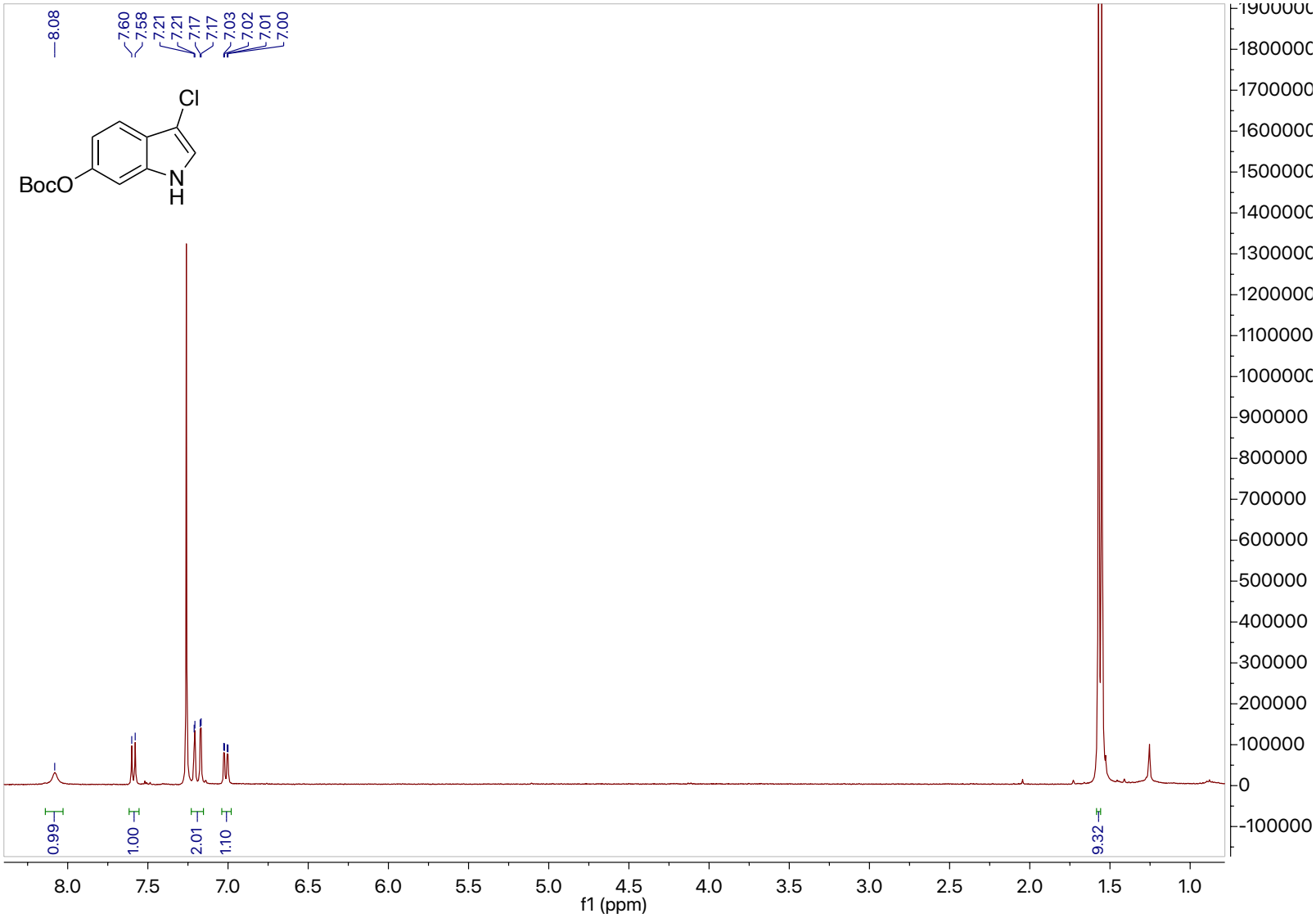

Figure A91. ^{1}H NMR Spectrum of compound **19** ($CDCl_3$).

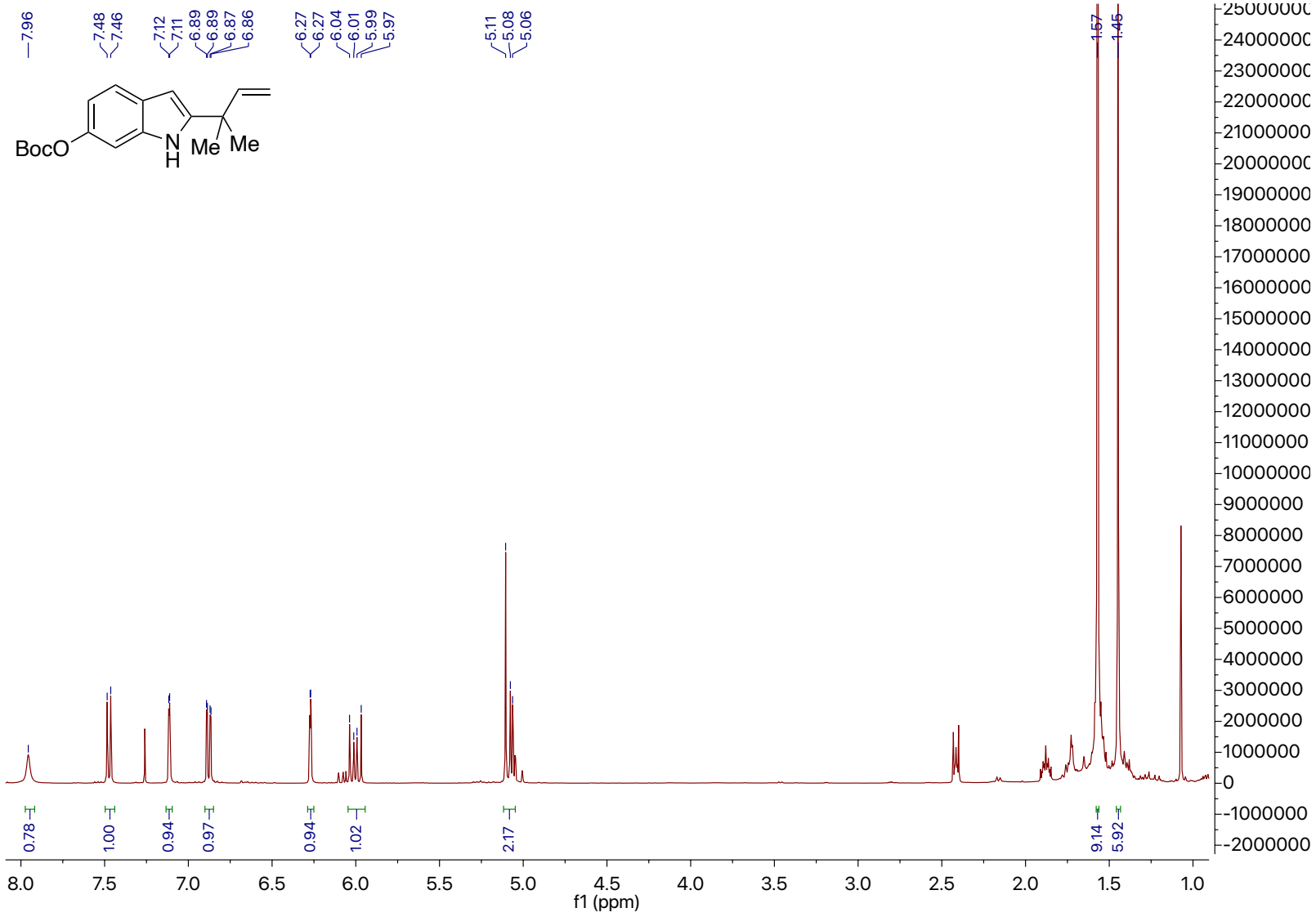

Figure A92. ^{1}H NMR Spectrum of compound **21** ($CDCl_3$).

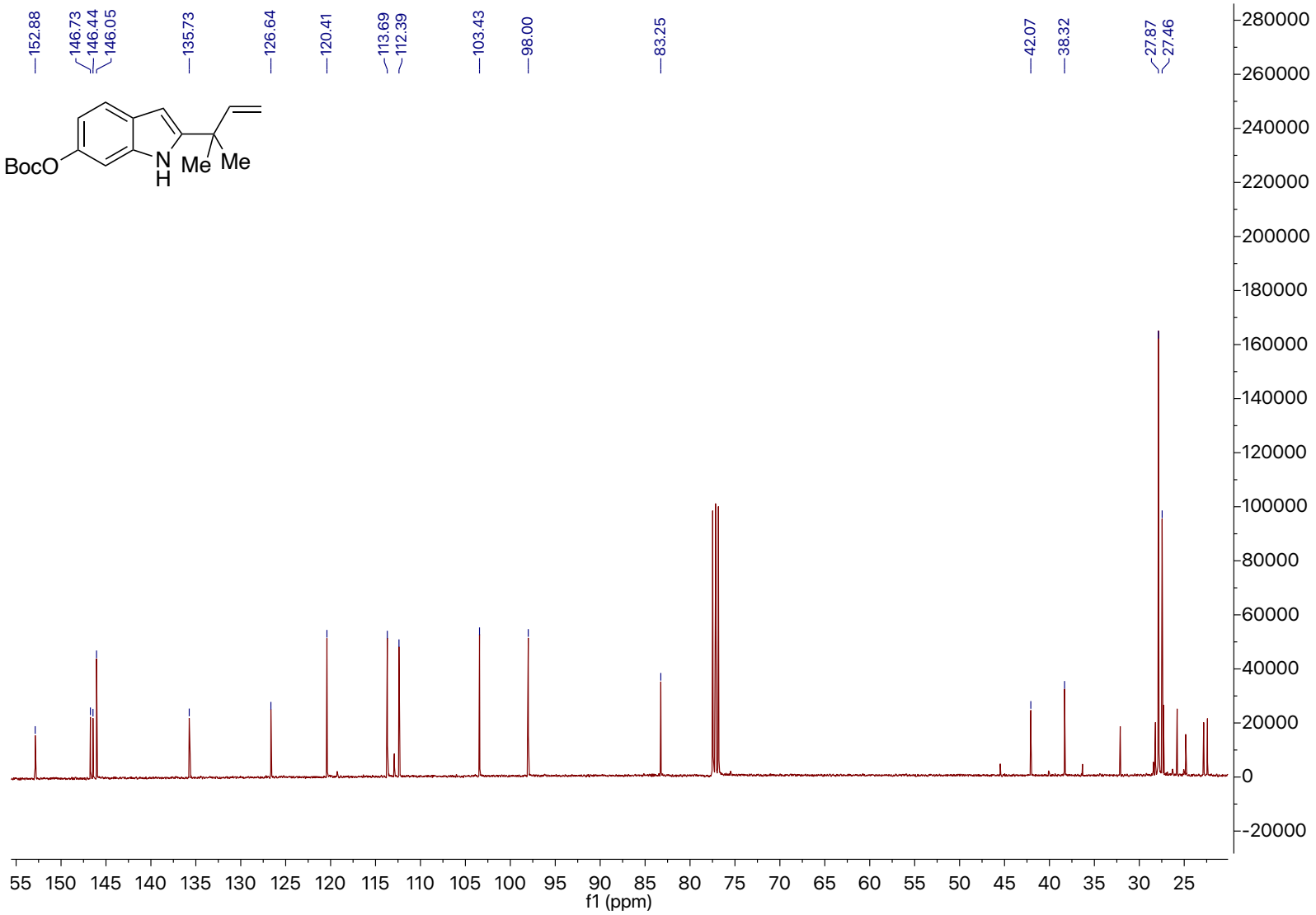

Figure A93. ^{13}C NMR Spectrum of compound **21** ($CDCl_3$).

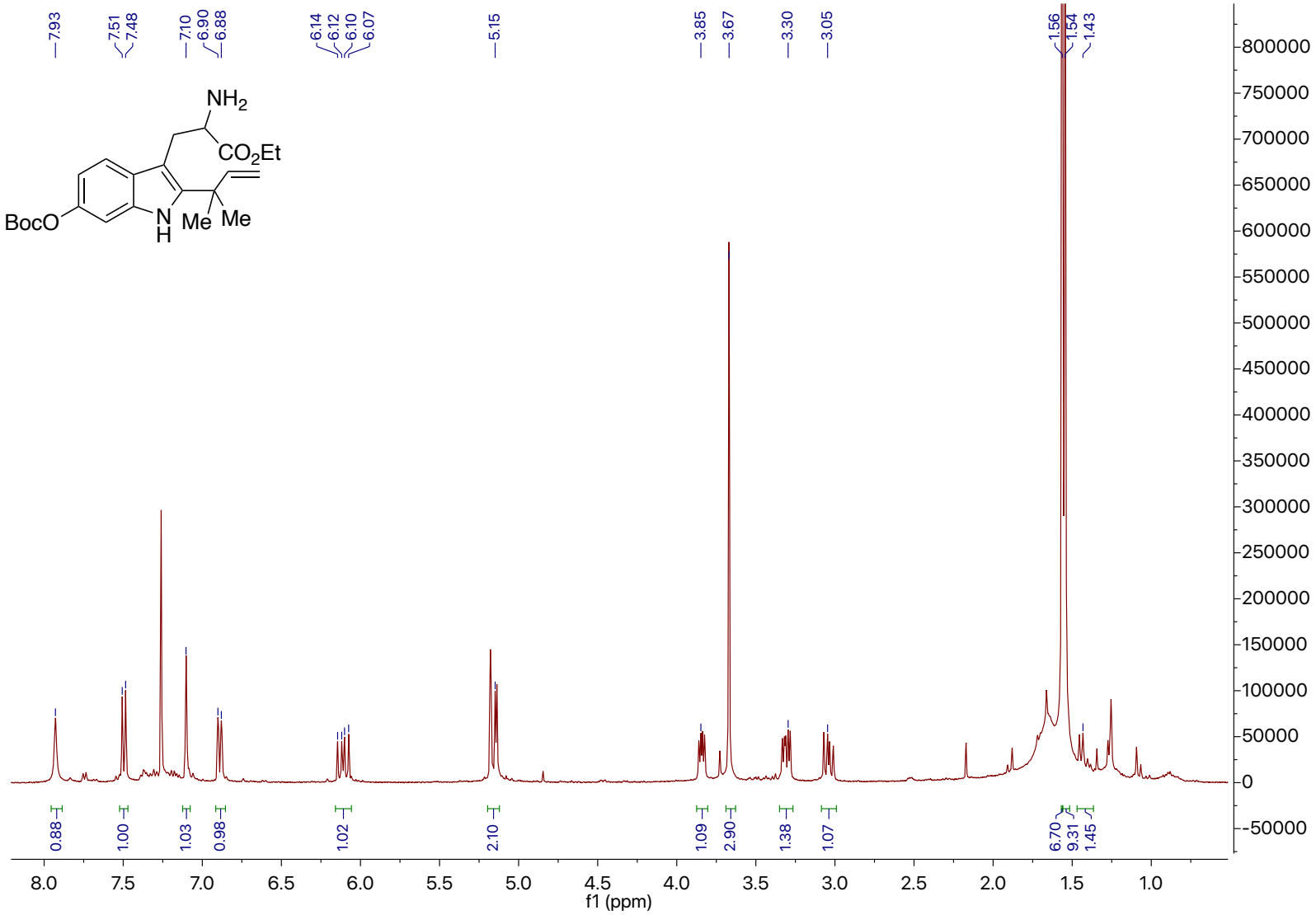

Figure A94. ^{1}H NMR Spectrum of compound **24** ($CDCl_3$).

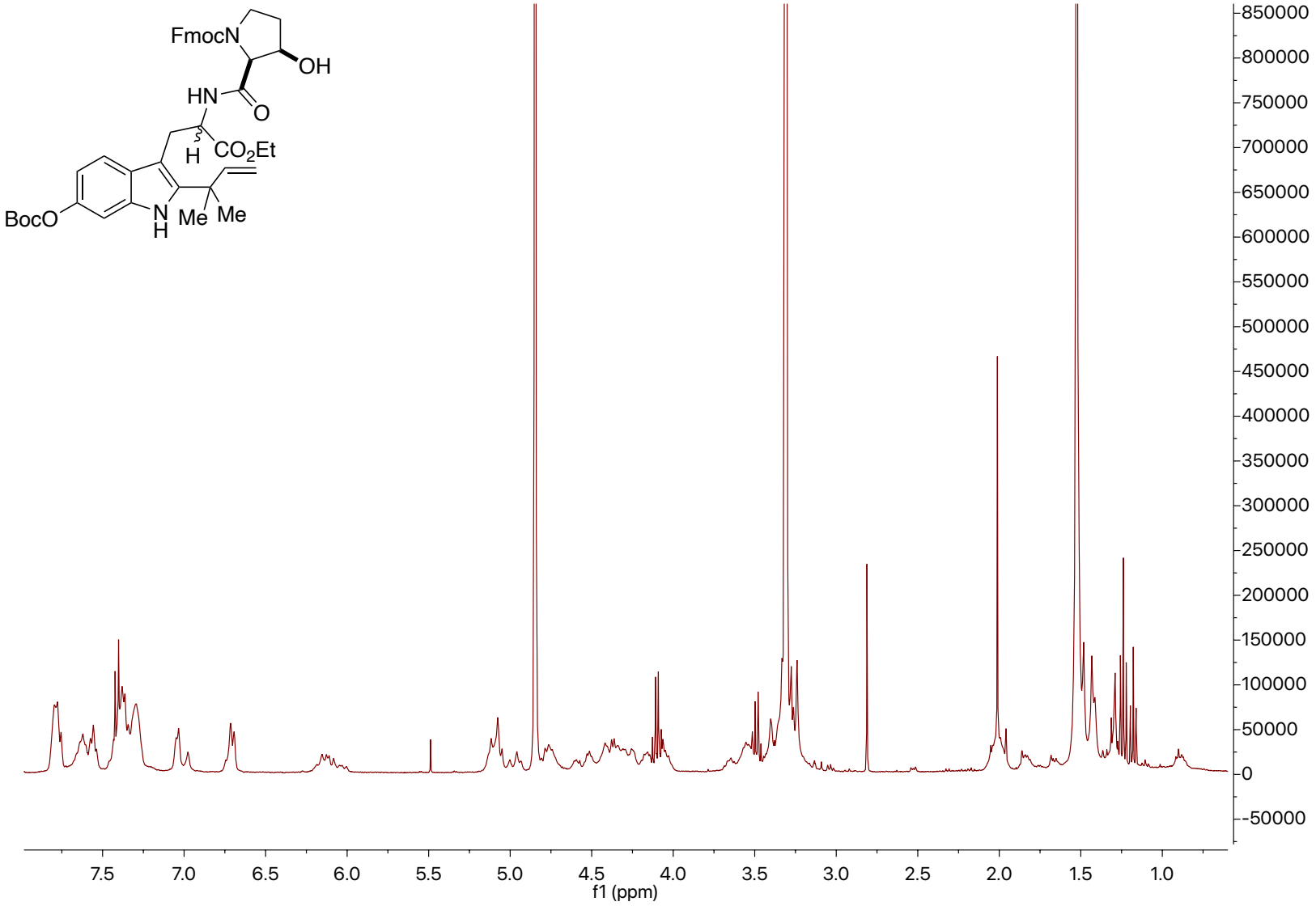

Figure A95. ^{1}H NMR Spectrum of compound **66** (MeOD).

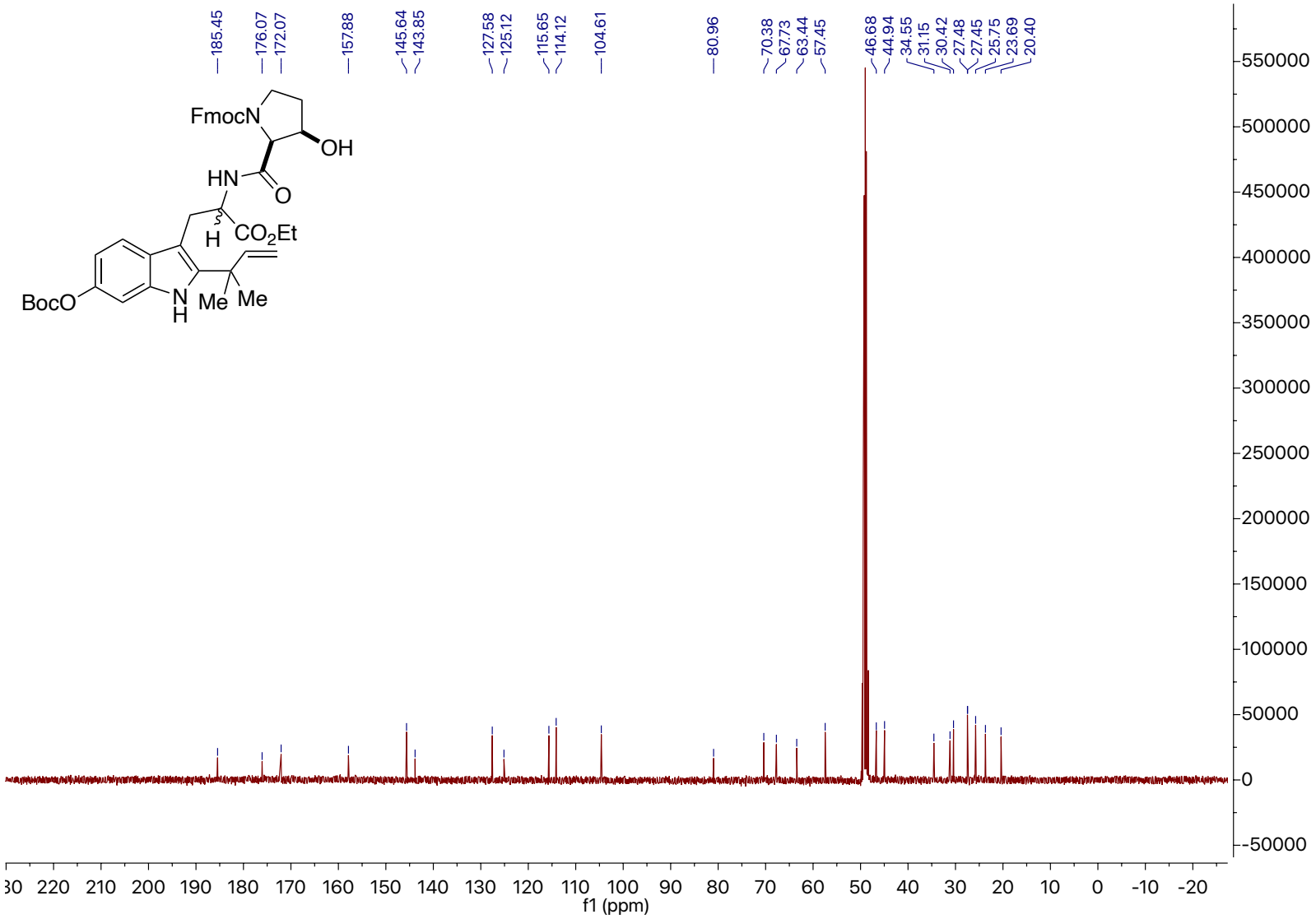

Figure A96. ^{13}C NMR Spectrum of compound **66** (MeOD).

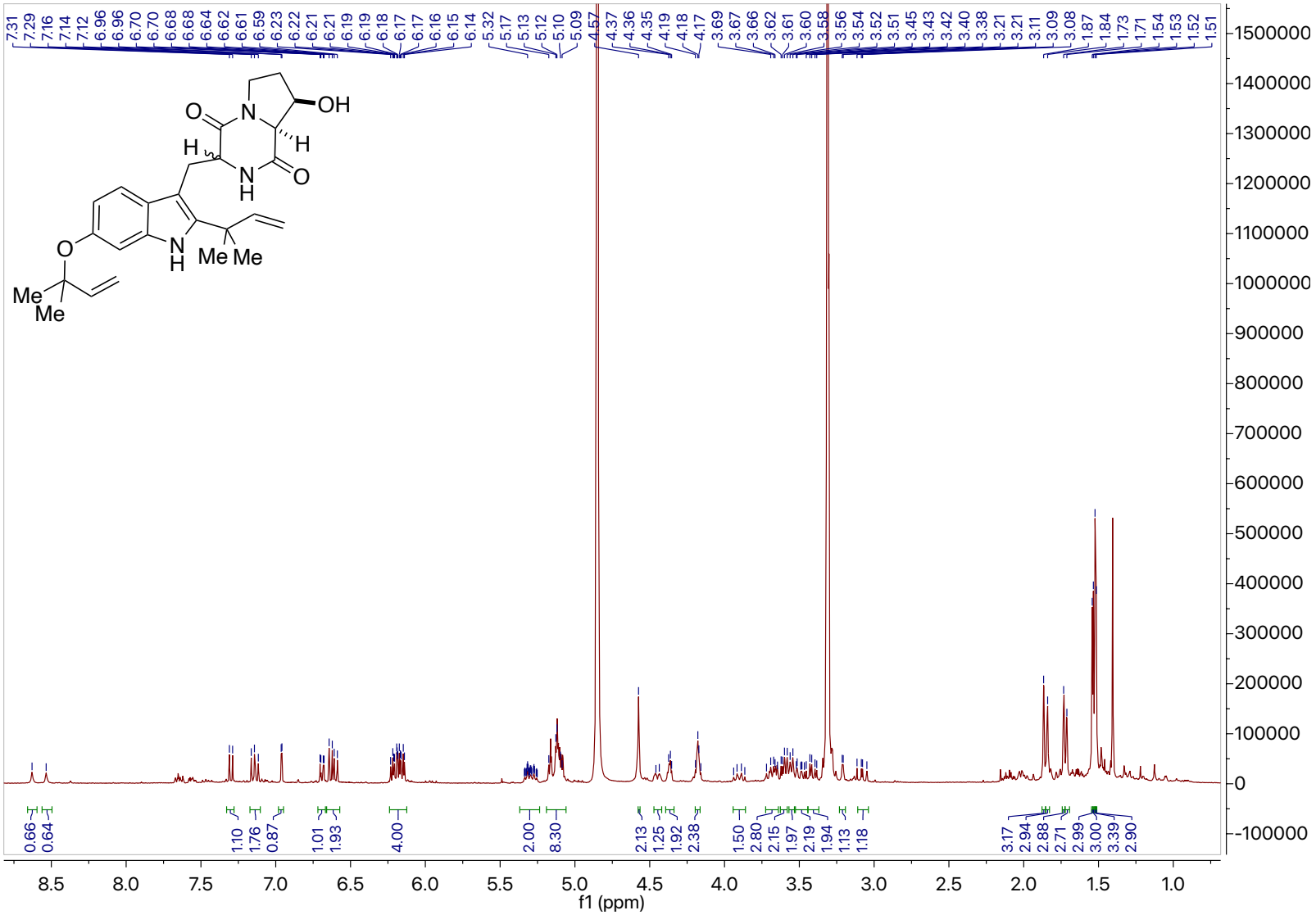

Figure A97. ^{1}H NMR Spectrum of compound **70** (MeOD).

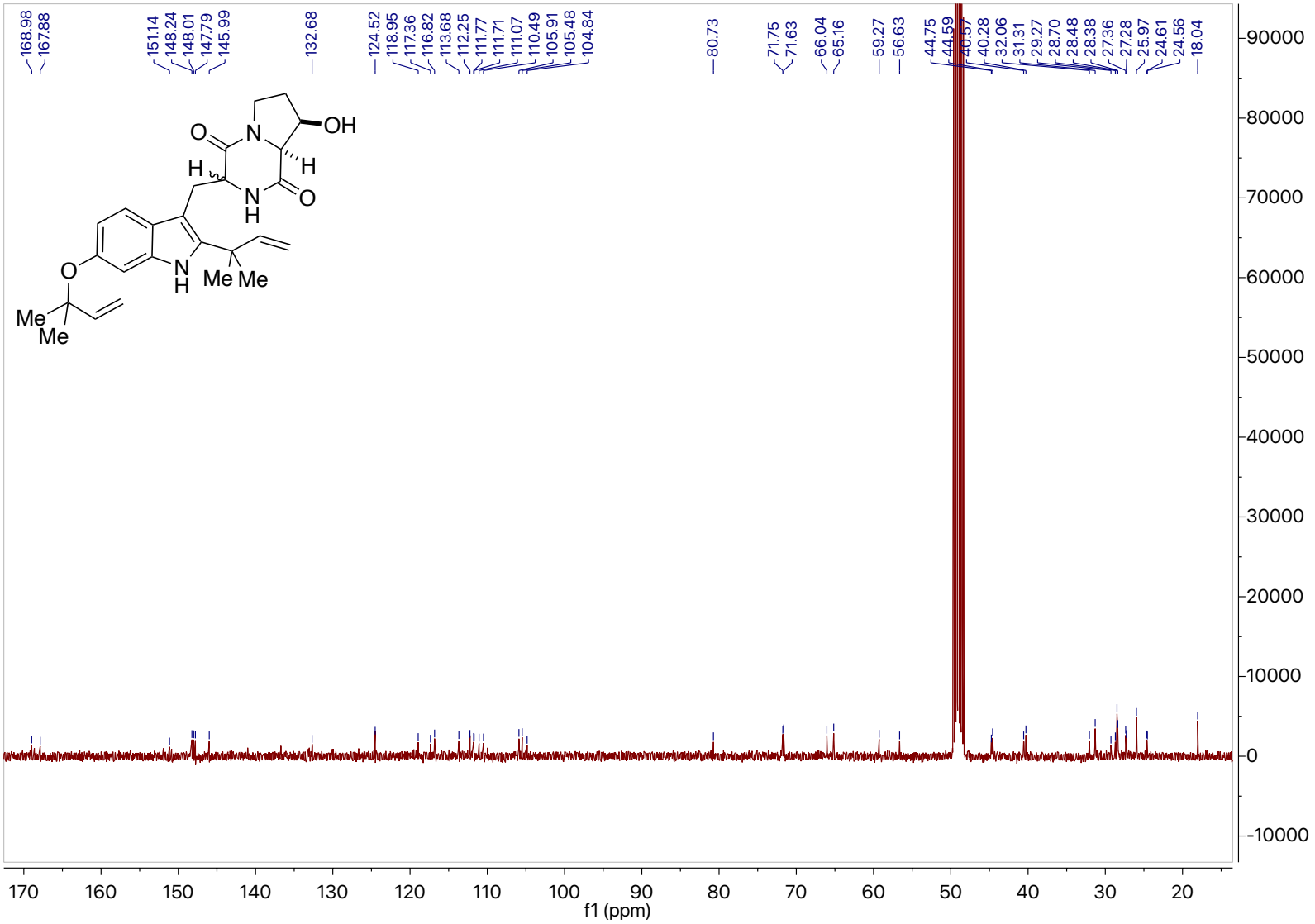

Figure A98. ^{13}C NMR Spectrum of compound **70** (MeOD).

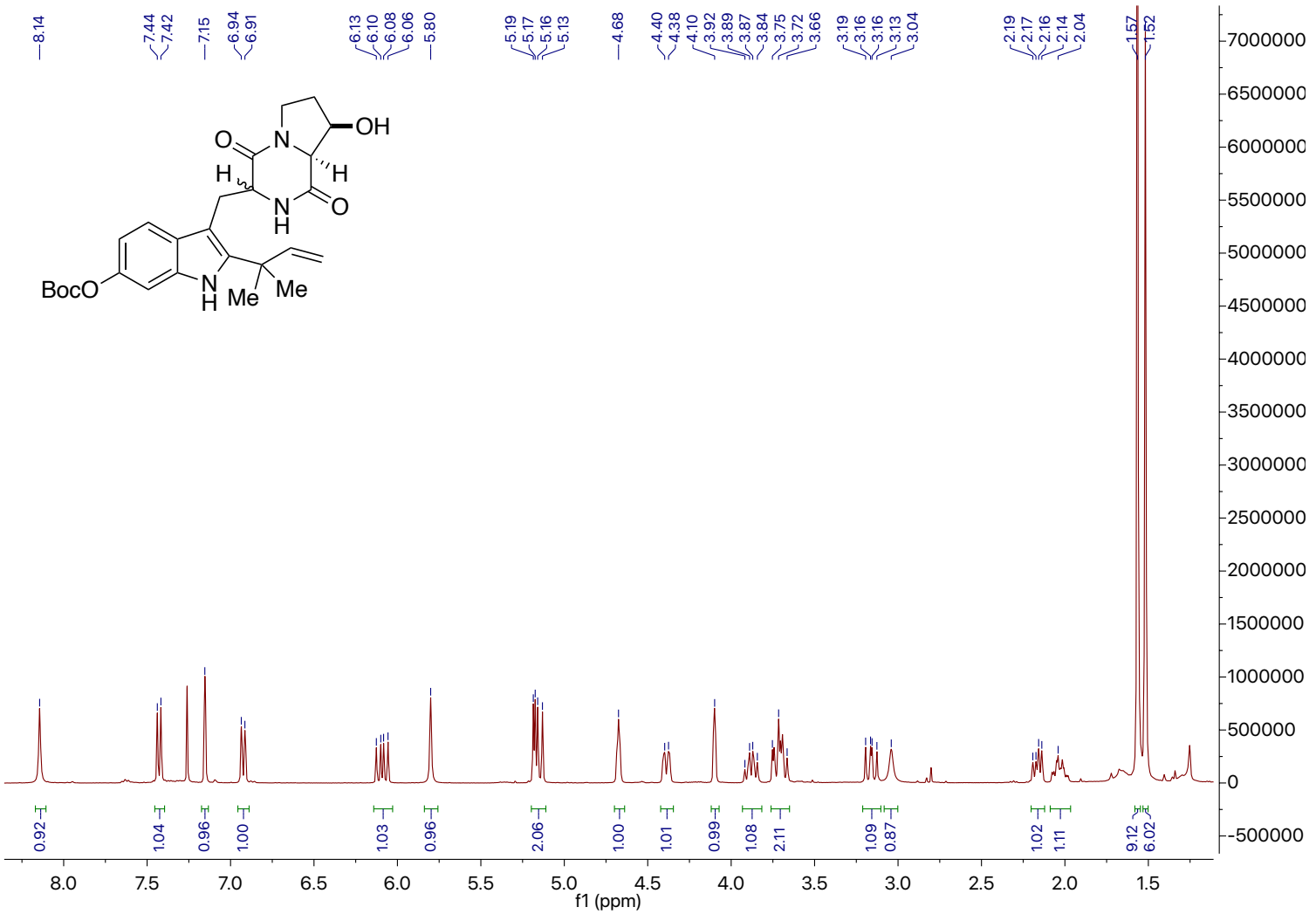

Figure A99. ^{1}H NMR Spectrum of compound **67a** ($CDCl_3$).

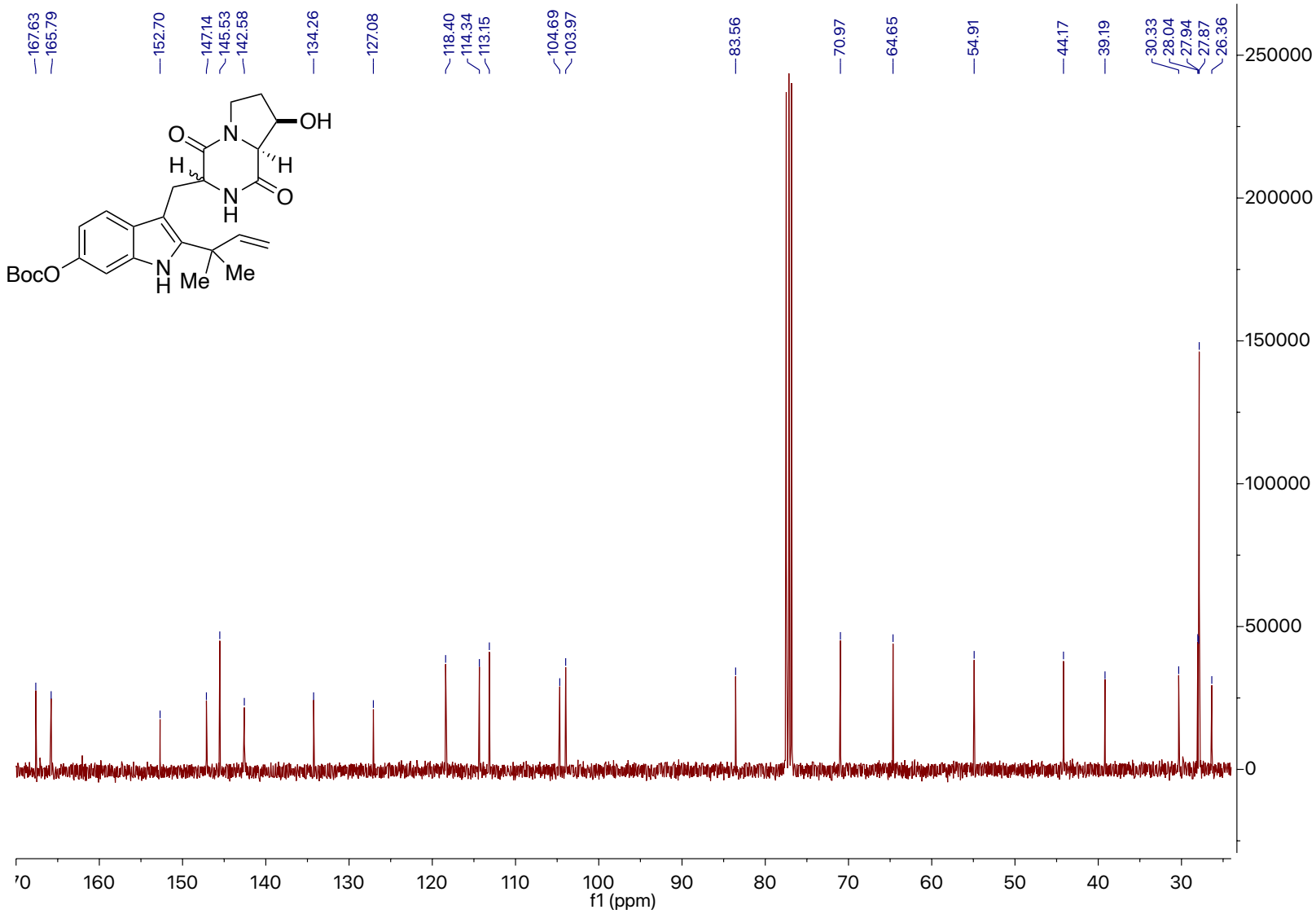

Figure A100. ^{1}H NMR Spectrum of compound **67a** ($CDCl_3$).

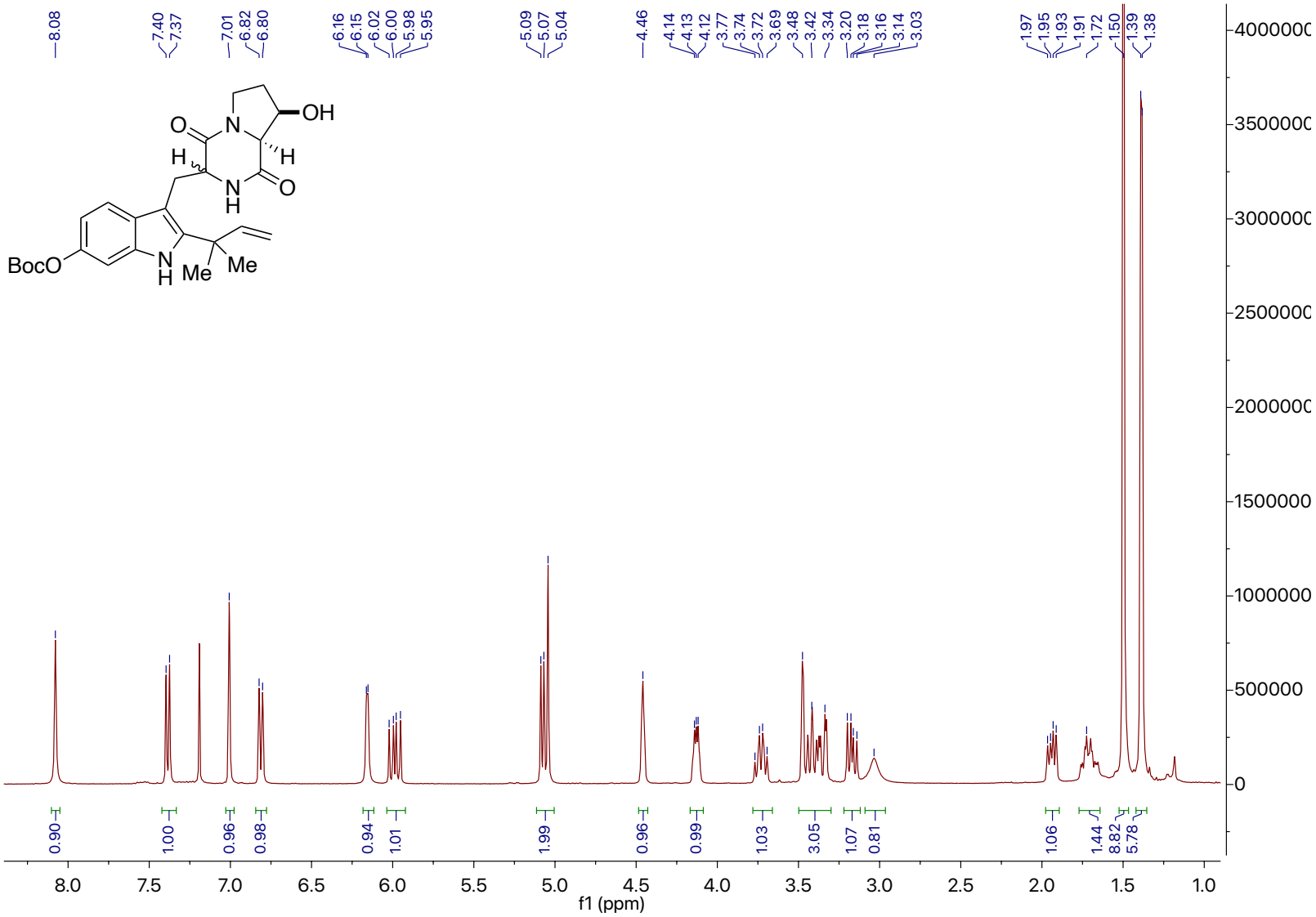

Figure A101. ^{1}H NMR Spectrum of compound **67b** ($CDCl_3$).

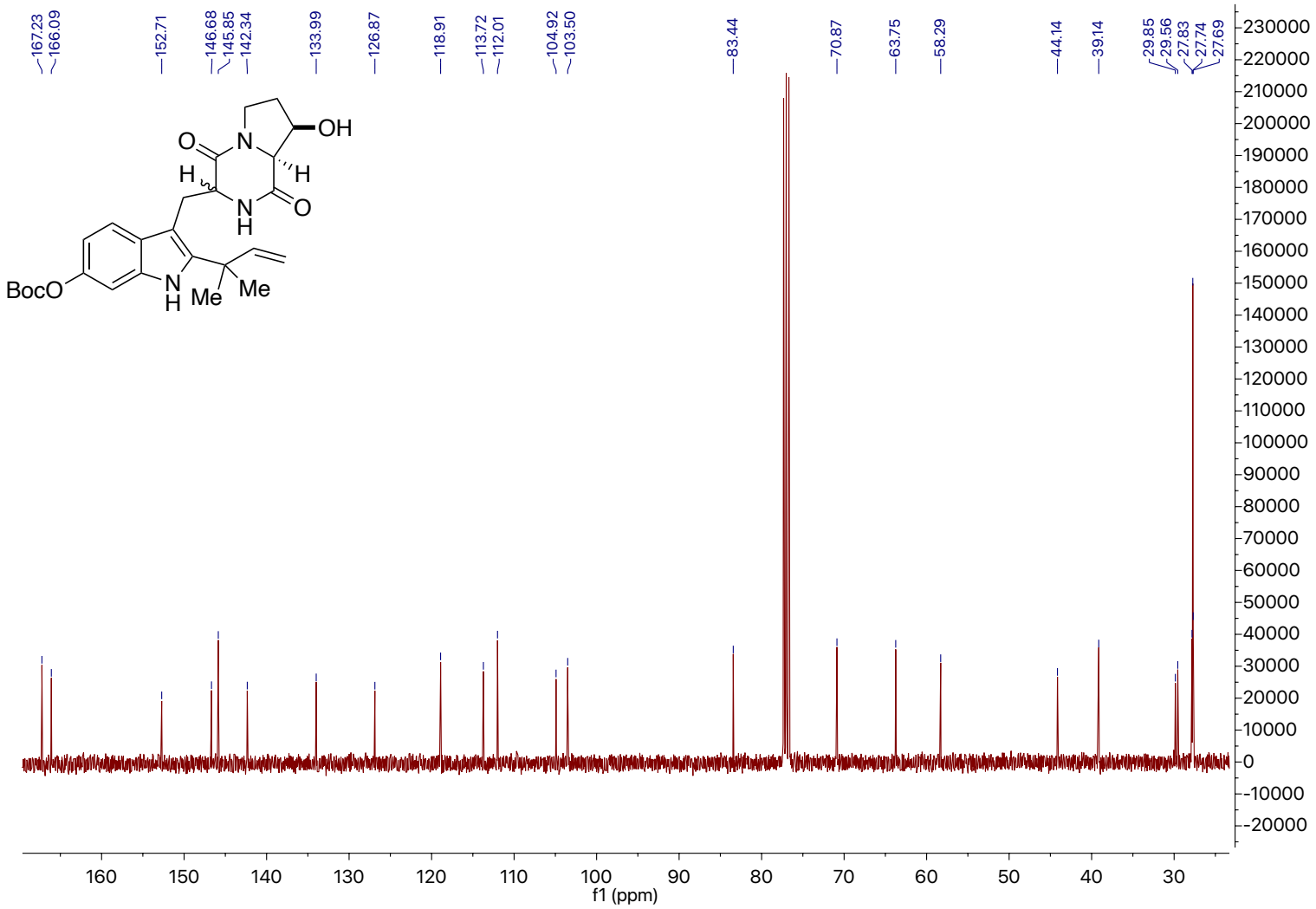

Figure A102. ^{1}H NMR Spectrum of compound **67b** ($CDCl_3$).

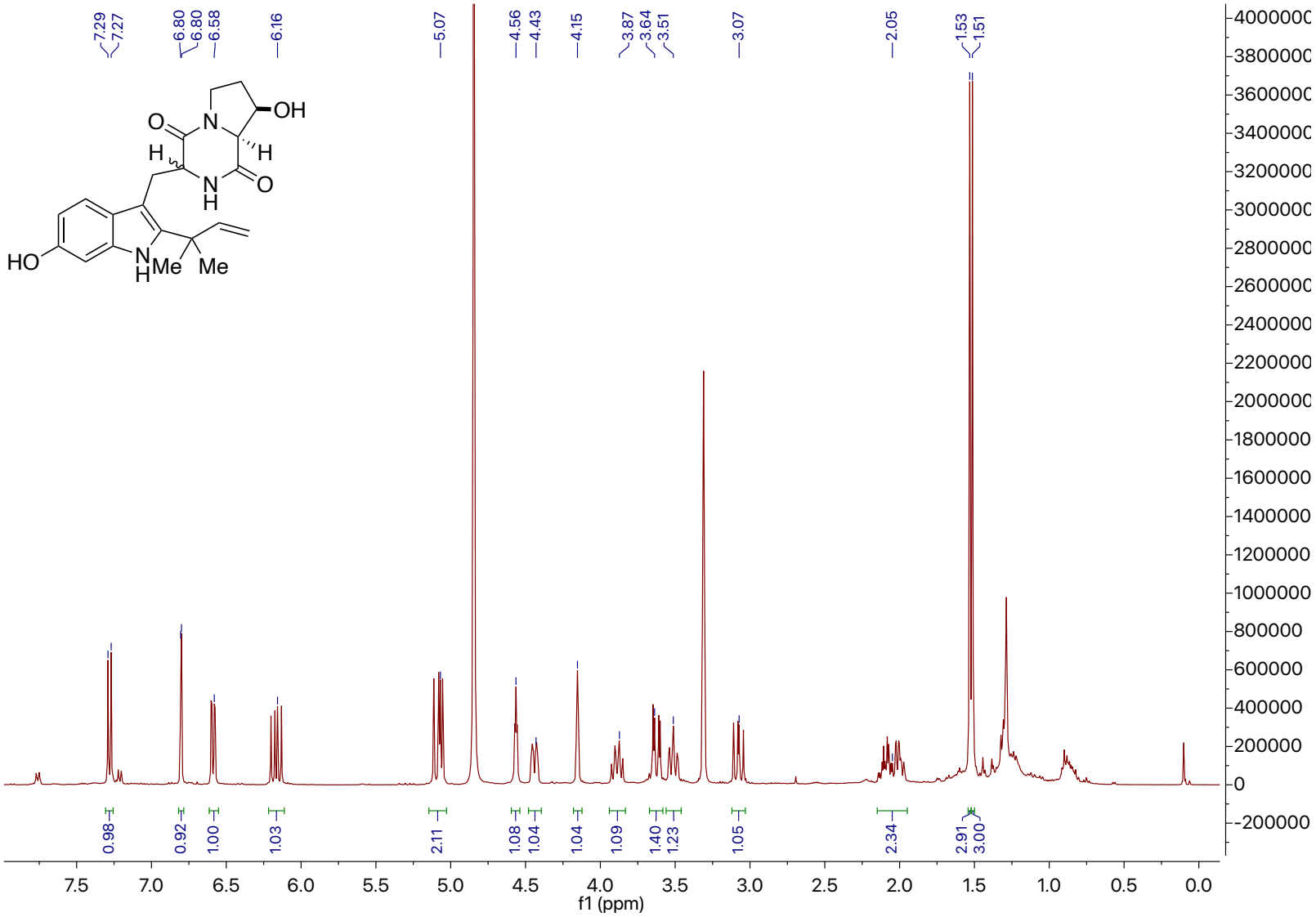

Figure A103. ^{1}H NMR Spectrum of compound **68** (MeOD).

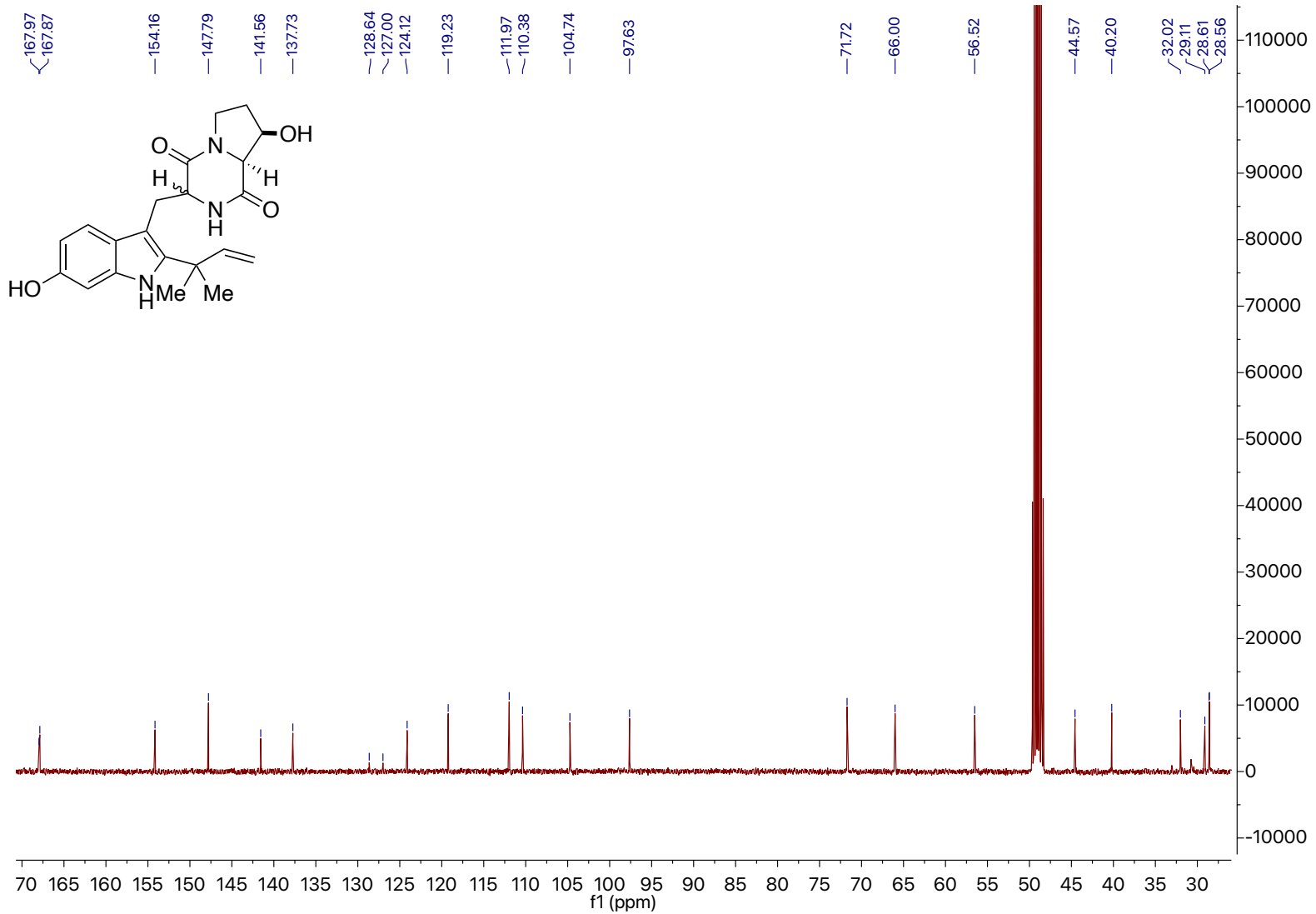

Figure A104. ^{1}H NMR Spectrum of compound **68** (MeOD).

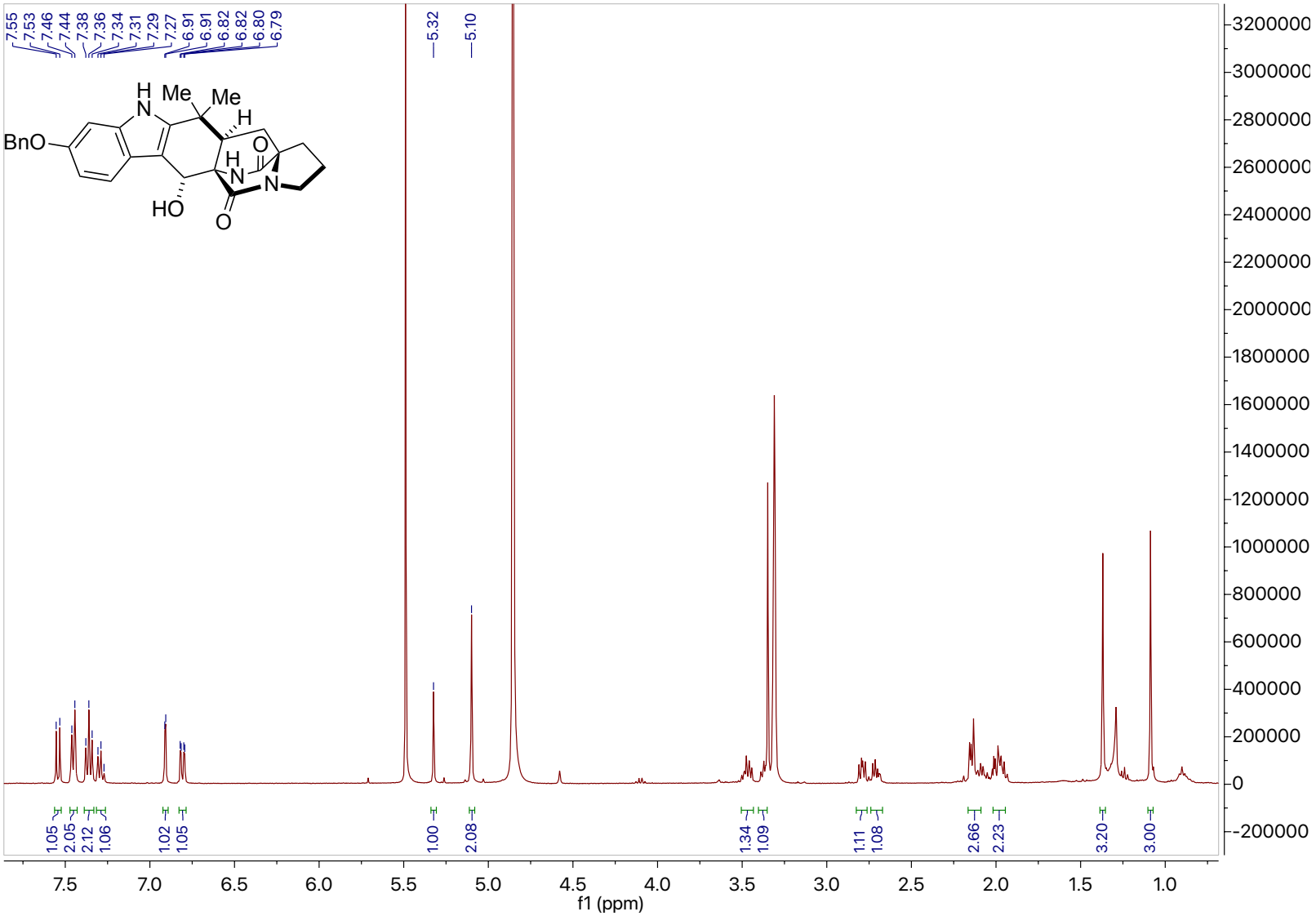

Figure A105. ^{1}H NMR Spectrum of compound **89** (MeOD).

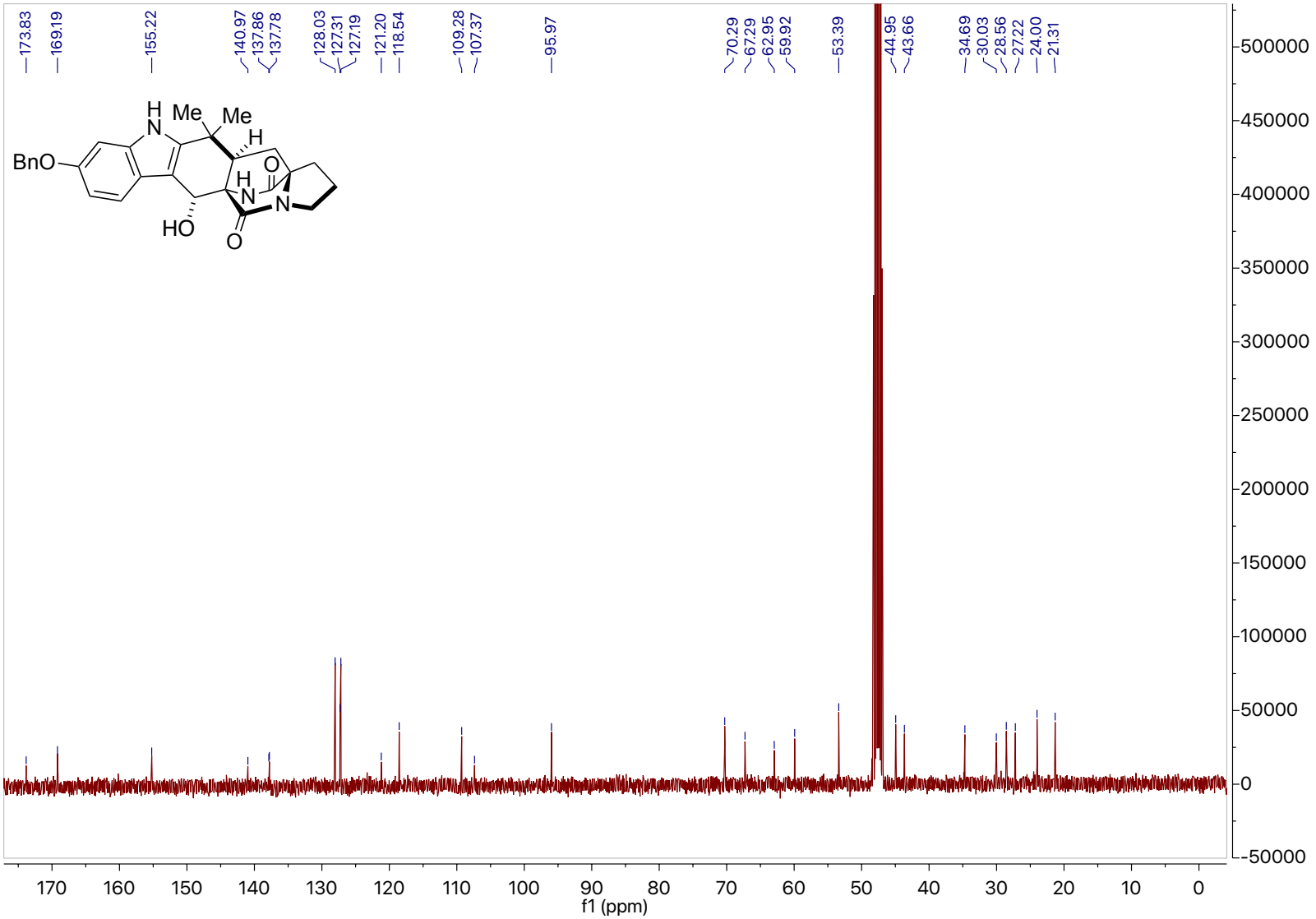

Figure A106. ^{13}C NMR Spectrum of compound **89** (MeOD).

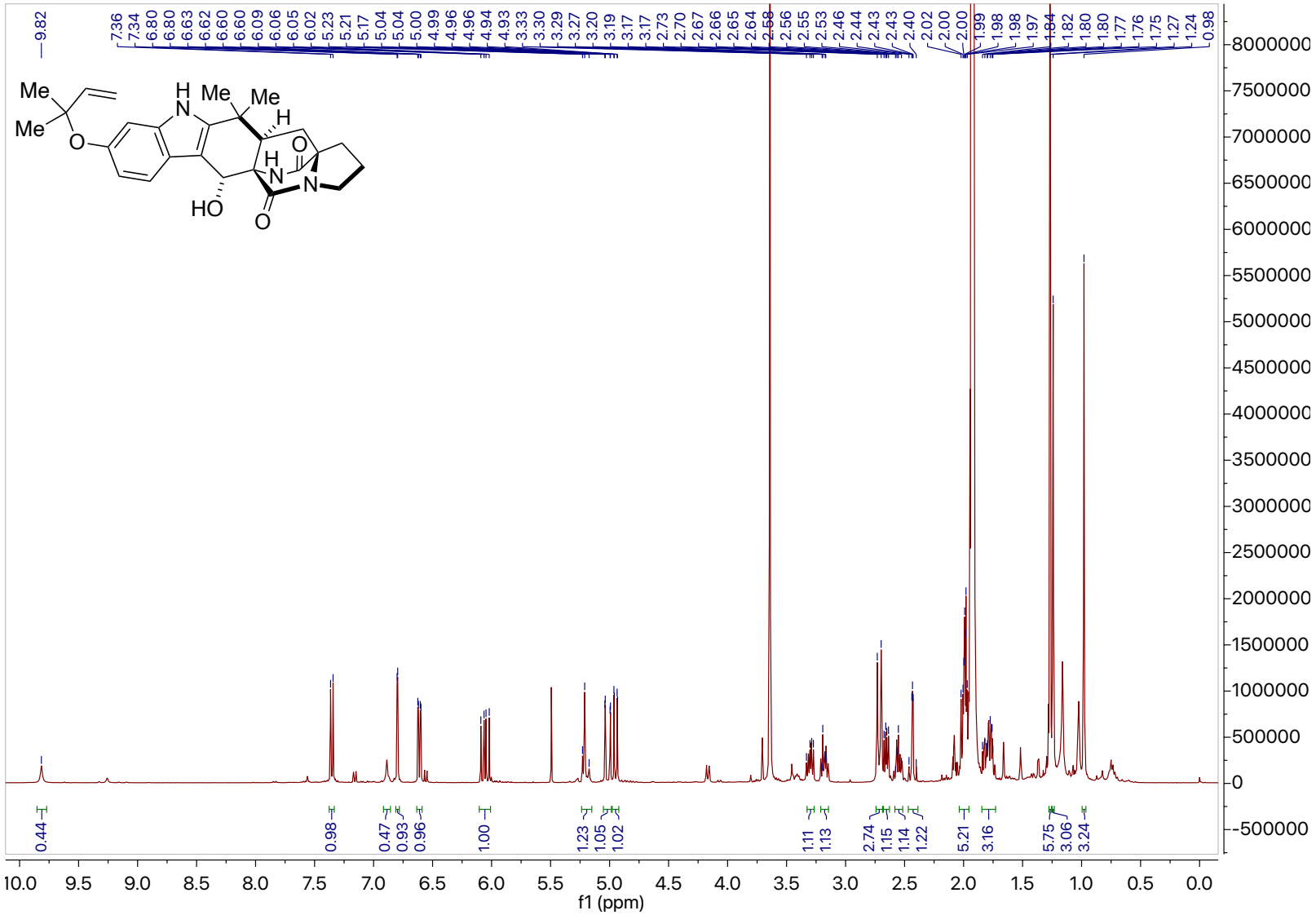

Figure A107. ^{1}H NMR Spectrum of compound **91** (Acetone).

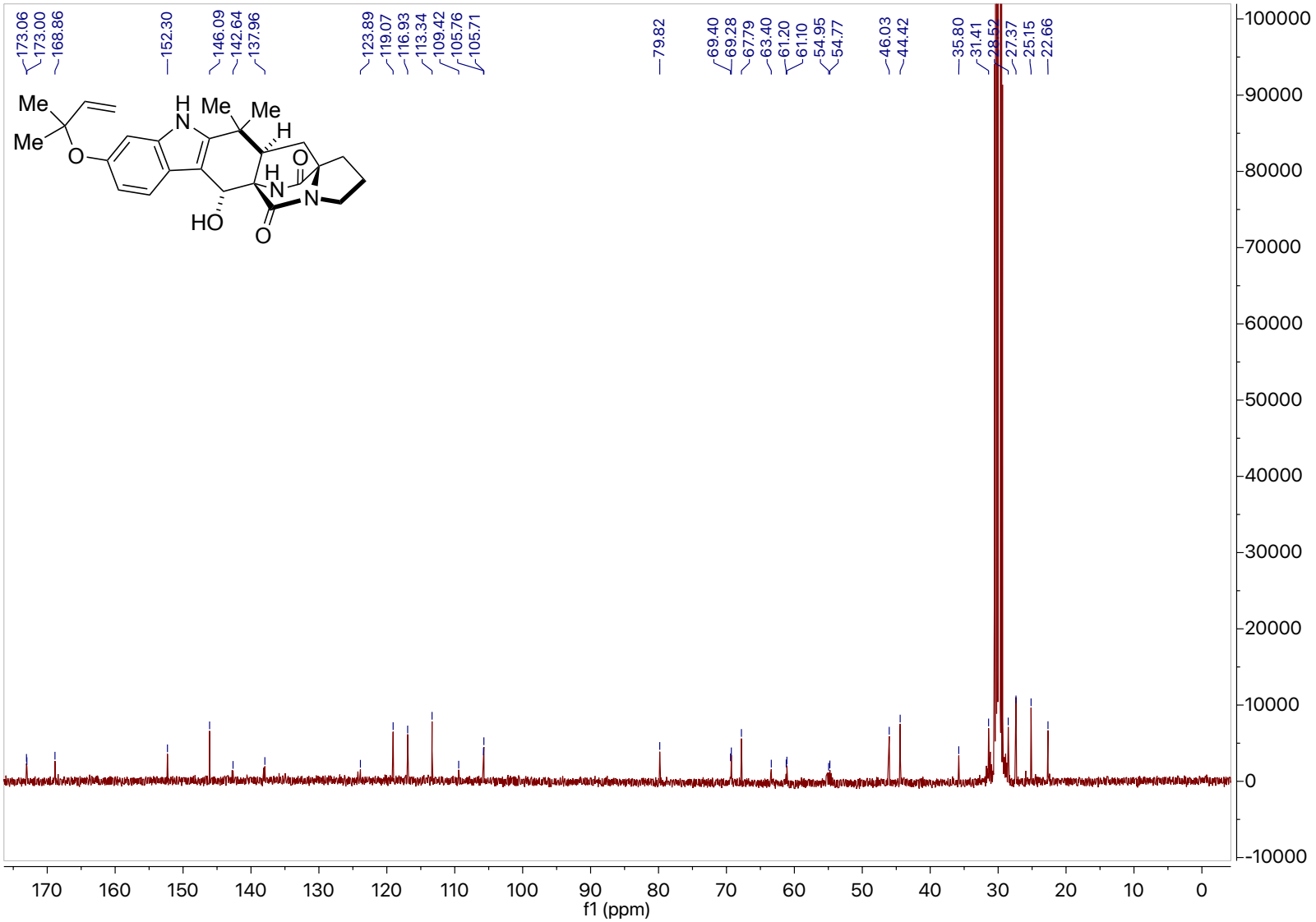

Figure A108. ^{13}C NMR Spectrum of compound **91** (Acetone).

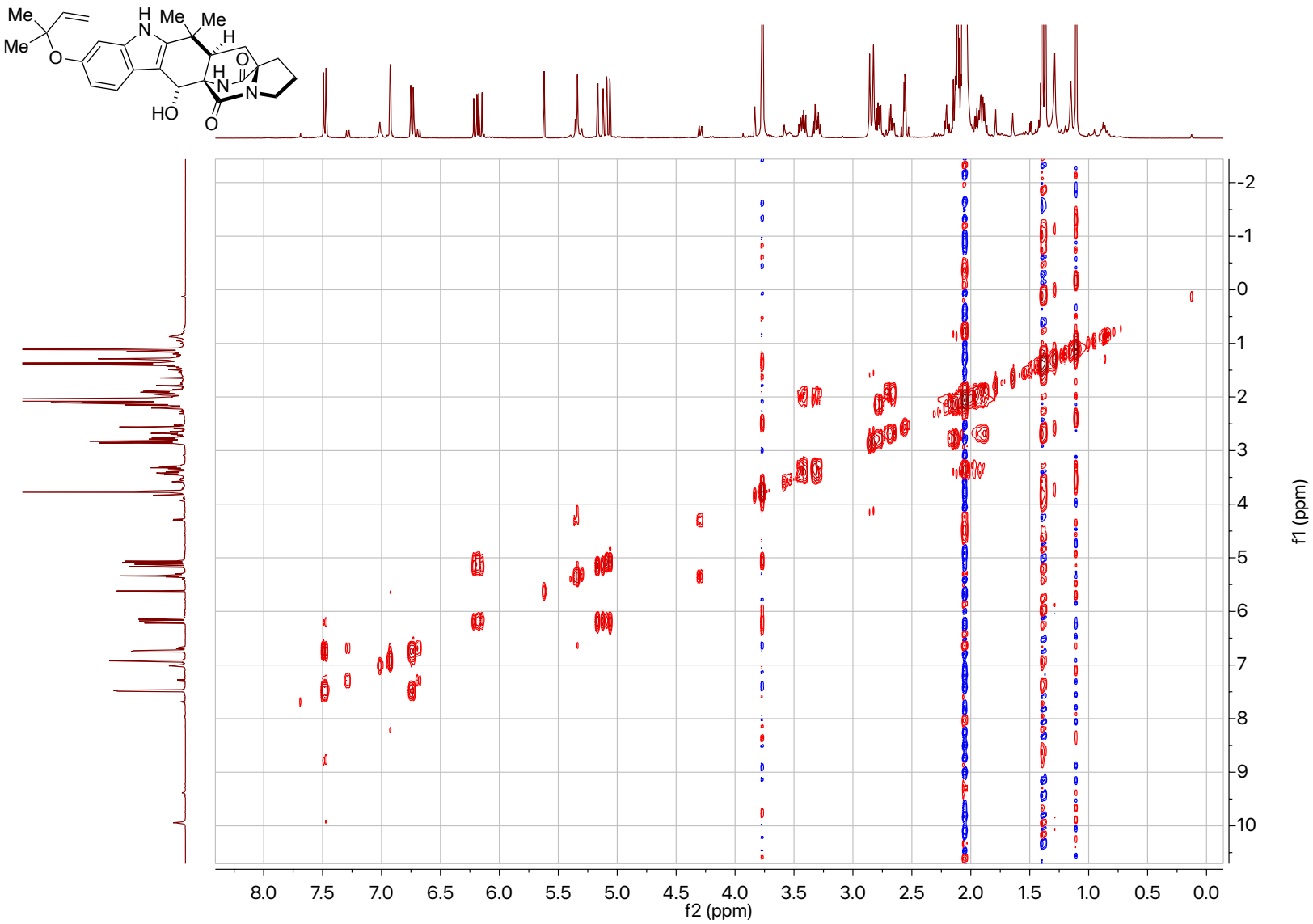

Figure A109. COSY NMR Spectrum of compound **91** (Acetone).

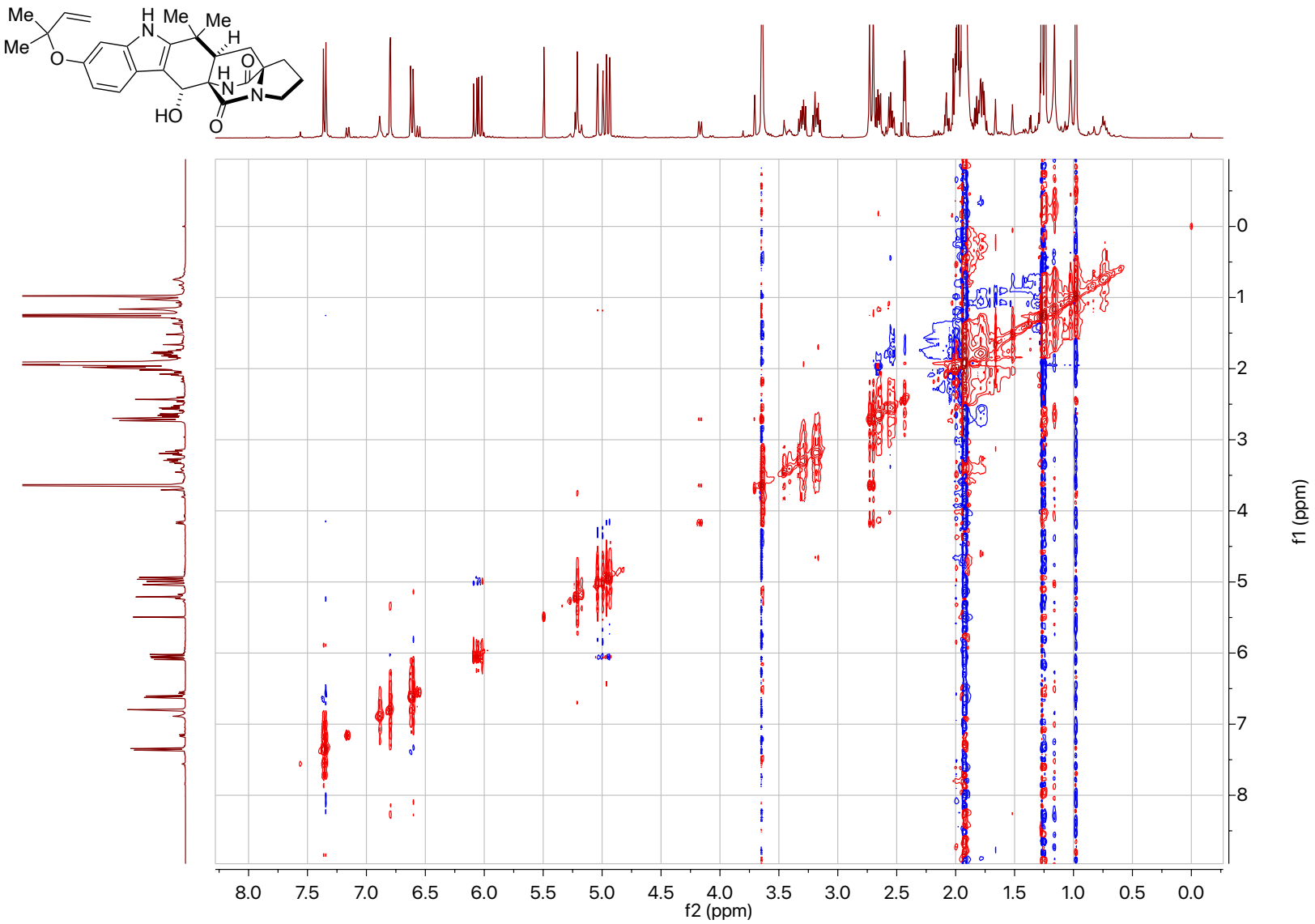

Figure A110. NOESY NMR Spectrum of compound **91** (Acetone).

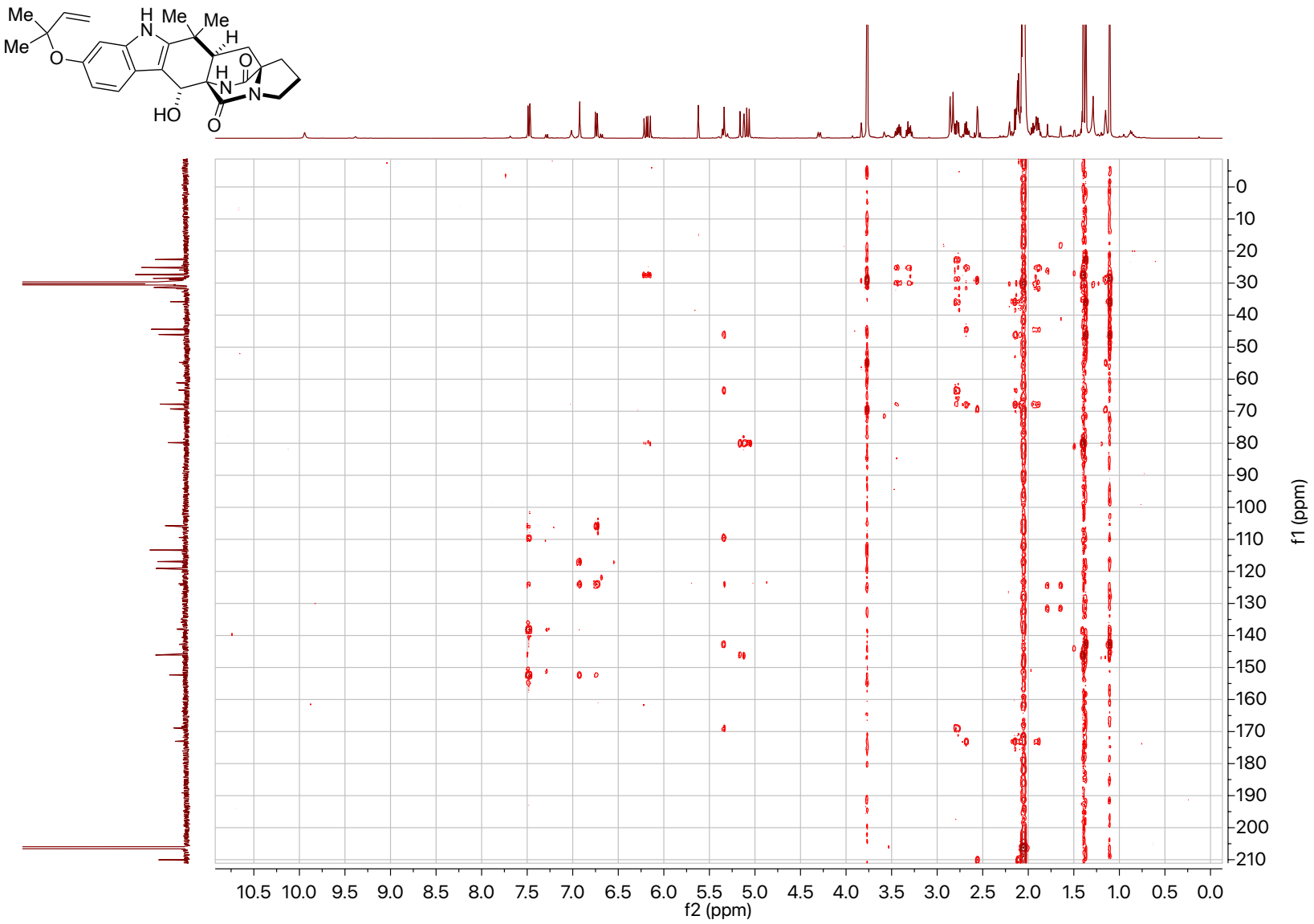

Figure A111. HMBC NMR Spectrum of compound **91** (Acetone).

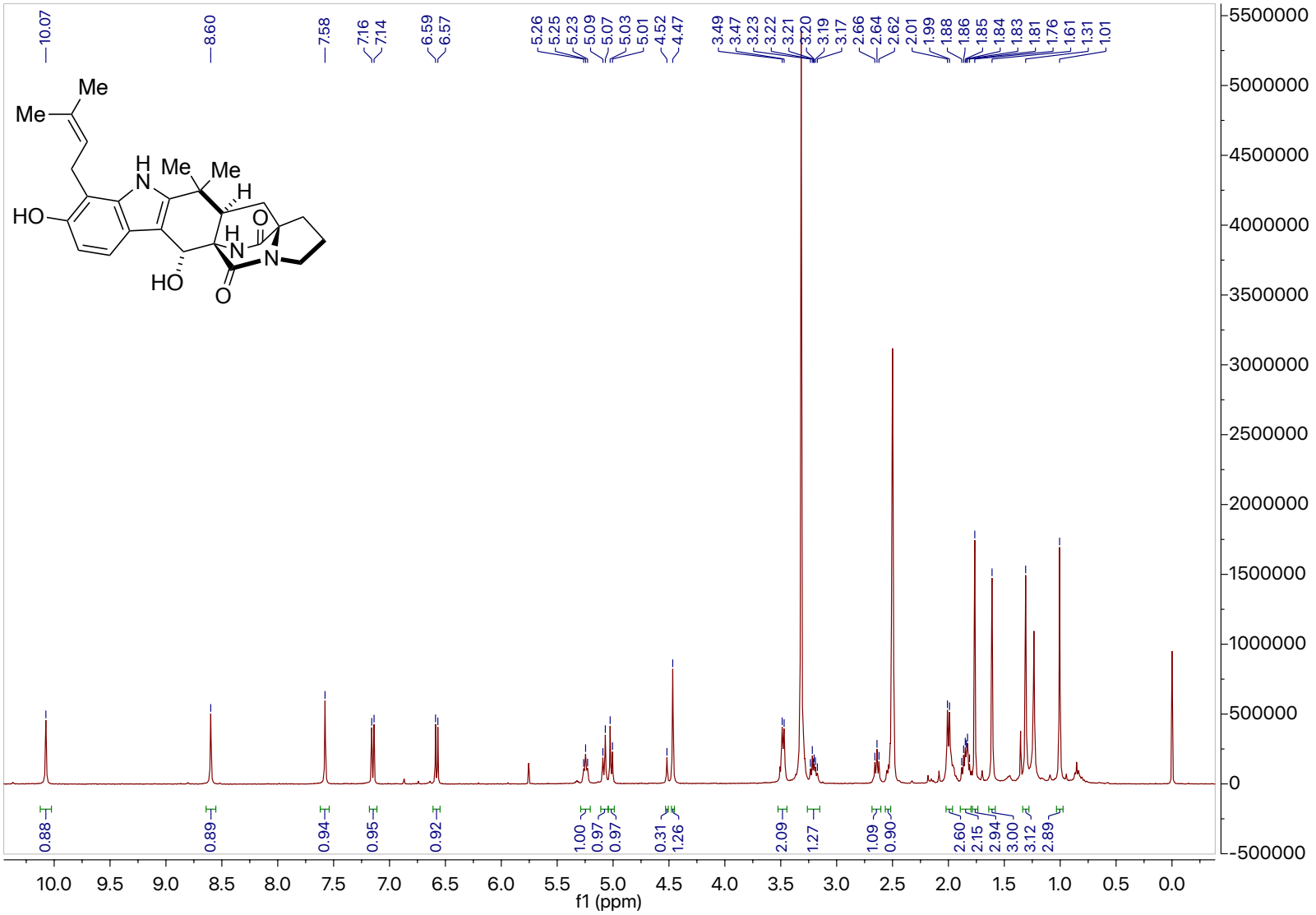

Figure A112. ^{1}H NMR Spectrum of Notoamide T2 (DMSO).

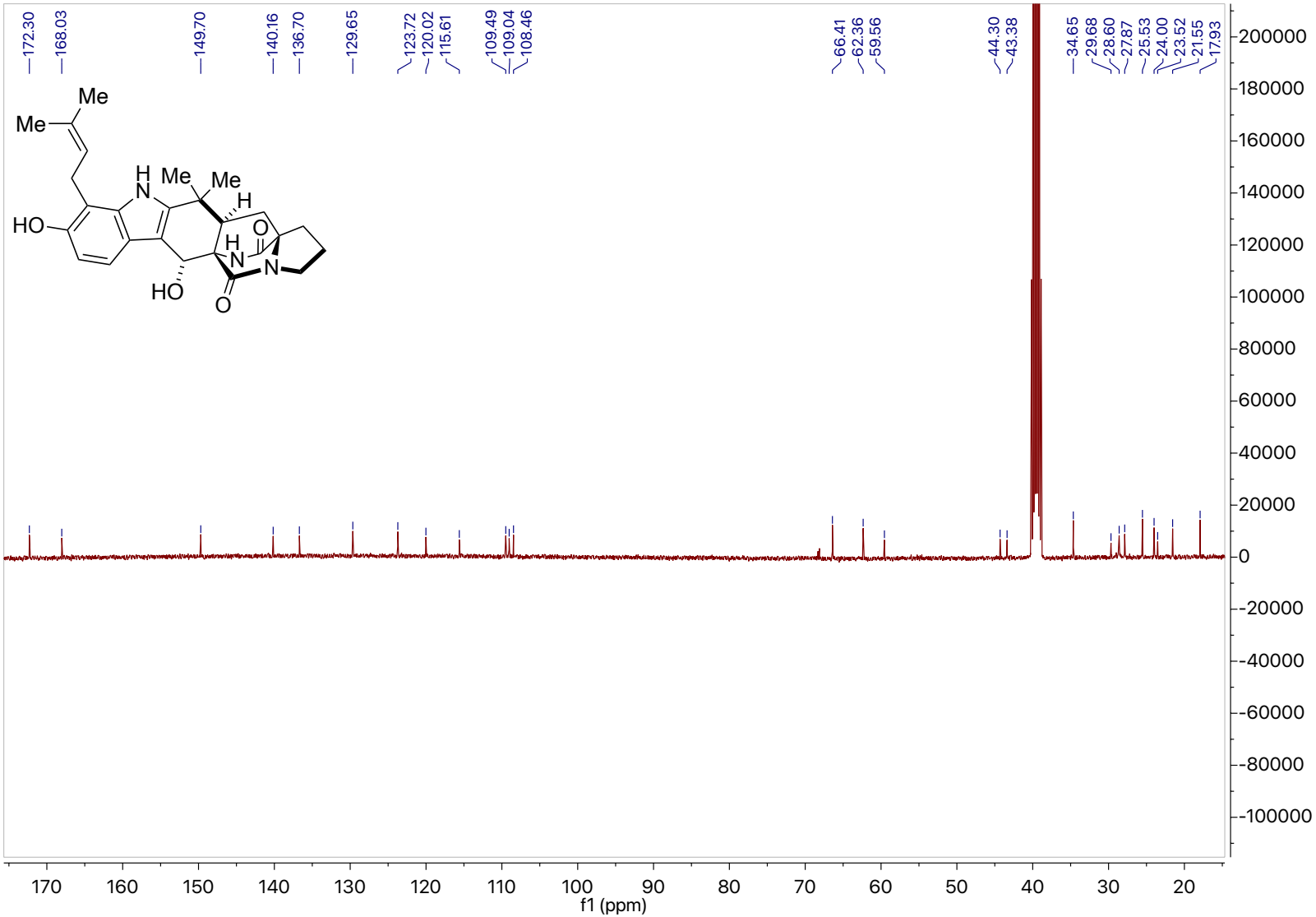

Figure A113. ^{13}C NMR Spectrum of Notoamide T2 (DMSO).

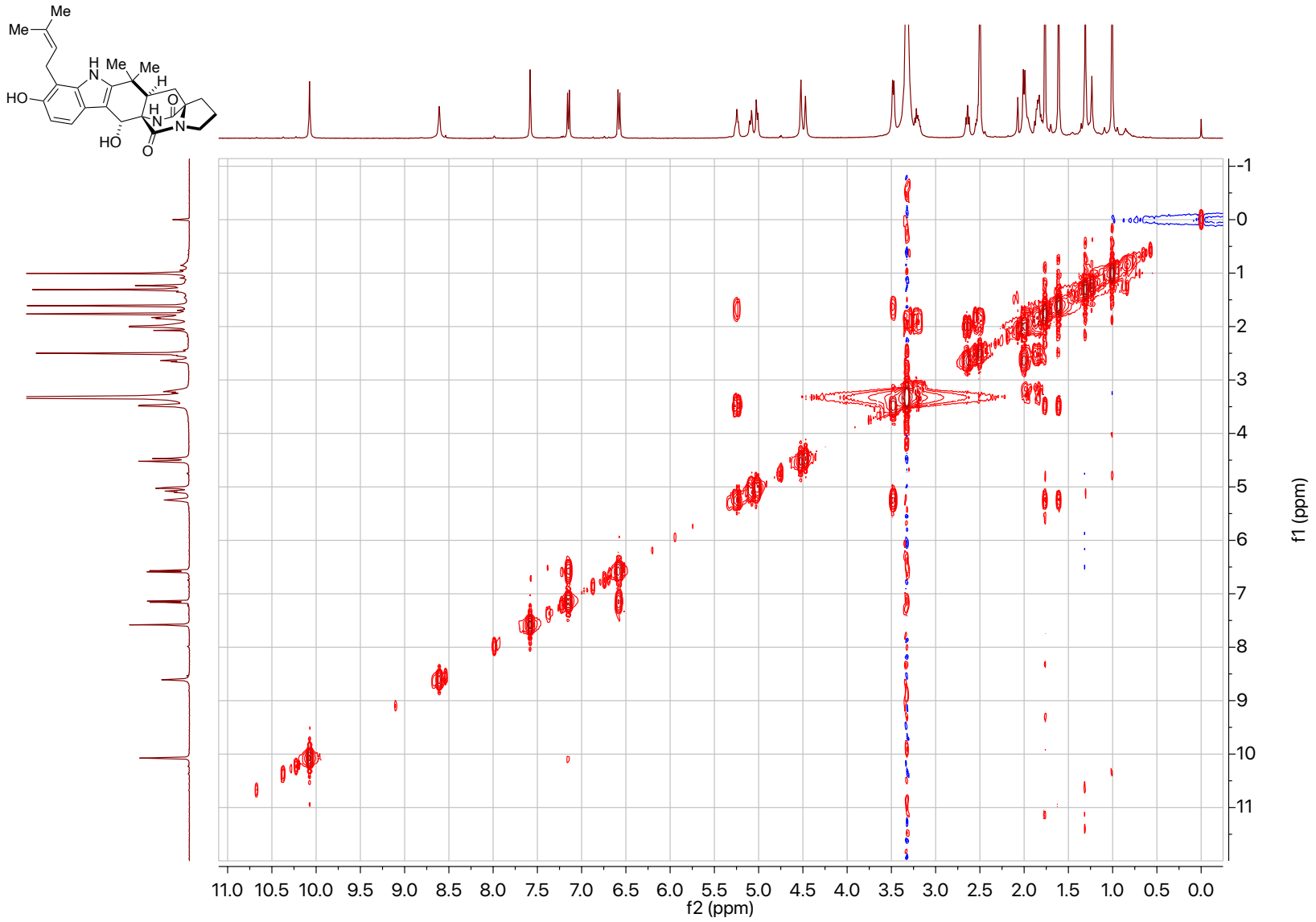

Figure A114. COSY NMR Spectrum of Notoamide T2 (DMSO).

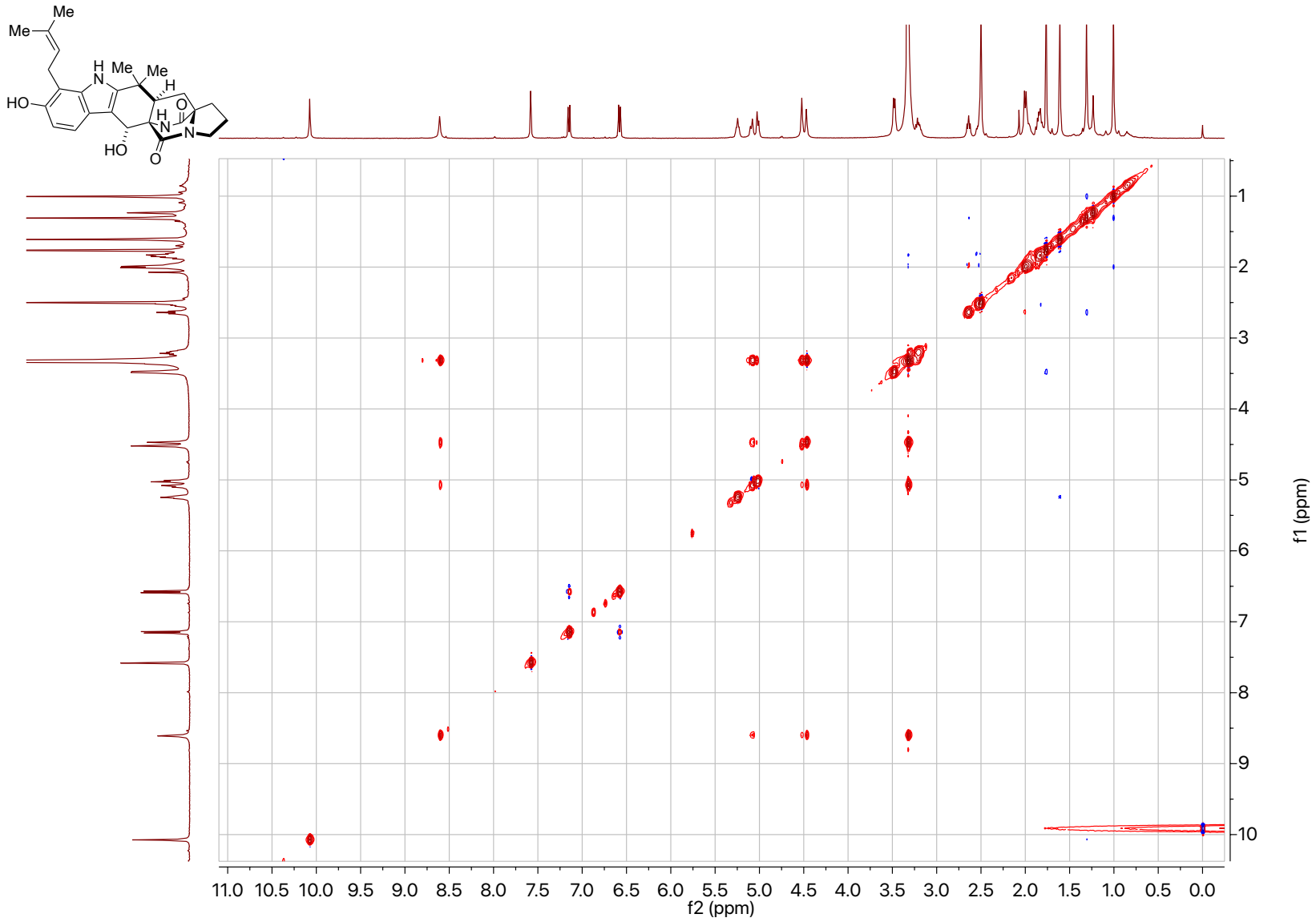

Figure A115. NOESY NMR Spectrum of Notoamide T2 (DMSO).

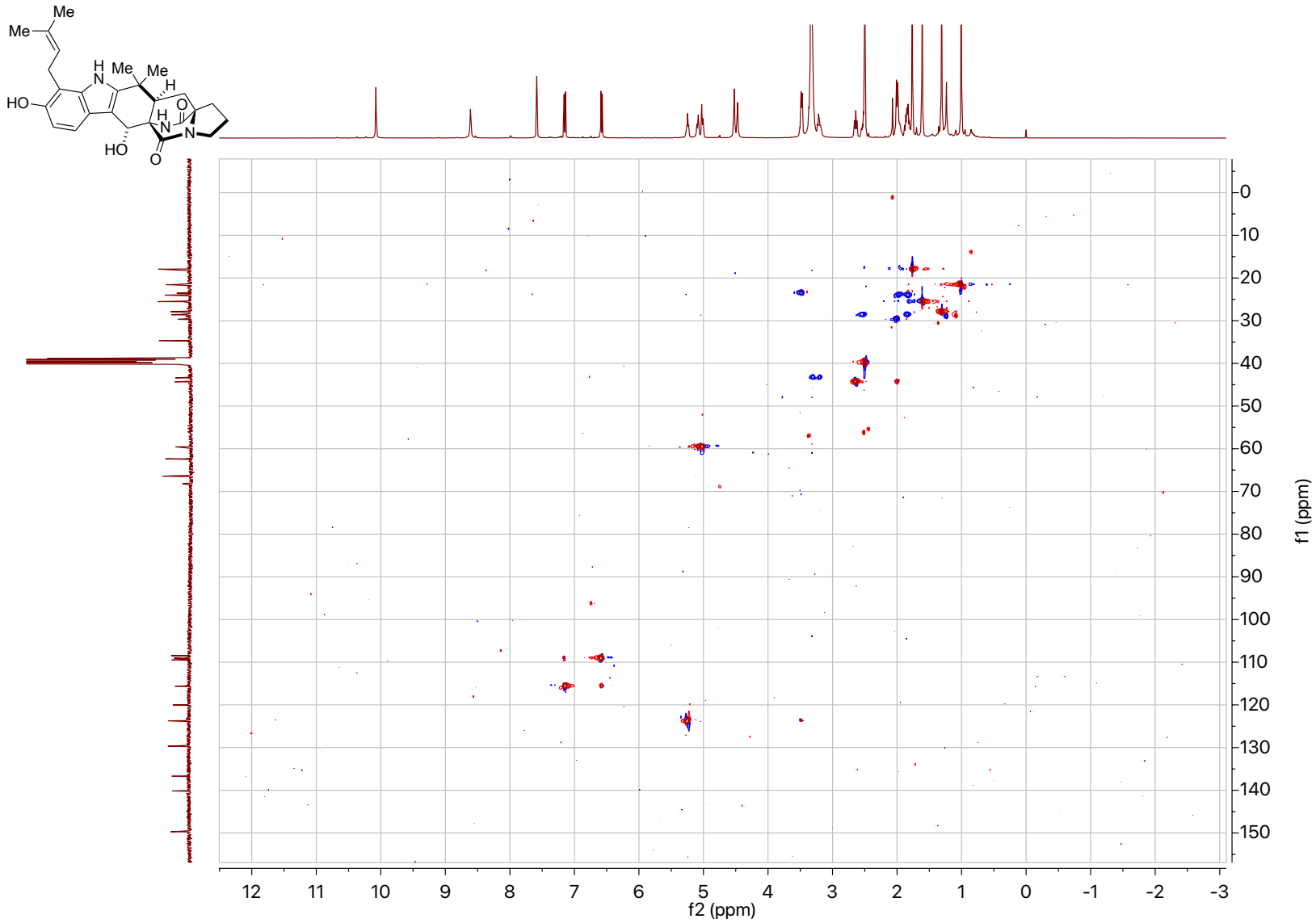

Figure A116. HSQC NMR Spectrum of Notoamide T2 (DMSO).

List of Abbreviations

AcOH	Acetic Acid
9-BBN	9-Borabicyclo[3.3.1]nonane
Boc	*tert*-Butoxycarbonyl
Boc_2O	Di-*tert*-butyl dicarbonate
BF_4OMe_3	Trimethyloxonium tetrafluoroborate
Bn	Benzyl
BOPCl	Biphosphinic chloride
BuLi	Butyllithium
$CDCl_3$	Deuterated Chloroform
$CHCl_3$	Chloroform
CO_2H	Formaldehyde
Cs_2CO_3	Cesium Carbonate
DA	Diels-Alder
DBU	1,8-diazabicyclo[5.4.0]undec-7-ene
DCM	Dichloromethane
DDQ	2,3-dichloro-5,6-dicyano-1,4-benzoquinone
DEAD	Diethyl azocarboxylate
DIBAL	Diisobutylaluminum hydride
DIPEA	Diisoproplethlamine
DMF	Dimethylformamide

DMSO	Dimethylsulfoxide
DO	Davis Oxaziridine
Et	Ethyl
EtOAc	Ethyl Acetate
Et_2O	Diethyl ether
EtOH	Ethanol
Fmoc	Fluorenylmethyloxycarbonyl
FmocOSu	Fluorenylmethoxycarbonyloxy succinimide
HATU	*O*-(7-Azabenzotriazol-1-yl)-*N,N,N',N'*-tetramethyluronium
HPLC	High Performance Liquid Chromatography
IMDA	IMDA Intramolecular Diels-Alder
K_2CO_3	Potassium carbonate
KO	Knock-out
*m*CPBA	*meta*-Chloroperbenzoic acid
MDRO	Multi-drug resistant organisms
Me	Methyl
MeCN	Acetonitrile
MeOH	Methanol
Ms	Methanesulfonyl (mesylate)
MsCl	Methanesulfonyl chloride
$NaBH_4$	Sodium borohydride
NADH	Nicotinamide adenine dinucleotide
NADPH	Nicotinamide adenine dinucleotide phosphate

NaH	Sodium Hydride
NCS	N-chlorosuccinimide
$NHMe_2$	Dimethylamine
NMR	Nuclear magnetic resonance
NRPS	Nonribosomal peptide synthetase
PBu_3	Tributylphoshine
PhMe	Toluene
PPTS	Pyridinium p-toluenesulfonate
pTLC	Preparative thin layer chromatography
i-Pr	Isopropyl
Py. or Pyr	Pyridine
$Sc(OTf)_3$	Scandium Triflate
SM	Starting Material
t-Bu	*Tert*-butyl
*t*BuOCl	*Tert*-butyl hypochlorite
TFA	Trifluoroacetic acid
THF	Tetrahydrofuran
TLC	Thin layer chromatography
TMS	Trimethylsilyl
TMSCl	Trimethylsilyl chloride
pTLC	Preparative thin layer chromatography
i-Pr	Isopropyl
2-OH-py	2-Hydroxypyridine